The effects of ocean acidification on photosynthesis, growth, and carbon and nitrogen metabolism of *Macrocystis pyrifera*

by

Pamela A. Fernández Subiabre

A thesis submitted

in fulfillment of the requirements for the degree of Doctor of Philosophy

in Botany at the University of Otago, Dunedin, New Zealand

June 2015

This thesis was conducted under the supervision of:

Assoc. Prof. Catriona L. Hurd (Primary supervisor)

Department of Botany, University of Otago,
Dunedin, New Zealand
and
University of Tasmania,
Hobart, Australia

and

Dr. Michael Roleda (Primary co-supervisor)

Department of Botany, University of Otago,
Dunedin, New Zealand,
and
Bioforsk, Norway

and

Dr. Christopher Hepburn (Secondary supervisor)

Department of Marine Sciences, University of Otago,
Dunedin, New Zealand.

Abstract

Increases in atmospheric CO_2 concentrations due to anthropogenic activities also cause an increase in oceanic $CO_{2(aq)}$, which will lead to a decline of 0.3-0.4 pH units in the surface ocean by 2100, termed ocean acidification (OA). To date, most OA studies have evaluated the effects of high $CO_{2(aq)}$ and low pH on calcified organisms, but little attention has been paid to determine the effects of OA on non-calcifying organisms such as fleshy macroalgae. Macroalgae depend on CO_2 to support their photosynthesis, and therefore the future predicted changes in inorganic carbon (Ci) availability may directly affect their carbon metabolism, photosynthesis and consequently, growth. The giant kelp *Macrocystis pyrifera* (hereafter *Macrocystis*) is a widely distributed and highly productive macroalga of temperate reef ecosystems that plays an important ecological role in nearshore trophic dynamics. This thesis examines the effects of OA on photosynthesis, growth and carbon and nitrogen metabolism of the giant kelp *Macrocystis*.

Macrocystis is known to be a mixed CO_2 and bicarbonate (HCO_3^-) user, but little is known about its Ci acquisition mechanisms. Here, an optimized method for measuring carbonic anhydrase (CA) in *Macrocystis* was developed. Using the optimized method, both external CA (CA_{ext}) and internal CA (CA_{int}) activities were readily detected in *Macrocystis*. The CA_{int} activity was 2× higher than CA_{ext}. The higher CA_{int} activity was related to the Ci uptake mechanism of *Macrocystis*. As shown in the subsequent examination on the Ci acquisition mechanisms under different HCO_3^-: CO_2 ratios at high (9.00) and low (7.65) pH, the main mechanism for HCO_3^- utilization in *Macrocystis* is via an anion exchange (AE) protein. Regardless of the CO_2 concentration present in the medium, the second HCO_3^- utilization mechanism, i.e. external catalyzed

HCO_3^- dehydration via CA_{ext} makes a lesser contribution to the photosynthetic Ci acquisition. The CA_{int} plays an important role in maintaining internal Ci pools, cellular pH homeostasis and in dehydrating HCO_3^- to supply CO_2 to RuBisCO.

Subsequent examination on the effects of OA on *Macrocystis* photosynthetic performance, growth, and CA_{ext} and CA_{int} activities showed that increased $CO_{2(aq)}$ and low pH did not affect the physiology of *Macrocystis*. Their ability to use HCO_3^- as the main Ci source remained unaffected by increased $CO_{2(aq)}$. The photosynthesis and growth of *Macrocystis* are likely Ci saturated under the current Ci conditions, and therefore, their photosynthetic Ci uptake and growth will not be affected by increased $CO_{2(aq)}$/low pH under a future OA scenario. Thereafter, *Macrocystis* nitrogen physiology relative to tissue nitrogen (N) status was examined to determine whether other environmental factors such as nutrient availability will regulate the species response to OA. However, I found that the thallus N status of *Macrocystis* (deplete and replete N pool) did not modify its response to OA. Consequently, OA affected neither the growth nor NO_3^- uptake and assimilation (i.e. NR) in *Macrocystis*, but some distinct responses such as enhanced NO_3^- uptake were observed in N-deplete *Macrocystis* blades grown under an OA treatment.

Kelp forests of *Macrocystis* are known to modify bulk water carbonate chemistry inside and outside the canopy. Seaweeds can also modify their microenvironment, i.e. at the thallus surface within the diffusion boundary layer (DBL) via physiological processes such as photosynthesis, respiration, and nutrient uptake. Knowledge of the metabolic fluxes (OH^-/H^+) is of great importance to elucidate how macroalgae may respond to a low pH (high $[H^+]$) under a future OA scenario. The present study showed that metabolic fluxes related to the high photosynthetic rates of

Macrocystis rather than due to inorganic nutrient uptake (i.e. NO_3^- and NH_4^+) are responsible for modifying pH within their DBL. Moreover, the pH within the DBL was greatly increased under an OA treatment compared to the ambient seawater pH condition.

Overall, this thesis reveals that OA will not affect rates of photosynthesis, growth, and carbon and nitrogen metabolisms of the giant kelp *Macrocystis*. The results obtained in the present study also suggest that other predicted environmental local changes such as eutrophication and low light availability may have a more significant effect on the physiology of *Macrocystis* than OA. This thesis elucidates how this species might respond to OA, and to the understanding of the carbon and nitrogen metabolism of the species, which will be of great importance for further studies to determine how future predicted global and local environmental changes might interactively affect *Macrocystis'* physiology and ecology.

Acknowledgements

I would first to thanks to my supervisors Catriona Hurd, Michael Roleda, and Chris Hepburn for your valuable assistance, knowledge, encouragement, support and patience throughout this study. Thanks to Catriona for your inspirational work that brought me to New Zealand, and for the amazing opportunity to work with you and your incredible research team. Thanks so much for your continued encouragement, advice and faith, and for always be so cheerful. Thanks also for giving me the opportunity to finish my studies in Hobart closer to you and around vibrant scientists that confirm for me that this the path I want to follow. Thanks to Maikee, for your continued encouragement, constant support, patience, and valuable advices and long conversations, and for always pushing me and keeping me on track. Thanks to both of you to make this journey so enjoyable and exciting, I have learned so much from both of you. I just can say that I was lucky to have both of you during this amazing journey, and it could not be better.

Many thanks to everyone at the Botany Department for always being so helpful and supportive. Special thanks to Vickey Tomlinson for all your help in the lab, to Hadley O'Sullivan for always be willing to help me, to Stewart Bell for your joy and making me smile every morning, and to Michelle McKinlay, Kath McGilbert and Kath Dickinson for all your help, support and caring about me while Catriona was away. Many thanks to my fellow students at the Botany Department and our lab group, Rocio Suarez, Yuanyuan Feng, Chris Cornwall, Daniel Pritchard, Derek Richards, Katja Schiwert, Ralf Rautenberger, Mauro Cubillos, and Pablo Leal for all your help in the field, lab and for making this journey so far away from home so enjoyable. I would also to thank to Kim Currie at the Chemistry Department for always be willing to help me, and caring about me and my research.

Many thanks to my friends in Dunedin, who always make feel like at home full of loved and around of good food and wine. Special Thanks to the Chiwi's Family Benavides-Moore for all the adventures in this beautiful country and cheer me up every time that I needed.

I would also thank to my beautiful family. Thanks to my parents and sister for always believing in me, and pushing me to follow my dreams no matter how crazy they sound.

Last but not least, thanks to my amazing partner Pablo, thank you so much for sharing this journey with me, for believing in me and following me in this crazy adventure so far away from home. Thank you so much for your patience, constant encouragement, wise advices and cheering me up when most I need it. Love you more than ever…. Te Amo.

Table of contents

List of Tables

List of Figures

Chapter 1: General introduction

1.1 Ocean acidification (OA)

Since the Industrial Revolution, the emissions of CO_2 into the atmosphere have increased considerably due to human activities such as fossil fuel combustion, cement manufacture and deforestation (The Royal Society 2005, Caldeira and Wickett 2003, Doney et al. 2009, IPCC 2013). The result is that atmospheric concentrations of CO_2 have increased from 280 (pre-industrial) to 392 µatm (present). Atmospheric CO_2 concentrations are projected to increase to ≈1000 µatm by the year 2100, based on the RCP8.5 business-as-usual-scenario (IPCC 2013). Approximately one third of these emissions will be absorbed by the world's oceans, increasing $CO_{2(aq)}$ and decreasing the pH of the surface waters, making them more acidic and altering the seawater carbonate chemistry, a process known as ocean acidification (OA) (The Royal Society 2005, Guinotte and Fabry 2008).

Oceanic $CO_{2(aq)}$ concentrations are projected to increase from 11.8 to 31 µmol kg^{-1} by the year 2100, causing an estimated drop in pH of 0.3-0.4 units from the current global ocean surface average of 8.15-7.75 (Koch et al. 2013, IPCC 2013). This decline in pH units will mean an increase of about 150% in the hydrogen ion concentration $[H^+]$ of seawater (Doney et al. 2009). These changes will alter the seawater carbonate equilibrium, changing the proportion of each dissolved inorganic carbon (DIC) form: $CO_{2(aq)}$, HCO_3^- and CO_3^{2-}. Today's ocean contains approximately 2000 µmol kg^{-1} of DIC at pH 8.07, where $CO_{2(aq)}$ makes the smallest contribution (1%), and HCO_3^- contributes 91% and CO_3^{2-} 8% of the total DIC. By the year 2100, total DIC will increase to 2180 µmol kg^{-1}, and $CO_{2(aq)}$ concentration will increase by 200%, whereas

HCO_3^- only will increase by 14% and CO_3^{2-} ions will decrease by 51% (The Royal Society 2005, Koch et al. 2013). However, despite a 200% increase in $CO_{2(aq)}$, HCO_3^- concentrations will remain much higher than $CO_{2(aq)}$. These significant changes in the ocean chemistry, with an increase in [$CO_{2(aq)}$] and [HCO_3^-], but a decrease in [CO_3^{2-}] will probably affect both photosynthetic and calcifying marine organisms (both autotrophs and heterotrophs) due to the potential changes in physiological processes including photosynthesis, respiration and calcification (The Royal Society 2005, Martin et al. 2013).

1.1.1 Response of non-calcifying photosynthetic marine organisms to OA

A substantial part of research into OA has been focused on calcified organisms (autotrophs and heterotrophs), mostly because they form calcareous structures that may be negatively affected by either the predicted decline in [CO_3^{2-}] or reduced pH (high [H^+]) (Jokiel et al. 2008, Fabry et al. 2008, Jokiel 2011, Kroeker et al. 2013). However, less attention has been paid to non-calcifying organisms, some of which might benefit from OA. Opposite to calcified algae, fleshy macroalgae and diatoms may benefit under OA (Kroeker et al. 2013). A recent meta-analysis study showed that under OA, growth of fleshy algae can increase by 22% and by 18% for diatoms (Kroeker et al. 2013). However, photosynthetic responses to OA appear to be more variable among taxa and species (Kroeker et al. 2013). For seagrass and macroalgae (= seaweeds), photosynthesis seems to be unaffected or positively affected by OA (Kroeker et al. 2013).

The increase in [$CO_{2(aq)}$] and [HCO_3^-], and the change in the relative proportion of each can affect photosynthetic organisms because both Ci forms can be used to support photosynthesis (Giordano et al. 2005, Raven and Hurd 2012). In several

seagrass species, photosynthesis and growth have been enhanced by high [$CO_{2(aq)}$] (Koch et al. 2013 and references therein). For macroalgal species, the photosynthetic response to OA has been heterogeneous and species-specific relative to their carbon physiology (Kübler et al. 1999, Israel and Hophy 2002, Raven and Hurd 2012). Although the majority of seagrass and macroalgae have the ability to use HCO_3^- as an Ci source for photosynthesis, mechanisms of acquisition vary among species, and photosynthesis and/or growth may not always be saturated by the current Ci concentrations. Therefore, high [$CO_{2(aq)}$] could enhance these physiological processes in some macroalgal species.

1.1.2 Carbon physiology of macroalgae and responses to OA

Photosynthesis of macroalgae would be severely limited if they were dependent only on the diffusive entry of CO_2 from the bulk seawater (SW) to the fixation site of the carbon assimilating enzyme ribulose-1,5-bisphosphate carboxylase/oxygenase (RuBisCO) (Beardall et al. 1998, Kawamitsu and Boyer 1999). RuBisCO is a bifunctional enzyme that fixes both CO_2 and O_2 (Kawamitsu & Boyer 1999). Oxygen competes with CO_2, hence CO_2 fixation might be less in solutions with high O_2 availability (normal air) (Kawamitsu and Boyer 1999). Furthermore, RuBisCO has a low affinity for CO_2 (Raven and Johnston 1991, Beer et al. 2014), and current ambient CO_2 concentrations ($\approx$ 12 µM) only half saturates the carboxylation reaction (Beer et al. 2014). For example, brown macroalgae can have RuBisCO with K_m values between 12 and 60 µM (Beer et al. 2014). Therefore, is not surprising that most macroalgae also use HCO_3^- as a Ci source for photosynthesis, after being converted to CO_2 by the internal carbonic anhydrase (CA_{int}) enzyme (Maberly 1990, Raven and Hurd 2012). To overcome these constraints of RuBisCO most marine macroalgae have developed several mechanisms to make efficient use of DIC, termed CO_2 concentrating mechanisms (CCMs), which

allow a more rapid C assimilation per unit of biomass. The mechanisms are quite diverse, but in all cases, they are composed principally of at least three functional elements: (1) influx of CO_2 and/or HCO_3^-, (2) capture of Ci inside the cell (usually as HCO_3^-) and (3) production of CO_2 from the dissolved inorganic carbon (Ci) pool around RuBisCO. These processes serve to increase the concentration of CO_2 around RuBisCO, hence RuBiSCO can function at much closer to its maximum carboxylase activity. Consequently, this reduces the rate of photorespiration and therefore improves the efficiency of CO_2 fixation (Mercado et al. 2006, Magnusson et al. 1996, Giordano et al. 2005, Beardall et al. 2005).

The changes in $[CO_{2(aq)}]$ and $[HCO_3^-]$ predicted by the year 2100 could have significant consequences on the ability of macroalgae to acquire Ci and the magnitude of this response will depend principally on their ability to use HCO_3^- relative to CO_2. Although $CO_{2(aq)}$ is the smallest pool of DIC, this uncharged molecule readily diffuses through the lipid bilayer of the plasma membrane into the cells, and some macroalgal species depend only on this Ci source for photosynthesis. For these macroalgae, strictly CO_2–users, e.g. *Lomentaria articulata*, the increase in $[CO_{2(aq)}]$ could reduce the energy cost for assimilation of CO_2, which consequently will enhance photosynthesis and growth (Raven 1991, Kübler et al. 1999). Unlike $CO_{2(aq)}$, HCO_3^- cannot diffuse through the lipid bilayer of the plasma membrane (Raven 1997), and is taken up by active transport from seawater to the inside of the cell. Three main mechanisms have been proposed for HCO_3^- acquisition by macroalgae: (1) active Ci uptake involving a P–type H^+–ATPase pump that might facilitate the transport of CO_2 or HCO_3^- into the cell. It is assumed that proton motive force would create a secondary transport (e.g. CO_2 and HCO_3^-) (Klenell et al. 2004). (2) The external conversion of HCO_3^- to CO_2, which is catalyzed by the external carbonic anhydrase (CA_{ext}), an enzyme located in the cell wall

in the majority of macroalgae, and (3) direct HCO_3^- uptake through a plasmalemma–located anion exchange (AE) protein (Axelsson et al. 1999, 2000, Kübler et al. 1999, Madsen and Maberly 2003, Klenell et al. 2004, Giordano et al. 2005). For mixed CO_2 and HCO_3^- users, direct and/indirect mechanisms for HCO_3^- utilization may be down-regulated at high [$CO_{2(aq)}$] (Magnusson et al. 1996, Madsen and Maberly 2003, Hurd et al. 2009). However, it has been suggested that for macroalgal species that possess an effective CCM neither photosynthesis nor growth will be affected by high [$CO_{2(aq)}$] (Beardall et al. 1998, Israel and Hophy 2002).

The HCO_3^- acquisition mechanisms vary among macroalgal species, and although some species may use HCO_3^-, photosynthesis and growth may still be limited by the current Ci concentrations due to a less effective mechanism for Ci acquisition. Mixed HCO_3^- and CO_2 users species with carbon-limited photosynthesis, e.g. *Hizikia fusiformis* and *Hypnea spinella* may exhibit positive responses to elevated [$CO_{2(aq)}$], as projected for strictly CO_2–users, where high [$CO_{2(aq)}$] did enhance growth and photosynthesis (Zou 2005, Suárez-Álvarez et al. 2012, Koch et al. 2013). Some studies have reported a reduction in the ability to use HCO_3^- in macroalgae cultured at [$CO_{2(aq)}$] (Björk et al. 1993, Garcia-Sanchez et al. 1994, Mercado et al. 1997, Gordillo et al. 2001). For example, for the green macroalga *Ulva* sp. cultured at high [$CO_{2(aq)}$] (seawater bubbled with 5% CO_2); this reduction was interpreted as a deactivation of the CCM, and CA_{ext} and CA_{int} activity was also reduced (Björk et al. 1993). In contrast, for *Porphyra leucostica* cultivated in a high CO_2 treatment (seawater bubbled with 1% CO_2), there was no reduction in CA_{ext} activity, but the mechanism for using HCO_3^- was also partially inactivated (Mercado et al. 1997). The same response was observed for *Fucus serratus* (Johnston and Raven 1990) and for *Gracilaria tenuistipitata* (Garcia-Sanchez et al. 1994), which had a reduced ability to use HCO_3^- as a carbon source after

they were cultured in a high CO_2 treatment (seawater bubbled with 5% CO_2). In the latter species, the CA activity, the maximum photosynthetic rate as well as the photosynthetic efficiency were lower in algae cultivated in the high CO_2 treatment than the ambient treatment. Similarly, Gordillo et al. (2001) observed the inactivation of CCMs in *U. rigida* in response to high [$CO_{2(aq)}$] (10,000 μl^{-1}). Therefore, the response of macroalgae to the predicted changes in the seawater chemistry due to OA might be species-specific depending on its Ci acquisition mechanism, their affinity for either HCO_3^- and/or CO_2 and their ability to spontaneously switch from one Ci source to the other. However, it is also important to highlight the culture conditions, in all studies mentioned above the concentrations of $CO_{2(aq)}$ used during incubations were higher than the ones expected by 2100.

1.1.3 Other biochemical or physiological parameters of macroalgae that might be affected by OA

The mechanisms of Ci acquisition, photosynthesis and growth are not the only physiological processes that could be affected by the changes in the [$CO_{2(aq)}$], [HCO_3^-] and pH predicted by the year 2100. Some studies have described important consequences on the distribution, abundance, and nutrient-uptake of fleshy macroalgae (Chung et al. 2011). The high [$CO_{2(aq)}$] might affect the nutrient metabolism, e.g. nitrate uptake rate and NR activity, and cell components such as soluble proteins contents and phycobiliprotein affecting the cellular C:N ratio (Zou and Gao 2010). In addition, a secondary effect of OA will be a possible decrease in nitrification rates (Beman et al. 2011), which will reduce the [NO_3^-] relative to that of [NH_4^+] and organic nitrogen in seawater. This change in the relative proportion of NO_3^-:NH_4^+ might influence the function of the CCMs (Raven et al. 2011).

1.2 Nitrogen metabolism

Nitrogen is usually the main factor limiting the productivity of macroalgae and in coastal waters is mostly available in two forms, nitrate (NO_3^-) and ammonium (NH_4^+) (Gerard 1982ab, Wheeler and North 1981, Fram et al. 2008, Hurd et al. 2014). In temperate regions, concentrations of inorganic nitrogen (N_i) usually vary during the season, reaching maximal concentrations during the fall and winter, and minimal between spring and summer (Haines and Wheeler 1978, Gerard 1982ab, Harrison and Hurd 2001). However, NH_4^+ might not always vary seasonally, and it might be present year around in low concentrations (Hepburn et al. 2007, Hurd et al. 2014). In addition, NH_4^+ may also be provided by epibionts organisms living on the macroalgal surface, being an important source of N_i when NO_3^- concentrations decline (Hepburn et al. 2007). Some macroalgal species, e.g. *Macrocystis pyrifera* and *Xiphophora chondrophylla*, are able to take up both N_i sources simultaneously and the presence of one source does not alter the uptake of the other, whereas for other species, e.g. *Ulva intestinalis* (= *Enteromorpha intestinalis*) and *Gracilaria pacifica*, NH_4^+ uptake may inhibits NO_3^- uptake by up to 50% (Haines and Wheeler 1978, Thomas and Harrison 1987, Harrison and Hurd 2001, Rees et al. 2007).

Although there is extensive knowledge about N_i kinetics in macroalgae, little is known about the transport mechanism of N_i sources into the algal cell. It is generally assumed that in eukaryotic algae, NH_4^+ is taken up by facilitated diffusion, whereas NO_3^- is taken up by active transport (Raven 1984, Lobban and Harrison 1997, Hurd et al. 2014, Pritchard et al. 2015). However, the presence of active NH_4^+ uptake has also been suggested for macroalgae (Rees et al. 1998, Raven and Giordano 2015). Unlike the N_i transport mechanism, it is well established that the energy cost required for NH_4^+ assimilation is lower than that of NO_3^- assimilation, which must be first reduced to

ammonium (Solomonson and Barber 1990, Hurd et al. 2014). NO_3^- and NH_4^+ uptake rates may vary frequently over time depending on the N_i availability in seawater and the physiological status of the algae (e.g. nitrogen status of the thallus), but might also be influenced by environmental factors such as light, temperature, water motion or other biological factors such as the age of the alga, nutritional history or interplant variability (Ahn et al. 1998, Hurd et al. 1996).

After NO_3^- uptake, the next step of pathway is the reduction of NO_3^- to nitrite (NO_2), catalyzed by the enzyme nitrate reductase (NR). This is a key enzyme in N metabolism and is considered to be the limiting step in nitrate assimilation (Solomonson and Barber 1990, Berges 1997). When NO_3^- uptake rate exceeds the NR capacity, unassimilated NO_3^- might be stored in storage vacuoles, and be assimilated later by NR (McGlathery et al. 1996, Hurd et al. 2014). NO_2 is then reduced to NH_3/NH_4 by the nitrite reductase (NiR). It is generally accepted that NR is mainly cytosolic, but there is some evidence that may be also associated with plastid membrane and the plasma membrane, whereas NiR may be located in the chloroplast (Ullrich 1983, Berges 1997, Hurd et al. 2014). Finally, NH_4^+ is assimilated into amino acids, the monomeric components of protein, by the enzyme complex glutamine synthetase (GS) - glutamine 2-oxoglutarate amino-transferase (GOGAT). NH_4^+ that is not immediately assimilated might also be stored in storage vacuoles, but in less concentration than NO_3^-; free amino-acids (FAA) and proteins can also be stored intracellularly (McGlathery et al. 1996, Rees et al. 1998). These intracellular N reserves are essential to support physiological processes such as growth and photosynthesis when external N_i concentrations decline (McGlathery and Pedersen 1999). Therefore, knowledge of the factors controlling N_i uptake, and interaction between N_i uptake, assimilation and

storage capacity are essential for a better understanding of the nitrogen metabolism in macroalgae.

Furthermore, the N metabolism is complexly associated with CCMs because the amount of resources invested by algal cell in acquiring Ci is likely associated with the availability of other nutrients, and also nitrogenous compounds are required to maintain operational the enzymatic system (Beardall and Giordano 2002, Giordano et al. 2005). The C and N metabolism might be tightly coupled in macroalgae (McGlathery and Pedersen 1999). Therefore, the N_i availability in seawater may have significant effects on the down-regulation of CCMs. For example, *Chlamydomonas reinhardtii* cultivated under N-limitation (NH_4^+ as N_i source) shows a clear reduction of photosynthetic affinity for Ci compared with algae that are N-sufficient (Beardall and Giordano 2002). This response may be a consequence of the lack of an essential element for the formation of other substances such as proteins involved in Ci acquisition. Furthermore, this response may depend on the availability and N_i source supplied (e.g. NO_3^- or NH_4^+); some algal cells cultivated on NH_4^+ have a higher affinity for CO_2 than cells cultivated with NO_3^- as a N_i source (Beardall and Giordano 2002, Raven and Beardall 2014).

1.2.1 Effects of OA on the N metabolism of macroalgae

The increase in [$CO_{2(aq)}$] projected by the end of this century may have significant consequences on the nitrogen metabolism of macroalgae. For example, it is anticipated that macroalgae which exhibit carbon-limited photosynthesis, e.g. strictly CO_2–users, might respond positively by increasing rates of CO_2 assimilation, causing higher growth rates at high [$CO_{2(aq)}$] than at low or current [$CO_{2(aq)}$]. This may lead to a greater demand for nutrients, particularly nitrogen and phosphorus because they play an

important role in the formation of amino acids and in the expression of the CCMs in marine algae (Raven and Beardall 2014), and increased nutrient uptake rate and assimilation by macroalgae. However, this depends on the availability of nutrients and the way in which they are utilized by alga (Zou and Gao 2010a, Xu et al. 2010). Gordillo (2001) observed an enhanced growth rate and N_i assimilation (nitrate uptake rate and NR activity) in *U. rigida* cultured at high [$CO_{2(aq)}$], while photosynthesis and protein soluble content decreased. Similarly, for *Hizikia fusiformis* and *Hypnea spinella* cultured under high [$CO_{2(aq)}$], an increase in growth and nitrogen assimilation (NO_3^- uptake rate and NR activity, and NH_4^+ uptake) was observed (Zou 2005, Suárez-Álvarez et al. 2012). The increase in N_i uptake and assimilation is probably associated with the high growth rate observed, as more nitrogen is required to support the higher growth under high $CO_{2(aq)}$. In contrast, high [$CO_{2(aq)}$] caused a decrease in N_i uptake and a change in the allocation of internal N compounds in *Gracilaria* sp. (Andria et al. 1999).The same pattern was observed for *G. tenuistipitata* (García-Sánchez et al. 1994), where NO_3^- uptake was lower at high [$CO_{2(aq)}$] than in the ambient treatment. Therefore, high [$CO_{2(aq)}$] may affect the growth and N metabolism of macroalgae in diverse ways, likely depending on the culture conditions (e.g. N_i availability) and on the internal N status of the algae (N-deplete or N-replete). However, the response of N metabolism to elevated CO_2 could be also species-specific.

1.3 Water motion

Water motion affects important environmental variables, which are biologically relevant to macroalgal communities, such as nutrient supply, light availability, herbivore activity, which often have direct influence on physiological processes of macroalgae such as resource acquisition (e.g. inorganic C and N), growth, photosynthesis and morphology, affecting indirectly their production (Kraemer and Chapman 1991, Hurd

2000, Koch et al. 2006). Therefore, water motion influences greatly the physiology and ecology of macroalgal species.

The effects of water motion on some physiological processes are directly related to the availability of resources that reach the thallus surface. At the surface of all submerged marine organisms, a thin layer of fluid forms, termed the viscous sub-layer (VSL), the thickness of which is greatly reduced under a turbulent flow (Hurd 2000). Within the VSL, the flow is laminar, and for organisms that have metabolic exchange across their surface (e.g. algae) a concentration gradient termed the diffusion boundary layer (DBL) or concentration boundary layer (CBL) is formed by the uptake or efflux of molecules by the organism (Wheeler 1980, Denny 1993, Hurd 2000). Thus, the transfer of mass (i.e. nutrients) to the organism's surface occurs across a concentration gradient. In a laminar flow, molecular diffusion is the only mechanism available for transferring substances down a concentration gradient whereas under a turbulent flow the transport of substances is mainly controlled by the turbulent eddies, which enhances the transfer of mass and momentum to the organism's surface (Denny and Wethey 2001). Therefore, the mass transfer of carbon, inorganic nitrogen or other essential nutrients under a laminar flow is in part regulated by the thickness of the DBL.

The thickness of the DBL determines the concentration gradient of those inorganic nutrients, and consequently determines the flux rates of delivery to the algae surface (Lesser et al. 1994). The thickness of the DBL is controlled by water motion (Wheeler 1980, Hurd et al. 1996). Fast flows around the seaweed cause a decrease of the DBL thickness, reducing the distance over which molecules travel, and thus metabolic processes can be enhanced. In slow flows, the flux of molecules to the thallus surface might be reduced by a thick DBL, which could limit metabolic processes (Hurd and Pilditch 2011, Hurd et al. 2014). Thus, important physiological processes of

seaweed may likely be limited by a reduction in the mass transfer of essential nutrients (e.g. CO_2, HCO_3^-, NO_3^-, NH_4^+) (Wheeler 1980, Koch 1994, Hurd 2000).

The DBL plays an important role in the diffusion of ions and molecules to/from the thallus surface. However, physiological processes may not only be affected by the reduced supply of inorganic nutrients or carbon across the DBL, but also by the accumulation of products (e.g. OH^- and O_2) released by the alga after a metabolic process, which may modify the pH within the DBL, affecting the rate of other physiological processes such as photosynthesis (Hurd 2000, Madsen et al. 1993). The seawater chemistry adjacent to the thallus surface could also be influenced by differently charged ions. Some studies have revealed that photosynthesis is negatively affected by the flow-dependent removal of O_2 from the organism's surface rather than by the influx of dissolved nutrients or molecules from seawater to thallus surface (Finelli et al. 2006). This means that under a slow flow, the accumulation of O_2 at the thallus surface might increase photorespiration, reducing the affinity of RuBisCO for CO_2. Similarly, Mass et al. (2010) suggested that the increase in photosynthesis in organisms such as coral, algae and seagrass during high-flow is not only due to the increase of dissolved substances to thallus surface, but also for enhancement of O_2 efflux from the organism to medium, increasing the affinity of RuBisCO for CO_2. Therefore, water motion should be considered as fundamental a factor as light and nutrients, which is capable of regulating processes such as photosynthesis, nutrient uptake rate and growth.

Furthermore, some metabolic processes may also alter the chemistry of seawater within the DBL (De Beer and Larkum 2001, Hurd 2000, Hurd et al. 2011, Beer et al. 2014). Processes such as calcification and respiration reduce the pH at the thallus surface, whereas photosynthesis increases it (Hurd et al. 2014). Those changes in pH at

the thallus surface of macroalgae affect the form of Ci source available: CO_2, HCO_3^- and CO_3^{2-}. Hurd et al. (2011) showed that the pH at the thallus surface of coralline seaweeds increased within the DBL during photosynthesis and decreased during dark periods. The same pattern was observed for *Gracilaria* sp. and *G. chilensis* (Gao et al. 1993). This trend was opposite to that of Ci concentration in the medium, where the highest values were found in the dark and associated with efflux of CO_2 (including CO_2 from respiration); the lowest were during the light period, associated with the consumption of photosynthetic inorganic carbon which exceeded the rate of dissolution of CO_2 into the seawater in equilibrium with the air (Gao et al. 1993). Furthermore, Beer et al. (2008) observed an increase in pH at the surface of *U. rigida* during light periods, but after 2-4 min of illumination pH decreased significantly within its DBL, indicating a light-dependent mechanism involving acidification, e.g. H^+ extrusion via an ATPase to facilitate the production of CO_2 by CA_{ext}. Thus, the mechanism of Ci utilization may also play an important role in pH changes at the macroalgal surface (Beer et al. 2008, Suárez-Álvarez et al. 2012, Hurd and Pilditch 2011, Gao et al. 1993).

There are other metabolic processes that also affect the pH within the DBL, such as N_i uptake. For example, when NH_4^+ is the N_i source, NH_4^+ assimilation contributes to the production of H^+ in the medium, whereas when NO_3^- is the N_i source, the NO_3^- uptake and assimilation yield OH^- (or influx of H^+) (Raven and De Michelis 1979, 1980, Fuggi et al. 1981). Therefore, NH_4^+ uptake might cause a decrease in pH within the DBL, whereas NO_3^- uptake might cause an increase in pH within the DBL. However, if NO_3^- and NH_4^+ are both available as N_i source and they are assimilated in a ratio of 2: 1 would give the synthesis of primary metabolites with production of neither excess OH^- nor excess H^+, hence the intracellular pH will be less perturbed (Stumm and Morgan 1981, Raven 1986, Raven 1991, Hurd 2000). Therefore, the fixation of C and

N_i assimilation, CO_2 and NH_4^+ respectively, are the major causes of net intracellular acidification. However, some authors have indicated that the effect of nutrient uptake on pH changes may be insignificant in comparison with utilization of Ci (Raven 1991, Gao et al. 1993, Suárez-Álvarez et al. 2012).

1.4 *Macrocystis pyrifera*

The giant kelp *Macrocystis pyrifera* (Linnaeus) C. Agardh (hereafter, *Macrocystis*) is widely distributed in the world, being present in both Northern and Southern hemispheres, localized mainly along the Pacific coast in the northeast, from Alaska to México, and in the southeast coasts of South America from Perú to Argentina, and in isolated regions of South Africa, Australia and New Zealand, and around most of the sub-Antarctic Islands to 60°S (van Tussenbroek 1989, Brown et al. 1997, Graham et al. 2007). This species grows in environments with different hydrodynamic regimes, from bays with slow water motion to sites with strong tidal currents and moderate wave exposure (Kain 1989, Graham et al. 2007, Hepburn et al. 2007).

In New Zealand, *Macrocystis* is restricted to cool waters, with temperatures between 13 and 17 ˚C during winter and summer months, respectively, and does not persist long in areas with temperatures > 18 ˚C for several days (Hay 1990). Its distribution is closely correlated to the Southland current, growing in southern and central open coastal waters, mainly along the east coast. It is also found in Campebell and Auckland Islands (Hay 1990, Brown et al. 1997). It tolerates a wide range of wave action, inhabiting in waves-exposed sites, but also in sheltered harbours, where it can form extensive beds in shallow waters (Hay 1990, Brown et al. 1997). In the South Island, the Otago coast has the largest quantities of *Macrocystis* around New Zealand, forming dense forests in outer coastal waters such as Karitane, Cornish head, Shag

Point, Moeraki and Kakanui, but also around shallow habitats and waves sheltered sites around the Otago Peninsula (Hay 1990, Brown et al. 1997).

The *Macrocystis* underwater forests play an important ecological role in the marine environment because they provide habitat, food, structure and protection for other species and are a classic an autogenic ecosystem engineer. For this reason *Macrocystis* is considered a foundation species (Graham et al. 2007). Due to their complex morphology, this species can modify its surroundings by altering biotic and abiotic properties of the environment. For example, the mechanical interaction of the kelp with flow can reduce the water motion or currents near and inside of the kelp forest as well as the irradiance which can be reduced to less than 5% of surface irradiance due to dense kelp canopies (Stewart et al. 2009, Foley and Koch 2010, Gerard 1984). Indeed, these large beds of kelp provide large amounts of nutrients, e.g. fixed carbon and nitrogen, to surrounding habitats due to their high rates of productivity (Graham et al. 2007, Fram et al. 2008, Rosman et al. 2007, Gaylord et al. 2007). They can also modify the surrounding SW chemistry due to physiological processes such as photosynthesis and respiration. Inside a kelp forest, pH fluctuates greatly during the day, reaching high values (9.11) and low values (7.92) during night time (Delille et al. 2000, Cornwall et al. 2013). These changes in pH modifies the proportion of each Ci source to the total DIC. Despite being an important macroalgal species, little is known about its Ci acquisition mechanisms, and on how this species will respond to the predicted changes in pH and SW carbonate chemistry predicted by the year 2100.

1.5 Objectives

Most OA studies have evaluated the effects of high [$CO_{2(aq)}$] and low pH on calcified organisms and on physiological processes such as calcification and photosynthesis.

However, little attention has been paid to determine the effects OA on non-calcifying organisms. *Macrocystis* has a very important ecological role in nearshore marine ecosystems. Therefore, how this species will respond to OA could have important consequences for associated organisms. As a first step to evaluate how populations of *Macrocystis* could be affected by OA, it is necessary to have a clear understanding of the functioning of the main physiological processes of the species. Therefore, the main goal of the present study was to examine the effects of OA on photosynthesis, growth, and carbon and nitrogen metabolism of *Macrocystis*.

The first part of this study was to elucidate the Ci acquisition mechanisms present in this species. The main mechanism for Ci utilization described in macroalgae is the external dehydration of HCO_3^- mediated by CA_{ext}. Therefore, in chapter 2 a literature review was conducted to determine the range of CA activities recorded in macroalgal species and evaluate the advantages and disadvantages of various extraction protocols used. After that an optimized assay for measuring external and internal CA activity in *Macrocystis* was developed.

In chapter 3, pH drift experiments were conducted to confirm that HCO_3^- is the main Ci source utilized by *Macrocystis*, and then the contribution of both CA_{ext} and direct HCO_3^- uptake via an AE protein to the photosynthetic Ci acquisition was examined with the aid of specific inhibitors to determine which is the main mechanism of Ci utilization in this species. In addition, as *Macrocystis* inhabits environments with naturally high fluctuations in pH (different HCO_3^-: CO_2 ratio), with a maximum *in situ* pH value of 9.11 and a minimum of 7.92, the contribution of each Ci acquisition mechanism (i.e. CA_{ext} and AE protein) to photosynthesis was determined at pH 9.00 (HCO_3^-: CO_2 = 940:1) and at pH 7.65 (HCO_3^-: CO_2 = 51:1). CA_{int} activity was also

measured to determine its role in photosynthesis, e.g. providing CO_2 to RuBisCO, after intracellular HCO_3^- conversion.

After determining the mechanisms for HCO_3^- utilization by this species, chapter 4 was focus on determining how changes in the carbonate system predicted for 2100, high [$CO_{2(aq)}$] and [HCO_3^-] but low pH will affect the photosynthetic performance, CA activities and growth of *Macrocystis* compared to today's conditions. *Macrocystis* blades were cultured for 7 days under a worst case scenario predicted by 2100 (OA treatment: pCO_2 1200 µatm; pH 7.59) and under today's conditions (ambient treatment: pCO_2 400 µatm; pH 8.00). At the end of the experiment the physiological parameters were compared between treatments. This chapter helped to determine whether external Ci concentrations are the main factor regulating photosynthesis and growth in this species.

Chapter 5 was focus on examining the interactive effects of OA and nitrogen status on the nitrogen physiology of *Macrocystis*, including NR activity, internal NO_3^- and NO_3^- uptake rates. Prior to assess the interactive effects OA and nitrogen status, the regulation of the N metabolism by external NO_3^- concentrations were determined. The effects of low and high NO_3^- availability on the NO_3^- uptake and assimilation (i.e. NR), and internal NO_3^- pools and total tissue N content were assessed. This work provided important information about the interaction between NO_3^- uptake and assimilation pathway, and how this species respond to different NO_3^- availability. After that, I determined how *Macrocystis* N status might affect the response of this species to OA, and the interactive effects of algae N status and OA on growth and photosynthesis. *Macrocystis* blades with different N status, N-deplete and N-replete, were obtained after a pre-experimental incubation under low and high NO_3^- concentrations. This work

provided important information about the interaction between the C and N metabolism in this species.

Chapter 6 was focus on determining how other physiological processes such as NO_3^- and NH_4^+ uptake and assimilation might modify the pH at the thallus surface within the DBL of *Macrocystis*. In addition, both of these processes involve fluxes of H^+/OH^- between the medium and the algae, and the effect of low pH (high $[H^+]$) (pH = 7.65) on NO_3^- and NH_4^+ uptake and assimilation was compared to today's conditions (pH = 8.00). To date the main physiological processes described in non-calcareous macroalgae modifying the pH at the thallus surface, within the DBL, are photosynthesis and respiration. Therefore, this chapter provided important new information about how other metabolic processes may contribute to the changes in pH within the DBL, which will be important under an OA scenario.

Finally, chapter 7 synthesized all the findings from the previous chapters and explain how *Macrocystis* might respond to OA. In addition, the interaction between C and N metabolism in *Macrocystis* was considered. Future directions on what we need to know about C and N metabolisms to predict macroalgal responses to OA was also discussed. Finally, the interactive effects of OA with other predicted environmental changes by the next century were discussed, highlighting the possible effects on *Macrocystis*, and the importance of including both local (e.g. eutrophication) and global environmental changes in our studies.

1.6 Academic papers

This thesis was conceived with the intension to make different aspects of the study as separate publishable chapters. In this regard, repetitions may be expected in different sections of each chapter, e.g., species ID and its ecological functions, and on the

environmental stress factor, i.e. ocean acidification, under investigation, among others. Chapters 3 and 4 were recently published (See below and table 1.1). In both publications, I primarily designed and performed the experiments, analyzed the data, and wrote the papers. My supervisors, Associate Prof. Catriona L. Hurd and Dr. Michael Y. Roleda, assisted in every aspect of the study and publication including providing advice on how to revise the manuscript based on the reviewer's comments. The format of these papers has been changed to that of the PhD, but they are otherwise the same as the published papers. The two chapters published (see Appendix 1 and 2 for the first page publication proof) are:

Chapter 3 published as:

Pamela A. Fernández, Catriona L. Hurd, Michael Y. Roleda (2014) Bicarbonate uptake via an anion exchange protein is the main mechanism of inorganic carbon acquisition by the giant kelp *Macrocystis pyrifera* (Laminariales, Phaeophyceae) under variable pH. *Journal of Phycology* 50:998–1008. DOI: 10.1111/jpy.12247.

Chapter 4 published as:

Pamela A. Fernández, Michael Y. Roleda, Catriona L. Hurd (2015) Effects of ocean acidification on the photosynthetic performance, carbonic anhydrase activity and growth of the giant kelp *Macrocystis pyrifera*. *Photosynthesis Research* 124:293–304. DOI: 10.1007/s11120-015-0138-5.

Chapter 2 has been submitted for publication and is currently 'under revision'. As for Chapters 3 and 4, my supervisors advised on the preparation of the manuscript for submission (see table 1.1). The thesis chapter 2 is very similar to the submitted manuscript, with a few changes to the methodology that were based on reviewer's comments.

Pamela A. Fernández, Michael Y. Roleda, Ralf Rautenberger, Catriona L. Hurd. Carbonic anhydrase activity in seaweeds: method overview and recommendations for

assay optimization using the giant kelp *Macrocystis pyrifera*. It has been submitted to the *Journal of Phycology*.

Chapters 5 and 6 have been written as thesis chapters, and a target journal has not been decided upon. In these chapters, my supervisors provided feedback on experimental design, data analyses and chapter structure and content, but have made little editorial contributions beyond the grammar.

Table 1.1: Thesis chapters (Chp), paper titles, authorship and candidate contribution, target journal and current publication status for each of the three journal articles produced for this thesis.

Chp	Paper title	Authors	Contribution of the candidate	Journal	Status
2	Carbonic anhydrase activity in seaweeds: method overview and recommendations for assay optimization using the giant kelp *Macrocystis pyrifera*	Fernández Roleda Rautenberger Hurd	Performed the literature review and designed the experiments, analyzed the data, and wrote the paper. Co-authors provided guidance on every aspect of the study	Journal of Phycology	Under revision
3	Bicarbonate uptake via an anion exchange protein is the main mechanism of inorganic carbon acquisition by the giant kelp *Macrocystis pyrifera* (Laminariales, Phaeophyceae) under variable pH	Fernández Hurd Roleda	Designed and performed the experiments, analyzed the data, and wrote the paper. Co-authors provided guidance on every aspect of the study	Journal of Phycology	Published
4	Effects of ocean acidification on the photosynthetic performance, carbonic anhydrase activity and growth of the giant kelp *Macrocystis pyrifera*	Fernández Roleda Hurd	Designed and performed the experiments, analyzed the data, and wrote the paper. Co-authors provided guidance on every aspect of the study	Photosynthesis Research	Published

Signed by all authors as follows:

Pamela A. Fernández 

Ralf Rautenberger 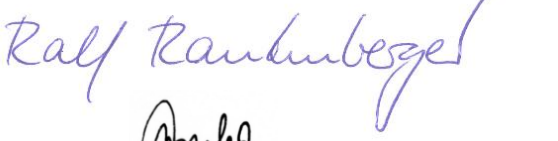

Michael Y. Roleda 

Catriona L. Hurd 

Date: 15 June 2015

Chapter 2: Carbonic anhydrase activity in seaweeds: method overview and recommendations for assay optimization using the giant kelp *Macrocystis pyrifera*

2.1 Introduction

Carbonic anhydrase (CA) is a ubiquitous metalloenzyme that catalyzes the interconversion of CO_2 and HCO_3^-: $H_2O + CO_2 \leftrightarrow H^+ + HCO_3^-$, which can use both zinc or cadmium as a catalityc metal (Young et al. 2008). The presence of CA is ubiquitous among eukaryotes and prokaryotes, having been reported in terrestrial plants, algae, animals and bacteria (Waygood 1955, Bowes 1969, Weaver and Wetzel 1980, Badger and Price 1994). The uncatalyzed interconversion between inorganic carbon (Ci) species proceeds slowly, and so CA is essential to accelerate the formation of either CO_2 or HCO_3^- (Sültemeyer et al. 1990). The reversible catalyzed hydration of CO_2 is fundamental to many physiological and metabolic processes such as photosynthesis and respiration, and pH homeostasis (Sharma et al. 2009). In algae, as in terrestrial plants, CA permits the rapid formation of the Ci substrate for photosynthesis (Surif and Raven 1989, Raven 1995).

The crucial role of CA in algae was not clearly established in the early research articles of the 1960-1970s, but it was presumed to be related to photosynthesis, being involved in the uptake and fixation of CO_2 (Graham et al. 1971, Graham and Smillie 1976). Later studies described two forms of CA: external CA (CA_{ext}), usually located on the cell surface of the alga, and internal CA (CA_{int}) located in the cytosol and/or chloroplast, depending on the species (Bowes, 1969, Graham and Smillie 1976, Tsuzuki et al. 1984, Miyachi et al. 1983, Cook et al. 1986, 1988, Surif and Raven 1989, Giordano and Maberly 1989). CA_{ext} increases the steady-state CO_2 concentration at the

membrane surface after the conversion of HCO_3^- to CO_2 especially at an 'average' seawater (SW) pH of ~8.07 where most of the Ci exists as HCO_3^- (Bowes 1969, Miyachi et al. 1983, Tsuzuki 1983). CA_{int} plays an important role in maintaining internal Ci pools, cellular pH homeostasis and in dehydrating HCO_3^- to supply CO_2 to RuBisCO (Graham et al. 1984, Tsuzuki and Miyachi 1989, Sültemeyer et al. 1990). This early research triggered interest in the mechanisms of Ci acquisition by marine algae. However, in the following decades, a wide range of protocols were developed, making it difficult to compare CA activity between algal species.

The reaction catalyzed by CA has been extensively studied using CA from animal sources, including humans. Therefore, is not surprising that the first methods utilized for measuring CA activity in algae were adapted from methods originally described for animals. In early studies (1940s-1950s), three main categories of method were described for measuring CA activity in animals: manometric, colorimetric and electrometric. In the manometric methods, CA activity is determined either by the rate of CO_2 produced from the dehydration of HCO_3^- when a HCO_3^- solution is shaken with a phosphate buffer (pH 6.6–6.8) and enzyme or by the increased rate of CO_2 uptake when gaseous CO_2 is shaken with a Veronal buffer (pH 8.0) and enzyme (Roughton and Booth 1946, Waygood 1955, Datta and Shepard 1959). In the colorimetric and electrometric methods, CA activity is determined by the hydration of CO_2, measured by the rate of pH shift using either indicators (i.e. phenol red or bromothymol blue) or pH electrodes, respectively (Wilbur and Anderson 1948, Waygood 1955, Datta and Shepard 1959). In both the colorimetric and electrometric methods, a cold saturated solution of CO_2, which acts as substrate for CA, is mixed with an alkaline buffer (i.e. 0.02 M Veronal, pH 7.95-8.15) at 0 ˚C. After the addition of CO_2 the pH drops rapidly because of the reaction catalyzed by CA: $CO_2 + OH^- \rightarrow HCO_3^- + H^+$ accompanied and followed

by the hydration of CO_2. The hydration of CO_2 is usually measured in a pH range from 8.0 to 6.3 in the uncatalyzed and catalyzed reactions. In an uncatalyzed reaction the rate of pH shift usually takes 100 to 120 sec whereas in a catalyzed reaction might takes half of that time (50–70 sec) (Wilbur and Anderson 1948). The latter two methods were the most commonly used in the first studies of measuring CA in micro- and macroalgal species (Nelson et al. 1969, Bowes 1969, Atkins et al. 1972, Graham and Smillie 1976).

Bowes (1969) was the first to use the electrometric method on macroalgae, and described the presence of CA in ten macroalgal species, including the giant kelp *Macrocystis pyrifera* (Linnaeus) C. Agardh (from California, USA); prior to this, CA was reported in the green macroalga *Ulva pertusa* Kjellman, but the activity was measured using the manometric method (Ikemori and Nishida 1968). These first studies in macroalgae found that CA activity was not inhibited by sulfhydryl inhibitors, but might be strongly inhibited by sulfonamides, which are known to be specific inhibitors for animal CA (Krebs and Roughton 1948, Kernohan 1965, Ikemori and Nishida 1968, Bowes 1969, Okazaki 1972). These findings suggested that CA in macroalgae might have a greater similarity with the animal enzyme than with terrestrial plants for which little or no inhibition by sulphanilamide was found (Ikemori and Nishida 1968). Therefore, the effects reported from early studies on CA from animals such as the influence of pH on the stability of the enzyme, effect of substrate concentration and type of buffer on CA activity (Roughton and Booth 1946, Datta and Shepard 1959, Kernohan 1965) may also affect CA activity in macroalgae. However, recent studies have shown that there are six types of CAs so far found in living organisms, and they are categorized from α to ζ (Matsuda and Kroth 2014 and references therein). Therefore, some forms of CAs found in algae may be similar to the animal ones (e.g. α-CAs) and some may be more similar to the higher plants ones (e.g. γ-CAs).

The electrometric method described by Wilbur and Anderson (1948) has been widely used for measuring CA in macroalgae; however many modifications have been included. For example, the hydration of CO_2 reaction has been measured at different pH ranges, i.e. 8.2-6.3, 8.5-7.5 and 8.2-7.8; also different buffers and reaction volumes have been used; and the method has also been adapted for measuring CA_{ext} (Cook et al. 1986, Cook et al. 1988, Surif and Raven 1989, Giordano and Maberly 1989, Haglund et al. 1992b, Mercado et al. 1997a, b). These modifications might affect directly CA activity, making the results not comparable between studies. Indeed, some studies have reported problems with the accuracy of the assay, indicating that the temperature dependence of the reaction as well as errors in the pH measurements contribute to the lack of accuracy of the method (Mercado et al. 1997a, van Hille et al. 2014). However, even though the electrometric method might present some disadvantages, and other methods have been developed to estimate CA activity in algae, e.g. mass spectroscopy, modified pH drift experiment and use of CA-specific inhibitors (Mercado et al. 1997a, van Hille 2001, van Hille et al. 2014), the electrometric method is still the most used for measuring CA in macroalgal species.

Interest in CA activity (CA_{ext} and CA_{int}) in marine algae has increased substantially in recent years because of the predicted changes in the seawater chemistry by the year 2100 due to ocean acidification (OA). By 2100, the average surface SW pH is predicted to decrease by 0.3-0.4 pH units with a corresponding 200% and 14% increase in CO_2 and HCO_3^-, respectively (The Royal Society 2005, IPCC 2013). These changes in pH and SW carbonate chemistry affect algal carbon metabolism (Hurd et al. 2009). An increasing number of studies have focused on determining the mechanisms involved in Ci utilization (Zou and Gao 2004, Zou and Gao 2009, Zou and Gao 2010b, Moulin et al. 2011, Zou et al. 2011a, Zou et al. 2011b, Olischläger and Wiencke 2013),

including determinations of CA activity in different algal species (Zou et al. 2003, Zou et al. 2004, Zou and Gao 2010ab, Hofmann et al. 2012, 2013). However, due to the diverse protocols developed for measuring CA and the variability found between algal species, the results between studies are mostly not comparable. Furthermore, most studies use 'standard assay conditions', taken from literature, and do not optimize the CA assay including extraction buffers, substrate concentration or buffer properties for each species being tested.

Macrocystis pyrifera (Linnaeus) C. Agardh (hereafter, *Macrocystis*), is widely distributed along the northeast Pacific coast from Alaska to Mexico, the east and west coasts of South America, in isolated regions of South Africa, Australia and New Zealand, and with an isolated population in the sub-Antarctic islands and has an important role in coastal regions as an ecosystem engineer (Steneck et al. 2002; Graham et al 2007). Despite its ecological importance, little is known about its mechanisms of Ci acquisition until recently described by Fernández et al. (2014). Bowes (1969) was the first to determine the presence of CA in *Macrocystis*; thereafter some studies reported the total CA activity, using the electrometric method described by Wilbur and Anderson (1948), modified by Haglund et al. (1992a) (Huovinen et al. 2007, Rothäusler et al. 2011). However, because the protocols used in previous studies were not the same, the results are not comparable (Bowes 1969, Huovinen et al. 2007, Rothäusler et al. 2011). Although all three studies used the electrometric method, there are differences in the types of buffer, reaction time and the extraction procedure, each of which could potentially affect CA activity. The aims of our study were: (1) conduct a literature search to determine the range of CA activities recorded in macroalgal species and evaluate the advantages and disadvantages of the various protocols used, (2) experimentally evaluate the effects of different type of buffers, other components in the

buffer and the reaction time (rate of pH shift) on the relative CA activity measured in *Macrocystis*, and (3) develop an optimized protocol for external and internal CA activity in *Macrocystis*.

2.2 Materials and Methods

2.2.1 Literature review

The literature search was conducted using the electronic database of Science Direct (http://www.sciencedirect.com/). The publications were mainly filtered using the keywords: carbonic anhydrase, macroalgae, electrometric method described by Wilbur and Anderson (1948). However, some key publications using the colorimetric method were also included. A total of 52 research publications on CA in macroalgae were reviewed (from 1960-present) to assess the assay, compare the CA values obtained and determine the coefficient of variation (% CV) reported in each study.

2.2.2 Seaweed collection

Adult *Macrocystis* sporophytes were collected during low tide from the upper subtidal in Aromoana (45°47'S, 170°43'E), Otago Harbour, New Zealand between October 2012 and March 2013. From different individual sporophytes (n = 11), young blades, i.e. the first pneumatocyst-bearing lamina below the apical scimitar, were removed. Blades were kept moist and dark inside an insulated container for transport to the laboratory, 20 minutes away. In the laboratory, blades were gently cleaned of any visible epiphytes and rinsed with filtered natural seawater (NSW) (0.5 µm pore size).

For CA assay optimization, 0.8-1.0 g tissue, excised 2 cm above the base of the blade was used (meristematic region). Tissue was frozen in liquid N_2 and ground to a fine powder using chilled mortar and pestle. Sub-samples each weighing 0.06-0.08 g were used to optimized CA assay protocol described below.

After protocol optimization, the precision of the method was determined using different individual *Macrocystis* sporophytes (n = 7); a disc of 0.06-0.08 g was excised

from each individual of *Macrocystis* blades. Disc was frozen in liquid N_2 and separately stored at –80 °C for one week until subsequent analyses of total, external and internal CA activities.

2.2.3 Assay optimization

The protocol for measuring total CA activity (CA_{ext} plus CA_{int}) in *Macrocystis* was optimized using a modified version of the electrometric method described by Wilbur and Anderson (1948) (Graham and Smillie 1976, Haglund et al. 1992a, Table 2.1). A step-wise optimization was followed: (1) the type of buffer (Table 2.2); (2) the molarity of the optimal buffer; (3) the different components in the optimal buffer (Table 2.3); (4) the pH range at which the hydration of CO_2 reaction is measured.

The three buffers commonly used in CA studies are Veronal, Tris and phosphate (see Table 2.1). However, Veronal buffer is difficult to obtain because of its hypnotic drug properties. Therefore, Tris-HCl and phosphate (Na_2HPO_4/NaH_2PO_4) were selected to determine the effect of different buffers on CA activity in *Macrocystis*. For these analyses the reaction time used was selected according to Giordano and Maberly (1989) and Haglund et al. (1992a), because they were used in a wide range of macroalgae species. Polyvinlpyrrolidone (PVP) and ditiothreitol (DTT) were incorporated into the buffers (Table 2.3) to prevent interference by brown seaweed phenolic compounds and to avoid oxidation of the extract: PVP absorbs polyphenols and DTT prevents the irreversible oxidation of the protein thiols structure (Graham and Smillie 1976, Hurd et al. 1995). The molarity of phosphate buffer was increased to 200 mM as recommended for another enzyme assay, i.e. nitrate reductase (Hurd et al. 1995), because using 25 mM, pH dropped substantially from 8.3 to 7.4 after the additions of PVP, DTT and Na-EDTA (data not shown).

To determine the sensitivity of the buffer and effects on the reaction times, CA activity was first measured using purified CA from bovine erythrocytes (C3934, Sigma-Aldrich, St Louis, MO, USA). The activity of purified CA, expressed as Wilbur-Anderson units (WA), was insensitive to different buffers, exhibiting comparable activity with either Tris-HCl or phosphate buffers, but longer uncatalyzed reaction times were observed using Tris-HCl than phosphate buffer.

CA activity was then measured using *Macrocystis* sub-samples. Frozen ground sub-samples (0.06 ± 0.02 g) were individually transferred into a 20 mL chilled glass vial, containing 10 mL of the extraction buffer (0-2˚C), either 200 mM phosphate (pH 8.3; n = 8) or 100 mM Tris-HCl (pH 8.5; n = 6). The ratio of algal fresh weight (FW, in g) to volume of buffer (in mL) of 0.006:1 was selected to give the highest CA activities according to a preliminary experiment. Each chilled glass vial, containing the algal sample and the extraction buffer, was vortex mixed for 20 s. To keep the extraction buffer temperature within the range (0-2˚C), the sample was dipped in ice for 5 s, for every 10 s vortex mixing. Thereafter, the temperature of the ice-cold extract was kept constant by sitting on ice and continuously stirred at 900 rpm, using a micro stirrer bar (10 × 3 mm), for the duration of the enzymatic reaction. Temperature and pH were simultaneously measured using a ROSS electrode (Orion 8107BNUMD) coupled to Orion 3-Stars Plus pH Benchtop meter (Orion, Thermo Scientific, San Jose, CA, USA). When pH stabilized at 8.3, the reaction was started by adding 5 mL of ice-cold CO_2-saturated MilliQ water (pH = 4.05-4.55). The time taken for the pH to drop by 0.4 units, from 8.3 to 7.9, was recorded.

The CO_2-saturated ultrapure MilliQ water (18.3 MΩ cm) was prepared by bubbling with pure CO_2 1 h before the assay, and kept cold on ice. During the assay, a sustained slow CO_2 bubbling through a rubber tubing into the rubber-stopper sealed 250

mL glass flask was maintained to keep a CO_2-saturated MilliQ water. The 5 ml of CO_2-saturated water was collected through a glass syringe, connected to another line of rubber tubing through the rubber stopper. The pH of the solution was monitored throughout the experiment.

The relative enzyme activity (REA) was determined using equation 1:

$$REA = (T_b/T_s) - 1 \qquad \text{(eq. 1)}$$

where T_b and T_s are the times in seconds required to drop by 0.4 pH units in the uncatalyzed extraction buffer (T_b, without algae) and in the enzyme-catalyzed reaction of the sample (T_s), respectively. The REA was standardized to the sample's fresh weight (REA g^{-1} FW).

The use of Tris-HCl buffer resulted in higher total CA activities compared to the phosphate buffer (see Results). Thereafter, the molarity of, and the components in, the Tris-HCl buffer were further optimized for the 2nd and 3rd step of the optimization process, respectively. Both the 50 mM and the 100 mM Tris-HCl buffers (pH 8.5) resulted in similar CA activities (see Results). A 50 mM Tris-HCl buffer was used for the 3rd step optimization because it was the most used in previous studies. For the 3rd step of optimization, different components, e.g. DTT, PVP, EDTA, AA were included or excluded from the buffer (see Table 2.3). Several tests showed that Buffer III (50 mM Tris-HCl, pH 8.5, containing DTT, PVP, Na-EDTA and AA, Table 2.3) resulted in the lowest coefficient of variation (% CV; see result) and this was used for the 4th step of the optimization process, i.e. the pH range at which the reaction time is recorded.

For the 4th step of the optimization process, two of the most commonly used pH ranges were selected, i.e. the time taken for a linear pH drop by: (1) 0.4 units from pH 8.3 to 7.9 (Reiskind et al. 1988, Giordano and Maberly 1989, Haglund et al. 1992a,

Mercado et al. 1999, 2001, 2002, Table 2.1) and (2) 1.0 unit from 8.3 to 7.3 (Mercado et al. 1997b, 1998, Gómez et al. 1998, Kevekordes et al. 2006, Table 2.1). The pH range 8.3-7.9 was optimal (see results) and used for the subsequent analyses (the same used in previous determinations).

2.2.4 External and internal CA activity

After the protocol for measuring total CA was optimized, CA_{ext} and CA_{int} activity were measured using the optimized method described above. From seven blades, each from an individual *Macrocystis* sporophyte, one disc of 0.074 ± 0.001 g FW was excised; the same disc was used for both CA_{ext} and CA_{int} measurements, and the total CA activity was calculated from the sum of CA_{ext} and CA_{int}. A preliminary experiment showed no statistical differences between total CA activity measured from one disc (14.05 ± 3.46 REA g^{-1} FW, n = 4) and calculated from the sum of the two CAs (5.28 ± 2.04 REA g^{-1} FW CA_{ext} + 10.01± 1.34 REA g^{-1} FW CA_{int}, n = 4) (Student's t-test, t = –0.902, df = 7, P = 0.397).

For CA_{ext} measurements, whole frozen discs (average weight= 0.074 ± 0.001 g FW) were individually rinsed with MilliQ water (0-2 ˚C) for 10 s and transferred into a 20 mL glass vial, containing 10 mL of extraction buffer. The enzymatic reaction was started by adding the CO_2-saturated MilliQ water. The CA activity was measured by recording the reaction time required to lower the pH by 0.4 units as optimized above.

After CA_{ext} had been extracted and assayed, each disc was ground to fine powder and used for measuring CA_{int} activity; the activity detected account only for CA_{int} as CA_{ext} was measured before to ground the disc. Individually pre-chilled vials were used for each measurement to avoid interference with the subsequent CA measurements.

CA activities measured using the optimized protocol were compared with the first results obtained using the standard, but non-optimized protocol. The % CV between samples was compared.

2.2.5 Statistical analyses

The effect of each variable evaluated on the CA assay was separately tested using analysis of variance (ANOVA, $P < 0.05$) or Student's t-test ($P < 0.05$) after both homogeneity of variance (Levene's test) and normal distribution (Shapiro-Wilk W-test) were satisfied. Significantly different groups were classified after Tukey's HSD post-hoc test ($P = 0.05$). All analyses were performed using the statistical software SigmaPlot version 11.0 (Systat Software, Inc., San Jose, CA, USA).

Table 2.1 Carbonic anhydrase (CA) assays based on the electrometric method 'Wilbur and Anderson 1948' used for measuring CA in macroalgae.

no.	Described by	Buffer properties									Reaction time		Adapted by
		Buffer	Molarity (mM)	pH	PVP (%w/v)	DTT (mM)	EDTA (mM)	AA (mM)	BSA (%w/v)	TX (%v/v)	pH ranges	pH units	
1	Wilbur and Anderson 1948	[1]Veronal	30/34[a]	8.1/8.6[a]	–	–	–	–	–	–	8.0–6.3	1.7/0.4[a]	Graham and Smillie 1976 Surif and Raven 1989 Haglund et al. 1992b[a]
2	Bowes 1969	[1–2]K_2HPO_4	4	7	–	–	–	–	–	–	7.0–5.0	2	–
3	Atkins et al. 1972	[1]Veronal	25	8.2	–	–	–	–	–	–	8.0–6.3	1.7	Graham and Smillie 1976
		[2]Tris–borate	100	8.3	–	100[c]	1		–	–			
4	Graham and Smillie 1976	[1]Veronal	25	8.2	–	–	–	–	–	–	8.0–6.3	1.7	Surif and Raven 1989
		[2]Tris–borate	300	8.3	2[b]	25	5		0.5	0.1			
5	Miller and Colman 1980	[1]K_2HPO_4	25	8.36	–	–	–	–	–	–	8.3–7.8	0.5	Cook et al. 1986 Giordano and Maberly 1989

6	Ramazanov and Semenko 1988	[1–2]Tris	50	8.5	–	15	5	25	–	–	‡	0.4	Björk et al. 1992
7	Giordano and Maberly 1989	[1]K_2HPO_4	25	8.36	–	–	–	–	–	–	8.2–7.8	0.4	Axelsson et al. 1995
		[2]Tris–borate	300	8.3	2[b]	25	5	–	0.5	0.1			Zou et al. 2004 Zou and Gao 2010ab
8	Haglund and Pedersén 1992	[1] Veronal	18	8.2	–	–	–	–	–	–	‡‡	0.1–0.2	Andría et al. 2000, 2001
		[2]Tris	50	8.5	20[b]	25[c]	5	25	–	–			
9	Haglund et al. 1992	[1–2]Tris	50	8.5	–	25	5	25	–	–	‡	0.4	García and Sanchez 1994 Mercado et al. 1999 Zou et al. 1993 Hofmann et al. 2012ab
10	Haglund et al. 1992 modified	[1–2]Tris	100	8.5	–	–	5	25	–	–	††	0.4	Mercado et al. 1997a
		[1–2]Tris	50	9.0	–	–	5	25	–	–	8.5–7.5	1.0	Mercado and Niell 1999 Mercado et al. 2000 Mercado et al. 2001 Mercado et al. 2002 Mercado et al. 1997b Mercado et al. 1998 Gómez et al. 1998 Flores–Moya et al. 1998

													Figueroa and Viñegla 2001 Gordillo et al. 2006 Viñegla et al. 2006
		[1–2]Tris	50	9.0	–	–	5	25	–	–	8.5–8.1	0.4	Huovinen et al. 2007 Rothäusler et al. 2011
11	Current study	[1–2]Tris	50	8.5	0.3	2	5	20	–	–	8.5–8.1	0.4	Fernández et al.

[1]: Buffer used as an assay buffer during CA measurements (CA_{ext} and/or CA_{total})
[2]: Buffer used as extraction buffer for total CA extraction; and also used as assay buffer.
[b]: Polyclar AT (insoluble PVP); [c]: Mercaptoethanol
†: Colorimetric assay
‡: drop of 0.4 pH units measured within the pH ranges from 8.1 to 7.1 or from 8.1 to 7.4 ††
‡‡: drop of 0.1–0.2 pH units measured within of a pH range between 8.6–8.0
Abbreviations: AA: Ascorbic acid; BSA: Bovine serum albumin; TX: Triton X–100.

Table 2.2: Extraction buffers tested in the carbonic anhydrase (CA) assay of *Macrocystis.*

Buffer	Concentration (mM)	pH	PVP (% w/v)	DTT (mM)	Na–EDTA (mM)	Ascorbic acid (mM)
Phosphate	200	8.3	0.3	2	5	–
Tris-HCl	100	8.5	0.3	2	5	20

Table 2.3: Components incorporated in a 50 mM Tris–HCl (pH 8.5) extraction buffer to evaluate their effects on the carbonic anhydrase (CA) assay of *Macrocystis.*

Medium	DTT (mM)	PVP (% w/v)	Na–EDTA (mM)	Ascorbic acid (mM)
Buffer I	–	–	5	15
Buffer II	–	0.3	5	15
Buffer III	2	0.3	5	15

2.3 Results

2.3.1 Literature review

The most common method used among the reviewed articles was the electrometric, with modifications by subsequent authors (Table 2.1). Most of the articles detected CA activity in the macroalgal species investigated (except by Cook et al. 1986, 1988 and some species investigated by Giordano and Maberly 1989). Three main steps for determining total CA activity were identified: (1) extraction of total CA, where fresh algal material is ground with a specific buffer, known as the 'extraction buffer', (2) centrifugation of the algal extract and collection of the supernatant, and (3) measurement of the total CA activity from the supernatant (0.1 mL) using an 'assay buffer' (15 mL) also termed 'sample buffer' by some authors, which is usually different to the extraction buffer (Atkins et al. 1972, Graham and Smillie 1976, Giordano and Maberly 1989, Björk et al. 1992, Haglund and Pedersen 1992). However, over the years the extraction procedure described by Wilbur and Anderson (1948) was gradually changed. For example, in some studies the centrifugation step was removed from the assay and the total CA activity was determined directly from crude extracts, obtained after grinding the fresh algal tissue with N_2 liquid and the extraction buffer (Björk et al. 1993, Mercado et al. 1997b, 2000, Huovinen et al. 2007, Table 2.1). In some cases, the extraction buffer was also used as the sample buffer (Ramazanov and Semenko 1988, Haglund et al. 1992a, Table 2.1). Furthermore, this method, originally developed for total CA measurements, was later adapted for the estimation of CA_{ext} activity, incorporating algal pieces into a sample buffer. Finally, different sample buffers were identified between studies, and total CA and CA_{ext} activities and the coefficient of variation were registered from each study (Tables 2.4 and 2.5).

Table 2.4: Total carbonic anhydrase (CA) activity and the coefficient of variation (% CV) registered in each study.

Phylum	no. of species	Total CA range	Total CA units	Range of % CV	Reference	Method used
Chlorophyta	4	0.061–0.303	REA?/mg^{-1} protein	No inf.	Bowes 1969	2
	13	62–3400	EU/mg chlorophyll	No inf.	Graham and Smillie 1976	1–3
	2	187.0–194.2	EU/mg chlorophyll	2.67–10.85%	Reiskind et al. 1988	4–Hogetsu & Miyachi 1976
	6	(-)76–2308	EU/g^{-1} FW	6.90–137.5%	Giordano and Maberly 1989	4–5
	1	5	REA/ g^{-1} FW	10%	Björk et al. 1992	6
	3	ND–13.4	REA/ g^{-1} FW	24%	Björk et al. 1993	1–6
	1	31	REA/ g^{-1} FW	21.30%	Gómez et al. 1998†	10
	1	6.5	REA/ g^{-1} protein	10.61%	Andria et al. 2001	8
	1	2.5	REA/ mg^{-1} SP protein	20.00%	Mercado et al. 2003†	1–10
	1	140	REA/ g^{-1} FW	28.60%	Figueroa and Viñegla 2001	10
	1	25	REA/ g^{-1} FW	12.00%	Viñegla et al. 2006	10
	4	100–150	REA/ g^{-1} FW	7–30%	Huovinen et al. 2007	10
Ochrophyta	2	0.004[b]–0.11	REA?/mg^{-1} protein	No inf.	Bowes 1969	2
	3	442–1110	EU/mg chlorophyll	No inf.	Graham and Smillie 1976	1–3
	10	114–1407	EU/mg chlorophyll	11.64–69.50%	Surif and Raven 1989	1–4
	12	(-)88–3111	EU/g^{-1} FW	3.328%	Giordano and Maberly 1989	4–5
	1	500	REA/ g^{-1} FW	5%	Figueroa and Viñegla 2001	10
	1	344.2[a]	REA/ g^{-1} FW	27.86%	Zou et al. 2003	9
	1	215	EU/mg chlorophyll	26.00%	Zhang et al. 2006	Israel et al. 1999
	1	250	REA/ g^{-1} FW	48.00%	Viñegla et al. 2006	10
	6	70–120[b]	REA/ g^{-1} FW	3–30%	Huovinen et al. 2007†	10

	1	134.4	EU/ g^{-1} FW	14.30%	Zou and Gao 2010a	7
	1	41.8	EU/ g^{-1} FW	45%	Zou and Gao 2010a	7
	1	15–85[b]	REA/ g^{-1} FW	%	Rothäusler et al. 2011†	1–10
Rhodophyta	4	0.151–0.294	REA?/mg^{-1} protein	No inf.	Bowes 1969	2
	7	201–4800	EU/mg chlorophyll	No inf.	Graham and Smillie 1976	1–3
	16	40–3269	EU/g^{-1} FW	5.5–37.5%	Surif and Raven 1989	1–4
	1	1.76	Relative to the blank	10.20%	Israel and Beer 1992	Beer and Israel 1990
	1	1.2	REA/ mg^{-1} protein	No inf.	Haglund et al. 1992a	9
	1	0.2	REA/ mg^{-1} protein	No inf.	Haglund and Pedersen 1992	1
	1	40.09	REA/ g^{-1} FW	15%	Mercado et al. 1997b	10
	1	2.05	Relative to the blank	17.10%	Israel and Friedlander 1998	No Inf. (5mM Tris buffer)
	1	200	REA/ g^{-1} FW	45%	Flores and Moya 1998†	10
	1	138	REA/ g^{-1} FW	2.12%	Mercado and Niell 1999	10
	1	1.36	Relative to the blank	12.50%	Israel et al. 1999	5 mM Tris buffer (8.0–6.5)
	1	1.61	REA/ mg^{-1} protein	40.37%	Mercado et al. 2000	10
	1	12.3	REA/ g^{-1} protein	4.22%	Andria et al. 2001	8
	3	11.16–20.12	REA/ g^{-1} FW	12.9–69.0%	Mercado et al. 2001	10
	1	150	REA/ g^{-1} FW	16.70%	Figueroa and Viñegla 2001	10
	1	24.4	REA/ g^{-1} FW	29.50%	Mercado et al. 2002	10
	1	75.6	REA/ g^{-1} FW	34.00%	Zou et al. 2004	7
	12	40–160	REA/ g^{-1} FW	9.10–50.0%	Huovinen et al. 2007†	10
	1	43.75[a]	REA/ g^{-1} FW	3.20%	Xu and Gao 2009†	7
	1	43.42	REA/ g^{-1} FW	4.20%	Hofmann et al. 2012	9

† SD and Means estimated from the graph; for method used see table 2.1; Formulas: EU = ((Tb/Te) –1) x 10); REA = (Tb/Te) –1
ND: activity no detected; No inf.: information no given in the article; [a]: REA units x 10; [b]: Study in *Macrocystis pyrifera*

Table 2.5: External carbonic anhydrase (CA) activity and the coefficient of variation (% CV) registered in each study.

Phylum	Species (n)	External CA range	External CA units	Range of % CV	Reference	Method used
Chlorophyta	6	(-)2.4–15.2	EU/g^{-1} FW	32.7–340.0%	Giordano and Maberly 1989	4–5
	1	1.12	Not specified	18.75	Beer and Israel 1990	25 mM Tris buffer
	1	4	REA/ g^{-1} FW	27.50%	Björk et al. 1992	1–6
	3	ND–1.2	REA/ g^{-1} FW	141.7–200.0%	Björk et al. 1993	6
	1	35.8	EU/g^{-1} FW	15.10%	Axelsson et al. 1995	7
	6	(-)0.2–3.76	REA/ g^{-1} FW	5.3–114.7%	Mercado et al. 1997a	10
	6	(-)1.83–19.22	REA/ g^{-1} FW	18.2–81.8%	Mercado et al. 1998	10
	1	17.86	REA/ g^{-1} FW	13.57%	Andría et al. 2001	8
	5	9.7–59	REA/ g^{-1} FW	1.4–23.7%	Gordillo et al. 2006	10
	8	4–30	REA/ g^{-1} dry WT	No inf.	Kevekordes et al. 2006	1–Miyachi 1983
Ochrophyta	2	ND	–	–	Cook et al. 1986	5
	10	21–95	EU/mg chlorophyll	11.6–47.7%	Surif and Raven 1989	1
	12	(-)3.9–11.5	EU/g^{-1} FW	17.9–2300.0%	Giordano and Maberly 1989	4–5
	2	2.2–3.2	REA/g^{-1} FW	38.6–44.2%	Haglund et al. 1992b	1
	3	0.15–6.18	REA/ g^{-1} FW	18.8–146.7%	Mercado et al. 1997a	10
	5	0.08–3.16	REA/ g^{-1} FW	11.0–2800%	Mercado et al. 1998	10
	1	7.3	REA/ g^{-1} FW	11.00%	Flores-Moya and Fernández 1998	9
	1	17.3[a]	REA/ g^{-1} FW	19.10%	Zou et al. 2003	
	9	8.4–32.0	REA/ g^{-1} FW	2.4–36.9%	Gordillo et al. 2006	10
	1	43	EU/mg chlorophyll	14.80%	Zhang et al. 2006	Israel et al. 1999
	1	15.8	EU/ g^{-1} FW	31.60%	Zou and Gao 2010a	7
	1	11.6	EU/ g^{-1} FW	37.10%	Zou and Gao 2010b	7

Rhodophyta	15	ND	–	–	Cook et al. 1986	5
	4	ND	–	–	Cook et al. 1988	1–5
	16	(-)71.6–62.5	EU/g^{-1} FW	37.8–1300.0%	Giordano and Maberly 1989	1–4
	1	1.25	No specified	8%	Israel and Beer 1992	Beer and Israel 1990
	1	0.5–1.5	REA/g^{-1} FW	No inf.	Haglund et al. 1992a	9
	7	1.94–15.87	REA/ g^{-1} FW	9.4–73.9%	Mercado et al. 1997a	10
	1	6.05	REA/ g^{-1} FW	26.00%	Mercado et al. 1997b	10
	5	(-)1.11–5.26	REA/ g^{-1} FW	5.8–300.0%	Mercado et al. 1998	10
	1	1.52	No specified	17.10%	Israel and Friedlander 1998	5 mM Tris buffer (8.0–6.5)
	1	11.63	REA/ g^{-1} FW	25.20%	Mercado & Niell 1999	10
	1	1.29	Relative to the blank	9.30%	Israel et al. 1999	5 mM Tris buffer (8.0–6.5)
	1	1.03	REA/ m^{-2} 10^3	23.30%	Mercado et al. 2000	10
	1	32.93	REA/ g^{-1} FW	29.10%	Andría et al. 2001	8
	3	(-)0.91–0.03	REA/ g^{-1} FW	74–2800%	Mercado et al. 2001	10
	1	13.1	REA/ g^{-1} FW	48.90%	Zou et al. 2004	7
	7	3.6–24.9	REA/ g^{-1} FW	0–38.9%	Gordillo et al. 2006	10
	1	ND	–	–	Xu and Gao 2009	7

† SD and Means estimated from a graph; for method used see table 2.1; Formulas: EU = ((Tb/Te) -1) x 10); REA = (Tb/Te) -1
ND: activity no detected; No inf.: information no given in the article
[a]: REA units x 10

2.3.2 Buffer effect on CA assay

The total CA activity of *Macrocystis* was considerably higher when measured with 100 mM Tris-HCl buffer (pH 8.5) than 200 mM phosphate buffer (pH 8.3), 8.89 ± 2.46 REA g^{-1} FW and 4.01 ± 1.69 REA g^{-1} FW, respectively (Student's t-test, t = 4.409, df = 12, P = < 0.001, Fig. 2.1).

2.3.3 Effect of molarity of the Tris-HCl buffer and its components on CA activity

The comparison between 50 mM and 100 mM Tris-HCl buffer (pH 8.5) resulted in similar CA activities of 9.94 ± 2.27 and 7.94 ± 2.14 REA g^{-1} FW (means ± SD), respectively (Student's t-test, t = –1.907, df = 14, P = 0.077). Therefore, the effect of different components in the buffer on CA activity was tested using 50 mM Tris (pH 8.5) (as recommended by Haglund et al. 1992a).

The addition of PVP and DTT to the extraction buffer (buffer III: 50 mM Tris-HCl, pH 8.5) resulted in a more stable CA assay than the control buffer (buffer I: without PVP or DTT), reducing the coefficient of variation from 35% in buffer I to 19% in buffer III (Fig. 2.2). However, no differences between total CA activities were found between buffers (Buffer I: 9.33 ± 3.29 REA g^{-1} FW; Buffer III: 8.14 ± 1.56 REA g^{-1} FW), but in both cases, total CA activity was significantly higher than using buffer II (ANOVA: $F_{5,14}$ = 12.684, P < 0.001; Tukey test, P < 0.05: buffer I ≥ III > II; Fig. 2.2). The addition of PVP into buffer II, without adding DTT, not only resulted in the lowest total CA activity, but also the highest variation between samples (79% CV) (Fig. 2.2).

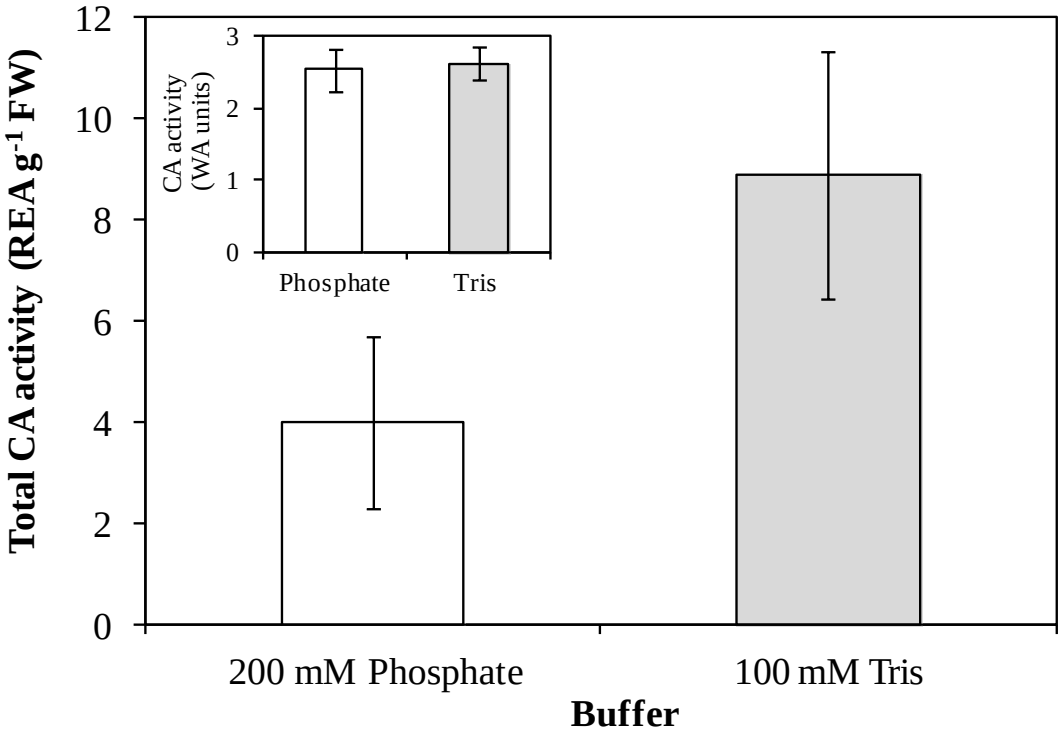

Figure 2.1: Effects of different extraction buffers on the total carbonic anhydrase (CA) activity of *Macrocystis*. Values are means ± SD (phosphate buffer, n = 8; Tris-HCl buffer, n = 6; sub-samples from one blade). Inset: Effect of Tris-HCl and phosphate buffer on purified bovine CA activity (Sigma-Aldrich) (in WA units). Values are means ± SD (n = 6). REA-relative enzyme activity, WA-Wilbur-Anderson units.

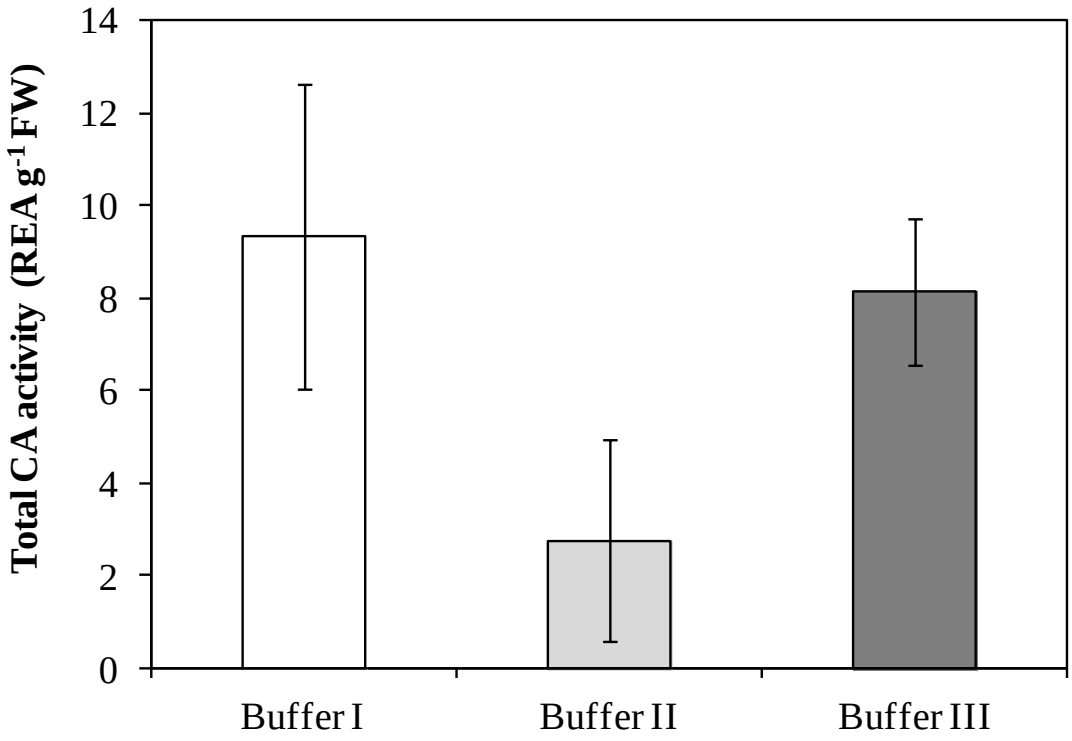

Figure 2.2: Effects of different components in the buffer on the total carbonic anhydrase (CA) activity of *Macrocystis*. Values are means ± SD (buffer I and III, n = 7; buffer II, n = 6; sub-samples from one blade). REA-relative enzyme activity, FW-fresh weight.

2.3.4 Effect of the reaction time on CA activity

The total CA activity was significantly affected by the pH intervals at which the hydration of CO_2 reaction was measured. The total CA activity was 33% (9.34 ± 1.88 REA g^{-1} FW) higher and more accurate (20% CV) when the enzymatic reaction was measured during the pH intervals between 8.3-7.9 than between 8.3-7.3 (6.23 ± 1.57 REA g^{-1} FW) (Student's t-test, t = 4.897, df = 28, P = < 0.001, Fig. 2.3).

2.3.5 External and internal CA activity of different individuals of *Macrocystis* using the optimized protocol

The external and internal CA activities of *Macrocystis* (n =7) were determined using the new optimized protocol for the species. After measuring CA_{ext} from one single disc, CA_{int} was readily measured using the ground powder from the same disc. CA_{int} activity (9.09 ± 2.18 REA g^{-1} FW, 20% CV) was 41% higher than CA_{ext} (5.33 ± 1.07 REA g^{-1} FW, 24% CV) (Student's t-test, t = –4.076, df = 12, P = 0.002, Fig. 2.4). The sum of both CA activities resulted in a total CA activity of 14.42 ± 3.08 REA g^{-1} FW (21% CV).

2.3.6 External and internal CA measurements before and after CA protocol optimization for *Macrocystis*.

After optimizing the CA assay for *Macrocystis*, the % CV between samples decreased considerably from 72% to 24% for the CA_{ext} activity, and from 32% to 24% for the CA_{int} activity. The CA_{ext} activity recorded before and after the protocol optimization was 6.33 ± 4.61 and 5.33 ± 1.07 REA g^{-1} FW, respectively, whereas for the CA_{int} activity was 14.73 ± 4.73 and 9.09 ± 2.18 REA g^{-1} FW, respectively (Fig. 2.5).

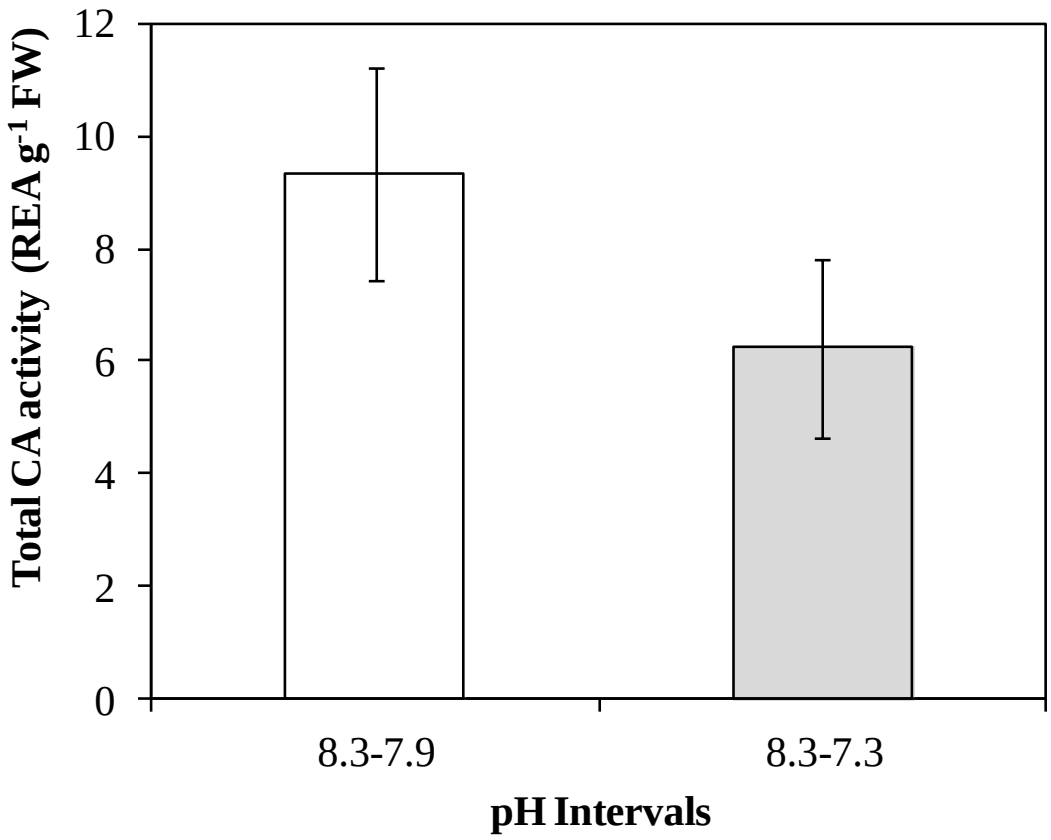

Figure 2.3: Effects of pH intervals on the carbonic anhydrase (CA) activity reaction of *Macrocystis.* pH intervals between 8.3-7.9 (ΔpH 0.4 units) and between 8.3-7.3 (ΔpH 1.0 unit). Values are means ± SD (n = 15; sub–samples from one blade).

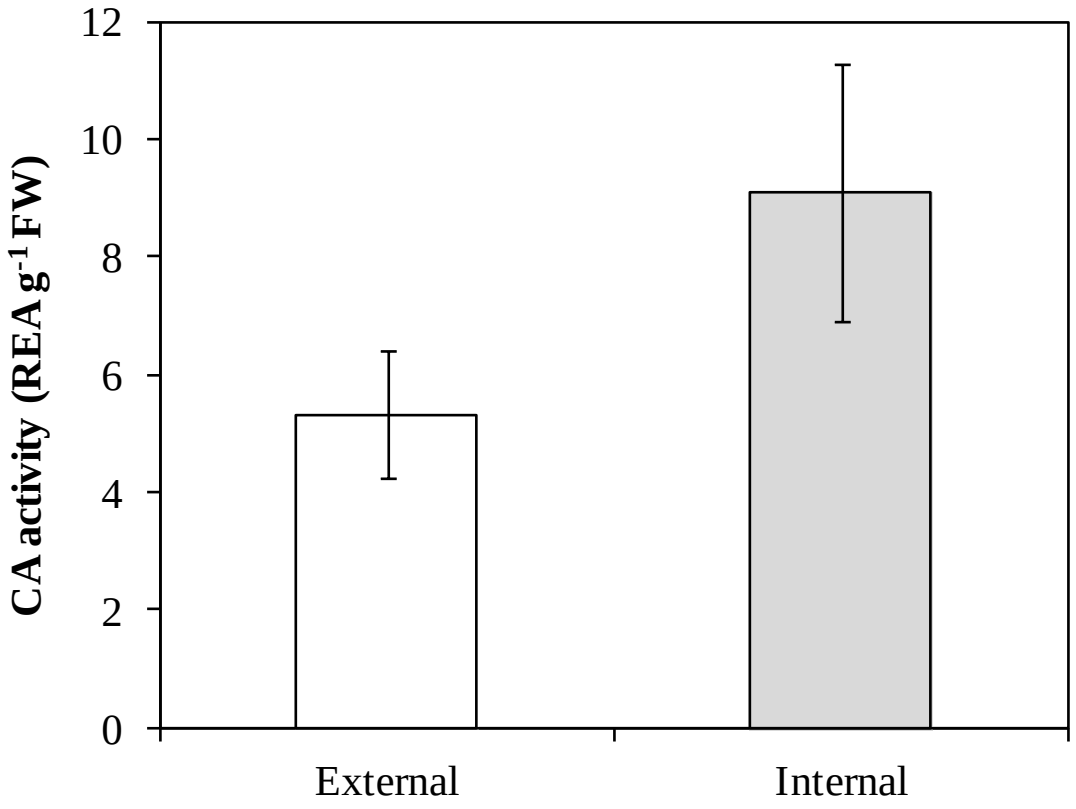

Figure 2.4: External and internal carbonic anhydrase (CA) activities in *Macrocystis* directly after collection, using the optimized CA assay. Values are means ± SD (n = 7; different individuals).

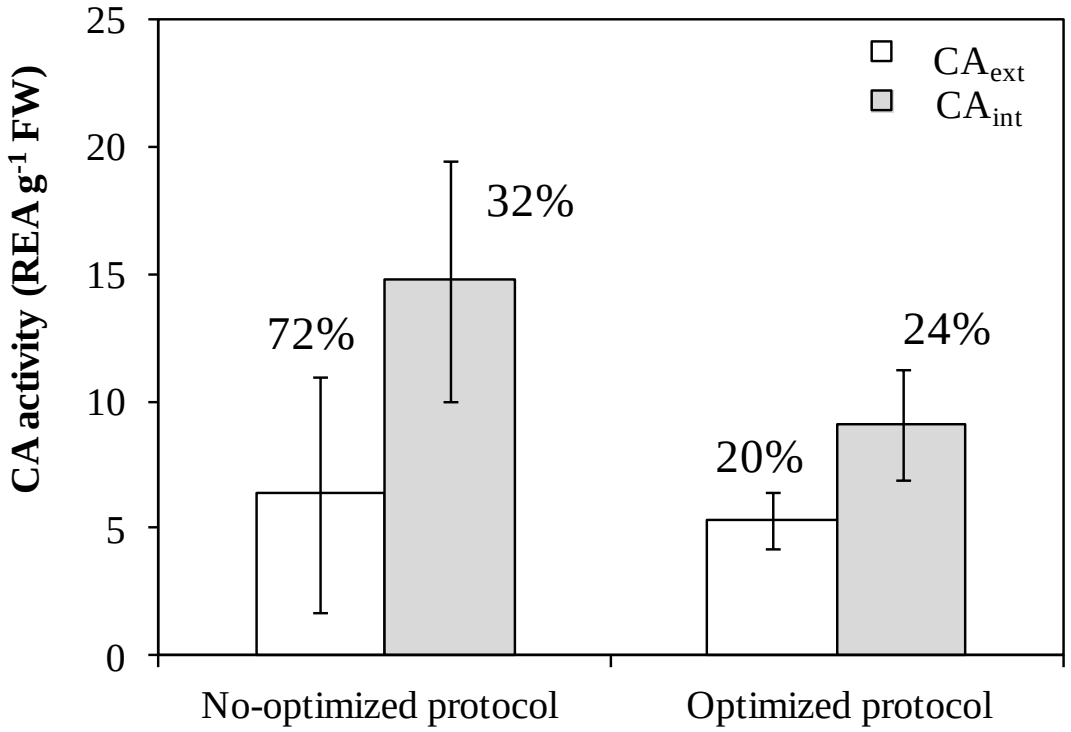

Figure 2.5: Comparison of external and internal carbonic anhydrase (CA_{ext} and CA_{int}) activities before and after the protocol optimization of the CA assay in *Macrocystis*. % values indicated the %CV for each measurement. Values are means ± SD (n = 7-8; different individuals).

2.4 Discussion

The results of this study suggest that the buffer chosen for the CA assay has a significant effect on CA activity recorded in the giant kelp *Macrocystis*. The use of Tris-HCl buffer as both an extraction and sample buffer resulted in a higher total CA activity than phosphate buffer. A 200 mM phosphate buffer has a stronger buffer capacity than a 50 or 100 mM Tris-HCl buffer. Therefore, the phosphate buffer used in this study can repress any changes in pH in the reaction medium during the CA measurement, which potentially results in a reduction of CA activity. Moreover, it has been reported that high concentrations of phosphate can directly inhibit the α-CA II isozyme present in humans (Dodgson et al. 1991), and apparently at high concentrations phosphate might behave as a competitive inhibitor of the enzyme, increasing the K_m during the catalyzed reaction (DeVoe and Kistiakowsky 1961, Maren 1967). However, the CA activity may also vary depending on the chemical nature of the buffer. For example, low CA activity registered in certain buffers such us HEPES and MEPS has been related to the capacity of the buffer of providing or accepting protons from the CA active site (Dodgson et al. 1991, Lindskog 1997, Ren and Lindskog 1992). Similarly, in CA from terrestrial plants, the activity varied depending on the buffer used during the assay (i.e. Phosphate, Tris, Veronal and HEPES), and the response to each buffer was species-specific (Hatch 1991, Warrier et al. 2014). Thus, though CA varies among animals, terrestrial plants, algae and cyanobacteria, i.e. α-CA, β-CA and γ-CA, all three types of CA are Zn^{2+} metalloenzymes, and all seem to share a similar catalytic mechanism (Lindskog 1997, Moroney et al. 2001, Fu et al. 2012). Therefore, the CA-catalyzed reaction in algae may also be dependent on the properties of buffer as reported in CA from animals and terrestrial plants.

Datta and Shepard (1959) indicated that there are at least two main criteria to select a suitable buffer for the CA assay: (1) the reaction time in an uncatalyzed reaction has to be sufficiently long and (2) the buffer does not interfere with the enzymatic reaction. When we first evaluated the buffering effect on CA activity purified from bovine erythrocytes, the reaction times in an uncatalyzed reaction were considerably longer when measured with Tris (131 ± 7.65 s) than with phosphate buffer (88 ± 6.04 s). Similar results were also found when the buffer effect was evaluated on CA from *Macrocystis.* The reaction time has to be sufficiently long to measure accurately the reaction because with the addition of CA the reaction time will be shortened to half, and thus any variation in the measured values would give a large variation between measurements. Therefore, the short reaction time together with the low CA activity obtained using the phosphate buffer suggests that phosphate is not a suitable buffer for measuring CA activity in *Macrocystis*.

The reaction time might also be influenced by the concentration of the buffer and/or its pH. Datta and Shepard (1959) showed that at a given buffer pH (Tris-HCl; pH = 8.0) the reaction time in an uncatalyzed reaction was much longer when measured in a buffer with a higher molarity (57 mM) than with low molarity (25 mM). Similar results were also observed when the buffer pH was increased from 8.0 to 10.0 (Datta and Shepard 1959). These buffer effects on the uncatalyzed reaction time might affect considerably the measured CA activity. No prior studies were found on CA from macroalgae in relation to the interaction between the buffer molarity and/or its pH, and the CA activity. In this study, no difference in either the reaction time or CA activity using Tris buffer of either 50 or 100 mM was observed. However, the pH effect on the CA activity was not tested. Therefore, the possibility cannot be discarded that the

effects of buffer pH and/or its molarity reported by Datta and Shepard (1959) on CA from human erythrocytes may also affect the CA activity of macroalgae.

Studies on the buffering effects on CA kinetics in macroalgae are scarce, and although there are a few earlier studies using Tris, Veronal or phosphate buffer in the CA assay, the differences found in CA activity were not explained by the interaction between buffer - enzyme. An early study in macroalgae evaluated the effect of different extraction buffers on total CA activity (Graham and Smillie 1976) and, as found for *Macrocystis*, in most of the species investigated, the use of a Tris-borate buffer (300 mM; pH = 8.3) resulted in a higher total CA activity compared to the sodium phosphate buffers tested (100 mM; pH = 7.0 and 7.8). Similar results were later reported by Giordano and Maberly (1989). Although both studies reported lower CA activity using phosphate buffer, the potential negative effects of the buffer during the enzyme extraction were not mentioned. Also, because the pH, molarity and components between extraction medium were also varied, it is difficult to conclude that the differences observed in CA activity were only due to the type of buffer. Further detailed studies on the CA kinetics in macroalgae are required for a better understanding of the interaction of the buffer with the enzyme.

Bowes (1969) first reported the presence of CA in *Macrocystis.* However, total CA activity (0.004 REA mg^{-1} protein) was much lower than the total CA activity measured in this study (14.42 ± 3.08 REA g^{-1} FW). Although the method and procedure used by Bowes (1969) to measure CA make these results not comparable, the use of 4 mM phosphate buffer (NaH_2PO_4/Na_2HPO_4) during the extraction and CA assay may explain in part the low activities reported. The low buffer concentration used could decrease the specific activity of CA, probably due to a decrease in the proton transfer

between the active site of the enzyme and the reaction medium (Rowlett and Silverman 1982, Rowlett et al. 1994, Dodgson et al. 1991).

Several modifications in the CA assay such as different buffer volumes, types of buffer and components, and reaction times were identified between the previous studies on macroalgae (Table 2.1). These modifications might contribute to the large variance and lack of accuracy reported in some studies (Cook et al. 1986, Giordano and Maberly 1989, Surif and Raven 1989, Björk et al. 1993, Mercado et al. 1998, Mercado et al. 2001, Tables 2.4 and 2.5). We found that the components of the buffer might interfere with CA activity found and the accuracy of the method. The addition of PVP and DDT to the extraction buffer reduced considerably the % CV from 33% down to 19% compared to the control buffer without PVP and DTT, which confirms the importance of including both reagents in the extraction buffer of brown seaweeds. PVP is important to avoid interference by soluble polyphenolic cell compounds of brown algae (i.e. phlorotannins), which are sequestered in physodes in the cytosol (Toth and Pavia 2001, Gómez and Huovinen 2010). Although the content of soluble phlorotannin is low in *Macrocystis* ($\leq$ 1mg g^{-1} DW; Steinberg 1985, Huovinen et al. 2010), the homogenization and cutting process involved in the total CA and CA_{ext} assays may increase the release of phenolic compounds, which might affect the enzyme measurements. Bowes (1969) suggested that the abundant amount of mucilage present in the algal extract of the brown algae *Eisenia arborea* Areschoug and *Macrocystis* produced interference with the CA assay. Similarly, determinations of other enzymes, i.e. nitrate reductase (NR), are also affected by brown seaweed phenolic compounds, and the importance of including DTT and PVP in the extraction buffer was highlighted (Thomas and Harrison 1988). However, it has been noted that the requirement DTT and

PVP might be species-specific for nitrate reductase (Hurd et al. 1995, Young et al. 2005), and this may also be the case for CA.

The coefficient of variation in this study was lower than that of other studies in brown macroalgae, and we attribute this to careful optimization of the assay for this species. Indeed, this is the first study to demonstrate that it is possible to measure CA_{ext} and CA_{int} activity from the same disc, and to report the presence of CA_{ext} using an electrometric method in *Macrocystis*. Although, the total CA activity measured in this study (14.42 ± 3.08 REA g^{-1} FW) was lower than in previous studies (Huovinen et al. 2007, Rothäusler et al. 2011), where CA ranged from 15 REA g^{-1} FW to 116 REA g^{-1} FW, the activity registered was within of the range reported for the species. For $CA_{ext,}$ the activity measured was comparable with other Laminariales species, i.e. *Saccharina latissima* (Linnaeus) C.E Lane, C. Mayes, Druehl & G.W. Saunders [=*Laminaria saccharina*] (3.20 REA g^{-1} FW) (Haglund et al. 1992b). We suspect that the differences observed between studies in the total CA activity may lie in the method used. The main differences found between previous reports and this optimized CA assay were: buffer pH (9.00), reaction time, the exclusion of DTT from the buffer and no use of PVP. Although we found that the inclusion of DTT and PVP into the buffer reduced the error of the method, CA activity measured was the same between buffers with or without the addition of DTT and PVP. Therefore, the higher CA activity reported in previous studies may not be explained by these additions. If the differences are because of the buffer pH, testing will be necessary to determine the effect of buffer pH on CA activity. However, it is also possible that other biological or physical factors may be responsible for the differences found in CA activity measured among studies. Environmental factors, e.g. temperature, UV radiation and salinity might affect considerably CA activities in algal species (CA_{ext}, CA_{int} or total CA) (Booth and Beardall 1991, Gómez et

al. 1998, Flores-Moya et al. 1998, Rothäusler et al. 2011). Moreover, diurnal and seasonal changes in total CA activity have also been observed (Berman-Frank and Zohary 1994, Flores-Moya et al. 1998, Gómez et al. 1998).

The present study showed that with proper optimization, the relative error in a CA assay can be reduced considerably, and although the electrometric method may still present some disadvantages, this is the only method that provides a quantitative estimation of CA activity. Therefore, I recommended carrying out assay optimization prior to experimental studies on CA activity in seaweed species. The present study indicates that important considerations when optimizing a CA assay are: (1) Buffer selection - the reaction time in an uncatalyzed reaction needs to be long enough to follow the reaction and to reduce the variation in measured values; (2) pH, molarity and components of the buffer selected - each component in the buffer has to meets the requirements for the species studied, e.g. PVP to avoid interference with phenolic compounds in brown macroalgae; (3) extraction procedure - use liquid N_2 to freeze the thallus before grinding and for homogenization. After homogenization ensure that the homogenized mixture is well mixed with the extraction buffer before starting the reaction (keeping the temperature constant between 0-2˚C), and (4) fresh weight/volume buffer - larger samples might interfere with the assay.

Chapter 3: Bicarbonate uptake via an anion exchange protein is the main mechanism of inorganic carbon acquisition by the giant kelp *Macrocystis pyrifera* (Laminariales, Phaeophyceae) under variable pH

3.1 Introduction

Seaweeds are the base of the food web and major contributors to benthic primary production in coastal ecosystems, providing both food and habitat for fish and invertebrates. Their high productivity enables them to fix large amounts of carbon, contributing around 2–10% of total marine production (Charpy–Roubaud and Sournia 1990, Graham et al. 2007, Bensoussan and Gattuso 2007, Koch et al. 2013). To support photosynthesis and growth, seaweeds require an exogenous inorganic carbon (Ci) source. Today's oceans contain approximately 2.1 mol m^{-3} of dissolved inorganic carbon (DIC) at pH ~8.07 and 15 ˚C, which exist as bicarbonate (HCO_3^-; 91%), carbonate (CO_3^{2-}; 8%) and dissolved carbon dioxide ($CO_{2\ (aq)}$; 1%) (Roleda and Hurd 2012); only CO_2 and HCO_3^- can be used as CO_2 source for photosynthesis. Although only a small proportion of Ci exists as CO_2, this uncharged molecule readily diffuses through the lipid bilayer of the plasma membrane into the seaweed cell, whereas the most abundant form of Ci, HCO_3^-, cannot diffuse through the lipid bilayer of the plasma membrane (Raven 1997). Due to the low CO_2 concentration in seawater, it is not surprising that most seaweed have developed mechanisms for using the abundant external pool of HCO_3^- as an exogenous Ci source (Axelsson et al. 1999, Maberly 1990, Larsson and Axelsson 1999).

Three main mechanisms have been proposed for HCO_3^- acquisition by seaweed: (1) the extracellular dehydration of HCO_3^- to CO_2, catalyzed by external carbonic anhydrase (CA_{ext}), an enzyme that is located in the cell wall in the majority of

seaweeds: the resulting CO_2 is then taken into the cell by passive diffusion, (2) the direct uptake of HCO_3^- through a plasmalemma–located anion exchange (AE) protein, and (3) active Ci uptake involving a proton motive force through a P–type H^+–ATPase pump that might facilitate the transport of CO_2 or HCO_3^- into the cell by the proton motive force generated by the proton excretion (Axelsson et al. 1999, 2000, Kübler et al. 1999, Madsen and Maberly 2003, Klenell et al. 2004, Giordano et al. 2005). The first two mechanisms are well described in seaweeds whereas studies on the active Ci uptake are more scarce.

The presence of these mechanisms in algae can be demonstrated with the aid of specific inhibitors. The externally catalyzed dehydration of HCO_3^- via CA_{ext} can be inhibited using acetazolamide (AZ), while direct HCO_3^- uptake via the AE protein can be inhibited using 4, 4'–diisothiocyanatostilbene–2, 2'–disulfonate (DIDS). Both inhibitors are membrane–impermeable, highly specific and widely used to inhibit HCO_3^- use mechanisms in algae (Drechsler and Beer 1991, Björk et al. 1992, Drechsler et al. 1993, Axelsson et al. 1995, 1999, 2000, Young et al. 2001, Herfort et al. 2002, Suffrian et al. 2011, van Hille et al. 2014). Both mechanisms, external HCO_3^- dehydration and direct HCO_3^- uptake, are able to operate independently, and thus the addition of both inhibitors can result in an almost complete inhibition of net photosynthesis (Axelsson et al. 1995, Larsson and Axelsson 1999). Similarly, active Ci uptake through a plasma membrane P–type H^+–ATPase pump can be inhibited using vanadate (VAN) (Klenell et al. 2004) and the activity of both external and internal CA can be inhibited using ethoxyzolamide (EZ). The difference in inhibitory activity between EZ and AZ is used to account for the relative internal carbonic anhydrase activity (Mercado et al. 2006).

Although most seaweed have the capacity to use HCO_3^- as an exogenous source of Ci, the mechanisms of acquisition vary among taxa and/or species (Maberly 1990). One or both mechanisms of HCO_3^- utilization, i.e. the extracellular catalyzed dehydration of HCO_3^- and direct HCO_3^- uptake, have been reported in green seaweeds (e.g. several *Ulva* species; Björk et al. 1992, Drechsler et al. 1993, Axelsson et al. 1999), red seaweeds (e.g. *Gracilaria* species, Haglund and Pedersén 1992, Andria et al. 1999; *Pyropia leucosticta* (Thuret) Neefus & J. Brodie [=*Porphyra leucostica*], Mercado et al. 1999), and in brown seaweeds. Among brown seaweeds, some species in the order Laminariales (kelps) are reported to use HCO_3^- via the external dehydration of HCO_3^-, catalyzed by CA_{ext} (Surif and Raven 1989, Flores–Moya and Fernández 1998, Axelsson et al. 1999). For example, when this HCO_3^- utilization mechanism was inhibited by the CA_{ext} inhibitor (AZ) in *Saccharina latissima* (Linnaeus) C.E Lane, C. Mayes, Druehl & G.W. Saunders [=*Laminaria saccharina*] its photosynthetic rate was reduced by around 80% (Axelsson et al. 2000). The presence of CA_{ext} in this species was also described by Haglund et al. (1992b). Both HCO_3^- utilization mechanisms have been described for the filamentous brown seaweed, *Ectocarpus siliculosus* (Dillwyn), which is one of the few brown seaweed species with a known direct HCO_3^- uptake mechanism: here two genes coding for putative bicarbonate transport in addition to CA have been reported (Gravot et al. 2010). In addition, a P–type H^+ –ATPase is involved in Ci acquisition in *Saccharina latissima* and *Laminaria digitata* (Hudson) J.V. Lamouroux. This proton pump might support either a H^+/HCO_3^- counter transport or a H^+ extrusion–enhanced dehydration of HCO_3^- to CO_2 in the periplasmic space (Klenell et al. 2004).

Ci acquisition mechanisms are extensively studied and well known in microalgae (Giordano et al. 2005, Spalding 2008). For example, regardless of the Ci

form (CO_2 or HCO_3^-) taken up by the microalga *Chlamydomonas reinhardtii*, HCO_3^- is the primary form accumulated into the cell, limiting CO_2 leakage (Spalding 2008). The internal interconversion of HCO_3^- and CO_2, catalyzed by CA_{int}, plays an important role in maintaining the internal Ci pool, pH homeostasis, and supplying CO_2 to RuBisCO (Moroney et al. 2001). Different isoforms of CA_{int} may be localized in the cytosol, chloroplast envelope, or in the stroma of microalgae (Graham et al. 1984, Moroney et al. 2001). Although the presence of CA_{int} has been detected in most of seaweed species investigated so far, its specific locations and functions inside the cell are unknown and more studies are required (Sültemeyer 1998). However, CA_{int} might have the same important roles in seaweed as it has in microalgae (Björk et al. 1992, 1993, Badger and Price 1994, Sültemeyer 1998).

The giant kelp, *Macrocystis pyrifera* (Linnaeus) C. Agardh (hereafter, *Macrocystis*) is widely distributed along the northeast Pacific coast from Alaska to Mexico, the east and west coasts of South America, in isolated regions of South Africa, Australia and New Zealand, with an isolated population in the sub–Antarctic islands, and has an important role in coastal regions as an ecosystem engineer (Steneck et al. 2002, Graham et al. 2007). The high productivity of *Macrocystis* controls the diurnal oscillation in proximate bulkwater pH, causing pH to increase during the day due to photosynthesis and decrease pH at night due to respiration (Cornwall et al. 2013). For example, a maximum daytime *in situ* pH 9.10 has been observed inside a *Macrocystis* bed (Delille et al. 2000). Under such a high pH, photosynthetic organisms are constrained to use the available Ci species in the form of HCO_3^- and photosynthesis will be severely limited if the algae depends only on CO_2. The seawater carbonate chemistry status may trigger and enhance the expression of different HCO_3^- use mechanisms (Axelsson et al. 1995, Larsson et al. 1997, Israel and Hophy 2002). Despite being a fast

growing species inhabiting an environment with a dynamic range of diel pH, we know little of the carbon acquisition mechanisms in *Macrocystis*. Such knowledge is particularly relevant as scientists assess how species and ecosystems might respond to the predicted pH reduction of 0.3–0.4 units (~8.07 to 7.65) and changes in seawater carbonate chemistry (200% increase in CO_2, 9% increase in HCO_3^-) predicted for year 2100 under ocean acidification (OA) (The Royal Society 2005). Because marine producers depend on Ci to support photosynthesis, these predicted changes in pH and seawater carbonate chemistry might affect directly their metabolism (Hurd et al. 2009, Roleda et al. 2012b, Kroeker et al. 2013). Given this, an understanding of Ci acquisition mechanisms is crucial to elucidate how seaweed species will respond to the predicted changes in seawater chemistry due to OA (Hurd et al. 2009, Hepburn et al. 2011). However, it should be noted that despite the predicted 200% increase in CO_2, the HCO_3^- concentration will remain 97% higher than that of dissolved CO_2 (The Royal Society 2005, Roleda et al. 2012a).

Macrocystis is known to be mixed CO_2 and HCO_3^- user, based on its stable isotope signatures and pH–drift experiments (Hepburn et al. 2011). However, knowledge about its Ci acquisition mechanisms are limited to measurements of total CA activity (e.g. Huovinen et al. 2007, Rothäusler et al. 2011) using the potentiometric method described by Wilbur and Anderson (1948). Other putative mechanisms such as direct HCO_3^- uptake via an AE–like system, active carbon uptake (CO_2 or HCO_3^-) using a plasma membrane P–type H^+–ATPase pump, or the inhibitor–sensitive external and internal CA activities, that have been found in other seaweeds, could be present but have not been investigated. In this study, we investigate the carbon acquisition mechanisms in *Macrocystis* following acclimation to two pH_T regimes (7.65; 9.00) and measure O_2–evolution under two pH_T incubation treatments (7.65; 9.00). We

hypothesized that (1) HCO_3^- is the primary exogenous source of Ci to support photosynthesis by *Macrocystis*, (2) external HCO_3^- dehydration mediated by CA_{ext} is the main mechanism for Ci acquisition, and (3) under higher concentrations of CO_2 (pH_T = 7.65), diffusive uptake of CO_2 will support photosynthesis when external HCO_3^- dehydration and other putative transport mechanisms are blocked by inhibitors.

3.2 Materials and Methods

3.2.1 Seaweed collection

During low tide in February 2013, one young blade, i.e. the first pneumatocyst–bearing lamina below the apical scimitar, was removed from each of 30 individual adult *Macrocystis* sporophytes, from the upper subtidal in Aromoana (45°47'S, 170°43'E), Otago Harbour, New Zealand. Blades were kept moist and dark inside an insulated bin for transport to the laboratory, 20 minutes away. In the laboratory, blades were gently cleaned of any visible epiphytes and rinsed with filtered natural seawater (NSW). From each of the 30 blades, a disc of 0.25–0.3 g was excised using a cork borer, 2 cm above the base of the blade. For the initial physiological status measurements, excised discs were allowed to recover for two hours. The initial physiological status was assessed using sacrificial discs: photosynthesis, measured at pH 7.65 (n = 3), 8.10 (n = 3) and 9.00 (n = 3), and CA_{int} and CA_{ext} activity (n = 3), were each measured as described below.

3.2.2 pH drift experiment

Preliminary experiments were conducted in June 2012 to verify the use of HCO_3^- as a Ci source by *Macrocystis* (Hepburn et al. 2011). Eight discs obtained from 8 individual adult sporophytes were incubated at two pHs: 8.10 (n = 4) representing today's seawater pH and 7.65 (n = 4) representing seawater pH predicted for 2100 (see below for method of pH modification). Each disc was incubated individually in a 20 mL sealed transparent container following the methods detailed in Hepburn et al. (2011) except that pH drift was recorded for 12 h of incubation. If the algal disc raised the seawater pH to > 9.00, this confirmed its capacity to use HCO_3^- (Maberly 1990).

3.2.3 Acclimation to different ratios of HCO_3^- and CO_2

The rest of the field–collected *Macrocystis* excised discs (n = 18) were acclimated for 2 days under two pHs, measured on the total scale (pH_T): 9.00 and 7.65 (see Roleda et al. 2012b). Each disc was individually incubated in a 250 mL glass flask containing the pH–adjusted seawater (n = 9 for each pH treatment). The filtered NSW, pH_T 8.10 (Ci = 1850 µM HCO_3^-; 13.63 µM CO_2), was adjusted to pH_T 9.00 and pH_T 7.65 using equal amounts of 0.2 M NaOH and 0.2 M $NaHCO_3$, and 0.2 M HCl and 0.2 M $NaHCO_3$, respectively (Hurd et al. 2009, Gattuso et al. 2010, Roleda et al. 2012b) and pH was then measured spectrophotometrically (McGraw et al. 2010). Seawater samples were fixed with mercuric chloride for total alkalinity (A_T) and DIC measurements. A_T was measured using the closed–cell titration method and DIC was measured directly by acidifying the sample (Dickson et al. 2007). A_T, DIC, pH, salinity, and temperature were used to calculate carbonate chemistry parameters using the program SWCO2 (Hunter 2007). The concentrations of HCO_3^- and CO_2 in pH_T 9.00 was 940 µM and < 1 µM, respectively (940:1) and in pH_T 7.65 was 2040 µM and 40.35 µM, respectively (51:1). The pH–adjusted seawater was replaced twice daily and each 250 mL glass flask was aerated using an aquarium pump. A preliminary experiment, i.e. without algae, showed no change in the seawater carbonate chemistry after 12 h. The 2–day pH acclimation period was at 12 ºC under a 12:12 h light: dark photoperiod of 150 µmol photons m^{-2} s^{-1} of PAR, provided by metal halide lamps (Philips HPI- T 400 W quartz), which corresponds to the saturating light intensity (E_k) of the species estimated from published studies (e.g. Gerard 1986, Colombo–Pallota et al. 2006) and from a preliminary P–E curve analysis in this study (E_k = 119.94 ± 18.47 µmol photons m^{-2} s^{-1}; n= 2). No photoinhibition of photosynthetic O_2 evolution was observed up to a maximum photon flux density (PFD) of 500 µmol photons m^{-2} s^{-1}.

3.2.4 Photosynthetic oxygen evolution

Photosynthetic O_2 evolution was measured inside a 154 mL acrylic chamber equipped with an optic fiber FOXY–R probe coupled to a USB–2000 spectrophotometer (Ocean Optics, Florida, USA) connected to a laptop. The chamber was equipped with a magnetic stirrer and sat on a stirring plate at 650 rpm to constantly stir the medium to create a homogenous vertical O_2 profile. The seawater was initially bubbled with N_2 to reduce the O_2 concentration from 271 µM to the experimental starting concentration of 100 ± 20 µM O_2. Then, seawater was buffered to either pH_T 9.00 or pH_T 7.65 for photosynthetic measurements (short term incubation). A single *Macrocystis* disc was then enclosed in the acrylic chamber and oxygen concentration was recorded every second using the OOISensor 1.0 software (Ocean Optics, Inc.). Measurements were conducted under a higher but non–photoinhibiting PFD of 250 µmol photons m^{-2} s^{-1}, at 12 °C. Incident light was provided by metal halide lamps (Philips HPI- T 400 W quartz). A control measurement at 2 hours, i.e. without algae, did not change the seawater dissolved O_2 concentration nor the carbonate chemistry. The oxygen concentration was expressed as µM O_2 as calculated using the formulas and coefficient of Millero and Poisson (1981) and Garcia and Gordon (1992). To determine acclimated versus transient responses to the two ratios of DIC species (HCO_3^-: CO_2), photosynthetic rates of discs that were acclimated at pH_T 9.00 were measured at both pH_T 9.00 (n = 3) and pH_T 7.65 (n = 3) (pH modified in the photosynthetic chamber, short term incubation). Likewise, discs acclimated at pH_T 7.65 were measured at both pH_T 9.00 (n = 3) and pH_T 7.65 (n = 3).

3.2.5 Application of the inhibitors DIDS and AZ

A concentration of 300 µM DIDS to inhibit the direct HCO_3^- uptake via the AE protein and 100 µM AZ to inhibit CA_{ext} were selected based on the dose response curves of Herfort et al. (2002), and the standard utilization of these concentrations across studies on the Ci–use mechanisms of micro– and macroalgal species (e.g. Smith and Bidwell 1989, Björk et al. 1992, Axelsson et al. 1995, 1999, 2000, Mercado et al. 1997ab, 2006, Larsson et al. 1997, Larsson and Axelsson 1999, Israel et al. 1999, Granbom and Pedersén 1999, Young et al. 2001, Choo et al. 2002, Israel and Hophy 2002, Moulin et al. 2011, van Hille et al. 2014).

The 0.03 M stock solution of DIDS (Sigma, ≥80% elemental analysis) was prepared by dissolving the powder in MilliQ water (Axelsson et al. 1999, Larsson and Axelsson 1999). The 0.02 M stock solution of AZ (Sigma, ≥99%) was prepared in 0.02 M NaOH in MilliQ water as its dissolution requires a basic medium not lower than pH 8.20 (Beer and Israel 1990, Axelsson et al. 1999, 2000). Dissolution under lower pH and adjusting pH to treatment pH caused precipitation. The quantity of inhibitor stock solution (1.54 mL of DIDS and 0.77 mL of AZ) injected into 154 mL seawater to make up the final concentration of DIDS and AZ had no detectable effect on the pH of the experimental treatment. The stock solutions were prepared daily and kept at 4 ˚C and dark.

The inhibitory effects of DIDS and AZ were tested under acclimated and transient pH conditions described above. The inhibitors were injected into the photosynthetic chamber one at the time. A specific inhibitor of the AE protein for direct HCO_3^- uptake, DIDS (Axelsson et al. 1995), was injected first into the chamber to a final concentration of 300 µM (Larsson et al. 1997, Axelsson et al. 1999). Then AZ,

which inhibits external CA activity (Axelsson et al. 1995), was injected into the chamber to a final concentration of 100 µM.

Oxygen concentration in the photosynthetic chamber was measured continuously for 20 min before the inhibitors were sequentially introduced. Initial photosynthetic rates, before inhibitor addition, were calculated from a linear regression of O_2 concentration versus time over the last 5 min. After the addition of each inhibitor, O_2 concentration was measured for another 15 min. The total O_2 evolution measurement was thus 50 min (20 + 15 + 15 min) for each experimental run under either pH_T 7.65 or 9.00. Photosynthetic rates after the addition of each inhibitor were calculated from a linear regression of O_2 concentration versus time for intervals of 0–5 min, 5–10 min and 10–15 min. For both inhibitors, the greatest inhibitory effect on the photosynthetic rate was observed during the first 5 minutes after addition and no additional inhibitory effect was observed to up 30 min (data not shown). No recovery in the photosynthetic rates was observed after 15 min, indicating no loss of inhibitor efficacy. pH was measured before and after each of the 50–min experimental runs, allowing the calculation of the change in pH (ΔpH). At the end of the experiment, each disc was flash frozen in liquid N_2 and stored at –80 °C until subsequent analyses of external and internal CA activities.

3.2.6 Carbonic anhydrase activity

CA activity was measured for discs following acclimation for 2 d at pH 7.65 or 9.00 (n = 3 each pH treatment), and for discs following the inhibition experiments. External and internal carbonic anhydrase (CA) activity was measured using the method described by Haglund et al. (1992a) with modifications (P. Fernández et al. in preparation). The extraction buffer was modified to prevent interference of brown seaweed phenolic compounds and to avoid oxidation of the extract: polyvinlpyrrolidone (PVP) and

ditiothreitol (DTT) were used to absorb polyphenols and to prevent the irreversible oxidation of the protein thiols, respectively. The tissue weight to buffer volume quotient was also optimized (6 mg:1 mL). The extraction buffer was composed of 50 mM Tris (adjusted to pH 8.5), 2 mM DTT, 15 mM ascorbic acid, 5 mM Na_2–EDTA, and 0.3% W/V PVP.

Frozen tissue discs (60 ± 20 mg f.w.) were initially analyzed for external CA activity. A 20 mL scintillation vial equipped with a micro stirrer bar (10x3 mm) was used for the enzymatic reaction. The glass vial was placed inside an ice–containing 100 mL plastic container to maintain the temperature at 0 ± 2 °C, sitting on top of a magnetic stirrer to stir the solution. A disc was transferred into the vial containing 10 mL of the extraction buffer. Temperature and pH were simultaneously measured using a ROSS electrode (Orion 8107BNUMD) coupled to Orion 3–Stars Plus pH Benchtop meter (Orion, Thermo Scientific). When pH stabilized at 8.3, 5 mL of ice–cold CO_2–saturated water was added. The time taken for the pH to drop 0.4 units, from 8.3 to 7.9, was recorded. Then the disc was ground to fine powder in liquid N_2–frozen mortar and pestle. The ground tissue (60 ± 20 mg) was analyzed for internal CA activity following the protocol described above.

The relative enzyme activity (REA) was determined using the equation:

$$REA = (T_b/T_s) - 1$$

where t_b and t_s are the times in seconds required to drop 0.4 pH units in the uncatalyzed extraction buffer (T_b, without algae) and in the enzyme–catalyzed reaction of the sample (T_s), respectively. The REA was standardized to corresponding sample fresh weight.

3.2.7 Statistical analyses

The effect of pH treatment on net photosynthesis, external and internal CA activities and photosynthetic inhibition using different inhibitors were separately tested using analysis of variance (ANOVA, $P < 0.05$) after homogeneity (Levene's test) and normality (Shapiro–Wilk test) were satisfied. Percentage data (photosynthetic inhibition) were logit transformed to satisfy the assumptions of normality and equal variance for ANOVA and Student's t-tests. Significantly different groups were classified after Tukey's HSD tests ($P = 0.05$). Within each group (i.e. pH treatment), the significant difference in responses, i.e. net photosynthesis, CA activities, and photosynthetic inhibition, were tested using a Student's t–test ($P < 0.05$). All analyses were performed using the statistical program SigmaPlot 11.0 (Systat Software, Inc.).

3.3 Results

3.3.1 pH drift experiment

Under both pH treatments, pHs: 8.10 and 7.65, and in all replicates, seawater pH was raised to pH 9.00 or above (9.014 ± 0.15 SD and 9.16 ± 0.04 SD measured at pH 7.65 and 8.10, respectively), thereby confirming that *Macrocystis* uses HCO_3^- as a Ci source.

3.3.2 Photosynthesis

Directly after collection (field collected material; ambient seawater pH_T = 8.10), photosynthetic rates of *Macrocystis* blades were highest when measured at pH_T 7.65 (66.32 µmol O_2 g^{-1} FW h^{-1}) and pH_T 8.10 (70.88 µmol O_2 g^{-1} FW h^{-1}), and significantly lower at pH_T 9.00 (32.98 µmol O_2 g^{-1} FW h^{-1}) (ANOVA: $F_{5,14}$ = 12.41, P < 0.05; Tukey test, P < 0.05: pH_T 8.10 ≥ 7.65 > 9.00; Fig. 3.1). The photosynthetic rate of discs acclimated for 2 days to pH_T 7.65 and measured under pH_T 7.65 were significantly higher than those measured at pH_T 9.00 (Student's t–test, t = 3.030, df = 4, P = 0.039, Fig. 3.1) and similar results were observed for discs acclimated for 2 d to pH_T 9.00 (Student's t–test, t = 3.274, df = 4, P = 0.031, Fig. 3.1), showing the same pattern as field–collected individuals. However, rates of photosynthesis measured at pH_T 7.65 and 9.00 were not significantly different between pH acclimation treatments (Student's t–test, P > 0.05). In contrast, the photosynthetic rate of discs acclimated for 2 days at pH_T 9.00 and measured at pH_T 7.65 were 25% higher than the discs measured at pH_T 7.65 directly after collection (field collected material) (Student's t–test, t = 3.282, df = 4, P = 0.030, Fig. 3.1).

3.3.3 Effects of AZ and DIDS on photosynthesis

After the 2–day acclimation to enhanced CO_2 (pH_T 7.65), the photosynthetic rate measured at both pH_T 7.65 and 9.00 was considerably reduced by the application of inhibitors (Fig. 3.2a). The pH at which photosynthetic measurements were made influenced significantly the inhibitory effect of both AZ and DIDS. A 55% reduction in net photosynthesis (NPS) of *Macrocystis* discs was observed when measured at pH_T 7.65 following the application of DIDS while a 65% reduction in NPS was observed when discs were measured at pH_T 9.00 (Student's t–test, t = -2.986, df = 4, P = 0.041: pH_T 9.00 > 7.65, Fig. 3.2a). After the application of AZ, NPS was inhibited by an additional 11% when measured at pH_T 7.65 while an additional 34% reduction in NPS was observed at pH_T 9.00 (Student's t–test, t = -3.097, df = 4, P = 0.036: pH_T 9.00 > 7.65, Fig. 3.2a). Regardless of the pH under which photosynthetic measurements were made the trend was the same, i.e. the inhibitory effect of DIDS was greater than that of AZ. For the pH_T 7.65–acclimated discs, a 67% and 99% inhibition of NPS was recorded following the application of both inhibitors (DIDS and AZ), when measured at pH_T 7.65 and pH_T 9.00, respectively (Fig. 3.2a).

Following acclimation to pH_T 9.00, the rate of NPS at pH_T 7.65 and pH_T 9.00 was considerably reduced by the application of inhibitors (Fig. 3.2b). However, the inhibitory effect of both DIDS and AZ was not significantly influenced by the pH at which the photosynthetic measurements were made. The NPS measured at pH_T 7.65 and 9.00 was inhibited by 55% following the DIDS application (Student's t–test, t = 0.0219, df = 4, P = 0.984: pH_T 9.00 = 7.65, Fig. 3.2b). After the AZ application, the photosynthetic rate was inhibited by an additional 17% and 21% when measured at pH_T 7.65 and pH_T 9.00, respectively (Student's t–test, t = -0.185, df = 4, P = 0.863: pH_T 9.00 = 7.65, Fig. 3.2b). Regardless of the pH at which the photosynthetic measurements were

made the trend was the same with the inhibitory effect of DIDS being greater than that of AZ. NPS was inhibited by a total of 70–75% after the application of both inhibitors at both pH_T 7.65 or 9.00 (Fig. 3.2b).

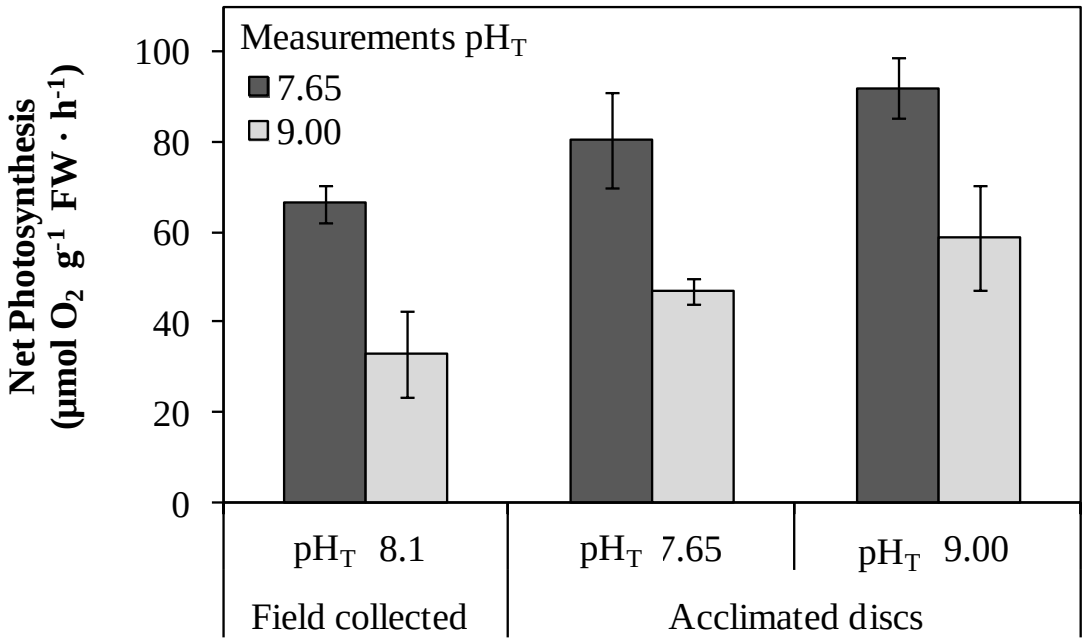

Figure 3.1: Net photosynthesis of *Macrocystis pyrifera* discs directly after collection (field collected material; ambient seawater pH_T = 8.10) at pH_T 7.65 and pH_T 9.00, and after two days of acclimation to pH_T 7.65 and pH_T 9.00. Values are the mean (n = 3) ± SE.

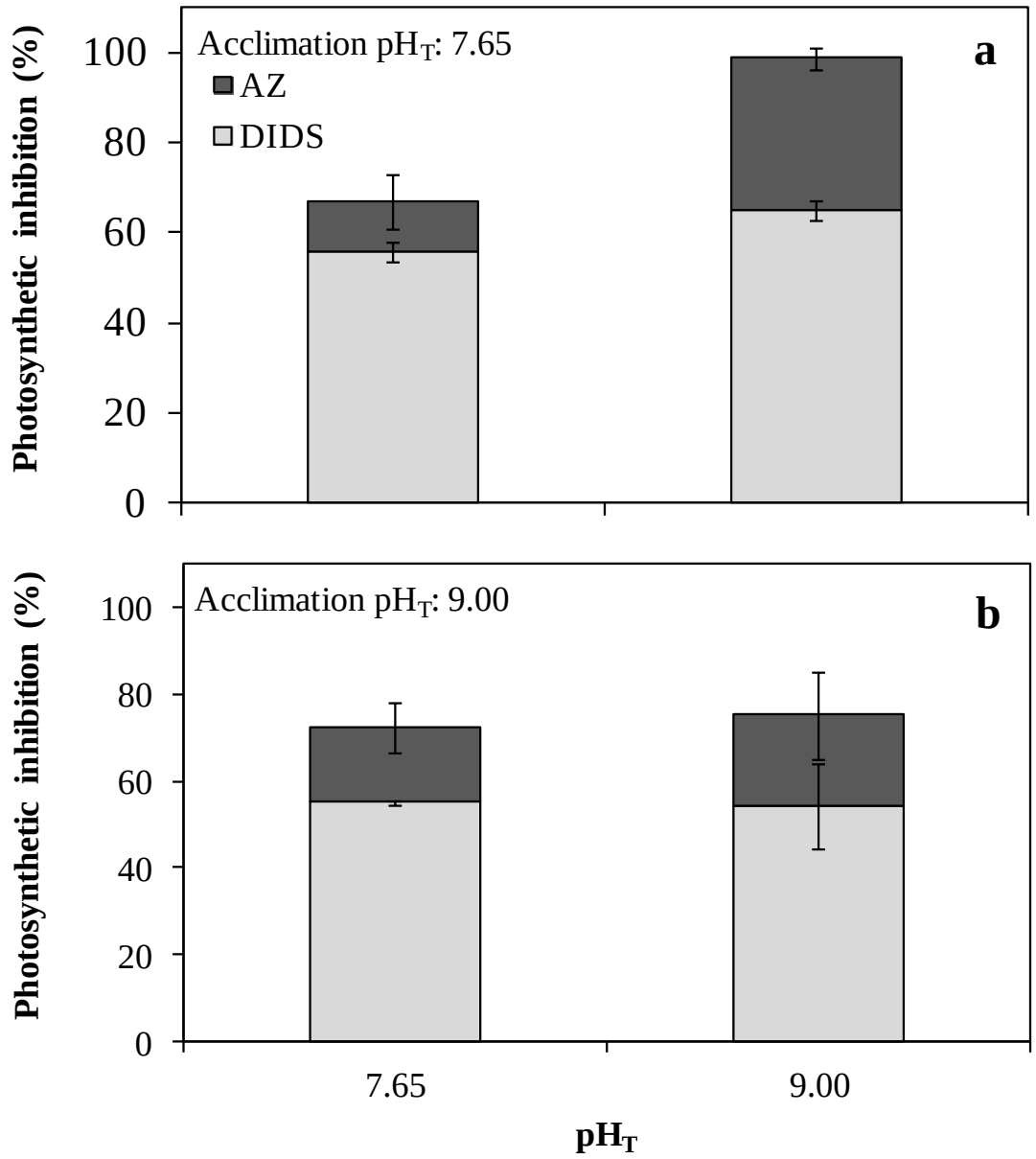

Figure 3.2: Photosynthetic inhibition after sequential blocking of the anion exchange (AE) protein and CA_{ext} activity by DIDS and AZ, respectively. Discs were acclimated for 2 days at (a) pH_T 7.65 and (b) pH_T 9.00. Photosynthesis of discs acclimated under (a) and (b) was measured at pH_T 7.65 and pH_T 9.00 in the photosynthetic chamber, plus inhibitors, over 15 min. Values are the mean (n = 3) ± SE.

3.3.4 External and internal carbonic anhydrase activities

CA_{ext} activity was 50% higher in blades directly collected from the field compared to those incubated for 2 days at pH_T 7.65 and pH_T 9.00 (ANOVA: $F_{5,14} = 7.715$, $P = 0.022$, Tukey test $P < 0.05$: pH_T 8.10 > 7.65 ≥ 9.00, Fig. 3.3). The CA_{ext} activity of discs incubated at pH_T 7.65 and pH_T 9.00 was similar at 1.70 ± 0.03 and 2 ± 0.07 REA g^{-1} FW, respectively (Tukey test, $P = 0.888$, Fig. 3.3). After the application of AZ during the photosynthetic measurements at pH_T 7.65 and 9.00, the CA_{ext} activity of discs acclimated to both pH_T 7.65 and 9.00 was reduced by the inhibitor (average between 0.12 – 0.90 REA g^{-1} FW; data no shown). CA_{int} did not change from the values of field collected material following incubation at either pH_T 7.65 or pH_T 9.00 (ANOVA: $F_{5,14} = 0.396$, $P = 0.689$, Fig. 3.3).

3.3.5 Inhibitor effects on CA_{int} activity

The CA_{int} activities of acclimated discs were 7.67 and 8.78 REA g^{-1} FW under pH_T 7.65 and pH_T 9.00, respectively (Fig. 3.4). After sequential applications of DIDS and AZ, the CA_{int} activity was affected by the disc acclimation history and photosynthetic pH measurements (Fig. 3.4). The CA_{int} activity of discs acclimated to pH_T 9.00 and measured at pH_T 7.65 was significantly higher (9.13 REA g^{-1} FW) than those acclimated at pH_T 7.65 and measured at pH_T 7.65 (2.87 REA g^{-1} FW) (Student's t–test, $t = 3.750$, df = 4, $P = 0.020$, Fig. 3.4). However, the CA_{int} of discs that were acclimated at pH_T 7.65 and measured at pH_T 9.00 were comparable (3.26 REA g^{-1} FW) to those of discs acclimated at pH_T 9.00 and measured at pH_T 9.00 (3.31 REA g^{-1} FW) (Student's t–test, $t = 0.0625$, df = 4, $P = 0.953$, Fig. 3.4).

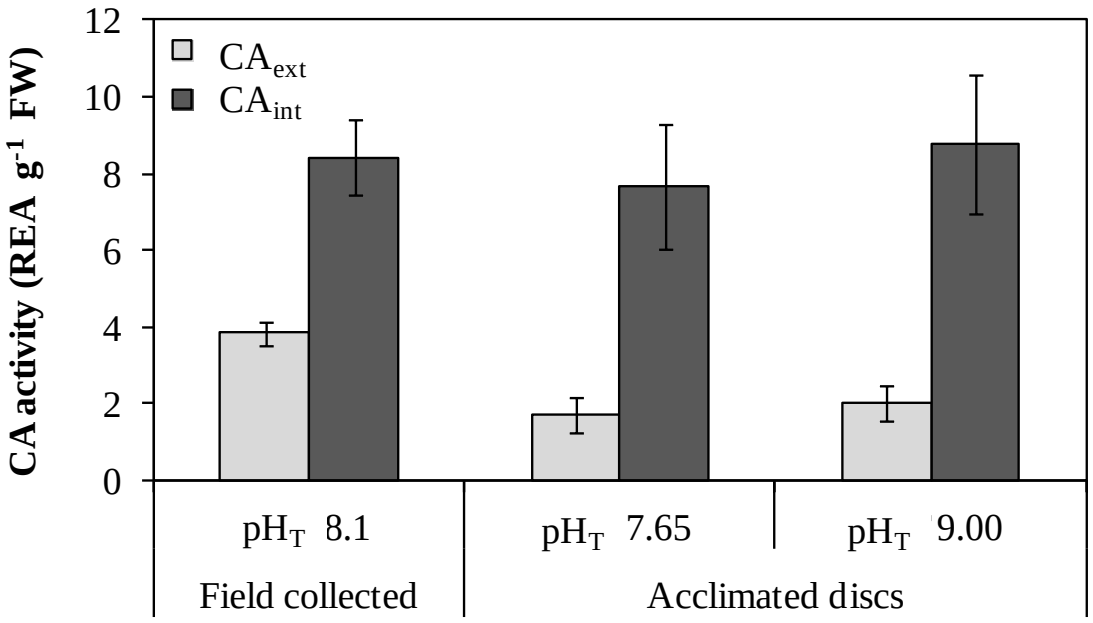

Figure 3.3: External and internal CA activities in *Macrocystis pyrifera* directly after collection (field collected material; ambient seawater pH_T = 8.10) and after two days of acclimation at pH_T 7.65 and pH_T 9.00. Values are the mean (n = 3) ± SE.

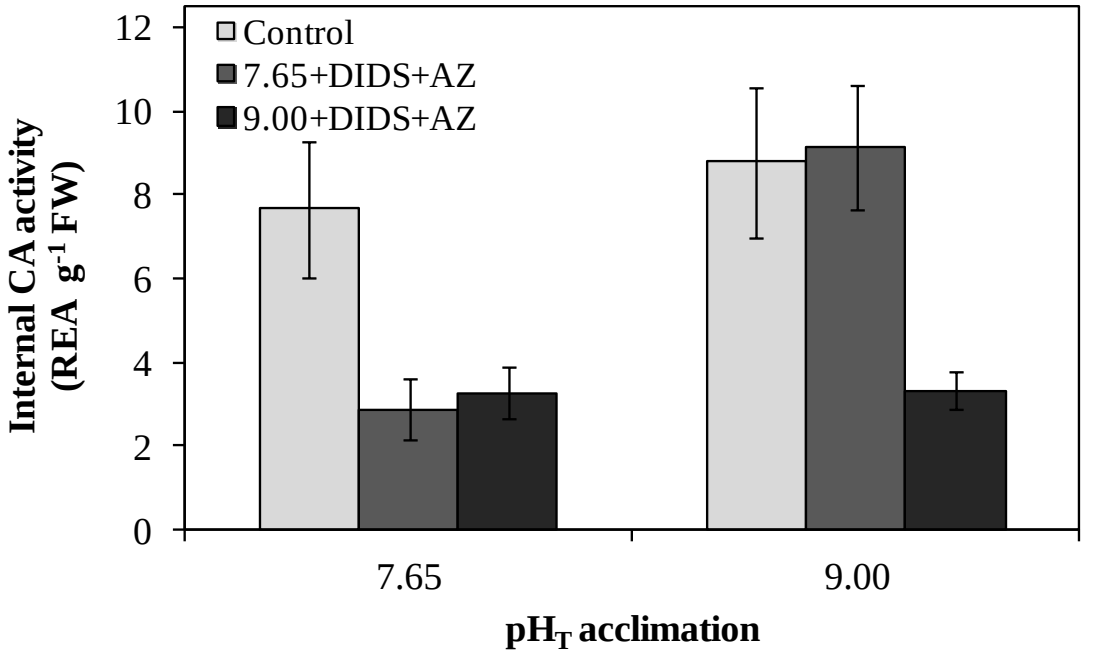

Figure 3.4: CA_{int} activity after sequential blocking of the AE protein and CA_{ext} activity by DIDS and AZ, respectively. The internal CA activity of discs acclimated for 2 days under pH_T 7.65 and pH_T 9.00 was immediately measured after photosynthetic measurements at pH_T 7.65 and pH_T 9.00, plus inhibitors and without inhibitors (control). Values are the mean (n = 3) ± SE.

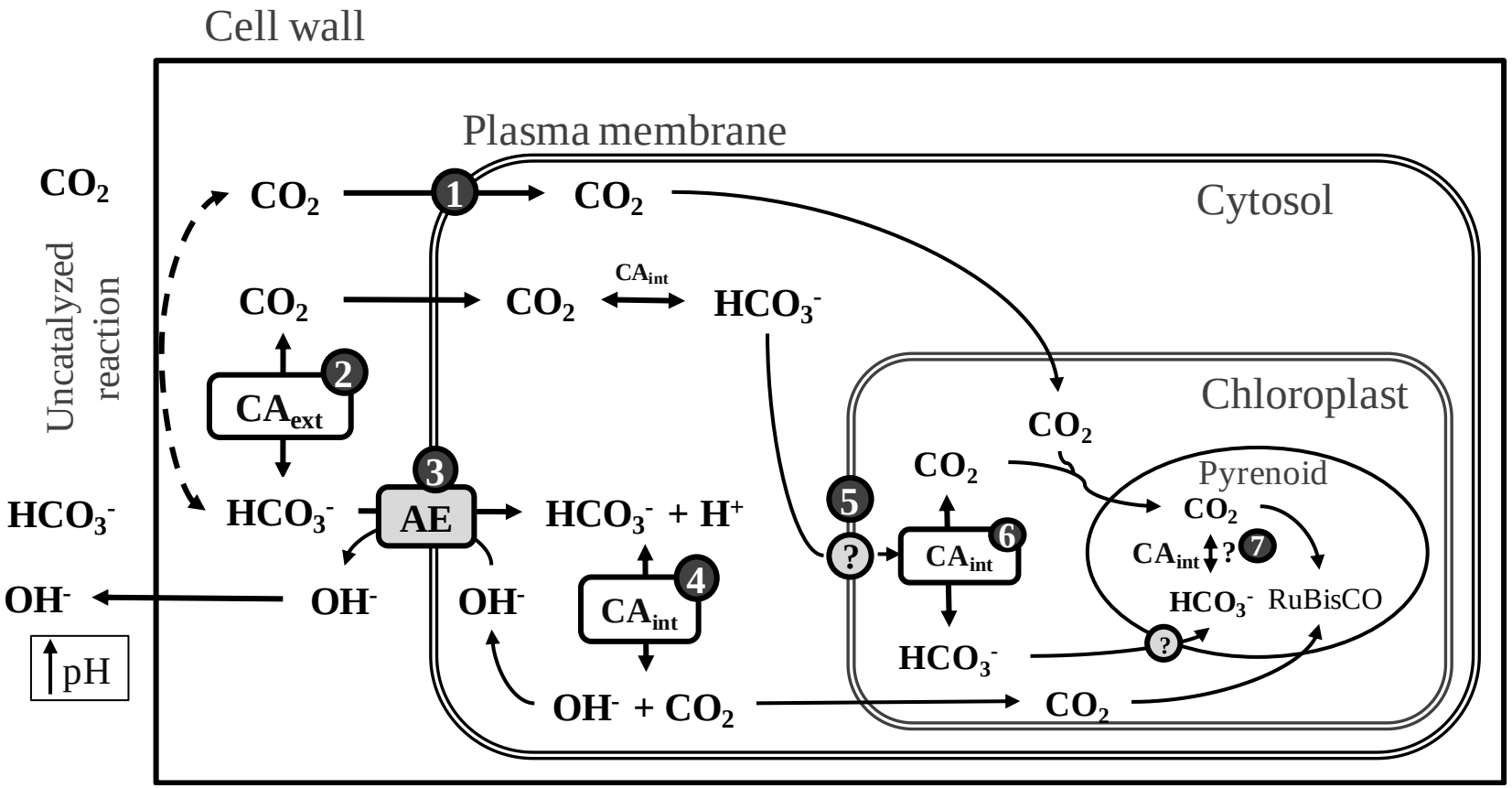

Figure 3.5: A schematic diagram on the photosynthetic carbon physiology of *Macrocystis pyrifera*: (1) passive transport of CO_2 through the plasma membrane; (2) external dehydration of HCO_3^- to CO_2, catalyzed by CA_{ext}, and CO_2 diffusion; (3) direct HCO_3^- uptake through the anion exchange (AE) protein; (4) HCO_3^-/CO_2 interconversion catalyzed by a putative CA_{int} isoform to maintain pH balance and internal Ci pool as HCO_3^-; (5) possible active transport of HCO_3^- into the chloroplast; (6–7) HCO_3^- dehydration in the chloroplast catalyzed by a putative CA_{int} isoform to supply CO_2 to RuBisCO.

3.4 Discussion

The results of this study support our first hypothesis that, for the giant kelp *Macrocystis*, HCO_3^- is the primary exogenous Ci species entering into cell to support photosynthesis. We found that the use of HCO_3^- occurs via two mechanisms: (1) the external catalyzed dehydration of HCO_3^- and (2) direct HCO_3^- uptake via an anion exchange (AE) protein (Fig. 3.5), and both external HCO_3^- dehydration and direct uptake mechanisms operate simultaneously irrespective of pH. The co–existence of both HCO_3^- utilization mechanisms has also been reported for *Ulva lactuca* (Linnaeus) (Axelsson et al. 1999), *U. intestinalis* (Linnaeus) [=*Enteromorpha intestinalis*] (Larsson et al. 1997), *Cladophora glomerata* (Linnaeus) Kützing (Choo et al. 2002) and *Gracilaria gaditana* nom. prov. (Andria et al. 1999). For *U. lactuca*, *U. instinalis* and *C. glomerata* the external HCO_3^- dehydration mechanism was predominant under lower pH whereas the direct HCO_3^- uptake was predominant under higher pH (Larsson et al. 1997, Axelsson et al. 1999, Choo et al. 2002). However, the simultaneous operation of both mechanisms under high and low pH, which we found for *Macrocystis*, has been reported only in *G. gaditana* (Andria et al. 1999). We suggest that the operation of both HCO_3^- use mechanisms in *Macrocystis*, that are functional at both pH_T 9.00 and pH_T 7.65, is required to support its high growth rate under the dynamic range of diurnally oscillating pH observed in coastal waters (Delille et al. 2000, Cornwall et al. 2013).

Our second hypothesis that the external HCO_3^- dehydration, catalyzed by CA_{ext}, is the main mechanism for Ci acquisition in *Macrocystis* was not supported. Instead, we found, for the first time, that direct HCO_3^- uptake via an AE protein is the main mechanism contributing to the internal Ci pool for *Macrocystis.* Regardless of pH–acclimation history and seawater pH during photosynthetic measurements, the inhibition of the AE protein resulted in 55–65% inhibition of *Macrocystis*

photosynthesis suggesting that it plays a crucial role in Ci acquisition. The greater inhibitory effects of DIDS compared to AZ on O_2 evolution rates of *Macrocystis* were also observed when the order of the addition of the inhibitors was reversed (AZ–DIDS; data not shown). The relatively low CA_{ext} activity observed in this study under pH_T 7.65 and pH_T 9.00 indicates that external catalyzed dehydration of HCO_3^-, and subsequent CO_2 uptake, plays a minor role in HCO_3^- use in *Macrocystis*. The high CA_{int} activity in *Macrocystis* is likely due to this enzyme actively catalyzing the dehydration of HCO_3^- that was taken up through the AE protein, to supply CO_2 to RuBisCO.

Utilization of exogenous Ci sources, CO_2 and HCO_3^-, and photosynthetic rates can affect the intracellular acid-base. Uptake of exogenous CO_2 and consequent intracellular conversion to HCO_3^- will produce H^+, while direct uptake of HCO_3^- will not. The rate of photosynthesis will also determine the amount of OH^- produced, affecting the internal acid-base balance. Different strategies might be employed by different algal groups for maintaining the intracellular acid-balance. The AE transport mechanism is involved in a one–for–one exchange of anions across the plasma membrane, i.e. in algae, the active transport of HCO_3^- into the cell might result in an outward flux of OH^- (Fig. 3.5; Smith and Bidwell 1989, Choo et al. 2002, Dreschler and Beer 1991, Beer 1994, 1996). While other mechanisms described in *Laminaria* species, i.e. *S. latissima* and *L. digitata*, depends on a plasma membrane associated H^+–ATPase pump that transports the excess cellular H^+ to the outside of the plasma membrane facilitating either a H^+/HCO_3^- co–transport or enhancement of the external uncatalyzed dehydration of HCO_3^- to CO_2 in the periplasmic space (Klenell et al. 2004, Zou et al. 2011a): these Laminariales have low levels (or even lack) of CA_{int} activity and it may be that the H^+–ATPase pump operates in lieu of CA_{int} (Mercado et al. 2006). In contrast, some green macroalgal species (e.g. *Ulva lactuca*) depend on the AE protein for Ci

acquisition along with a putative OH^- efflux (Beer 1996), and in this case the regulation of intracellular acid-base balance might be related to a high CA_{int} activity as plasma membrane associated H^+–ATPase pump has not been reported (Beer 1994, Mercado et al. 2006). Similar to *U. lactuca*, we measured high CA_{int} activity and direct HCO_3^- uptake via the AE protein in *Macrocystis*, and we suggest that a plasma membrane associated H^+–ATPase pump does not operate in *Macrocystis*.

This suggestion, that *Macrocystis* does not utilize a plasma membrane associated H^+–ATPase pump, is supported by another line of evidence. Proton buffers, e.g. Tris and Hepes are known to inhibit plasma membrane H^+–ATPase–facilitated Ci acquisition mechanism, because proton buffers dissipate any acid regions created by H^+ extrusion into the DBL, reducing effectively the photosynthetic rates (Axelsson et al. 2000, Klenell et al. 2004, Mercado et al. 2006). Application of 50 mM Tris–HCl did not reduce photosynthetic O_2 production in *Macrocystis* (preliminary experiment, data not shown) suggesting that this Ci acquisition mechanism is most likely not present in *Macrocystis*.

A direct HCO_3^- uptake mechanism had been identified, using the same AE inhibitor (DIDS) as we used, in several *Ulva* spp. (Drechsler et al. 1993, Axelsson et al. 1999, Larsson et al. 1997), and in *G. gaditana* (Andria et al. 1999), but ours is the first such record for a brown seaweed of the Order Laminariales. The other Laminariales tested, *S. latissima* and *L. digitata,* are insensitive to DIDS indicating that, in contrast to *Macrocystis,* direct HCO_3^- uptake via an AE protein is unimportant in active Ci uptake at ambient seawater pH (Larsson and Axelsson 1999). However, for *L. digitata* direct uptake via this HCO_3^- transporter may be activated at pH > 9.5 and become an important mechanism at extremely high pH (Klenell et al. 2004). Other brown seaweeds belonging to other Orders, e.g. *Endarachne binghamiae* J. Agardh (Scytosiphonales)

(Zou and Gao 2010b), *Hizikia fusiformis* (Harvey) Okamura and *Sargassum henslowianum* C. Agardh (Fucales) (Zou et al. 2003, 2011a) are also insensitive to DIDS, and they too rely primarily on the CA_{ext}–mediated external HCO_3^- dehydration to fill their internal Ci pool (Larsson and Axelsson 1999, Zou and Gao 2010b, Zou et al. 2003, 2011a).

A range of active HCO_3^- use mechanisms are utilized by various seaweeds, indicating that the uptake of Ci by the combination of CA_{ext}–mediated external dehydration of HCO_3^- plus diffusive CO_2 entry is insufficient to supply the internal Ci pool of most seaweed. Other active Ci uptake mechanisms include the HCO_3^- uptake driven by the P–type H^+ –ATPase pump described in *S. latissima*, *L. digitata* (Klenell et al. 2004), *E. binghamiae* (Zou and Gao 2010) and *C. glomerata* (Choo et al. 2002). For *Macrocystis*, regardless of pH acclimation history in this study, the low CA_{ext} activity (1.70 and 2.00 REA g^{-1} FW) suggests that externally catalyzed HCO_3^- dehydration is insufficient to fill the internal Ci pool to support the high growth rate of this species. However, the small brown seaweed *Hizikia fusiformis*, has a much higher CA_{ext} activity (17.3 and 9.5 REA g^{-1} FW; Zou et al. 2003) than *Macrocystis*, and no known other active Ci transport mechanisms, suggesting that for this species CA_{ext} + diffusive uptake of CO_2 may be sufficient to support its metabolic requirements. The question of if the suite of carbon uptake mechanisms employed by seaweed vary with seaweed size/growth rate would be an interesting line of enquiry.

In this study, the high CA_{int} activity, responsible for the inter–conversion of HCO_3^- and CO_2, is consistent with its function to maintain intracellular acid–base balance (Smith and Raven 1979) and the supply of CO_2 to RuBisCO. Different isoforms of CA_{int} may deliver different functions, e.g. cytosolic CA is responsible for keeping the equilibrium between these Ci forms and thus regulate the internal pH in the cytosol and

Ci storage in the form of HCO_3^- to limit CO_2 leakage when the concentration gradient is higher inside the cell, while CA on the plastid envelope and stroma is for the supply of CO_2 to RuBisCO (Lucas 1983, Spalding 2008, Moroney et al. 2001).

When the known HCO_3^- use mechanisms of *Macrocystis* were blocked, the CA_{int} activity was still detectable but was lower than the control. This is may be due to the reduced entry of new Ci into the cell and the possible direct use of diffusive CO_2 for photosynthesis. The unexpected higher CA_{int} activity for discs acclimated at pH_T 9.00 and measured at pH_T 7.65 requires further study. Here we suggest a possible 'luxury uptake' by passive CO_2 diffusion from the external medium into the cell, the CO_2 subsequently needs to be converted to HCO_3^- to prevent CO_2 leakage out of the cell and to accumulate internal Ci pool as HCO_3^-. However, this was not observed in discs acclimated at pH_T 7.65 and measured under the same pH. This acclimation–specific response might be related to the internal regulation of OH^- and H^+.

Our third hypothesis that under higher concentrations of CO_2 (pH_T 7.65), diffusive uptake of CO_2 will support photosynthesis when HCO_3^- dehydration and other HCO_3^- uptake mechanisms are blocked by inhibitors was supported. We found that when all known HCO_3^- uptake mechanisms are blocked by inhibitors at pH_T 7.65, (Fig. 3.2a) the higher CO_2 concentration of the seawater was able to support 30% of the photosynthesis in *Macrocystis.* The elevated CO_2 at low pH may allow higher CO_2 uptake to fill the Ci pool and may directly supply CO_2. Such a rapid initial CO_2 uptake has been shown in cyanobacteria (*Synechoccus sp*.), where CO_2 is the main substrate for Ci uptake within the first seconds after illumination, and HCO_3^- uptake is slowly activated in the following 20–60 s (Badger et al. 1985, Bédu et al. 1989, Price et al. 2008). However, before all of the known HCO_3^- use mechanisms were blocked, the photosynthetic rate of *Macrocystis* was not enhanced by elevated CO_2 (pH_T 7.65);

similar photosynthetic rates were measured under ambient SW carbonate chemistry (pH_T 8.10; see Results).

The response of seaweeds to future elevated CO_2 will depend on their carbon physiology, e.g. strictly CO_2–user versus mixed CO_2 and HCO_3^- user (Hurd et al. 2009). However, most seaweeds have evolved an effective Ci–use strategy to compensate for the low availability of CO_2 (Giordano et al. 2005). The direct and indirect use of HCO_3^- ions demonstrate that for most micro– and macroalgal species, photosynthesis is already saturated under the current seawater Ci concentration (Beer 1994, Beardall et al. 1998). Moreover, Ci use mechanisms can be modulated by the environment (Giordano et al. 2005). Therefore it is unlikely that the future elevated CO_2 (~40.35 µM) or the small increase in HCO_3^- ion concentration (~190 µM) will substantially stimulate photosynthesis in species that use HCO_3^- (Beardall et al. 1998), as we found for *Macrocystis*. However, after a period (several days to months) of elevated CO_2 acclimation some species may down–regulate their direct and/or indirect HCO_3^- use mechanisms (Zou et al. 2003, 2011b, Hurd et al. 2009, Stojkovic et al. 2013), an idea that requires experimental testing.

Our study looks at the mechanisms of Ci acquisition in one of the most ecologically important coastal primary producers. Knowledge of its carbon physiology is very important for understanding the ecological impact of OA. Aside from acidification, the world's ocean is also getting warmer. The surface ocean temperature is predicted to increase between 1.4 and 5.8 ˚C by 2100 (IPCC, 2013). The interactive effect of OA and ocean warming is reported to increase *Macrocystis* spore mortality (Gaitán–Espitia et al. 2014). Long–term studies through the whole life cycle, including microscopic (i.e. spores and gametophytes) and macroscopic (i.e. sporophytes) stages and different generations (successive cohorts of sporophytes), and the interactive effects

of OA and ocean warming may show different responses and thus warrant further investigation.

In summary, *Macrocystis* is primarily dependent on HCO_3^- as an exogenous Ci source, and up to 99% of its photosynthesis was arrested when both HCO_3^- uptake mechanisms, direct HCO_3^- uptake via an AE protein and external HCO_3^- dehydration mediated by CA_{ext}, were blocked at pH_T 7.65 (HCO_3^-: CO_2 = 51:1) and pH_T 9.00 (HCO_3^-: CO_2 = 940:1). We suggest that, for the giant kelp *Macrocystis*, the direct HCO_3^- uptake via an AE protein and/or its preference for HCO_3^- as the main exogenous Ci source will not be affected by higher CO_2 concentrations and lower pH under a future OA scenario. However, further long–term studies (several days to months) on elevated CO_2 acclimation will be important to elucidate if *Macrocystis* can down–regulate its direct and/or indirect HCO_3^- use mechanisms under OA. Finally, the mechanism of HCO_3^- uptake in *Macrocystis* (AE protein) differs from that found in other members of the Order Laminariales (CA_{ext} + H^+–ATPase; *S. latissima* and *L. digitata*, Larsson and Axelsson 1999, Klenell et al. 2004), highlighting that a variety of Ci uptake strategies are employed by seaweeds, even those within the same Order; understanding how seaweed–based ecosystems might respond to a future high CO_2 ocean will require fundamental information on species–specific carbon uptake mechanisms.

Chapter 4: Effects of ocean acidification on the photosynthetic performance, carbonic anhydrase activity and growth of the giant kelp *Macrocystis pyrifera*

4.1 Introduction

Over the last 200 yr, the atmospheric CO_2 pool has increased by ~ 3.3 Pg C yr^{-1}, from a value of ~280 (28 Pa) in 1800 to 395 µatm (39 Pa) at the present, due to human activities such as burning fossil fuels, deforestation, cement manufacture, and others land-use changes (Caldeira and Wickett 2003; Beardall and Raven 2004, The Royal Society 2005). This trend is projected to continue by a minimum rate of 0.5% per year throughout the next century, reaching values of ~1000 µatm of CO_2 by 2100 (IPCC 2013). Approximately one third of these CO_2 emissions will be absorbed by the world's oceans, increasing $CO_{2(aq)}$ and decreasing the pH of the surface waters, making them more acidic and altering the seawater carbonate chemistry, a process known as ocean acidification (OA) (The Royal Society 2005; Guinotte and Fabry 2008). By 2100, the $CO_{2(aq)}$ concentration will be double the existing level, leading to an estimated drop in pH of 0.3–0.4 units from the current global ocean surface average of ~8.15 to 7.75 (IPCC 2013). These predicted changes in seawater carbonate chemistry can influence important biological and physiological processes of calcifying and non-calcifying marine organisms (both autotrophs and heterotrophs) (The Royal Society 2005).

Seaweeds are the base of the food web and major contributors to benthic primary production in coastal ecosystems (Charpy-Roubaud and Sournia 1990; Bensoussan and Gattuso 2007). To support photosynthesis and growth, seaweeds require an exogenous inorganic carbon (Ci) source. Today's oceans contain approximately 2.1 mol m^{-3} of dissolved inorganic carbon (DIC), which exists as bicarbonate (HCO_3^-), carbonate

(CO_3^{2-}) and dissolved carbon dioxide ($CO_{2\ (aq)}$); only CO_2 and HCO_3^- can be used as CO_2 source for photosynthesis.

CO_2 is the substrate for photosynthesis and $CO_{2(aq)}$ diffuses easily into algal cells, but only 1% of Ci present in today's oceans exists as CO_2 while 91% exists as HCO_3^-, which cannot diffuse through the lipid bilayer of the plasma membrane (Raven 1997). Consequently photosynthesis of seaweeds would be severely carbon limited if they were dependent only on the diffusive entry of CO_2 from the medium to the site of fixation via the carbon assimilating enzyme RuBisCO, a bifunctional enzyme that fixes both CO_2 and O_2 (Beardall et al. 1998; Kawamitsu and Boyer 1999). Therefore, is not surprising that most seaweeds are able to utilize HCO_3^- from the bulk seawater (Maberly 1990; Raven and Hurd 2012). The HCO_3^- transported into the cell can be either accumulated as an internal Ci pool or converted to CO_2 via an intracellular carbonic anhydrase (CA_{int}). The CO_2 produced by CA_{int} then diffuses to the active site of RuBisCO, thereby increasing the CO_2 concentration and improving the efficiency of CO_2 fixation in the presence of O_2 (Magnusson et al. 1996; Kawamitsu and Boyer 1999; Beardall et al. 2005).

These mechanisms, termed CO_2 concentrating mechanisms (CCMs), are found in most of the algae to overcome the deficiencies of RuBisCO and to compensate for the low availability of $CO_{2(aq)}$ (Giordano et al. 2005). CCMs are quite diverse, but in all cases, they are composed principally of at least three functional elements: (1) influx of CO_2^- and/or HCO_3^-, (2) active capture of Ci into the cell (usually accumulated internally as HCO_3^-) and (3) production of CO_2 from the Ci pool around RuBisCO. The wide range of effective Ci-use strategies observed in seaweeds suggests that photosynthesis is saturated under the current Ci concentration in seawater (Beer 1994; Beardall et al. 1998).

The response of seaweeds to a future elevated CO_2 concentration can be heterogeneous and species-specific relative to their carbon physiology. For example, for species that are strictly CO_2-users, the increase in CO_2 concentrations may increase diffusive entry of CO_2 into the cell, and could reduce the energy cost for active Ci uptake mechanisms required to increase internal Ci accumulation; the energy saved could enhance growth (Raven 1991; Kübler et al. 1999). For mixed CO_2 and HCO_3^- users, direct and/or indirect mechanisms for HCO_3^- acquisition may be down-regulated (Magnusson et al. 1996; Madsen and Maberly 2003; Hurd et al. 2009). Two main mechanisms for HCO_3^- acquisition by seaweed are: (1) the extracellular catalyzed dehydration of HCO_3^- to CO_2, mediated by external carbonic anhydrase (CA_{ext}), an enzyme that is located in the cell wall in the majority of seaweeds: the resulting CO_2 is then taken into the cell by passive diffusion, and (2) direct HCO_3^-uptake through the plasma membrane via an anion exchange (AE) protein (Drechsler et al. 1993; Axelsson et al. 1999 2000; Giordano et al. 2005). However, the first mechanism seems to be the most prevalent for HCO_3^- utilization among seaweeds (Israel and Hophy 2002), but it may be non-functional under high pH (>9.00), whereas direct HCO_3^- uptake operates equally well at pH 8.4 and 9.4 (Axelsson et al. 1995, Fernández et al. 2014). Thus, a seaweed's response to elevated CO_2 concentration will depend not only on which Ci source it uses to support photosynthesis, but also on the mechanism(s) of Ci acquisition.

Consequently, the future increase in $CO_{2(aq)}$ and HCO_3^- concentrations, and the change in the relative proportions of each, could affect differently the photosynthesis and growth of different species of seaweed. It has been suggested that neither photosynthesis nor growth will be affected by elevated $CO_{2(aq)}$ concentrations for macroalgal species that possess an effective CCM and are therefore capable of using HCO_3^- (Beardall 1998; Israel and Hophy 2002). However, for some HCO_3^--using

species, photosynthesis may be carbon-limited and for these species, as well as for non-bicarbonate users, a positive response to increased $CO_{2(aq)}$ might be expected (Kübler et al. 1999; Zou 2005, Suárez-Álvarez et al. 2012). Other studies have shown negative effects of elevated $CO_{2(aq)}$ on photosynthetic rate, pigment content (Garcia-Sanchez et al. 1994) and/or growth of seaweeds (Swanson and Fox et al. 2007; Gutow et al. 2014). Furthermore, little attention has been paid to the effects of elevated $CO_{2(aq)}$ on chemical composition, for example, changes in cellular carbon and nitrogen content have been reported in *Porphyra leucosticta* when $CO_{2(aq)}$ was increased (Mercado et al. 1999). Therefore, the response of seaweeds to a future elevated $CO_{2(aq)}$ concentration might be complex and species-specific depending on the effective Ci-use strategy present in the alga.

Macrocystis pyrifera is a dominant, highly productive brown seaweed of temperate coastlines of the west coast of North America and southern hemisphere (Hay 1990; Graham et al. 2007). It is known to be a mixed CO_2 and HCO_3^- user (Hepburn et al. 2011) and two HCO_3^- utilization mechanisms have been described for this species: (1) extracellular catalyzed dehydration of HCO_3^- mediated by CA_{ext}, (Huovinen et al. 2007; Rothäusler et al. 2011; Fernández et al. 2014), and (2) direct HCO_3^- uptake via an AE protein (Fernández et al. 2014). However, the main mechanism of HCO_3^-utilization has been attributed to the direct uptake via the AE mechanism with CA_{ext} making little contribution (Fernández et al. 2014). The goal of this study was to examine how *Macrocystis* is affected by the changes in the carbonate system predicted for 2100 compared to today's conditions. This was achieved by investigating the growth and photosynthetic rates, external and internal carbonic anhydrase activity (CA), HCO_3^- vs CO_2 use, and carbon and nitrogen content, following 7 days' culture at current seawater conditions (ambient treatment: pCO_2 400 µatm; pH 8.00) and a worst case scenario

treatment predicted for 2100 (OA treatment: pCO_2 1200 µatm; pH 7.59). We hypothesized that (1) the affinity of *Macrocystis* for HCO_3^- as a Ci source will decrease after a 7 d incubation in the OA treatment compared to the ambient treatment, but (2) there will be no effect of pCO_2/pH treatment on the rates of photosynthesis and growth.

4.2 Materials and Methods

4.2.1 Seaweed collection and culture maintenance

During low tide in the austral summer 2012, one vegetative apical scimitar, i.e. the youngest blade (Leal et al. 2014), was cut off > 60 individual adult *Macrocystis* sporophytes inhabiting the upper subtidal in Aramoana (45°47'S, 170°43'E), Otago Harbour, New Zealand. Blades were transported to the laboratory in an insulated bin with ambient seawater (SW). In the laboratory, the blades of each apical scimitar were gently rinsed and cleaned of visible epibionts with natural seawater (NSW). Seawater used in the study was collected from Otago Harbour, New Zealand (45˚52.51'S, 170˚30.9'E) stored in a 1000 L plastic tank. For all experiments, SW was filtered using Filter Pure polypropylene spun melt (0.5 µm pore size) and UV sterilized, with an Aquastep 25 W Ultraviolet Sterilizer.

From each of the 60 collected blades, young meristematic discs were excised from the apical scimitar blades, using a 20 mm diam. cork borer, at 2 cm from the bulb-blade junction. For the Ci acquisition mechanism experiments, i.e. pH drift and inhibition of photosynthesis, one disc (0.07–0.08 g FW) was excised from each of 26 blades. These 26 discs were cultivated together in a 5 L culture flask bubbled with air. For the photosynthetic physiology and growth experiments, four discs (0.05–0.06 g FW) per blade were cut from the remaining 34 blades, and each group of four discs was grown together in an individual culture chamber (650 mL) of an automated pH-controlled culture system (McGraw et al. 2010; see below). The final ten discs were used to assess the initial physiological status of the discs (external and internal CA activity (n = 6), and stable isotope signature ($\delta^{13}C$ and $\delta^{15}N$) and total tissue carbon and nitrogen content (both n = 4)). All experimental discs were maintained in the laboratory

for at least 12 h to 2 days to heal marginal wounds. Prior to experiments, and during experiments, the cultures were maintained in a growth cabinet (Contherm Plant Growth Chamber, Contherm Scientific Co. Ltd., New Zealand) at 12 °C under a 12:12 h light:dark photoperiod and saturating light of 110 µmol photons m^{-2} s^{-1} of PAR. Incident light was provided overhead by metal halide lamps (Philips HPI- T 400 W quartz) and measured using a 4π-sensor (QSL-2101, Biospherical Instruments Inc., San Diego, CA, USA). Physiological measurements, i.e. photosynthesis and pH drift experiments, were conducted under the same experimental conditions.

4.2.2 Effect of internal and external CA inhibitors on photosynthetic rates of field-collected samples

The effect of highly-specific external and internal CA inhibitors on the photosynthetic rate of *Macrocystis* was investigated to determinate the contribution of CA to Ci uptake. Field-collected discs, acclimated for 2 days in the laboratory, were exposed to different pH treatments representing different HCO_3^-: CO_2 ratios and $CO_{2\ (aq)}$ availability: pH 7.59 (HCO_3^-: CO_2 = 2147 µmol kg^{-1}: 48 µmol kg^{-1}), pH 8.00 (1912 µmol kg^{-1}: 17 µmol kg^{-1}ratio), and pH 9.00 (1138 µmol kg^{-1}: 1.2 µmol kg^{-1}). Seawater pH was adjusted using NaOH, $NaHCO_3$, and HCl described in Roleda et al. (2012b).

The specific inhibitors used were acetazolamide (AZ), to which cell membranes are only weakly permeable and it thus inhibits only external CA (Moroney et al. 1985), and ethoxyzolamide (EZ) which passes readily through cell membranes and therefore inhibits both external and internal CA. The flux of AZ through the cell membrane is 1000-times slower than that of EZ (Geib et al. 1996). These inhibitors have been used together in many algal studies to show the relative contribution of both enzymes to photosynthetic Ci uptake (Haglund et al. 1992a; Axelsson et al. 1995; Mercado et al.

1997; Badger et al. 1998; Andría et al. 2001; Peréz-Lloréns et al. 2004; Mercado et al. 2006; Ihnken et al. 2011). Both AZ and EZ were prepared as stock solutions of 0.05 M in 0.05 M of NaOH in MilliQ water (Peréz-Lloréns et al. 2004). Final concentrations of 100 µM of AZ and EZ were used to inhibit CA_{ext} and CA_{int}, respectively. The effect of these inhibitors was tested on the photosynthetic rate of *Macrocystis* measured at pHs: 7.59; 8.00 and 9.00 (n = 6 in each pH treatment).

For photosynthetic measurements (procedure described below), individual discs (0.07–0.08 g FW) were separately enclosed in a 154 mL acrylic chamber, containing the pH-adjusted seawater. When steady-state photosynthesis had been reached (after 20 min), the inhibitors were injected into the culture chamber, one at the time. The inhibitor AZ was injected first to a final concentration of 100 µM (Axelsson et al. 1995). After 15 minutes, the inhibitor EZ was injected to a final concentration of 100 µM (Axelsson et al. 1995). As CA_{ext} was already blocked, the inhibitory effect of EZ was used to account only for the relative internal CA activity. Initial photosynthetic rates (without inhibitors) and the % inhibition on photosynthetic rates by each inhibitor were determined under each pH treatment in the same manner and experimental set-up as described in Fernández et al. (2014).

4.2.3 Incubation under pCO_2 400 µatm and 1200 µatm

After two days' acclimation, each culture chamber containing the 4 *Macrocystis* discs (each of 0.05–0.06 g FW, with a total weight per tank of 0.195 ± 0.029 g FW), was randomly assigned to 2 pCO_2/pH treatments: ambient (pCO_2 400 µatm; pH 8.00) and OA (pCO_2 1200 µatm; pH 7.59) (n = 12 replicates for each treatment). These treatments are representative of the current and future seawater carbonate system predicted for 2100 under a business-as-usual scenario (Table 1). The pCO_2 concentration of 1200

µatm is slightly higher than the maximum of 1142 µatm predicted by 2100 (IPCC 2013).

The experiment was performed in an automated pH-controlled culture system described by McGraw et al. (2010) and modified by Cornwall et al. (2013). The filtered NSW used for the experiment was enriched with 50 µM NO_3^- and 5 µM H_2PO_4. The ambient, nutrient-enriched seawater (pH 8.00) was adjusted using equal amount of 0.2 M HCl and 0.2 M $NaHCO_3^-$ to achieve the OA treatment (pCO_2 1200 µatm; pH 7.59); this acid-base manipulation is chemically the same as bubbling with CO_2 (Gattuso et al. 2010). The system continuously supplies either control (ambient SW pH ~8.00) or pH-adjusted (pH 7.59) seawater to each of the 24 culture chambers. The sequence is randomized and the SW in each culture chamber is replaced every 4.4 h. The pH is measured spectrophotometrically to an accuracy of ± 0.01 units, on the total scale (pH_T) (McGraw et al. 2010). Each culture chamber was equipped with a magnetic stirrer and sat on a stirring plate set at 650 rpm to vigorously mix the SW and minimize diffusion boundary layer at the surface of the blade discs (see Cornwall et al. 2013 for details).

After the first cycle of exposure to the corresponding pCO_2/pH treatment (4.4 h after the start of the experiment), one disc was removed from each of the 24-culture chambers to assess its physiological and biochemical status. Thereafter, 1 disc was removed on days 3 and 7 of the incubation.

4.2.4 pH drift experiment

To determine whether *Macrocystis* was using HCO_3^-, the pH drift method was used; the ability of the algal disc to raise the seawater pH to > 9.00 is evidence of its capacity to use HCO_3^- (Maberly 1990). The carbon-use mechanism of *Macrocystis* was investigated immediately after collection (initial seawater pH of 7.98; n = 8) and after 7

days' incubation in the ambient and OA treatments (n = 4). Discs were individually incubated in a 20 mL sealed transparent glass container containing either 20 mL of filtered NSW (pH 8.00) or pH-adjusted (pH 7.59) seawater, depending on which experimental treatment were grown in. The experiments were conducted following the methods detailed in Hepburn et al. (2011) except that pH drift was recorded over a 12 h incubation. A blank control, i.e. without algae, showed no change in the seawater pH after 12 h of incubation.

4.2.5 Photosynthetic rates

Photosynthesis was measured as O_2 evolution inside an acrylic chamber (154 mL) equipped with an fiber optic FOXY-R probe coupled to a USB-2000 spectrophotometer (Ocean Optics, Florida, USA), connected to a laptop. The chamber was equipped with a magnetic stirrer and sat on a stirring plate at 650 rpm. To avoid O_2 concentrations inside the chamber increasing to a level that might cause photo-respiration, the seawater was initially bubbled with N_2 to reduce the O_2 concentration from 271 µM to the experimental starting concentration of 100 ± 20 µM O_2. A single *Macrocystis* disc was then enclosed in the acrylic chamber contained either 154 mL of NSW (pCO_2 400 µatm; pH 8.00) (n = 4) or pH-adjusted NSW (pCO_2 1200 µatm; pH 7.59) (n = 4) under saturating light 110 µmol m^{-2} s^{-1}. O_2 evolution was registered for 40 min for each. The O_2 concentration was expressed as µM, as calculated using the formulas and coefficient of Millero and Poisson (1981) and Garcia and Gordon (1992). The photosynthetic rates were calculated using linear regression over the last 10 min of incubation and standardized to corresponding sample fresh weight. At the end of each photosynthetic measurement, the disc was dried for 48 h at 60 °C for subsequent determination of C/N content and stable isotopes. The pH before and after photosynthetic measurement was used as a proxy to determine the preference for HCO_3^- or CO_2 as a Ci source.

4.2.6 Carbonic anhydrase activity

The activities of CA_{ext} and CA_{int} of field collected discs (n = 5) and discs incubated under ambient and OA treatment after 1, 3, and 7 days were measured using the method of Haglund et al. (1992a) with some modifications for this species (Fernández et al. in prep.). The assay was carried out in 10 mL of Tris buffer (pH 8.5) (containing 2 mM DTT, 15 mM ascorbic acid, 5 mM Na_2-EDTA, and 0.3% w/v PVP) held at 0 ± 2 °C. Frozen discs (0.06 ± 0.02 g FW) were initially analyzed for CA_{ext} activity and then used for CA_{int} measurements. For CA_{ext} measurements, one disc was transferred into the vial containing 10 mL of the assay buffer and when pH stabilized at 8.3, the reaction was started by adding 5 mL of ice-cold CO_2-saturated MilliQ water. The time taken for the pH to drop 0.4 units, from 8.3 to 7.9, was recorded. Temperature and pH were simultaneously measured using a ROSS electrode (Orion 8107BNUMD) coupled to Orion 3-Stars Plus pH Benchtop meter (Orion, Thermo Scientific). For measurements of CA_{int} activity, the same method as described above was used, but the disc was ground to a fine powder in liquid N_2-frozen mortar and pestle. The relative enzyme activity (REA) was determined using the equation: $REA = (T_b/T_s) - 1$,where T_b and T_s are the times in seconds required to drop 0.4 pH units in the uncatalyzed buffer (T_b, without algae) and in the enzyme-catalyzed reaction of the sample (T_s), respectively. The REA was standardized to the corresponding sample fresh weight.

4.2.7 Growth rate

The relative growth rate (RGR, % d^{-1}) was determined according to Zou (2005): $RGR = \ln(W_t/W_0) \times t^{-1} \times 100$, where W_0 is the initial FW and W_t is the final FW after *t* days of incubation. Discs were gently blotted dry with tissue, before weighing, to remove excess water. Growth rates were determined on days 3 (n = 12) and 7 (n= 12) under

each pCO_2/pH treatment. After measuring growth (n = 12) on days 3 and 7, 8 replicates were frozen for CA determinations and 4 replicates were used to measure photosynthetic rates as described above. At the end of each photosynthetic measurement, the disc was dried for 48 h at 60 °C for subsequent determination of total tissue C/N content and stable isotopes.

4.2.8 Total tissue C/N content and stable isotopes

Dried samples were ground to a fine powder using a mortar and pestle, and stored in micro-centrifuge tubes. The total tissue C and N content and stable isotopes (δ^{15}N and δ^{13}C) were assayed by combustion of the whole material (1 mg) using a Carlo Erba NC2500 elemental analyzer (CE instrument, Milan) and measured using a Europa scientific '20/20 Hydra' (Europa Scientific, UK) isotope ratio mass spectrometer (IRMS) in continuous flow mode. Raw isotopes ratios were normalized to the IAEA (International Atomic Energy Agency) reference material and the standards USGS-40 and USGS-41.

4.2.9 Metabolically-induced ΔH^+ and inorganic carbon uptake

The pH before and after each of the 40-min photosynthesis experiments, described above, was recorded to calculate pH change in a closed system, expressed as ΔH^+ (Roleda et al. 2012b). Further, on day 1 of the 7-day incubation experiment in the automated pH-controlled culture system, the seawater from each of the 24-culture chambers was collected after the seawater-exchange cycle (4.4 h) to measure A_T, DIC and pH. The change in SW carbonate chemistry parameters between time zero of the control of both pCO_2/pH treatments and corresponding after 4.4 h was used as a proxy for Ci uptake in *Macrocystis* (n = 3). HCO_3^- and CO_2 uptake rates by *Macrocystis* were calculated by the disappearance of Ci from the medium after 4.4 h, and standardized by

the algal fresh weight (g) and time (h). Carbonate chemistry parameters in the SW samples were analyzed as described below.

4.2.10 Seawater carbonate chemistry and nutrient concentrations

The SW samples collected from each of the 24 culture chambers and controls were fixed with mercuric chloride. Total alkalinity (A_T) was measured using the closed-cell titration method and dissolved inorganic carbon (DIC) was measured directly by acidifying the sample (Dickson et al. 2007). A_T, DIC, pH, salinity, and temperature were used to calculate carbonate chemistry parameters using the program $SWCO_2$ (Hunter 2007) (Table 4.1).

Inorganic nutrient concentrations were measured for each pCO_2/pH treatment. SW samples were taken on days 1 and 7 from each culture chamber at the beginning and after the first cycle of incubation (time 0 and after 4.4 h). SW samples were frozen at –20 ˚C until defrosted and analyzed for nitrate (NO_3^-) and phosphate (PO_4^-) using a QuickChem 8500 series 2 Automated Ion Analyzer (Lachat Instrument, Loveland, USA).

4.2.11 Statistical analyses

Statistical significant differences between treatments were detected using either analysis of variance (ANOVA, $P < 0.05$) or Student's t-test ($P < 0.05$) after homogeneity (Levene's test) and normality (Shapiro-Wilk test) of data were satisfied. Significantly different groups were classified after Tukey's HSD tests ($P = 0.05$). All analyses were performed using the statistical program SigmaPlot 11.0 (Systat Software, Inc.).

4.3 Results

4.3.1 Effect of internal and external CA inhibitors on photosynthetic rates of field-collected samples

Photosynthetic rates of *Macrocystis* discs measured at low (7.59), current (8.00), and high seawater pH (9.00) were not significantly different (ANOVA: $F_{3,7} = 0.480$, $P = 0.628$, Fig. 4.1 inset). After the sequential application of the external and internal CA inhibitors, photosynthetic rates of *Macrocystis* were significantly reduced by 48% across all pH treatments. AZ inhibited photosynthesis by 25–28% across pH treatments. No significant differences were found between pH treatments (ANOVA: $F_{3,7} = 0.299$, $P = 0.746$, Fig. 4.1). Similarly, EZ inhibited photosynthetic rates of *Macrocystis* discs by a further 19–24% across all pH treatments, and no significant differences were found between pH treatments (ANOVA: $F_{3,8} = 0.191$, $P = 0.829$, Fig. 4.1).

4.3.2 pH drift experiment

The field-collected discs incubated under ambient SW (pH 7.98) were able to raise the SW pH by 1.18 units to pH 9.16 ± 0.01 (±SE) (n = 8, Fig. 4.2). Likewise, discs incubated for 7 days either under ambient (pCO_2 400 µatm; pH 8.00) or OA treatment (pCO_2 1200 µatm; pH 7.59), and measured under the same initial pH (8.00 or 7.59), were able to raise seawater pH to 9.09 ± 0.03 and pH 9.01 ± 0.09 (±SE), respectively (Student's t-test, $t = 0.935$, df = 5, $P = 0.393$, Fig. 4.2). The relative increase in pH units, expressed as ΔH^+, was greater under the OA treatment compared to ambient (Student's t-test, $t = -39.189$, df = 5, $P < 0.001$, Fig. 4.2).

Table 4.1: Seawater chemistry, carbonate parameters were calculated from the total alkalinity (A_T, n = 2) and DIC (n = 2) measurements of seawater corresponding to each pCO_2/pH treatment. Standard deviations (in parentheses).

	pCO_2-Treatment	
Carbonate Chemistry	**Ambient$_{400\ \mu atm}$**	**OA$_{1200\ \mu atm}$**
pH	8.05	7.59
DIC (µmol kg^{-1})	2043 (0.50)	2156 (0.26)
A_T (µmol kg^{-1})	2217 (0.53)	2195 (0.26)
HCO_3^- (µmol kg^{-1})	1897 (0.46)	2053 (0.25)
Dissolved CO_2 (µmol kg^{-1})	17 (0.01)	50 (0.01)
CO_3^{2-} (µmol kg^{-1})	128 (0.03)	53 (0.01)
pCO_2 (µatm)	447 (0.11)	1242 (0.27)

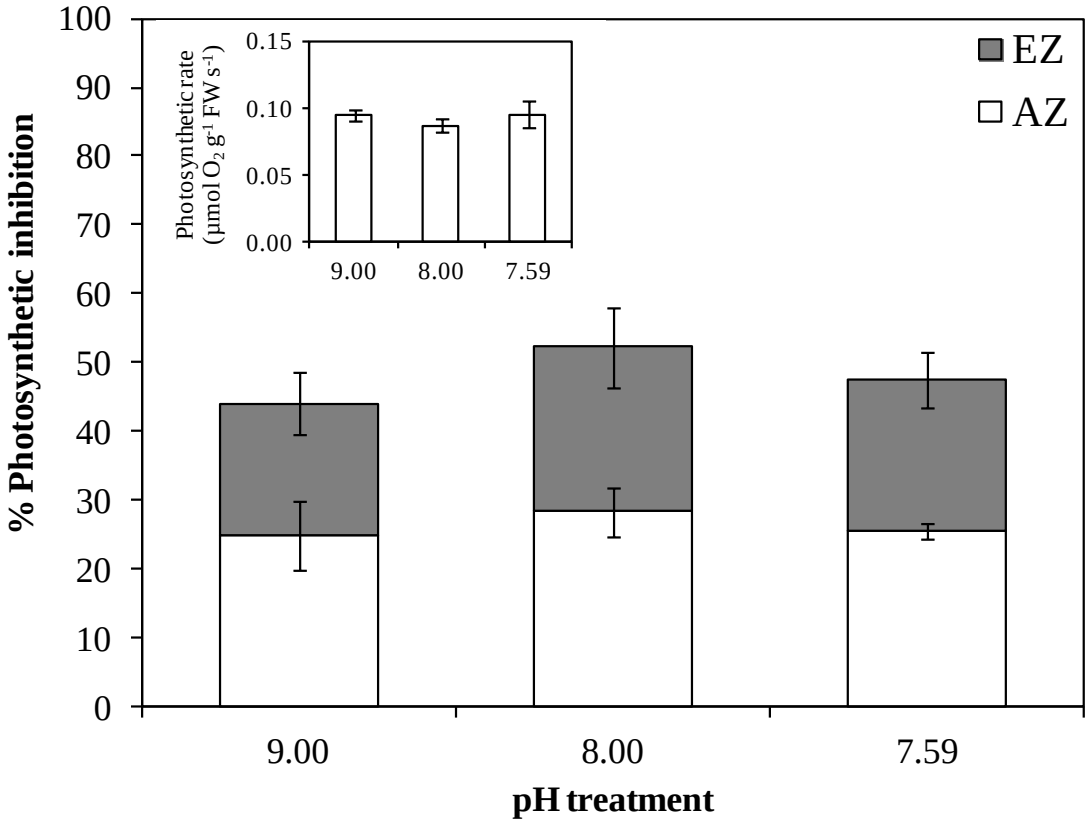

Figure 4.1: Initial photosynthetic rates of field collected *Macrocystis* discs exposed to different pH after two day acclimation at 12 ˚C under saturating light intensity (inset). The effect of inhibitor additions (AZ and EZ) on the photosynthetic rate of *Macrocystis*, expressed as % of inhibition of the initial NPS, measured under different pH treatments that represent different HCO_3^-:CO_2 ratios: pH 7.59 = 2147 µmol kg^{-1}: 48 µmol kg^{-1}; pH 8.00 = 1912 µmol kg^{-1}: 17 µmol kg^{-1}, and pH 9.00 = 1138 µmol kg^{-1}: 1.2 µmol kg^{-1}. Values are the mean (n = 6) ± SE.

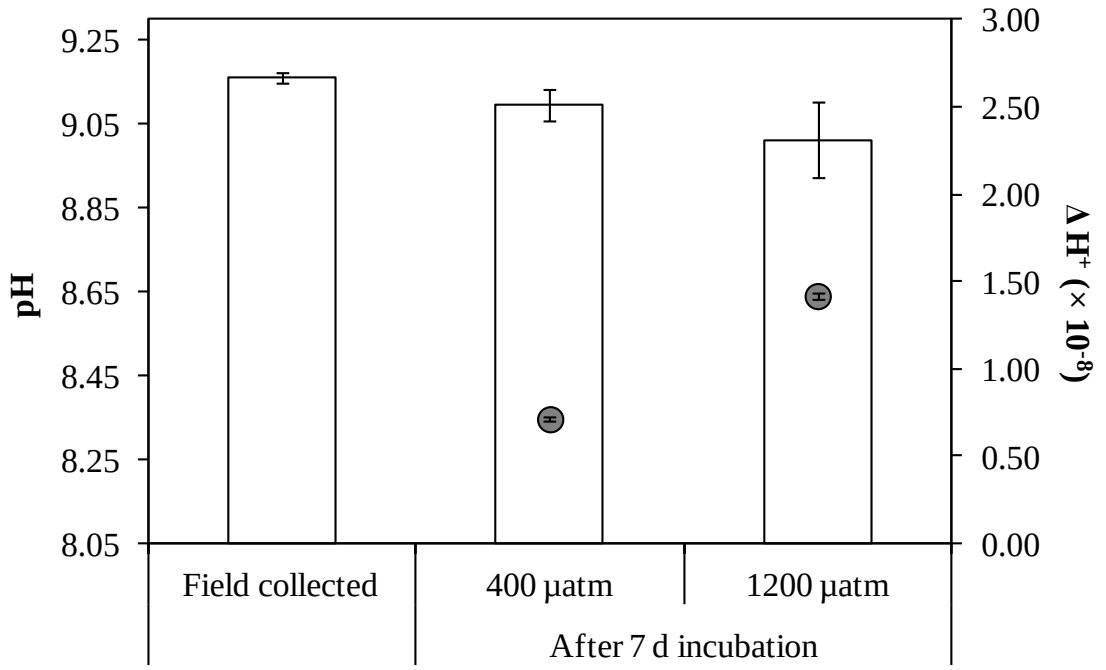

Figure 4.2: pH drift experiments performed in NSW with field-collected and laboratory incubated *Macrocystis* discs at ambient pCO_2 400 µatm (pH 8.00) and an OA treatment 1200 µatm (pH 7.59), and the change H^+ concentration, (ΔH^+) under two pCO_2/pH treatments. Final pH values > 9.0 indicate the ability of the algae to use HCO_3^-. Values are the mean (n = 4–8) ± SE. Gray circles in the middle of the bars represent the change H^+ concentration (y-secondary axis).

4.3.3 Photosynthetic rates

Photosynthetic rates of *Macrocystis* grown under ambient (pCO_2 400 µatm; pH 8.00) compared to the OA treatment (pCO_2 1200 µatm; pH 7.59) were not significantly different across all sampling days (Student's t-test, $P > 0.05$, Fig. 4.3).

4.3.4 Carbonic anhydrase activity

The internal CA activity was consistently 4-times higher than CA_{ext} activity in both pCO_2/pH treatments across all sampling days (Fig. 4.4). CA_{ext} was not significantly different between treatments on day 1 (Student's t-test, $t = 1.400$, df = 10, $P = 0.192$) and day 3 (Student's t-test, $t = -1.432$, df = 10, $P = 0.183$). On day 7, CA_{ext} activity was significantly higher under ambient compared to the OA treatment (Student's t-test, $t = 2.569$, df = 10, $P = 0.028$, Fig. 4.4). In contrast, CA_{int} activity was not affected under the OA treatment (pCO_2 1200 µatm; pH 7.59) across all sampling days and it remained active under both pCO_2/pH treatments (Student's t-test, $t = 1.693$, df = 10, $P = 0.121$, Fig. 4.4).

4.3.5 Growth rate

The relative growth rates (RGR) of *Macrocystis* did not significantly vary between pCO_2/pH treatments during two sampling periods (Fig. 4.5). The 7.65 % and 9.82 % per day growth rate observed on day 3 for ambient and OA treatment, respectively, was not significantly different (ANOVA: $F_{4,30} = 1.824$, $P = 0.191$, Fig. 4.5). The same was observed on the day 7 as RGRs of 3.96 ± 0.41 and 4.64 ± 0.77 (± SE) for ambient and OA treatment, respectively, were not statistically different (ANOVA: $F_{4,30} = 0.916$, $P = 0.349$, Fig. 4.5).

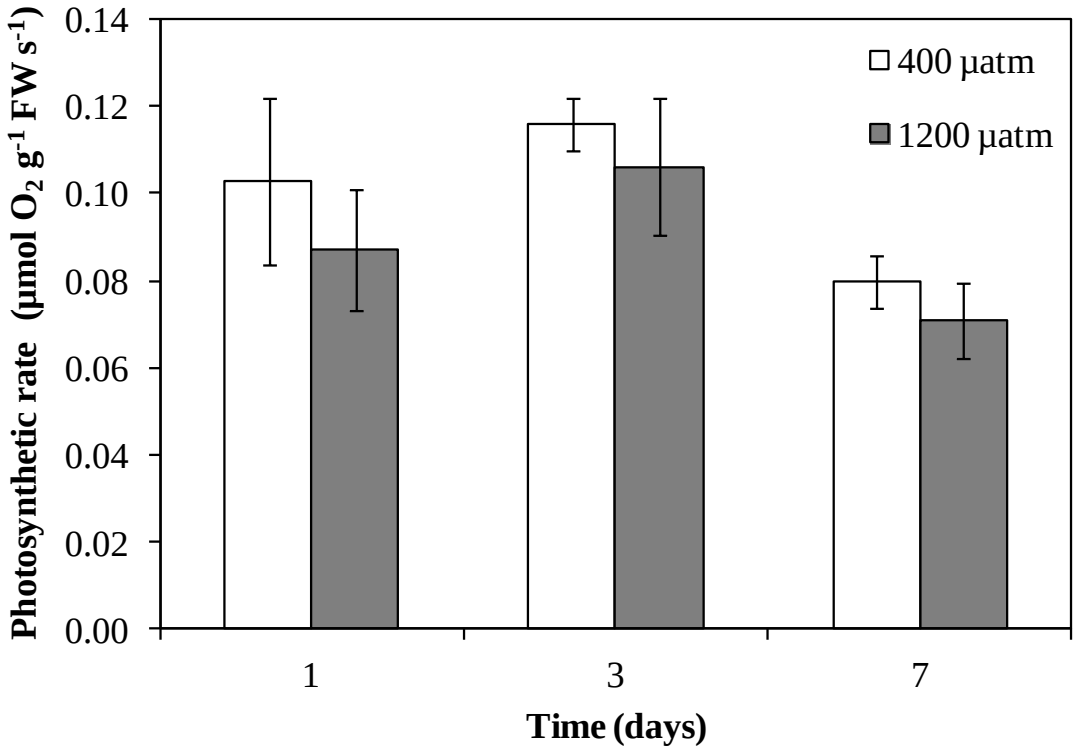

Figure 4.3: Time-series of photosynthetic performance of *Macrocystis* cultured at ambient pCO_2 400 µatm (pH 8.00) and in an OA treatment 1200 µatm (pH 7.59). Values are the mean (n = 4) ±SE.

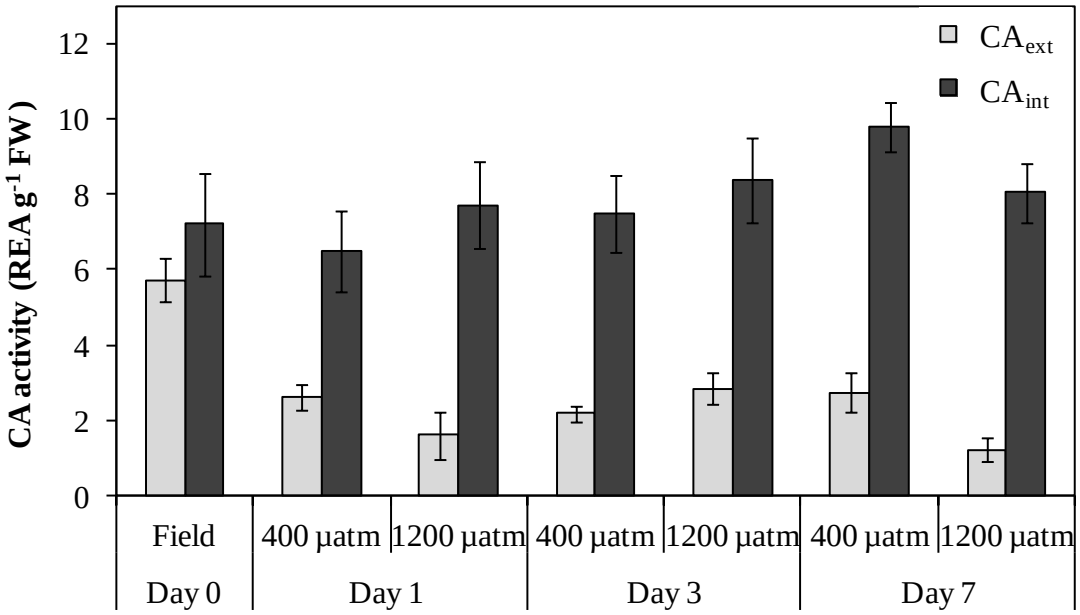

Figure 4.4: Time-series of external and internal carbonic anhydrase activity (CA_{ext} and CA_{int}) for field-collected and laboratory incubated *Macrocystis* discs at ambient pCO_2 400 µatm (pH 8.00) and in an OA treatment 1200 µatm (pH 7.59). Values are the mean (n = 8) ±SE.

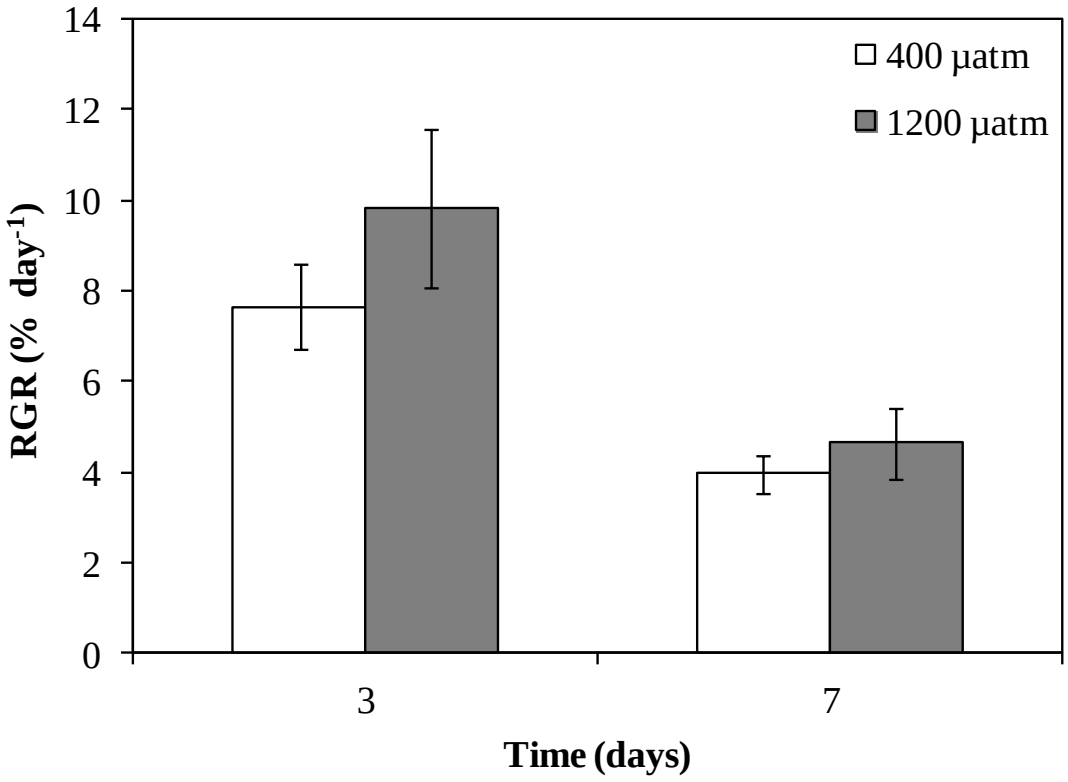

Figure 4.5: Relative growth rate (RGR) of *Macrocystis* after 3 and 7 days of incubation under ambient pCO_2 400 µatm (pH 8.00) and an OA treatment 1200 µatm (pH 7.59). Values are the mean (n = 12) ±SE.

4.3.6 Total tissue C/N content and stable isotopes

After seven days' incubation, the total tissue C and N contents, and C:N ratio (Table 4.2) were not significantly different between pCO_2/pH treatments (Student's t-test, $P > 0.05$). Likewise, the $\delta^{13}C$ signatures of –12.80 and –15.26 in disc grown under ambient and OA treatment, respectively, were not significantly different (Student's t-test, $t = 1.561$, df = 6, $P = 0.170$, Table 4.2). Similarly there was not a significant effect of experimental treatment on $\delta^{15}N$ (Student's t-test, $t = 0.603$, df = 6, $P = 0.569$, Table 4.2). A significant difference between tissue chemical composition (e.g. C, N, stable isotopes) was observed between the time zero field control samples and the 7-days laboratory incubated samples under both pCO_2/pH treatments (ANOVA: $F_{4,46} = 16.417$, $P < 0.01$, Table 4.2).

4.3.7 Metabolically-induced ΔH^+ and inorganic carbon uptake

At the end of each photosynthetic measurement on day 7, the seawater pH inside of the photosynthetic chamber showed that the $[H^+]$ decreased significantly in the medium when discs were grown in the OA treatment compared to discs that were grown in the ambient treatment (Student's t-test, $t = 2.793$, df = 4, $P = 0.049$, Fig. 4.6). The absolute mean change in H^+ ions was $0.29 \times 10^{-8} \pm 0.09 \times 10^{-8}$ and $0.040 \times 10^{-8} \pm 0.01 \times 10^{-8}$ units (± SE) in the OA treatment and ambient, respectively. However, no significant effect was observed on day 3 (Student's t-test, $t = 0.251$, df = 4, $P = 0.814$, Fig. 4.6).

The SW carbonate chemistry measured during day 1 of the experiment showed that HCO_3^- uptake within the 4.4 h incubation period was similar for both pCO_2/pH treatments (Student's t-test, $t = 1.284$, df = 4, $P = 0.269$, Fig. 4.7). Also, HCO_3^- uptake was higher than CO_2 uptake regardless of the pCO_2 concentration (Student's t-test, $t = -16.194$, df = 4, $P < 0.001$, Fig. 4.7).

Table 4.2: Stables isotopes and total tissue C/N content measured in discs of *Macrocystis* directly collected from the field (n= 5) and after 2 d of pre-incubation (n = 3) and 7 days of incubation under ambient pCO_2 400 µatm (pH 8.00) and an OA treatment 1200 µatm (pH 7.59). Standard deviation (in parentheses).

	Experimental condition			
Parameters	**Field**	**Pre-incubation**	**Ambient$_{400\ \mu atm}$**	**OA$_{1200\ \mu atm}$**
$\delta^{15}N$ (‰)	8.98 (0.76)	1.42 (1.08)	0.27 (0.57)	0.04 (0.54)
Nitrogen (% w/w)	1.07 (0.14)	2.10 (0.09)	2.35 (0.13)	2.38 (0.21)
$\delta^{13}C$ (‰)	-20.93 (0.75)	-21.93 (1.82)	-12.83 (0.90)	-15.26 (2.99)
Carbon (% w/w)	27.52 (0.52)	23.26 (0.05)	32.45 (0.78)	32.42 (1.13)
C:N mol ratio	30.31 (4.86)	12.97 (0.60)	16.09 (0.82)	15.99 (1.49)

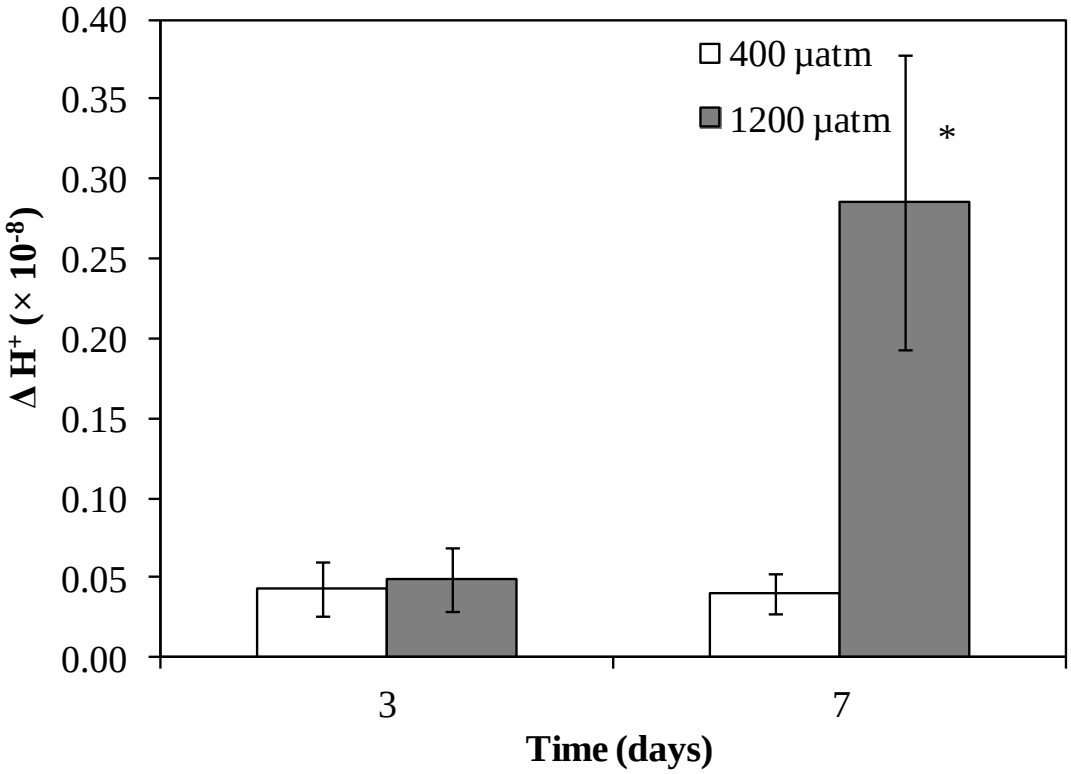

Figure 4.6: Change in H^+ ions (ΔH^+) from pH measurements after the photosynthetic rate was measured under ambient pCO_2 400 µatm (pH 8.00) and an OA treatment 1200 µatm (pH 7.59). Values are the mean (n = 4) ± SE. * indicates significant differences between treatments.

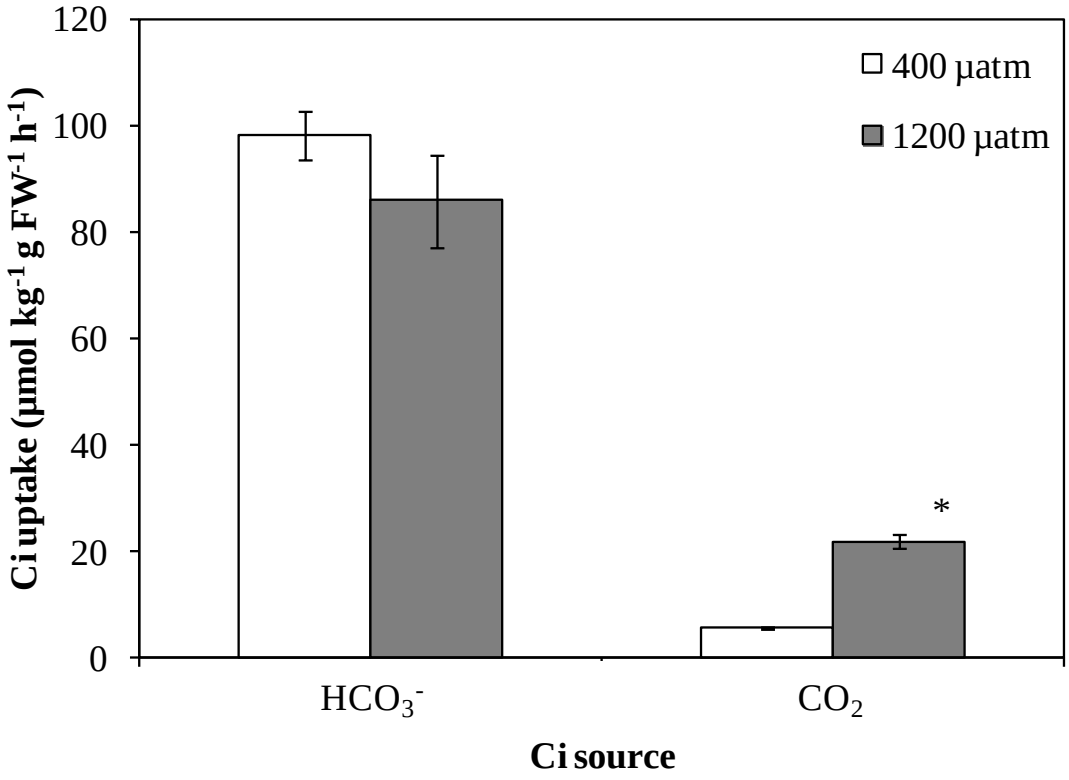

Figure 4.7: Inorganic carbon uptake by *Macrocystis* discs. The change in seawater carbonate chemistry over 4.4 h was used as a proxy for uptake of different inorganic carbon species. SW samples were taken on day 1 of incubation under ambient pCO_2 400 µatm (pH 8.00) and OA treatment 1200 µatm (pH 7.59). Values are the mean (n = 3) ±SE. * indicates significant differences between treatments.

4.4 Discussion

The first hypothesis that the preference of *Macrocystis* for HCO_3^- will decrease under the OA treatment, was not supported. The main exogenous Ci source used by *Macrocystis* was HCO_3^- under both current and future CO_2 concentrations, confirming the findings of Fernández et al. (2014). Even though there may be more diffusive entry of CO_2 into the cells under higher $CO_{2(aq)}$, the preference for HCO_3^- was not affected. Furthermore, photosynthetic rates and the sensitivity to pH and to both CA inhibitors (AZ and EZ) were not altered by the different pH treatments (different HCO_3^-: CO_2 ratio) indicating that *Macrocystis* exhibited the same capacity to use HCO_3^- as an exogenous Ci source regardless of the concentration of pCO_2 in the medium.

The second hypothesis, that photosynthetic and growth rates of *Macrocystis* will not change under OA treatment compared to current seawater conditions, was supported. Similar photosynthetic and growth rates were observed for discs grown under the ambient (pCO_2 400 µatm; pH 8.00) or OA treatment (pCO_2 1200 µatm; pH 7.59). These findings suggest that for *Macrocystis*, photosynthesis is saturated at current seawater Ci concentrations, likely due to their high capacity to use HCO_3^- as a Ci source by two different mechanisms. Therefore, it is unlikely that a future increase in $CO_{2(aq)}$ of ~40.35 µM or in HCO_3^- ion concentration of ~190 µM will substantially stimulate *Macrocystis* photosynthesis. As photosynthesis was not enhanced, it is not surprising that growth was not enhanced either. The enhancement of growth by elevated pCO_2 is commonly related to a reduction in the energy cost involved in the active HCO_3^- uptake and CCMs, and thus saved energy can be used to support other physiological processes such as growth (Beardall and Giordano 2002). The mechanisms present in *Macrocystis* for Ci acquisition (i.e. direct HCO_3^- uptake via an AE protein together with the CA_{int} required for the internal HCO_3^- dehydration to supply CO_2 to

RuBisCO) can be energetically costly and they are not down-regulated under low pH (Fernández et al. 2014). Therefore, the energy demand required to support photosynthesis in *Macrocystis* is not reduced by higher pCO_2 concentrations, and consequently growth rates are not enhanced.

Mixed CO_2 and HCO_3^- users that exhibit saturated photosynthesis under current ambient Ci concentrations are not expected to be substantially affected by future elevated $CO_{2(aq)}$ concentrations. Thus, as we found for *Macrocystis*, photosynthesis was not enhanced in the red alga *Chondrus crispus* cultured under elevated pCO_2 concentrations (Sarker et al. 2013). In a similar way, no effect of elevated pCO_2 on photosynthetic rates was reported by Israel and Hophy (2002) in 13 seaweed species, with representatives from each of the three algal divisions (Chlorophyta, Rhodophyta and Ochrophyta). The lack of response to elevated pCO_2 was attributed to an effective HCO_3^- use mechanism (Israel and Hophy 2002). However, not all HCO_3^- users species have shown the same response to elevated pCO_2. For example, in *Gracilaria tenuistipitata* photosynthetic rates were reduced under elevated pCO_2 (Garcia-Sanchez 1994); however, in this study the pCO_2 concentration was 150-times higher than current. Therefore, the experimental design and treatment of each study should be examined with care in order to make a physiologically and ecologically relevant interpretation of the results.

The use of HCO_3^- by *Macrocystis* was not affected by elevated pCO_2, despite a decrease in CA_{ext} activity that was observed on the last day of the incubation. Since CA_{ext} makes little contribution to Ci acquisition in *Macrocystis*, a reduction in CA_{ext} may not be metabolically significant for the species. This finding is opposite to that of other studies in which the regulation of both CA_{ext} and CA_{int} by the CO_2 concentration present in the medium has been reported. For example, a decrease in CA_{ext} activity in

algae grown under elevated CO_2 has been reported for a few species, including *Hizikia fusiformis* (Zou et al. 2003), *Gracilaria tenuistipitata* (Garcia-Sanchez 1994), and *Ulva rigida* (Björk et al. 1993). In contrast to *Macrocystis*, the reduction in CA_{ext} in those species affected their capacity to use HCO_3^- as a Ci source, reducing their photosynthetic rates (Garcia-Sanchez 1994; Björk et al. 1993; Gordillo et al. 2001). For the red alga *P. leucosticta*, CA_{ext} was not reduced at elevated CO_2, but a decrease in the total CA activity was observed, suggesting that only CA_{int} was regulated by Ci levels (Mercado et al. 1997). For *P. leucosticta*, the low CA_{int} observed was associated with reduced entry of Ci into the cell. For *Macrocystis*, CA_{int} was not reduced by the elevated CO_2 provided in the OA treatment, likely due to the continuous entry of Ci as either HCO_3^- or CO_2 into the cell: this suggests that the main mechanism present in *Macrocystis* for HCO_3^- acquisition, via an AE protein, was not affected by elevated pCO_2.

Fernández et al. (2014) demonstrated that CA_{int} in *Macrocystis* is regulated by Ci entry into the cell, i.e. when all HCO_3^--use mechanisms present were blocked, CA_{int} was reduced in almost all the pH treatments. Therefore, the high CA_{int} activity shown in this study throughout the experiment was likely due to the active intracellular dehydration of HCO_3^-, taken up via the AE protein, to supply CO_2 to RuBisCO. The absence of full photosynthetic inhibition by EZ, which inhibits the catalyzed dehydration of the internal HCO_3^- pool, suggests that a fraction of the internal Ci pool is readily available as CO_2 which supports photosynthesis. For example, cellular pH homeostasis maintains an internal pH between 5.0 and 8.0 in different cellular compartments (cf. Rautenberger et al. 2015 and references therein); this suggests that metabolically-generated protons (H^+) can facilitate uncatalyzed dehydration of HCO_3^- to supply CO_2 to RuBisCO, as previously proposed by Raven (1997b). In many

eukaryotic autotrophic marine organisms the vacuole occupies a large volume in the cells, and has a very acidic pH ranging from 6.5 to 1.0, depending on the species (Raven and Smith 1980, McClintock et al. 1982). These characteristics make them potential locations for non-catalyzed dehydration of HCO_3^- to CO_2, enhancing the CO_2 concentration inside the cell (Raven 1997b).

Irrespective of the pCO_2 present in the medium, HCO_3^- uptake was 85% higher than CO_2 uptake in both experimental treatments (ambient and OA). Even though a 75% higher CO_2 uptake rate was observed under the OA treatment compared to ambient, the overall contribution of CO_2 as Ci source to the photosynthetic Ci uptake was still around 25%. Our results thus suggest that for *Macrocystis,* the increase in CO_2 and HCO_3^- as a result of OA will affect neither their capacity nor preference for HCO_3^-. Similarly, Brown et al. (2014) reported no effect of elevated pCO_2 (pCO_2 1200–1500 µatm) on the photosynthetic Ci uptake by *Macrocystis,* compared to ambient concentrations (pCO_2 400–600 µatm), under either non-saturating or saturating irradiances. The greater decrease in H^+ observed after photosynthetic measurements in the closed system, for *Macrocystis* grown and measured under elevated pCO_2 (pH 7.59), might be associated with a higher entry of CO_2 into the cell. As CO_2 is in equilibrium with carbonic acid (H_2CO_3), a higher CO_2 uptake under elevated pCO_2 will leads to a decrease in the acidity of the medium (Beer et al. 2014).

The similar Ci uptake observed under both pCO_2/pH treatments suggests that carbon assimilation did not change with increasing pCO_2, which may explain why tissue C/N content, C:N ratio and stable isotopes ($\delta^{13}C$ and $\delta^{15}N$) were unaffected by the OA treatment. The differences observed between tissue chemical composition (e.g. C, N, stable isotopes) between field control samples and the 7-days laboratory incubated samples under both pCO_2/pH treatments may be explained by the nutrient enrichment

during the incubations, as C:N ratios decrease with increasing nitrogen sufficiency (Hurd et al. 2014).

Growth is an integrative parameter of all physiological processes, and different directional responses (positive, negative or no-response) to elevated pCO_2 have been reported among different seaweed species. Our finding that the growth rate of *Macrocystis* was not affected by OA supports that of Brown et al. (2014), also for *Macrocystis,* and Rautenberger et al. (2015) for *Ulva*. Similarly, growth rates of 13 seaweed species, including six members from the Orchrophyta phylum, were not significantly affected by increased pCO_2 in the culture medium (Isarel and Hophy 2002). In contrast, a positive growth response to elevated pCO_2 was reported for the kelp *Nereocystis luetkeana* (Thom 1996; Swanson and Fox 2007) and in the green alga *U. rigida* (Gordillo et al. 2001), whereas reduced growth rates were observed in the kelp *Saccharina latissima* (= *Laminaria saccharina*) (Swanson and Fox 2007). The differences observed between kelp species may be explained by the species-specific strategies for Ci utilization (Fernández et al. 2014), and different experimental treatments, e.g. light, pCO_2/pH, nutrient levels. This suggests that the responses of seaweeds to a future elevated pCO_2 may also depend on other metabolic processes, and be affected by other environmental factors.

Environmental factors that might modulate the response of seaweed to elevated pCO_2 include nutrient supply (nitrogen and phosphorus), light intensity and temperature; seasonal responses have also been reported (Zou and Gao 2009; Xu and Gao 2009; Zou et al. 2011b; Roleda and Hurd 2012, Longphuirt et al. 2013; Sarker et al. 2013). The response of *H. fusiformis* to elevated pCO_2 may depend on the nitrogen availability in the culture medium (Zou et al. 2011b, Zou 2005). Similarly, a positive response to elevated pCO_2 in *Gracilaria lemaneiformis* has been observed only under

an intermediate light intensity (Zou and Gao 2009) and for algae grown under a high phosphorus concentration (Xu and Gao 2009), whereas no response was observed under either low light intensity or low phosphorus concentration. For the red alga *Chondrus crispus*, the effect of pCO_2 on growth and photosynthesis became evident only in combination with either elevated temperature or reduced irradiance (Sarker et al. 2013). Similarly, a recent study showed that the interactive effect of increased temperature and pCO_2 might be beneficial physiologically for *Macrocystis*, increasing both photosynthesis and growth in the adult sporophytes (Brown et al. 2014); however, there was no effect of elevated pCO_2 alone on photosynthetic rates, growth, or C:N ratios, and there was a negative effect of high temperature alone on growth and photosynthesis. These findings show how complex and variable the response of *Macrocystis* to a future ocean (high pCO_2/low pH and elevated temperature) might be, and how the experimental conditions under which the alga is grown might modulates this response (Zou et al. 2011b).

In summary, *Macrocystis* carbon physiology and growth were not affected by higher pCO_2 and lower pH predicted for a future ocean. However, further studies are required to determine the combined effects of temperature, pCO_2, light, and nutrients on *Macrocystis* growth and photosynthesis, and also on other physiological processes including respiration and enzyme activities, in order to elucidate how this species might respond to the global environmental changes predicted for the future. Internal and external enzymes related either to carbon or nitrogen assimilation might be modulated by environmental factors such as temperature and light, and thereby different seasonal responses might also be expected.

Chapter 5: The interactive effects of seaweed nitrogen status and pCO_2 on the nitrogen physiology, growth and photosynthetic rates of *Macrocystis*.

5.1 Introduction

Since the Industrial Revolution, the atmospheric CO_2 concentration has risen from 280 to 395 μatm, and it is expected to reach levels of ≈1000 μatm by 2100 under a business-as-usual scenario (IPCC 2013). Increasing atmospheric CO_2 will affect seawater carbonate chemistry, increasing dissolved $CO_{2(aq)}$ and bicarbonate (HCO_3^-) concentrations, and reducing the global surface ocean pH by 0.3–0.4 units, termed ocean acidification (OA) (The Royal Society 2005, Guinotte and Fabry 2008, IPCC 2013, Chapter 1 section 1.1). In addition to the changes in the seawater carbonate chemistry associated with OA, changes at a local scale, such as increases in coastal eutrophication, are also expected in coastal ocean (Boyd and Hutchins 2012, Bender et al. 2014). These predicted changes in OA and nutrient supply can influence important biological and physiological processes of marine organisms (both autotrophs and heterotrophs) (Koch et al. 2013), and the interaction between global and local drivers may modify the response of seaweeds to the global environmental changes predicted for the ocean.

The future increase in $CO_{2(aq)}$ and HCO_3^- availability may enhance growth and photosynthetic rates in some macroalgae (Suárez-Álvarez et al. 2012, Raven and Hurd 2012, see Chapters 3 and 4). Therefore, elevated $CO_{2(aq)}$ may lead to an increased demand for nutrients to support the higher growth rates in macroalgal species that are carbon-limited under the current Ci conditions (Zou 2005, Xu et al. 2010, Suárez-Álvarez et al. 2012). However, most algal species, possess carbon concentrating

mechanisms (CCMs; see Chapter 3), and so are able to use HCO_3^- as a Ci source to support their photosynthesis, meaning that photosynthesis is saturated by dissolved inorganic carbon at current concentrations, but also depending on its affinity for HCO_3^- (Beardall 1998, Israel and Hophy 2002, Fernández et al. 2014/Chapter 3). In the latter case, the response of macroalgae to OA may be influenced by nutrient availability rather than external Ci concentrations. The effect of elevated $CO_{2(aq)}$ on nutrient uptake and assimilation may depend on the interaction between the functioning of CCMs and nutrient acquisition in terms of energy investment. The amount of resources invested by algal cells in acquiring carbon through a CCM is likely associated with the availability of nutrients (Giordano et al. 2005).

Nitrogen (N) is an essential nutrient in many macroalgal species, and is considered to be the nutrient that frequently limits *Macrocystis*' growth (Gerard 1982ab, Wheeler and North 1981, Brown et al. 1997, Fram et al. 2008). Inorganic nitrogen (N_i) is mainly available as nitrate (NO_3^-) and ammonium (NH_4^+), and their concentration may vary temporally and spatially in coastal waters (Haines and Wheeler 1978, Gerard 1982ab). The concentration of NO_3^- in surface seawater usually has a strong seasonal pattern, reaching winter concentrations that are about 10-fold higher than those in summer where concentrations might reach values close to zero. In summer, NH_4^+ might be an important source of N_i as it can be rapidly regenerated from bacterial decomposition or from excretion of marine epifauna; NH_4^+ does not exhibit a clear seasonal pattern, and it might be present in low concentrations all around the year (Phillips and Hurd 2003, Hepburn et al. 2006, Fram et al. 2008, Hurd et al. 2014, Pritchard et al. 2015). *Macrocystis* is a species capable of using both N_i sources to support its growth, and the presence of one source does not alter the uptake of the other (Haines and Wheeler 1978). NH_4^+ assimilation, however, is energetically less expensive

than NO_3^-, because it can be immediately incorporated into amino acids, whereas NO_3^- must be first reduced to ammonium. However, NH_4^+ concentrations in coastal surface waters in Otago coast, New Zealand are lower than NO_3^- concentrations (Brown et al. 1997, Phillips and Hurd 2003, Hepburn and Hurd 2005). Therefore, the major source of N_i incorporated by *Macrocystis* likely is NO_3^-, with exception of summer where NH_4^+ might be an important source of N_i.

NO_3^- can be transported into the algal cell, either by facilitated diffusion, i.e. carrier or channel proteins, or active transport, as it is a charged ion that cannot easily diffuse through the plasma membrane (Lobban and Harrison 1997, Hurd et al. 2014). The nitrate transported into the cell is reduced to nitrite (NO_2^-) by the enzyme nitrate reductase (NR). This is a key enzyme in N metabolism and is considered to be the limiting step in the nitrate assimilation (Solomonson and Barber 1990, Berges 1997). NR activity is mainly regulated by nitrate availability, but can be also influenced by other environmental factors such as light and temperature (Berges 1997, Lartigue and Sherman 2005, Young et al. 2007). After N_i has been incorporated into the cell, it can be accumulated in storage pools, e.g. soluble inorganic pools (i.e. NO_3^- or NH_4^+, stored in the vacuole/cytoplasm) or soluble organic pools (e.g. amino acids, pigments, proteins); both inorganic and organic pools contributed to the total tissue N content (Hwang et al. 1987, McGlathery et al. 1996, Naldi and Wheeler 1999). The size of these pools might be controlled by NR activity and N_i uptake rates, which are influenced by external N_i concentrations (Lartigue and Sherman 2005, Hurd et al. 2014). It has been shown that nitrate uptake and assimilation, including NR activity, internal NO_3^- pool and total tissue N content of *Macrocystis pyrifera* and *Laminaria digitata* are strongly influenced by seasonal variations in NO_3^- concentrations (Wheeler and North 1980, Wheeler and Srivastava 1984, Druehl 1984, Davison and Stewart 1984, Young et al.

2007). These results suggest that NR activity, internal NO_3^- pool and total tissue N content, can be useful indicators of the nitrogen status in the algae.

Some macroalgal species accumulate inorganic and organic nitrogen pools that support their growth, and hence other physiological processes such as photosynthesis when external nitrogen supply is reduced (Chapman and Craige 1977, Gerard 1982a). Species such as *Laminaria longicruris* are capable of accumulating inorganic NO_3^- pools of up to 28,000-fold the maximum external NO_3^- concentrations to support growth during months of low external NO_3^- supply; the depletion of this pool might occur in a lag period of 2 months after the disappearance of NO_3^- in the water (e.g. summer), helping to support a rapid growth at the beginning of the summer and a slow growth during late summer (Chapman and Craige 1977). However, other species, *Spyridea hypnoides*, might have less capacity of storage, but the accumulation or depletion of the inorganic NO_3^- pools might occur in much shorter scales of hours to days (McGlathery 1992) showing a tight correlation between growth and ambient nutrient supply (Edwards et al. 2006). These species might respond rapidly to external environmental changes. Unlike *L. longicruris*, *Macrocystis* has a smaller capacity for nitrogen-storage and inorganic NO_3^- pools and total tissue nitrogen content can be accumulated or depleted in a shorter time scale of hours to days (Gerard 1982a, Kopczak 1994). *Macrocystis* may store intracellular nitrogen reserves, exhibiting a positive correlation between external nitrogen (i.e. NO_3^- and NH_4^+) concentrations and total tissue N content, and inorganic N pools (i.e. NO_3^- and NH_4^+), which suggests that internal N is accumulated when N concentrations exceed those needed to support growth (Gerard 1982ab, Hurd et al. 1996, Brown et al. 1997, Hepburn et al. 2007). When external NO_3^- concentrations suddenly increase, *Macrocystis* might accumulate rapidly large amounts of NO_3^-, exhibiting different storage capacity depending on the

local environmental conditions (Kopczak et al. 1991, 1994). Kain (1989) and Brown et al. (1997) suggested that *Macrocystis* is a 'seasonal responder', i.e. it responds rapidly to variations in environmental conditions at a local scale.

The interaction between N_i availability and CCM functioning is complex, but may be explained by the relationship between cellular carbon and nitrogen metabolism. An increase in carbon assimilation may lead to an increased demand for nitrogen to maintain the correct internal balance between these nutrients (Beardall and Giordano 2002, Giordano et al. 2005). Carbon and nitrogen metabolisms can be strongly coupled in micro- and macroalgae (Vergara et al. 1995, McGlathery et al. 1996, McGlathery and Pedersen 1999), and in other organisms such as higher plants (Stitt and Krapp 1999). The energy and carbon skeletons required for nitrogen uptake and assimilation are provided by photosynthesis, and the content of chlorophyll, amino acids and proteins depend on intracellular N levels (Turpin et al. 1988, McGlathery et al. 1996). For microalgae grown under nitrogen-limited conditions, the resupply of N causes an increase in N assimilation, which can affect the photosynthetic metabolism due to carbon demands in excess of the capacity of photosynthetic carbon fixation (Turpin 1991, and references therein). Therefore, it is likely that algae grown under different inorganic N concentrations might exhibit a different response to a future elevated $CO_{2(aq)}$ as nitrogen limitation may affect photosynthesis and carbon metabolism of algae (Turpin 1991).

Fernández et al. (2015/Chapter 4) showed that neither photosynthetic nor growth rates of *Macrocystis* discs were affected by elevated pCO_2. However, experiments were conducted under a final NO_3^- concentration of 50 µM that is saturating for *Macrocystis* growth. The relationship between N_i assimilation and CO_2 availability seems to vary between macroalgae species. For some species, *Hizikia fusiformis* and *Ulva rigida*

grown under N-sufficient concentrations (60 µM and 5000 µM/per 10 days, respectively) NO_3^- uptake and assimilation (i.e. NR activity) increased under elevated $CO_{2(aq)}$ whereas photosynthesis was reduced (Gordillo et al. 2001, Zou 2005). In contrast, for *Gracilaria sp*. grown under N-sufficient concentrations (75 µM), NO_3^- uptake and assimilation was reduced under elevated $CO_{2(aq)}$ (Andria et al. 1999). The differences observed between studies may be due to the internal N status of the algae and/or by the experimental nutrient conditions used in each study. However, only a few studies have shown how the nitrogen status of the macroalgae may modulate their physiological response to a future elevated $CO_{2(aq)}$ concentration (Andria et al. 1999, Gordillo et al. 2001). The nutritional status of the algae might be a key factor in the regulation of their response to OA, since for example greater intracellular N pools (i.e. organic N pool and NH_4^+ internal pools) may result in a lower investment of energy in assimilating new N entering into the cell, and so more energy and internal N reserves will be available to support high growth and photosynthesis under an OA scenario.

The goals of this study were to test the hypotheses that (1) NO_3^- uptake and assimilation by *Macrocystis*, including the size of the internal NO_3^- pool, total tissue N content, C:N ratio and nitrate reductase (NR) activity, are dependent on NO_3^- supply, and (2) nitrogen status modulates the physiological response of *Macrocystis* under ambient and elevated pCO_2. That is, N-replete *Macrocystis* blades grown under elevated pCO_2 will exhibit higher photosynthetic and growth rates compared to N-deplete *Macrocystis* blades grown either under ambient or elevated pCO_2.

5.2 Materials and Methods

5.2.1 Seaweed collection

Young blades, i.e. the 2nd and 3rd blades below apical scimitar, of *Macrocystis* were collected from Aramoana (45°47'S, 170°43'E), Otago Harbour, New Zealand, in October 2013. A total of 56 blades, each collected from an individual of *Macrocystis*, were transported to the laboratory in an insulated container with ambient seawater. In the laboratory, blades were gently rinsed and cleaned with natural seawater (NSW) of any visible epiphytes. Each of the 56 blades were cut to a similar size of 14 cm × 3 cm (fresh initial weight 2.0 ± 0.2 g) at 2 cm from the neumatocyst/blade junction using a razor blade. Thereafter, blade sections were incubated in eight 5 L glass jars containing filtered NSW (0.5 µm pore size) at 12 °C for 2 h to allow marginal wounds to heal. Cultures were aerated constantly with an air pump. After two hour's incubation, 12 blade sections of *Macrocystis* were haphazardly selected from different jars to assess their initial physiological status: NO_3^- uptake rate, NR activity, soluble tissue NO_3^- pool, total tissue carbon and nitrogen content, C:N ratio, and stable isotopes were measured as described below. The rest of the blade sections were used for further incubations, described below.

5.2.2 Experimental design

In order to evaluate the effect of elevated pCO_2 on *Macrocystis* blades with different nitrogen statuses (deplete/replete), blade sections were first incubated under pre-experimental conditions for 3 days. Two N_i concentrations, using nitrate as the only N source, were used, ambient (<7 µM) and nitrate-enriched SW (80 µM). After that, pre-treated blade sections were incubated for an additional 3 days under ambient and

elevated pCO_2 (Fig. 5.1) (see below for details). All physiological parameters measured are described in Table 5.1.

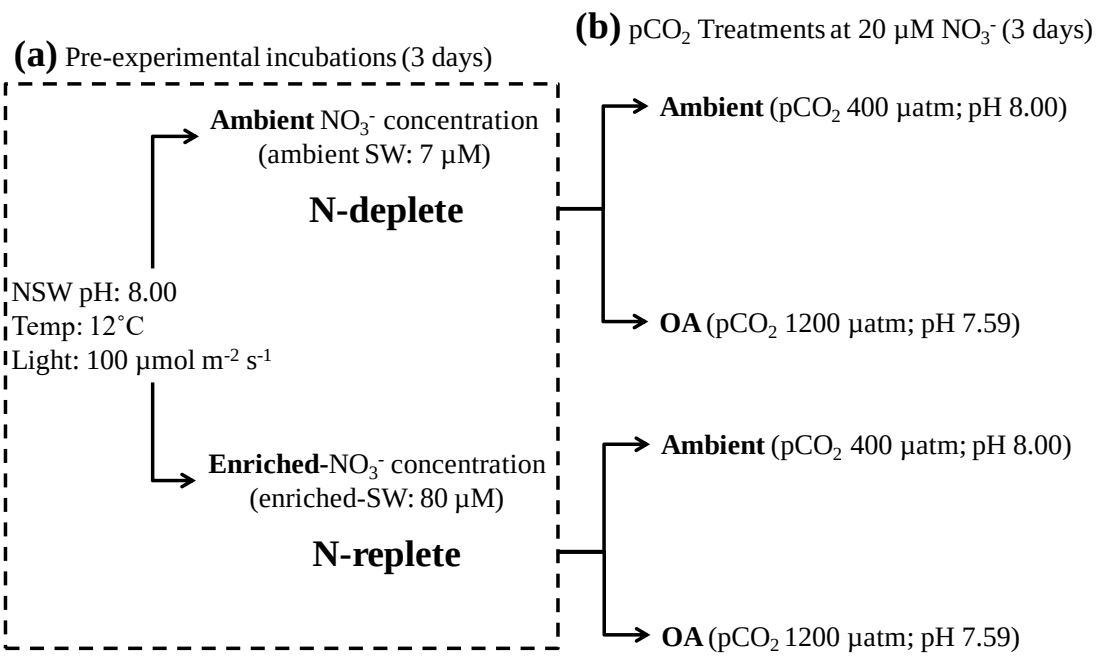

Figure 5.1: Illustration of the experimental design. *Macrocystis* blade sections were first incubated under (a) pre-experimental conditions for 3 days to obtain blades with different nitrogen status (deplete/replete). After that, pre-treated blade sections were incubated (b) for an additional 3 days under an ambient (pCO_2 400 µatm; pH 8.00) and OA treatment (pCO_2 1200 µatm; pH 7.59) at 20 µM NO_3^-.

Table 5.1: Biochemical and physiological parameters measured in *Macrocystis* blades following field collection, the pre-experimental incubations, the 1 h uptake measurement at 20 µM NO_3^-, and after the pCO_2 incubations. NM = not measured.

Biochemical and physiological parameters	**Field-collected blades**	**Pre-experimental incubations**		**After the 1 h uptake measurement**		**pCO_2 incubations at 400 µatm and 1200 µatm**	
		N-deplete	N-replete	N-deplete	N-replete	N-deplete	N-replete
Uptake rate (µmol NO_3^- g^{-1} FW h^{-1})	✓	✓	✓	✓	✓	✓	✓
Nitrate reductase (nmol NO_3^- g^{-1} FW min^{-1})	✓	✓	✓	✓	✓	✓	✓
Tissue soluble NO_3^- pool (µmol NO_3^- g^{-1} FW)	✓	✓	✓	✓	✓	✓	✓
$\delta^{15}N$	✓	✓	✓	✓	✓	✓	✓
$\delta^{13}C$	✓	✓	✓	✓	✓	✓	✓
N (% w/w)	✓	✓	✓	✓	✓	✓	✓
C (% w/w)	✓	✓	✓	✓	✓	✓	✓
C:N ratio	✓	✓	✓	✓	✓	✓	✓
Photosynthetic rate (µmol O_2 g^{-1} FW h^{-1})	N/M	N/M	N/M	N/M	N/M	✓	✓
Growth rate (% day^{-1})	N/M	✓	✓	N/M	N/M	✓	✓

5.2.3 Pre-experimental incubations under ambient NO_3^- (< 7 µM) and NO_3^--enriched (80 µM) conditions

The goal of the pre-experimental incubations in ambient and NO_3^--enriched SW was to produce blades of *Macrocystis* that had different nitrogen statuses (deplete/replete), that were subsequently used in an experiment in which pCO_2 was manipulated (i.e. an OA experiment). Blade sections of *Macrocystis* were placed in 5 L glass jars containing ambient filtered SW (< 7 µM) or nitrate-enriched SW (80 µM). A total of eight jars were used, each containing between five to six blade sections, each taken from a different individual (44 blades in total); four jars with ambient concentrations and four jars with NO_3^--enriched concentrations. NO_3^- was added as $NaNO_3$ into ambient filtered SW to a final concentration of 80 µM. Phosphate was added as NaH_2PO_4 to a final concentration of 16 µM to maintain the N: P ratio at 5:1 and avoid phosphate limitation. SW samples of 10 mL were taken every day before and after renewal of the medium, and stored at –20˚C for nutrient analysis. Cultures were maintained in a growth cabinet (Contherm Plant Growth Chamber, Contherm Scientific Co. Ltd., New Zealand) at 12 °C under a 12:12 h light:dark photoperiod and saturating light of 110 µmol photons m^{-2} s^{-1} of PAR, and aerated constantly with an air pump.

After 3 days of the pre-experimental incubations under ambient and NO_3^--enriched seawater, one blade section was randomly removed from each of the eight jars (i.e. four N-deplete blades and four N-replete blades) and immediately processed for NR activity, soluble tissue NO_3^- pool, total tissue C and N content, C:N ratio, and stable isotopes ($\delta^{13}C$ and $\delta^{15}N$). Another 12 blade sections (i.e. six N-deplete blades and six N-replete blades) were used to measure NO_3^- uptake rate, described below. The remaining

24 blade sections were used for further pCO_2 incubations (i.e.12 N-replete and 12 N-deplete blades).

5.2.4 Incubations under ambient pCO_2 400 µatm and elevated pCO_2 1200 µatm

After three days of the pre-experimental incubations in ambient and NO_3^--enriched SW, the 24 *Macrocystis* blades, each blade section with an initial fresh weight of about 2.38 ± 0.36 (g ± SD), were transferred to an automated pH-controlled culture system maintained in a growth cabinet (Contherm Plant Growth Chamber, Contherm Scientific Co. Ltd., New Zealand) at 12 °C under a 12:12 h light: dark photoperiod and saturating light of 110 µmol photons m^{-2} s^{-1} of PAR. N-deplete and N-replete blades were incubated under to two pCO_2/pH levels: ambient treatment (pCO_2 400 µatm; pH 8.00) and OA treatment (pCO_2 1200 µatm; pH 7.59) (n = 6 for each) for a further 3 days. Each blade section was individually incubated in each of the 24 culture chambers. The SW used in the system was enriched with 20 µM NO_3^- and 5 µM PO_4^{3-}, and fully renewed every 4.4 h (see Fernández et al. 2015/Chapter 4, for details).

After 3 days' incubation under two pCO_2 treatments, the experiment was terminated and the following physiological and biochemical measurements were made for each blade. Immediately upon termination of the experiment, nitrate uptake rates were measured (see below). At the end of each nitrate uptake measurement, photosynthetic rates were measured as described below. Finally, the blade sections were weighed to estimate growth rates, and divided into three parts for biochemical analysis, i.e., NR activity, soluble tissue NO_3^- pool, total tissue C and N content, C:N ratio, and stable isotopes ($\delta^{13}C$ and $\delta^{15}N$).

5.2.5 Biochemical and physiological parameters measured

Nitrate uptake rates were measured on blade sections immediately after the 3-day pre-experimental treatment, and after the 3-day culture in different pCO_2 treatments. Nitrate uptake rates were measured in twelve 1 L glass beakers, containing 620 mL of SW with a final concentration of 20 µM NO_3^-. To avoid the formation of boundary layers, each beaker was sitting on top of a stirrer plate and the medium was continuously stirred with a magnetic stirring bar at 650 rpm. Prior to the addition of the blade section, a 10 mL SW sample was drawn from each beaker to determine the initial nutrient concentration in the medium. Thereafter, each of the twelve *Macrocystis* blade sections with either a N-deplete pool (n = 6) and or a N-replete pool (n = 6) were incubated for 1 h under a saturating photon flux density of ≈120 µmol m^{-2} s^{-1}. At the end of each incubation period, each blade section was removed and a 10 mL SW sample was taken to determine the final nutrient concentration in the medium. All seawater samples were stored at –20°C until subsequent nutrient analysis. Seawater samples were analyzed using a a QuickChem 8500 series 2 Automated Ion Analyzer (Lachat Instrument, Loveland, USA). The same procedure was used to determine initial nitrate uptake rates from field-collected blades (n = 6). The nitrate uptake rate was determined using the following equation:

$$V = \frac{(S_i - S_f) \times Vol}{t \times ww}$$

where V is the uptake rate (µmol g^{-1} FW h^{-1}), S_i and S_f are the initial and final nutrient concentrations (µM), respectively, Vol is the incubation volume (L), t is the time (h) and ww is the fresh weight of the alga (g).

At the end of the incubation, each blade section was divided into three parts for biochemical analyses: NR activity (0.25 g FW), soluble tissue NO_3^- pool (0.5-0.6 g

FW), and total tissue C and N content and stable isotopes (0.1 g FW) analyzed from the same tissue. Samples for NR measurement and soluble tissue NO_3^- pool were stored at –80 ˚C and –20 ˚C, respectively, until analysis. Samples for tissue C and N content and stable isotopes were oven dried at 60 ˚C and processed as describe below.

Nitrate reductase activity (NR)

NR activity was measured by nitrite production in an *in vitro* assay (Hurd et al. 1995) on blades collected from the field, after pre-experimental incubations, after the NO_3^- uptake measurement, and after pCO_2 incubations (Table 5.1, Fig. 5.1). NR was extracted using an extraction buffer of 200 mM Na-phosphate (pH 7.9) containing 3% w/v bovine serum albumine (BSA), 0.3 % w/w polyvinylpyrrolidone (PVP), 2 mM dithiothreitol (DTT), 5 mM Na_2–EDTA and 1% w/v Triton X-100 (all Sigma, St Louis, MO, USA). Frozen tissue weighing 0.25-0.30 g was ground to a fine powder, using liquid nitrogen in a liquid N_2-frozen mortar and pestle. The powder was then transferred into a 2 mL microcentrifuge tube held in liquid N_2. For enzyme extraction, 3 mL of cold extraction buffer (4 ˚C) and the powdered algae (0.25-0.30 g) were mixed in a 10 mL glass tube and kept in a polystyrene box covered with ice. Tubes were vortex for 10 sec and stored on ice for 25 min (extraction time).

The enzymatic reaction was conducted in 1.5 mL microcentrifuge tubes containing a reaction mixture composed of 580 µL of 200 mM Na–phosphate buffer and 100 µL of 2 mM NADH. Before adding the extract, the reaction mixture was pre-equilibrated for 10 min to the reaction temperature (12 ˚C). To transfer 220 µL of homogenized extract into the reaction mixture, a 1 mL pipette tip with cut-off tips was used. The reaction was started by adding 100 µL of 100 mM KNO_3^-. Tubes were mixed by vortexing and incubated for 20 min at 12 ˚C in a temperature controlled growth

chamber. The reaction was stopped by adding 500 µL of 1 M Zn acetate, and tubes centrifuged at 12,000 rpm for 20 min. A sub-sample of 500 µL was collected from the supernatant and transferred into a new microcentrifuge tube to determine the nitrite concentration (Strickland and Parsons 1968) after the addition of 500 µL of 58 mM sulfanilamide and 500 µL of 3.68 mM N-(1-naphthyl)ethylenediaminedihydrochloride (NED). Absorbance of the samples was determined at 540 nm, and the concentration of nitrate was determined using a standard calibration curve prepared with a 5 mM $NaNO_2$ solution. The NR activity was expressed as nmol NO_3^- g^{-1} FW min^{-1} and calculated as:

$$N = \frac{c \times v}{t \times ww}$$

where N is NR activity (nmoles g^{-1} FW $min^{-1)}$, c is the concentration of nitrite produced (nmoles L^{-1}), v is the assay volume (L), t is the extraction time (min) and ww is the fresh weight of the alga (g).

Soluble tissue nitrate

The soluble tissue nitrate concentration was measured using the boiling-water extraction method (Thomas 1983, modified by Hurd et al. 1996), on blade sections collected from the field, and after pre-experimental incubation and pCO_2 incubations (Table 5.1, Fig. 5.1). A preliminary experiment, comparing boiling times of 40 and 20 min, showed that higher NO_3^- concentrations are obtained after 40 min boiling. Frozen samples weighing 0.5 ± 0.05 g were placed in a 50 mL glass tubes containing 40 mL of MilliQ water, and boiled for 40 min at 100 ˚C. Tubes were placed into a 1 L glass beaker sitting on top of an aluminum-top hot plate. After the first boiling, the water was cooled to room temperature and filtered using a 50 mL syringe with a 0.2 µM Whatman filter. The remaining tissue was boiled two more times; no further nitrate was released after the

third boiling. Filtered seawater samples were stored at –20 ˚C until subsequent NO_3^- analysis. The total soluble nitrate content of each sample was obtained after the sum of the three boiling, and expressed as µmol NO_3^- g^{-1} FW. Samples were analyzed for NO_3^- using a QuickChem 8500 series 2 Automated Ion Analyzer (Lachat Instrument, Loveland, USA).

Photosynthetic rates

Photosynthetic rates were measured as O_2 evolution using a fiber optic FOXY-R probe coupled to a USB-2000 spectrophotometer (Ocean Optics, Florida, USA) connected to a laptop. Photosynthetic rates were measured individually in each of the 24-culture chambers (620 mL) on the last day of pCO_2 incubation. Each culture chamber contained a single blade section of *Macrocystis* (3.64 ± 0.42 g FW), and was equipped with a magnetic stirrer, and sat on a stirring plate at 650 rpm under a saturating light of 110 µmol m^{-2} s^{-1}. O_2 evolution was registered for 15 min. The oxygen concentration was expressed as µM O_2 as calculated using the formulas and coefficient of Millero and Poisson (1981) and Garcia and Gordon (1992). The photosynthetic rates were calculated using linear regression over the last 5 min of incubation and standardized to corresponding sample fresh weight (g).

Growth rates

The relative growth rate (RGR, % d^{-1}) was determined according to the exponential model: $RGR = \ln(W_t - W_0) \times t^{-1} \times 100$ (Zou 2005), where W_0 is the initial FW of the algae while W_t is the final FW after *t* days of incubation. At the end of the photosynthetic measurements, each blade section of *Macrocystis* was gently blotted dry and the fresh weight measured. Growth rates were determined for each pCO_2/pH treatment.

Total tissue carbon and nitrogen content, and stable isotopes ($\delta^{13}C$ and $\delta^{15}N$)

To determine the total tissue carbon and nitrogen content, C:N ratio and stable isotope composition ($\delta^{13}C$ and $\delta^{15}N$), tissue samples from the field collection, from after the pre-experimental incubations, and the NO_3^- uptake measurements, and after pCO_2 incubations were dried at 60 ˚C for 48 h, ground to a fine powder with a mortar and pestle, and stored in a microcentrifuge tube of 0.2 mL until subsequent analysis. the total tissue carbon and nitrogen content and stable isotopes ($\delta^{13}C$ and $\delta^{15}N$) were assayed by combustion of the whole seaweed material (1 mg) using a Carlo Erba NC2500 elemental analyzer (CE instrument, Milan) and measured using a Europa scientific '20/20 Hydra' (Europa Scientific, UK) isotope ratio mass spectrometer (IRMS) in continuous flow mode. Raw isotopes ratios were normalized to the IAEA (International Atomic Energy Agency) reference material and the standards USGS-40 and USGS-41.

5.2.6 Statistical analyses

Statistically significant differences between treatments were detected using analysis of Student's t-test ($P < 0.05$) after homogeneity (Levene's test) and normality (Shapiro-Wilk test) of data were satisfied. All analyses were performed using the statistical program SigmaPlot 11.0 (Systat Software, Inc.).

5.3 Results

5.3.1 Physiological parameters of field-collected samples

Physiological parameters measured from field-collected samples, i.e. nitrate uptake rate, nitrate reductase (NR), soluble tissue NO_3^- pool, C/N total content and stable isotopes, are shown in Table 5.2. Both NO_3^- uptake rate and NR activity were observed in field-collected blades, however, the internal NO_3^- pool was close to zero. The C:N ratio of 15 is indicative of blades being nitrogen-sufficient at the onset of the experiment (see discussion section 5.4.1).

Table 5.2: Biochemical and physiological parameters measured in *Macrocystis* field-collected blades. Values are mean of 6 replicates ± standard deviation.

Biochemical and physiological parameters	**Means ± SD**
Uptake rate (µmol NO_3^- g^{-1} FW h^{-1})	4.62 ± 1.32
Nitrate reductase (nmol NO_3^- g^{-1} FW min^{-1})	6.24 ± 1.10
Tissue soluble NO_3^- pool (µmol NO_3^- g^{-1} FW)	0.42 ± 0.32
$\delta^{15}N$	10.55 ± 0.74
$\delta^{13}C$	-18.86 ± 1.57
N (% w/w)	2.07 ± 0.28
C (% w/w)	26.57 ± 1.01
C:N ratio	15.21 ± 2.25

5.3.2 Physiological parameters following a 3 days pre-experimental incubation under ambient NO_3^- (< 7 µM) and NO_3^--enriched (80 µM) conditions

Nitrate uptake rates

The nitrate uptake rates of *Macrocystis* blades varied significantly between NO_3^- treatments (Fig. 5.2). The NO_3^- uptake rates of N-deplete *Macrocystis* blades were 36% higher than in N-replete *Macrocystis* blades (Student's t-test, t = 2.872, df = 8, P = 0.021, Fig. 5.2, Table 5.3).

Nitrate reductase activity (NR)

The nitrate reductase (NR) activity of N-deplete *Macrocystis* blades was 63% lower compared to N-replete blades, after 3 days' pre-experimental incubation (Student's t-test, t = 5.782, df = 6, P = 0.001, Fig. 5.3a). NR activity was also measured following the 1 h measurement of NO_3^- uptake that was made at an initial concentration of 20 µM, directly after the 3-day pre-experimental treatment. NR activity of N-deplete *Macrocystis* blades was 35% lower compared to N-replete blades (Student's t-test, t = -2.918, df = 8, P = 0.019, Fig. 5.3b). For N-deplete blades, NR did not change after the 1h uptake experiment (Student's t-test, t = –1.188, df = 8, P = 0.269, Fig. 5.3b), whereas NR activity of N-replete blades was reduced by a 26% after the NO_3^- uptake measurements (Student's t-test, t = 2.419, df = 8, P = 0.052, Fig. 5.3b, Table 5.3).

Soluble tissue nitrate

After the 3-day pre-experimental incubation, soluble tissue NO_3^- concentrations in *Macrocystis* blades varied significantly between NO_3^- treatments (Fig. 5.4a). Tissue NO_3^- content (0.18 µmol NO_3^- g^{-1} FW) of N-deplete *Macrocystis* blades was 98% lower compared to N-replete blades (13.89 µmol NO_3^- g^{-1} FW) (Student's t-test, t = 34.417, df

= 9, $P < 0.001$, Fig. 5.4a). After the 1 h NO_3^- uptake measurement (at an initial concentration of 20 µM), soluble tissue NO_3^- content of N-deplete *Macrocystis* blades was 93% lower compared to N-replete blades (Student's t-test, t =18.795, df = 9, $P < 0.001$, Fig. 5.4b). Soluble tissue NO_3^- content of N-deplete blades increased by a 78% after the NO_3^- uptake experiment compared to values recorded before the uptake measurement (Student's t-test, $t = –7.503$, df = 7, $P < 0.001$, Fig. 5.4ab), whereas soluble tissue NO_3^- content of N-replete blades did not change after the uptake measurement (Student's t-test, $t = 1.306$, df = 8, $P = 0.228$, Fig. 5.4ab, Table 5.3).

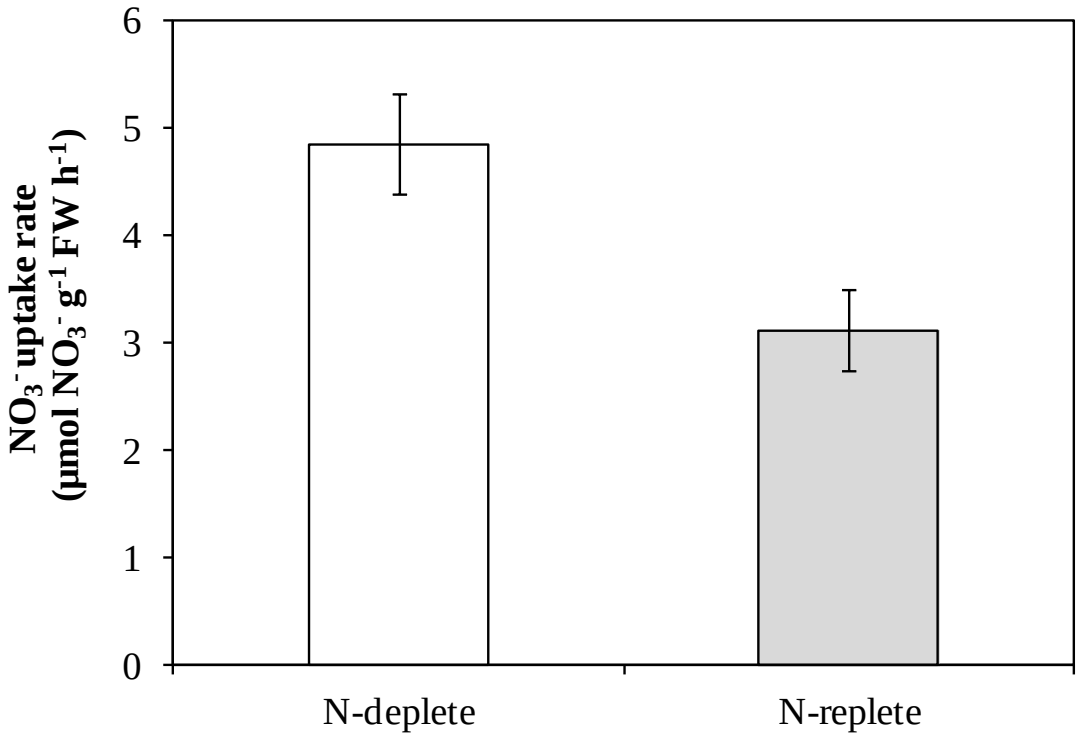

Figure 5.2: Nitrate uptake rates of *Macrocystis* blade sections after 3 days' incubation under ambient (< 7 µM) (N-deplete), and nitrate (80 µM) enriched SW (N-replete). Data are means of 5 replicates ± SE. N-deplete > N-replete (Student's t-test $p < 0.05$).

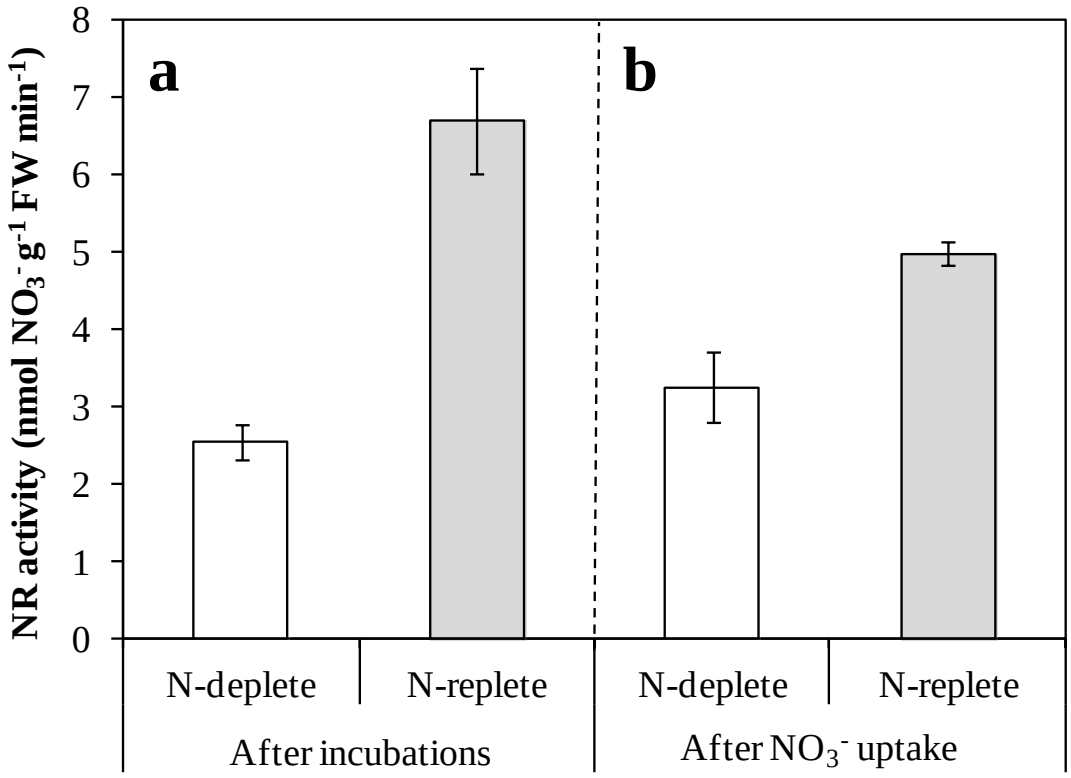

Figure 5.3: Nitrate reductase (NR) activity of *Macrocystis* blade sections after (a) 3 days' incubation under ambient (< 7 µM) (N-deplete), and nitrate (80 µM) enriched SW (N-replete) and (b) after the 1 h NO_3^- uptake measurements on day 3 at an initial concentration of 20 µM. Data are means of 4 replicates ± SE (after incubations) and 6 replicates ± SE (after NO_3^- uptake). Significantly different sub-groups: After incubations: N-deplete < N-replete; after NO_3^- uptake: N-deplete < N-replete; N-deplete: after incubations = after NO_3^- uptake; N-replete: after incubations > after NO_3^- uptake (Student's t-test).

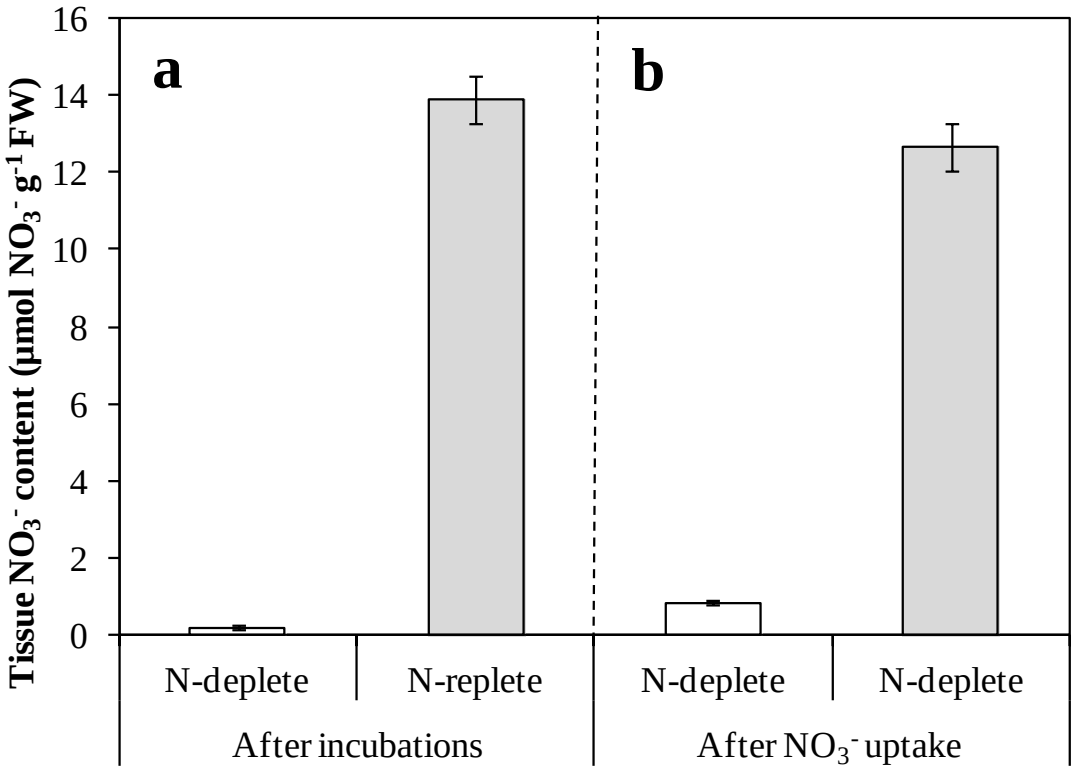

Figure 5.4: Tissue NO_3^- content (internal NO_3^- pool) of *Macrocystis* blade sections after (a) 3 days' incubation under ambient (< 7 µM) (N-deplete), and nitrate (80 µM) enriched SW (N-replete) and (b) after the 1 h NO_3^- uptake measurements on day 3 at an initial concentration of 20 µM. Data are means of 4 replicates ± SE (after incubations) and 6 replicates ± SE (after NO_3^- uptake). Significantly different sub-groups: After incubations: N-deplete < N-replete; after NO_3^- uptake: N-deplete < N-replete; N-deplete: after incubations < after NO_3^- uptake; N-replete: after incubations = after NO_3^- uptake (Student's t-test).

5.3.3 Total tissue carbon and nitrogen content, C:N ratio, and stable isotopes ($\delta^{15}N$ and $\delta^{13}C$)

After the 3-day pre-experimental incubation, the tissue chemical composition of *Macrocystis* blades varied significantly between NO_3^- treatments (Fig. 5.5a-c). The total tissue nitrogen content (1.42% of dry wt) of N-deplete *Macrocystis* blades was 41% lower than the N-replete blades (2.41% of dry wt) (Student's t-test, $t = –11.282$, df = 6, $P < 0.001$, Fig. 5.5a). The total tissue carbon content was 3.6% higher for N-deplete (25.35% of dry wt) *Macrocystis* blades than for N-replete blades (24.43% of dry wt) (Student's t-test, $t = 2.603$, df = 6, $P = 0.040$, Fig. 5.5b). The C:N ratio of N-deplete *Macrocystis* blades was 56% higher than N-replete blades, at 20.80% and 11.23% dry wt, respectively (Student's t-test, $t = 12.457$, df = 6, $P < 0.001$, Fig. 5.5c). After the 1 h NO_3^- uptake measurement, total tissue N and C content and C:N ratio of N-deplete *Macrocystis* blades did not change (Student's t-test, $t = –0.787$, df = 8, $P = 0.454$; $t = –0.0997$, df = 8, $P = 0.923$; $t = 0.786$, df = 8, $P = 0.454$, respectively, Fig. 5.5a-c), and a similar result was recorded for N-replete blades (Student's t-test, $t = –0462$, df = 8, $P = 0.656$; $t = –0.998$, df = 8, $P = 0.347$; $t = –1.183$, df = 8, $P = 0.271$, respectively, Fig. 5.5a-c, Table 5.3).

The $\delta^{15}N$ of N-deplete *Macrocystis* blades was 25% higher than that of N-replete blades (Student's t-test, $t = 14.676$, df = 6, $P < 0.001$, Fig. 5.6a). After the 1 h NO_3^- uptake measurement, same pattern was observed (Student's t-test, $t = 11.932$, df = 10, $P < 0.001$, Fig. 5.6a). However, the $\delta^{15}N$ of N-deplete *Macrocystis* blades decreased by a 5% after the NO_3^- uptake measurement (Student's t-test, $t = 2.725$, df = 8, $P = 0.026$, Fig. 5.6a), while $\delta^{15}N$ of N-replete blades did not change (Student's t-test, $t = 0.480$, df = 8, $P = 0.644$, Fig. 5.6a). For $\delta^{13}C$, there was no change between blades after 3 days' incubation under different NO_3^- treatments (Student's t-test, $t = –1.157$, df = 6, $P =$

0.291, Fig. 5.6b). After the 1 h NO_3^- uptake measurement, same results were observed for $\delta^{13}C$ (Student's t-test, $t = -1.777$, df = 10, $P = 0.106$, Fig. 5.6b). When compared the $\delta^{13}C$ before and after the NO_3^- uptake measurements, $\delta^{13}C$ values did not change either in N-deplete *Macrocystis* blades (Student's t-test, $t = -0.657$, df = 8, $P = 0.530$, Fig. 5.6b) or N-replete blades (Student's t-test, $t = -1.434$, df = 8, $P = 0.190$, Fig. 5.6b, Table 5.3).

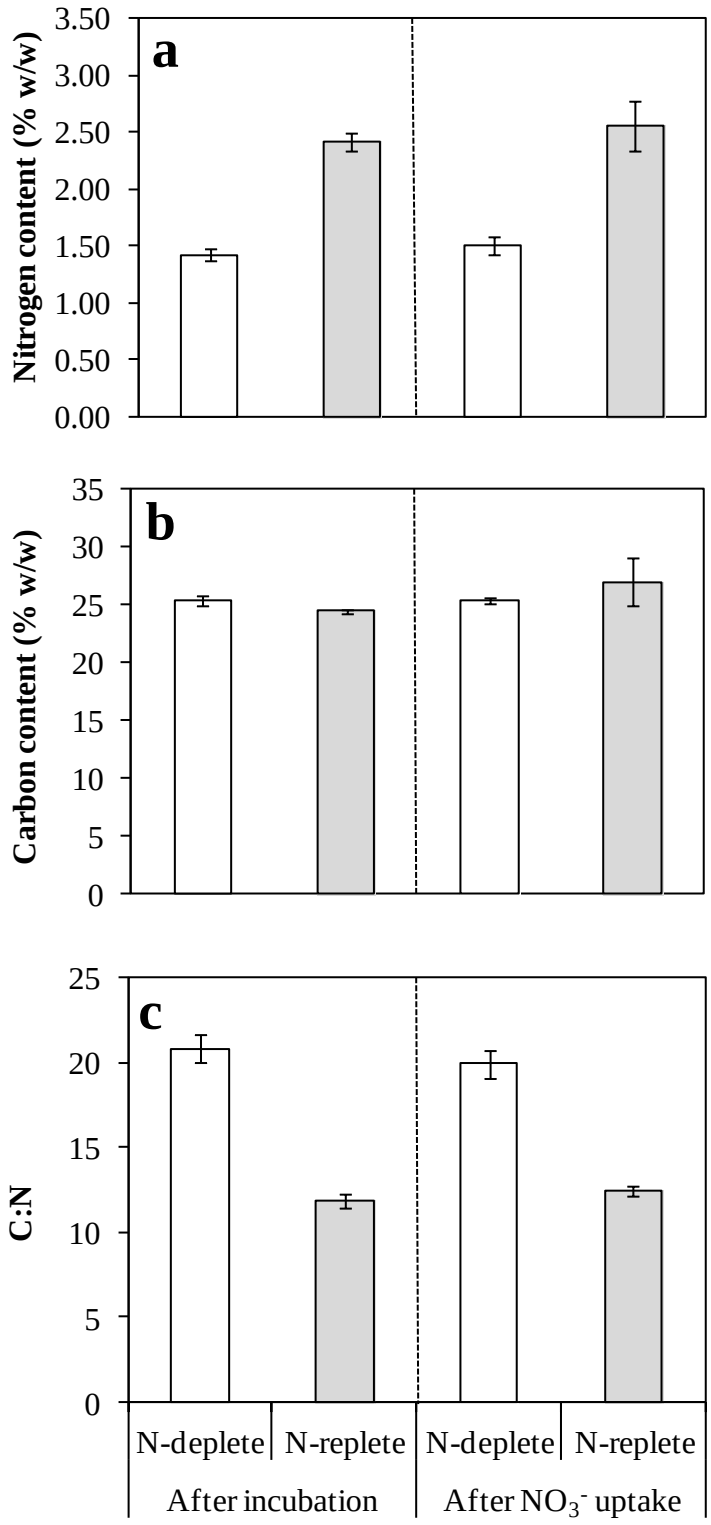

Figure 5.5: Total tissue nitrogen content (a), total tissue carbon content (b), and C: N ratio (c) of *Macrocystis* blade sections after 3 days' incubation under ambient (< 7 µM) (N-deplete), and nitrate (80 µM) enriched SW (N-replete) and after the 1 h NO_3^- uptake measurements on day 3 at an initial concentration of 20 µM. Data are means of 4 replicates ± SE (after incubations) and 6 replicates ± SE (after NO_3^- uptake). Significantly different sub-groups: (a) after incubations: N-deplete < N-replete; after NO_3^- uptake: N-deplete < N-replete, (b) after incubations: N-deplete > N-replete; after

NO_3^- uptake: N-deplete = N-replete, (c) after incubations: N-deplete > N-replete; after NO_3^- uptake: N-deplete > N-replete (Student's t-test). No significant differences in N-replete and N-deplete prior or after NO_3^- uptake (Student's t-test).

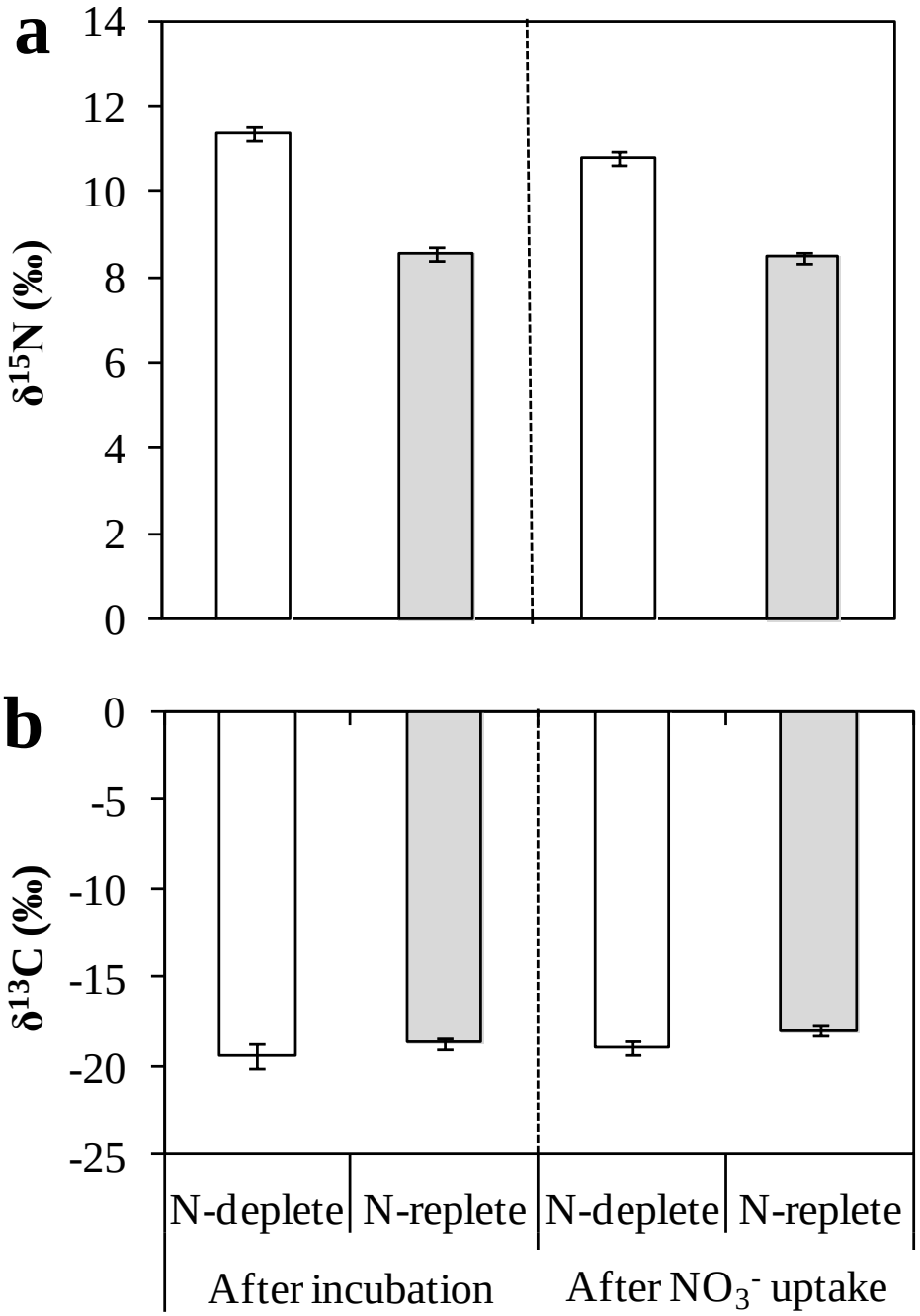

Figure 5.6: Stable isotopes $\delta^{15}N$ (a) and $\delta^{13}C$ (b) of *Macrocystis* blade sections after 3 days' incubation under ambient (< 7 µM) (N-deplete), and nitrate (80 µM) enriched SW (N-replete) and after the 1 h NO_3^- uptake measurements on day 3 at an initial concentration of 20 µM. Data are means of 4 replicates ± SE (after incubations) and 6 replicates ± SE (after NO_3^- uptake). Significantly different sub-groups: (a) after incubations: N-deplete > N-replete; after NO_3^- uptake: N-deplete > N-replete; N-deplete: after incubations > after NO_3^- uptake; N-replete: after incubations = after NO_3^- uptake, (b) no significant differences between sub-groups (Student's t-test).

5.3.4 Physiological parameters following incubations under ambient pCO_2 400 µatm and elevated pCO_2 1200 µatm

Nitrate uptake rates

Nitrate uptake rates of *Macrocystis* blades varied significantly between pCO_2/pH treatments (Fig. 5.7). The NO_3^- uptake rate of N-deplete *Macrocystis* blades incubated under the OA treatment (pCO_2 1200 µatm; pH 7.59) was 28% higher than N-deplete blades incubated under the ambient treatment (pCO_2 400 µatm; pH 8.00), at 2.11 and 1.51 µmol NO_3^- g^{-1} FW h^{-1}, respectively (Student's t-test, t = 2.717, df = 9, P = 0.024, Fig. 5.7, Table 5.3). Conversely, for N-replete blades, NO_3^- uptake did not change between the pCO_2/pH treatments (Student's t-test, t = 1.427, df = 9, P = 0.187, Fig. 5.7, Table 5.3). No significant differences in NO_3^- uptake rates were recorded between N-deplete and N-replete blades incubated under either the OA treatment (Student's t-test, t = –1.058, df = 9, P = 0.318, Fig. 5.7) or the ambient treatment (Student's t-test, t = –0.121, df = 9, P = 0.906 , Fig. 5.7, Table 5.3).

Nitrate reductase activity (NR)

NR activity of N-deplete *Macrocystis* blades was unaffected by the OA treatment (pCO_2 1200 µatm; pH 7.59). Similar NR activities of 3.60 and 2.95 nmol NO_3^- g^{-1} FW min^{-1} were observed in blade sections incubated under ambient (pCO_2 400 µatm; pH 8.00) and OA treatment (pCO_2 1200 µatm; pH 7.59), respectively (Student's t-test, t = 1.461, df = 9, P = 0.178, Fig. 5.8, Table 5.3). Conversely, for N-replete blades incubated under the ambient treatment (400 µatm; pH 8.00), NR activity was 55% lower than that of blades incubated under the OA treatment (1200 µatm; pH 7.59), at 1.69 and 3.77 nmol NO_3^- g^{-1} FW min^{-1}, respectively (Student's t-test, t = 2.686, df = 9, P = 0.025, Fig. 5.8, Table 5.3). For the OA treatment, there was no significant difference in NR activity between

N-deplete and N-replete *Macrocystis* blades (Student's t-test, t = 2.32, df = 9, P = 0.822, Fig. 5.8), whereas under the ambient treatment the NR activity of N-replete blades was 43% lower compared to N-deplete blades (Student's t-test, t = –2.893, df = 9, P = 0.018, Fig. 5.8, Table 5.3).

Soluble tissue nitrate

The soluble tissue NO_3 content (= internal NO_3^- pool) of *Macrocystis* blades varied significantly between pCO_2/pH treatments (Fig. 5.9). The tissue NO_3^- content of N-deplete *Macrocystis* blades was 81% higher under the OA treatment (pCO_2 1200 µatm; pH 7.59) than ambient (pCO_2 400 µatm; pH 8.00), at 0.91 and 0.16 µmol NO_3^- g^{-1} FW, respectively (Student's t-test, t = 3.590, df = 8, P = 0.007, Fig. 5.9, Table 5.3). Conversely, for N-replete blades, tissue NO_3^- content did not vary between pCO_2/pH treatments (Student's t-test, t = –0.241, df = 9, P = 0.815, Fig. 5.9, Table 5.3). For the OA treatment, tissue NO_3^- content was 89% higher in N-replete *Macrocystis* blades than that of N-deplete blades (Student's t-test, t = 7.182, df = 8, P < 0.001, Fig. 5.9). A similar result was observed for the ambient treatment (pCO_2 400 µatm; pH 8.00) as tissue NO_3^- content was 98% higher in N-replete blades compared to N-deplete blades (Student's t-test, t = 7.182, df = 8, P < 0.001, Fig. 5.9, Table 5.3).

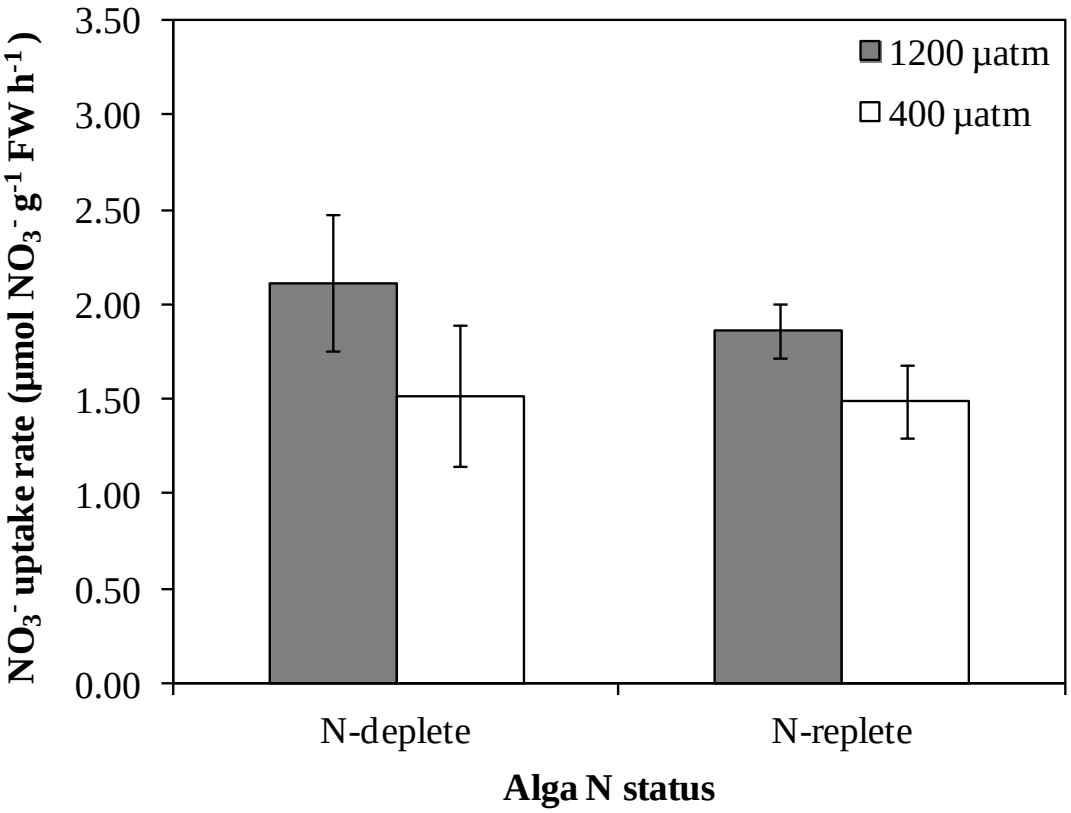

Figure 5.7: Nitrate uptake, measured at an initial concentration of 20 µM, of *Macrocystis* blade sections that were first incubated for 3-days in < 7 µM NO_3^- (N-deplete) or 80 µM NO_3^- (N-replete), and then incubated for a further 3 days at 20 µM NO_3^- in either ambient (pCO_2 400 µatm; pH 8.00) or an OA treatment (pCO_2 1200 µatm; pH 7.59). Data are means of 6 replicates ± SE. Significantly different sub-groups: N-deplete: 1200 µatm > 400 µatm; N-replete: 1200 µatm = 400 µatm; 1200 µatm: N-deplete = N-replete; 400 µatm: N-deplete = N-replete (Student's t-test).

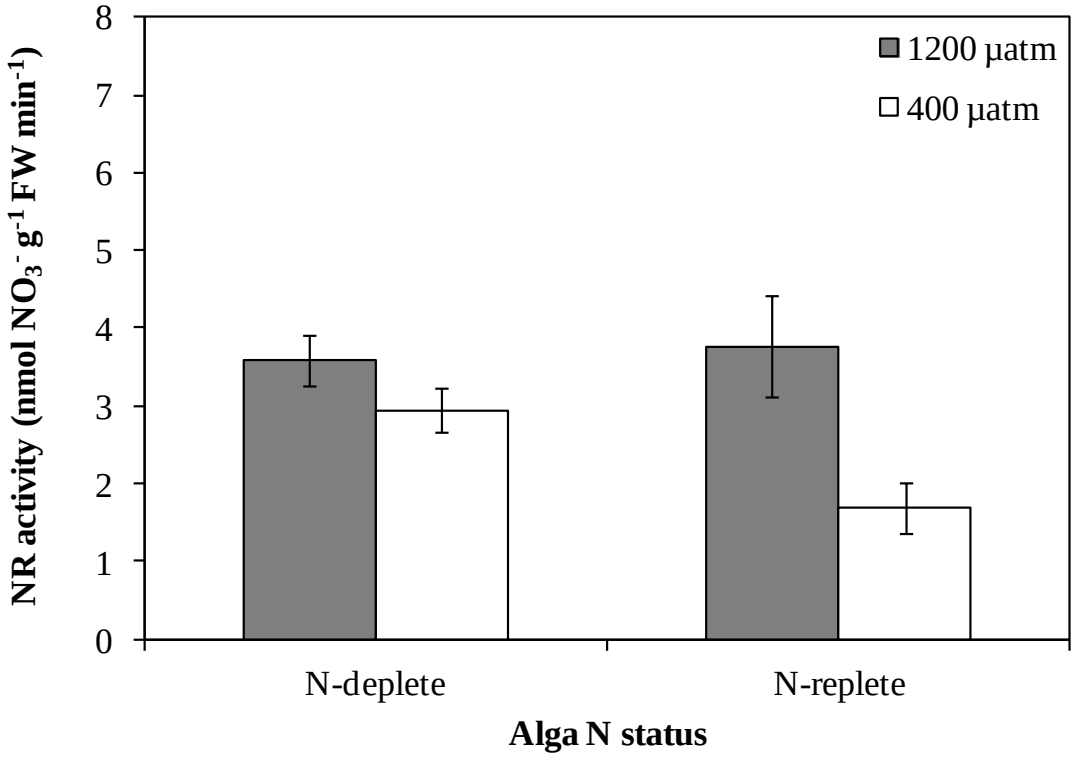

Figure 5.8: Nitrate reductase (NR) activity of *Macrocystis* blade sections that were first incubated for 3-days in < 7 µM NO_3^- (N-deplete) or 80 µM NO_3^- (N-replete), and then incubated for a further 3 days at 20 µM NO_3^- in either ambient (pCO_2 400 µatm; pH 8.00) or an OA treatment (pCO_2 1200 µatm; pH 7.59). Data are means of 6 replicates ± SE. Significantly different sub-groups: N-deplete: 1200 µatm = 400 µatm; N-replete: 1200 µatm > 400 µatm; 1200 µatm: N-deplete = N-replete; 400 µatm: N-deplete > N-replete (Student's t-test).

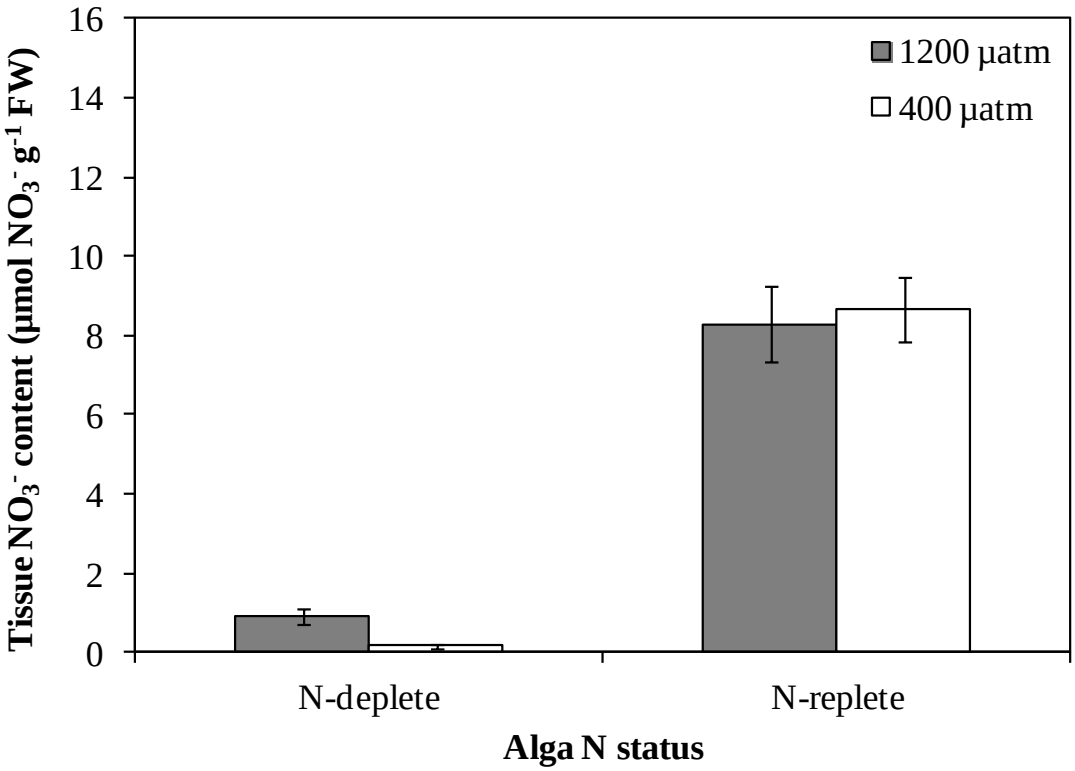

Figure 5.9: Tissue NO_3^- content of *Macrocystis* blade sections that were first incubated for 3-days in < 7 µM NO_3^- (N-deplete) or 80 µM NO_3^- (N-replete), and then incubated for a further 3 days at 20 µM NO_3^- in either ambient (pCO_2 400 µatm; pH 8.00) or an OA treatment (pCO_2 1200 µatm; pH 7.59). Data are means of 6 replicates ± SE. Significantly different sub-groups: N-deplete: 1200 µatm > 400 µatm; N-replete: 1200 µatm = 400 µatm; 1200 µatm: N-deplete < N-replete; 400 µatm: N-deplete < N-replete (Student's t-test).

Photosynthetic rate

The photosynthetic rates of N-deplete and N-replete *Macrocystis* blades did not significantly vary between pCO_2/pH treatments (Fig. 5.10). The photosynthetic rates in N-deplete blades recorded for the ambient (pCO_2 400 µatm; pH 8.00) and OA treatment (pCO_2 1200 µatm; pH 7.59), respectively, were similar (Student's t-test, t = 0.500, df = 10, P = 0.628, Fig. 5.10, Table 5.3). A similar result was observed in N-replete blades incubated under the ambient (pCO_2 400 µatm; pH 8.00) or OA treatment (pCO_2 1200 µatm; pH 7.59) where respective photosynthetic rates of 28.22 and 39.69 µmol O_2 g^{-1} FW h^{-1} were not statistically different (Student's t-test, t = 0.721, df = 7, P = 0.494, Fig. 5.10, Table 5.3). Photosynthetic rates did not vary between N-deplete and N-replete blades either under the ambient (Student's t-test, t = –0.079, df = 9, P = 0.938, Fig. 5.10) or OA treatment (Student's t-test, t = 0.433, df = 8, P = 0.677, Fig. 5.10).

Growth rate

The relative growth rates (RGR) of N-deplete and N-replete *Macrocystis* blades did not vary with pCO_2/pH treatments (Fig. 5.11). Growth rates were similar (13.02% and 13.57% per day) for N-deplete blades incubated either under the ambient (pCO_2 400 µatm; pH 8.00) or OA treatment (pCO_2 1200 µatm; pH 7.59), respectively (Student's t-test, t = 0.476, df = 10, P = 0.645, Fig. 5.11, Table 5.3). A similar result was observed in N-replete blades as RGRs of 14.11% and 16.38% for blades incubated under ambient (pCO_2 400 µatm; pH 8.00) and OA treatment (pCO_2 1200 µatm; pH 7.59), respectively (Student's t-test, t = 1.901, df = 10, P = 0.086, Fig. 5.11, Table 5.3). Growth rates did not vary between N-deplete and N-replete blades either under the ambient (Student's t-test, t = –1.154, df = 10, P = 0.275, Fig. 5.11) or OA treatment (Student's t-test, t = –2.049, df = 10, P = 0.068, Fig. 5.11).

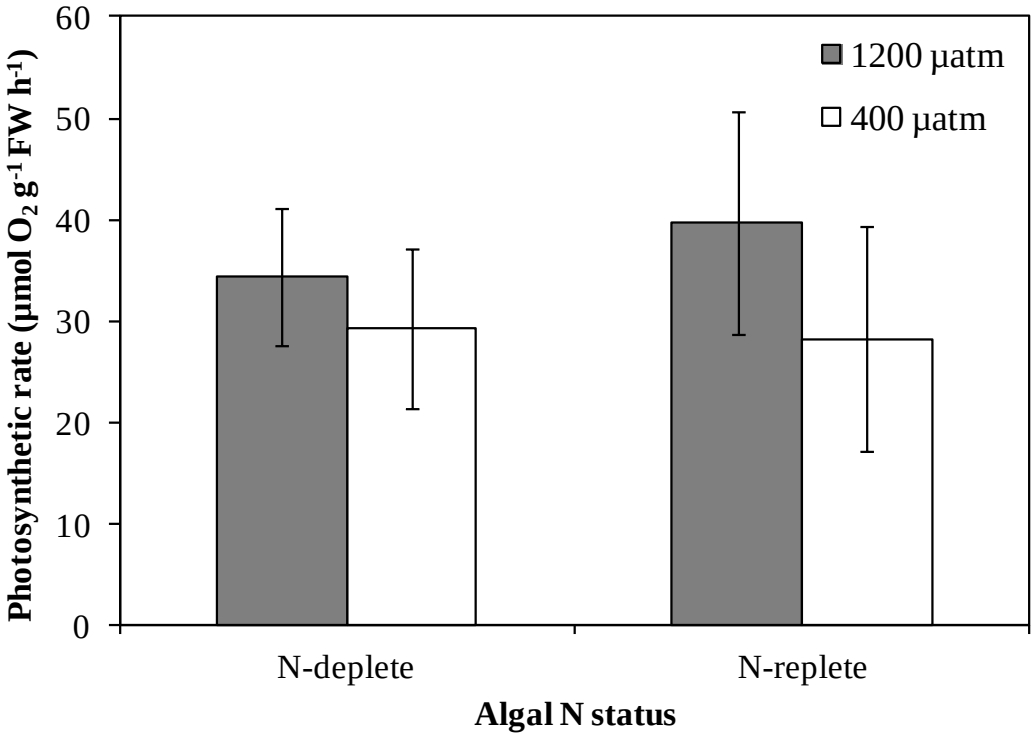

Figure 5.10: Photosynthetic rate of *Macrocystis* blade sections that were first incubated for 3-days in < 7 µM NO_3^- (N-deplete) or 80 µM NO_3^- (N-replete), and then incubated for a further 3 days at 20 µM NO_3^- in either ambient (pCO_2 400 µatm; pH 8.00) or an OA treatment (pCO_2 1200 µatm; pH 7.59). Data are means of 6 replicates ± SE. Significantly different sub-groups: N-deplete: 1200 µatm = 400 µatm; N-replete: 1200 µatm = 400 µatm; 1200 µatm: N-deplete = N-replete; 400 µatm: N-deplete = N-replete (Student's t-test).

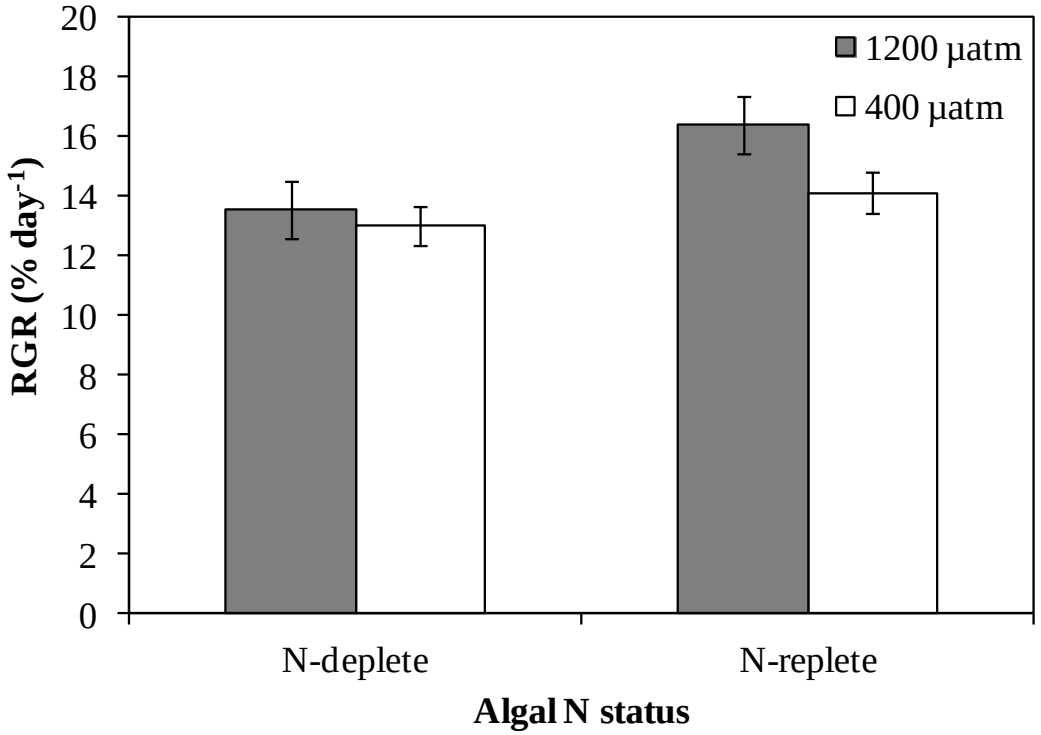

Figure 5.11: Relative growth rates (RGR) of *Macrocystis* blade sections that were first incubated for 3-days in < 7 µM NO_3^- (N-deplete) or 80 µM NO_3^- (N-replete), and then incubated for a further 3 days at 20 µM NO_3^- in either ambient (pCO_2 400 µatm; pH 8.00) or an OA treatment (pCO_2 1200 µatm; pH 7.59). Data are means of 6 replicates ± SE. Significantly different sub-groups: N-deplete: 1200 µatm = 400 µatm; N-replete: 1200 µatm = 400 µatm; 1200 µatm: N-deplete = N-replete; 400 µatm: N-deplete = N-replete (Student's t-test).

Total tissue carbon and nitrogen content, and stable isotopes ($\delta^{15}N$ and $\delta^{13}C$)

The chemical tissue composition of *Macrocystis* blades was mostly unaffected by the pCO_2/pH treatments (Fig. 5.12, Table 5.3). For N-deplete blades, neither total tissue N content, total C tissue content nor C:N ratio varied between pCO_2/pH treatments (Student's t-test, t = 1.940, df = 10, P = 0.081; t = –0.976, df = 10, P = 0.352; t = –1.730, df = 10, P = 0.114, respectively, Fig. 5.12a-c). Similarly, for N-replete blades neither total tissue N content, total tissue C content nor C:N ratio varied between pCO_2/pH treatments (Student's t-test, t = 0.614, df = 10, P = 0.553; t = –1.416, df = 10, P = 0.187; t = 2.119, df = 10, P = 0.060, respectively, Fig. 5.12a-c). For the OA treatment, total tissue N content was 31% lower in N-deplete *Macrocystis* blades than that N-replete blades (Student's t-test, t = 13.578, df = 10, P = < 0.001, Fig. 5.12a). A similar result was observed for the ambient treatment (Student's t-test, t = 7.418, df = 10, P = < 0.001, Fig. 5.12a). Otherwise, total tissue C content did not vary between N-deplete and N-replete blades either under the ambient (Student's t-test, t = 1.638, df = 10, P = 0.132, Fig. 5.12b) or OA treatment (Student's t-test, t = 0.327, df = 10, P = 0.70, Fig. 5.12b). The C:N ratio was significantly higher in N-deplete than in N-replete blades incubated either under the ambient (Student's t-test, t = –6.529, df = 10, P = < 0.001, Fig. 5.12c) or OA treatment (Student's t-test, t = –9.404, df = 10, P = < 0.001, Fig. 5.12c).

The $\delta^{15}N$ signature of N-deplete *Macrocystis* blades did not vary between pCO_2/pH treatments (Student's t-test, t = –0.326, df = 10, P = 0.751, Fig. 5.13a, Table 5.3), while the $\delta^{13}C$ signature changed between pCO_2/pH treatments (Fig. 5.13b). The $\delta^{13}C$ values of –16.54 and –17.64 recorded under the ambient and OA treatments, respectively, varied significantly (Student's t-test, t = –2.613, df = 10, P = 0.026, Fig. 5.13b, Table 5.3). For N-replete blades, neither the $\delta^{13}C$ signature nor the $\delta^{15}N$ signature

varied between pCO_2/pH treatments (Student's t-test, t = 0.206, df = 10, P = 0.841; t = –1.419, df = 10, P = 0.186, respectively, Fig. 5.13a-b, Table 5.3). The $\delta^{15}N$ signature was significantly higher in N-deplete than in N-replete blades incubated in both the ambient (Student's t-test, t = –6.289, df = 10, P = < 0.001, Fig. 5.13a) and OA treatment (Student's t-test, t = –5.976, df = 10, P = < 0.001, Fig. 5.13a). The $\delta^{13}C$ signature was significantly higher for N-deplete than in N-replete blades incubated either under the ambient (Student's t-test, t = 2.896, df = 10, P = 0.016, Fig. 5.13b) or OA treatment (Student's t-test, t = 7.884, df = 10, P = < 0.001, Fig. 5.13b).

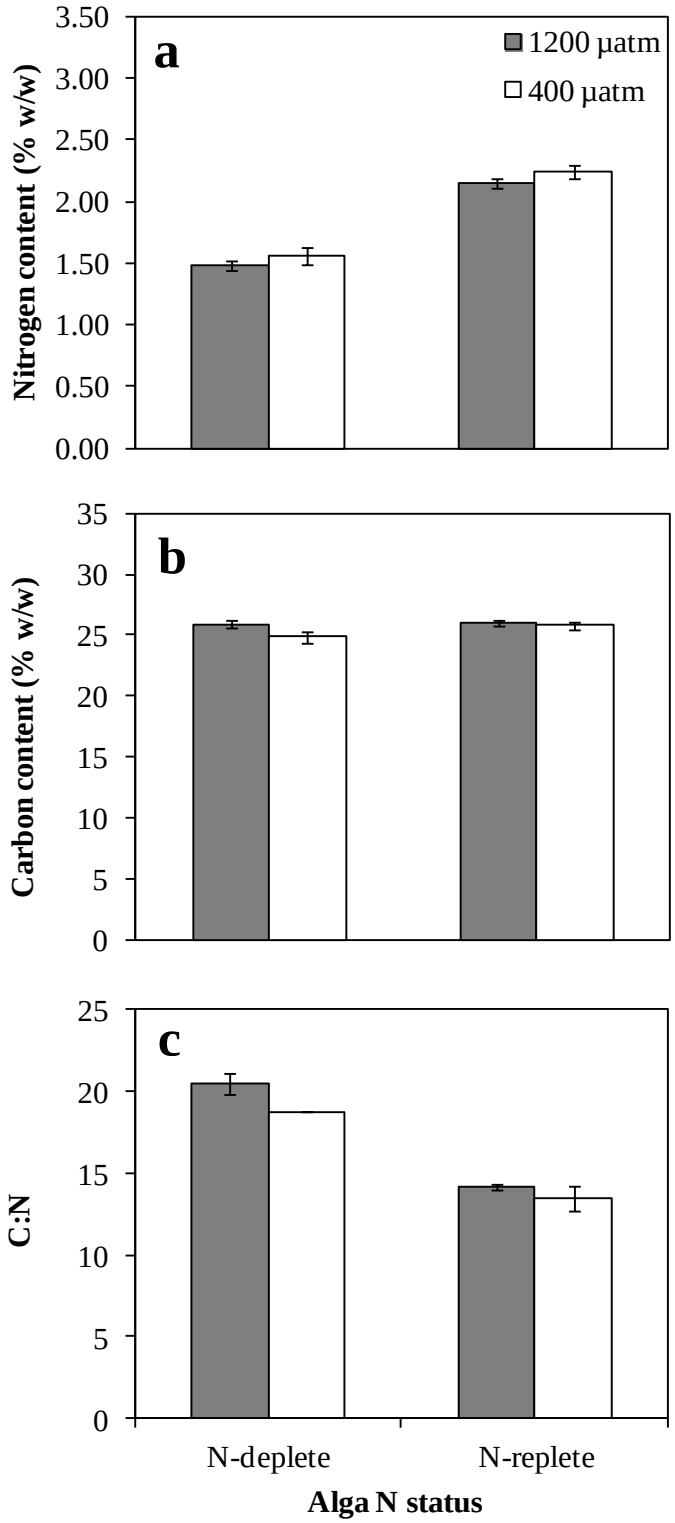

Figure 5.12: Total tissue nitrogen content (a), total tissue carbon content (b) and the C:N ratio (c) of *Macrocystis* blade sections that were first incubated for 3-days in < 7 µM NO_3^- (N-deplete) or 80 µM NO_3^- (N-replete), and then incubated for a further 3 days at 20 µM NO_3^- in either ambient (pCO_2 400 µatm; pH 8.00) or an OA treatment (pCO_2 1200 µatm; pH 7.59). Data are means of 6 replicates ± SE. Significantly different sub-groups: (a), (b) and (c) N-deplete: 1200 µatm = 400 µatm; N-replete: 1200 µatm = 400 µatm; (a) 1200 µatm: N-deplete < N-replete; 400 µatm: N-deplete < N-replete, (b)

did not vary significantly between sub-groups, (c) 1200 µatm: N-deplete > N-replete; 400 µatm: N-deplete > N-replete (Student's t-test).

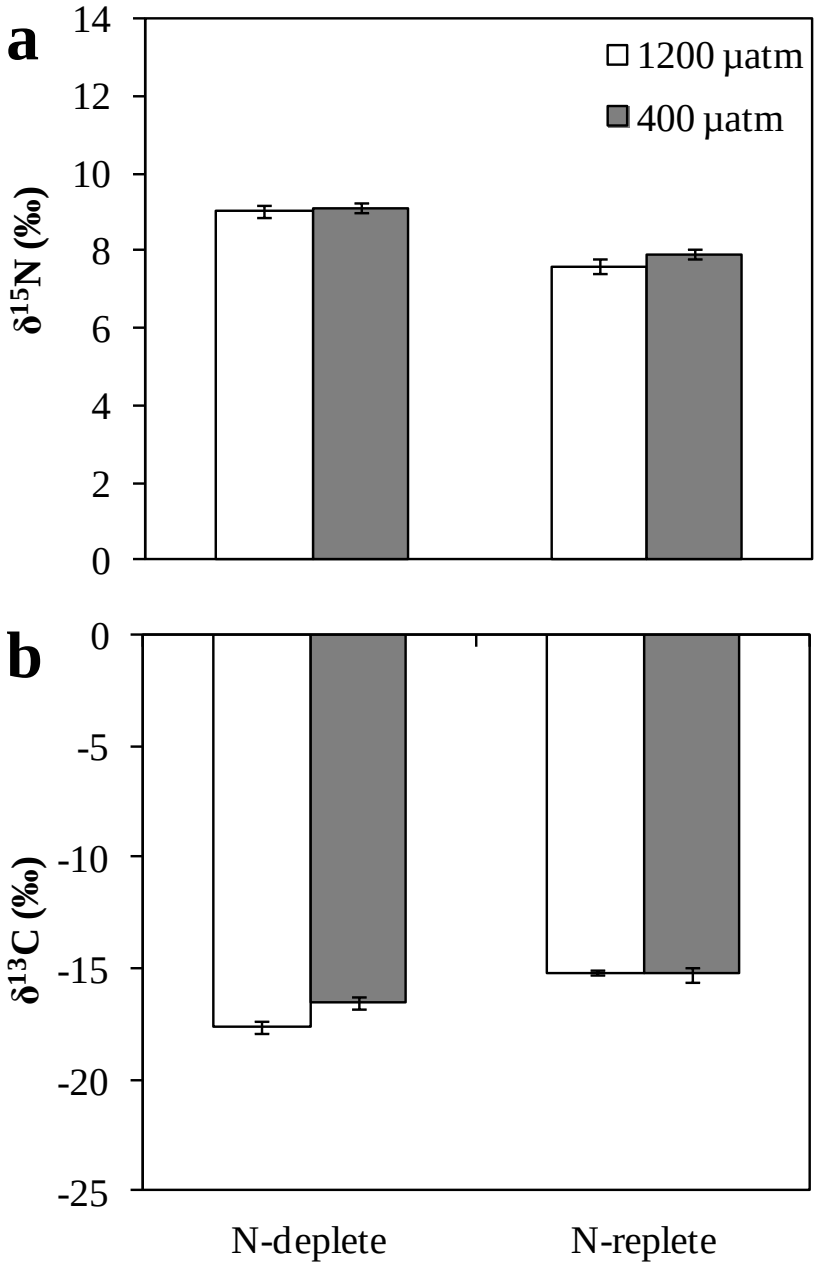

Figure 5.13: Stable isotopes $\delta^{15}N$ (a) and $\delta^{13}C$ (b) of *Macrocystis* blade sections that were first incubated for 3-days in < 7 µM NO_3^- (N-deplete) or 80 µM NO_3^- (N-replete), and then incubated for a further 3 days at 20 µM NO_3^- in either ambient (pCO_2 400 µatm; pH 8.00) or an OA treatment (pCO_2 1200 µatm; pH 7.59). Data are means of 6 replicates ± SE. Significantly different sub-groups: (a) N-deplete: 1200 µatm = 400 µatm; N-replete: 1200 µatm = 400 µatm; 1200 µatm: N-deplete > N-replete; 400 µatm: N-deplete > N-replete, (b) N-deplete: 1200 µatm > 400 µatm; N-replete: 1200 µatm = 400 µatm; 1200 µatm: N-deplete > N-replete; 400 µatm: N-deplete > N-replete (Student's t-test).

Table 5.3: A comparative table illustrating the results obtained after the 3-day pre-experimental incubations in <7µM NO_3^- (N-deplete) or 80 µM NO_3^- (N-replete), and after the 3-day incubations in different pCO_2 treatments, ambient (pCO_2 400 µatm; pH 8.00) and OA (pCO_2 1200 µatm; pH 7.59) at 20 µM NO_3^-. ↑: higher; ↓: lower; =: no differences.

Biochemical and physiological parameters	**Pre-experimental incubations**		**pCO_2 incubations at 400 µatm and 1200 µatm**	
	N-deplete	N-replete	N-deplete	N-replete
Uptake rate (µmol NO_3^- g^{-1} FW h^{-1})	↑	↓	↑ at 1200 µatm	No effect
Nitrate reductase (nmol NO_3^- g^{-1} FW min^{-1})	↓	↑	No effect	↓ at 400 µatm
Tissue soluble NO_3^- pool (µmol NO_3^- g^{-1} FW)	↓	↑	↑ at 1200 µatm	No effect
$\delta^{15}N$	↑	↓	No effect	No effect
$\delta^{13}C$	=	=	↑ at 1200 µatm	No effect
N (% w/w)	↓	↑	No effect	No effect
C (% w/w)	=	=	No effect	No effect
C:N ratio	↑	↓	No effect	No effect
Photosynthetic rate (µmol O_2 g^{-1} FW h^{-1})	N/M	N/M	No effect	No effect
Growth rate (% day^{-1})	=	=	No effect	No effect

5.4 Discussion

5.4.1 Nitrogen metabolism of *Macrocystis*

The first hypothesis, that the rates of NO_3^- uptake and assimilation of *Macrocystis* are dependent on the NO_3^- supply, was supported. The NR activity, internal NO_3^- pool and total tissue N content were considerably reduced when NO_3^- supply was low, indicating that these parameters are influenced by external NO_3^- concentrations. When NO_3^- becomes available, the uptake rate of N-deplete blades was 2-times higher than N-replete blades, suggesting that NO_3^- uptake by *Macrocystis* can be rapidly stimulated, especially in blades with a low internal NO_3^- pool. In addition, although NR activity of N-deplete blades did not vary significantly after the 1 h NO_3^- uptake measurement, there was a trend of increased NR activity, whereas for N-replete blades NR activity was significantly down-regulated after the 1 h NO_3^- uptake measurement; these findings indicate that NR activity may be rapidly (~1 h) up or down-regulated depending on the external NO_3^- concentrations. These results indicate that *Macrocystis* can rapidly up-regulate their N uptake, storage and assimilation (i.e. NR), which may be required to maintain its growth in environments where N supply fluctuates sporadically and seasonally; thus when NO_3^- availability increases suddenly *Macrocystis* has the ability for rapid NO_3^- uptake and assimilation, and NO_3^- that is not immediately assimilated may be stored for using during periods of external N limitation.

The total tissue N content and internal NO_3^- pool of *Macrocystis* might reflect external variations in NO_3^- concentrations (Wheeler and North 1980, Wheeler and Srivastava 1984). It has been shown that for *Macrocystis*, total tissue N content decreases considerably under low external NO_3^- concentrations (0-1.5 µM), reaching values of 0.7–1.0% dry wt (Wheeler and North 1980, Druehl 1984, Hurd et al. 1996,

Hurd et al. 2000, Stewart et al. 2009). Seasonal changes have been reported in *Macrocystis* populations from California, Canada and New Zealand, with maximal values of 2.2-3.0% dry wt in winter (high external [NO_3^-]) and minimal values of 0.8-1.7% dry wt in summer (low external [NO_3^-]) (Wheeler and North 1981, Wheeler and Srivastava 1984, Zimmerman and Kremer 1986, van Tussenbroek 1989, Brown et al. 1997, Hepburn et al. 2006).

The pattern observed in previous studies between total tissue N content and external NO_3^- concentrations agree with the results observed in this study. After the 3 day pre-experimental incubations under a low and high [NO_3^-], the total tissue N content of *Macrocystis* blade sections was 1.42 % dry wt and 2.42% dry wt, respectively. For N-deplete blades, total tissue N content was lower by 31% compared to initial values of the field-collected blades (2.06% of dry weight), whereas for N-replete blades was higher by 17.5%. These results suggest that for N-deplete blades, dilution of tissue N content and likely movements between the internal N pools occurred to support growth under limited NO_3^- concentrations (McGlathery et al. 1996), while for N-replete blades likely most of the new NO_3^- entered the cell was stored as internal inorganic or organic N pools, contributing to the increase in the total tissue N content. The rapid response of *Macrocystis* to external NO_3^- concentrations observed in this study provides evidence that this species can rapidly modify their nitrogen metabolism in response to the external NO_3^- availability, which might explain in part the differences observed in growth and storage nitrogen capacity between *Macrocystis* populations from different localities (Kain 1989, Kopczak et al. 1991).

The rapid accumulation of tissue N content in *Macrocystis* was also reflected in the size of the internal NO_3^- pool. Druehl (1984) and Wheeler and Srivastava (1984) found that the internal NO_3^- pool of *Macrocystis* may increase 30-40 fold after a short

period of incubation (hours-days) under a high [NO_3^-]. Similarly, in the present study, internal NO_3^- pools of *Macrocystis* blades increased 70-fold after a 3 day incubation in 80 µM NO_3^-. Seasonal variation in the internal NO_3^- pool in *Macrocystis* has also been reported, being positively correlated with external NO_3^- concentrations (Wheeler and Srivastava 1984, Hurd et al. 1996, Hepburn and Hurd 2005). In *Macrocystis integrifolia* (= *Macrocystis pyrifera*), maximum internal NO_3^- pools of 50-70 µmol g^{-1} FW were observed in winter, whereas undetectable values were observed in spring/summer (Wheeler and Srivastava 1984, Hurd et al. 1996). These latter values are comparable to the low values (0.18 µmol g^{-1} FW) observed in *Macrocystis* blade sections grown under low [NO_3^-] and the maximum values (13.89 µmol g^{-1} FW) observed in blades grown under higher concentrations, although this latter value is lower compared to the maximum recorded in previous studies, the differences observed with previous studies were likely due to the short incubation time utilized in our experiment. (Wheeler and Srivastava 1984, Hurd et al. 1996). The differences might be explained by the short-tem incubation (3 days) utilized in this experiment and by the experimental (80 µM NO_3^- pulse) and environmental conditions (constant supply of NO_3^-). Despite the differences observed between studies in the maximum internal NO_3^- pools, the same relationship between external NO_3^- concentrations and internal NO_3^- pool was observed.

Macrocystis exhibits a lower nitrate storage capacity than *L. longicruris*, which may accumulate to up 28,000-fold the external NO_3^- concentration (Chapman and Craige 1977, Wheeler and Srivastava 1984). *Macrocystis* might accumulate to up 3-6 fold the maximum external NO_3^- concentrations (Wheeler and Srivastava 1984, Hurd et al. 1996). Thus, the contribution of the internal NO_3^- pool in *Macrocystis* may not contribute greatly to the total tissue N content. In this study, for N-replete blades, the internal NO_3^- pool (1.38 µmol NO_3^- g^{-1} DW; using a wet-to dry mass conversion for

Macrocystis of 0.1; Wheeler and Srivastava 1984) was 98% higher than N-deplete blades (0.018 µmol NO_3^- g^{-1} DW), and contributed a 57.5% of the total N content (2.47% of dry weight). A similar result was observed in N-replete thalli of *F. serratus* and *F. vesiculosus*, where inorganic pools (mainly NO_3^-) contributed a 44% of the total tissue N content (Young et al. 2009). In contrast, the internal NO_3^- pool of N-deplete *Macrocystis* blades contributed only by a 1.6% of the total N content (1.42% of dry weight). These results suggest that most of the NO_3^- taken up by N-deplete blades was immediately assimilated by NR, and likely used to support growth. In other macroalgae such as *Ulva fenestrata* and *Chaetomorpha linum*, cultured in enriched NO_3^- seawater, the inorganic NO_3^- pool contributed to about 7-15% of the total tissue N content (McGlathery et al. 1996, Naldi and Wheeler 1999). In brown macroalgae, *Laminaria digitata* and *F. vesiculosus*, inorganic NO_3^- pool contributed to about 3-4% of the total tissue N content in winter (Young et al. 2007). The contribution of the inorganic N pools (i.e. NO_3^- and NH_4^+) to the total tissue N content change seasonally, depending on the external NO_3^- concentrations (Young et al. 2007). Wheeler and Srivastava (1984) suggested that internal NO_3^- pool is a relative term because it depends on the NO_3^- assimilation rate. Thus, the differences observed between species, and between *Macrocystis* blades with different N statuses might be explained by a different assimilation rate of NO_3^-, e.g. with a high NR activity most of the NO_3^- incorporated into the cell is rapidly assimilated rather than stored, and it may be stored as internal N organic pools (e.g. amino acids or proteins), but might also be explained by the growth demand of each species, as new NO_3^- entering into the cell might be immediately directed into growth rather than stored.

The results presented here support those of previous studies, indicating that macroalgal NO_3^- uptake rates might be controlled by small changes in internal NO_3^-

pools, and that uptake rates increase after periods of nitrogen starvation (Wheeler and Srivastava 1984, Thomas and Harrison 1985, Hwang et al. 1987, McGlathery et al. 1996, Lartigue and Sherman 2005, Young et al. 2009). At the end of the experiment, internal NO_3^- pools and total tissue N content were lower in *Macrocystis* blades incubated at low [NO_3^-], and NO_3^- uptake rates were higher, than blades incubated under higher concentrations. It has been shown for some macroalgae, *C. linum*, *Porphyra perforata*, *Gracilaria tikvahiae*, including *Macrocystis*, that NO_3^- uptake rates are inversely correlated with internal NO_3^- pools (Haines and Wheeler 1978, Wheeler and Srivastava 1984, Thomas and Harrison 1985, Kopczak 1994, McGlathery et al. 1996, Hepburn et al. 2006). Even though total tissue N content may remain high, uptake rates are increased to refill internal inorganic pools (i.e. NO_3^- and NH_4^+) utilized during low N availability (McGlathery et al. 1996). Increasing N uptake capacity when N availability is limited is an important adaptation of macroalgae that inhabit an environment where N supply may occur in episodic pulses (Zimmerman and Kremer 1984, Kopczak 1994). However, despite increases in NO_3^- uptake rate and internal NO_3^- pools in response to an episodic NO_3^- pulse after a period of N-limitation, the rate of filling other internal N pools (i.e. amino acids and proteins), depend on the assimilation rate of NR.

The NR activity in macroalgae seems to be controlled by the external NO_3^- concentrations (Lartigue and Sherman 2005), but it might also be influenced by changes in the size of internal NO_3^- pools (Young et al. 2007). In this study, NR activity in *Macrocystis* was lower under low external [NO_3^-], following the same pattern observed in the internal NO_3^- pool and total tissue N content. These results suggest that NR might be regulated by both external [NO_3^-] and internal NO_3^- pools, as reported for other brown macroalgal species, i.e. *F. serratus* and *L. digitata* (Young et al. 2007). NR

activity did significantly decrease for N-replete blades following NO_3^- resupply (during the 1 h at 20 µM uptake measurement); however, for N-replete blades NR did not change after the 1 h NO_3^- resupply. Young et al. (2009) showed that increases in NR activity were observed after 4-7 h of NO_3^- resupply (100 µM) in macroalgae *F. serratus* and *F. vesiculosus* grown for 3 weeks under N-starvation. This suggests that a longer incubation time (> 1 h) may be required to increase NR activity in *Macrocystis* after a period of N-limitation. Indeed, after the 1 h NO_3^- resupply to N-deplete blades, the internal NO_3^- pool increased by 5-fold, suggesting that the new NO_3^- incorporated into the cell was first stored internally, most likely within the vacuole (Corzo and Niell 1994), and then assimilated by NR. The decrease in NR activity observed in N-replete blades suggests a fast response to a change in the external NO_3^- availability, and also that NR activity may be down-regulated more rapidly than it can be up-regulated, likely due to the energy required for the NR synthesis. This idea also supported by the decrease observed in NR activity from field-collected blades (6.24 nmol NO_3^- g^{-1} FW) compared to N-deplete blades (2.52 nmol NO_3^- g^{-1} FW). The high NR activity observed in field-collected blades, when external and internal NO_3^- concentrations were low suggests that NR is always active to allow a rapid assimilation of an episodic NO_3^- pulse, but it is unclear as to whether the regulation of NR is by external and/or internal NO_3^- concentrations.

NR in brown macroalgae may depend on both an environmentally inducible and constitutive NR isoforms, as occur in higher plants (Solomonson and Barber 1990, Young et al. 2009). Earlier studies on microalgae reported the existence of two forms of NR enzymes: (1) located in the cytoplasm, and (2) located in the plasma-membrane, which may be involved in the NO_3^- uptake (Tischner et al. 1989, Solomonson and Barber 1990, Stöhr et al. 1993). NR located in the plasma-membrane appears to be

under a different regulatory control than the internal NR (Solomonson and Barber 1990). Butz and Jackson (1977) suggested that NR may be part of an enzyme complex involved in both the transport and reduction of NO_3^-. Hurd et al. (1995) proposed that one or more izoenzymes of NR may be present in macroalgae. Therefore, similar to microalgae, two forms of NR may exist in macroalgae, which may be regulated by different factors, that is plasma-membrane NR might be regulated by external NO_3^- concentrations while cytoplasmatic NR may be regulated by both external and internal NO_3^- concentrations. Therefore, each of the two forms of NR may be saturated under different NO_3^- concentrations. However, further studies (e.g. gene expression studies) on NO_3^- uptake and assimilation in macroalgae are required for a better understanding of the intracellular regulation on the synthesis of the relevant enzymes that are involved in the nitrogen metabolism (i.e. NR, NiR, GS).

Total tissue N content and C:N ratio are useful indicators of the N status of algae to assess N-limitation (Wheeler and North 1981). C:N ratios >20 indicate a possible N limitation in macroalgae (Hurd et al. 2014). In this study, both total tissue N content and C:N ratio varied as a function of external NO_3^- concentration and algal N status as shown in other macroalgal species (Vergara 1995, McGlathery and Pedersen 1999, Phillips and Hurd 2003, Young et al. 2009). After the pre-experimental incubations, total C content in *Macrocystis* blades ranged between 24.42-25.34 (% dry wt), similar to the mean reported for macroalgae (24.8± 6.3 % dry wt) (Duarte 1993), and N content ranged between 1.49, in *Macrocystis* blade sections incubated under low [NO_3^-] to 2.41 (% dry wt) in blades incubated under high [NO_3^-]. Duarte (1993) suggested that as the variability in N concentrations in macrocalgae is much greater than C concentrations, change in C:N should be dominated by changes in N content. This confirms that changes in C: N ratio observed in *Macrocystis* blades after the pre-experimental

incubations were mainly influenced by tissue N content rather than C content. *Macrocystis* blade sections incubated under low [NO_3^-] had a lower N content and a higher C:N ratio (= 20.80) than blades incubated under high [NO_3^-] (C:N = 11.83). This inverse relationship between C:N ratio and N content has been previously suggested by Duarte (1993). The high C:N ratio reported in *Macrocystis* blades incubated under low [NO_3^-] suggests that were likely N-limited, but it did not reach the critical low values of total tissue N content that might limit their growth (1.1% dry weight, Gerard 1982a).

Foley and Koch (2010) indicated that $\delta^{15}N$ signature of *Macrocystis* varied seasonally depending on the NO_3^- concentration present in the seawater, being inversely proportional to the NO_3^- concentration, which agrees with this study. *Macrocystis* blades incubated under low [NO_3^-] had a $\delta^{15}N$ signature of 11.38‰ while blades incubated under a high [NO_3^-] had a $\delta^{15}N$ signature of 8.56‰. Although values of $\delta^{15}N$ of macroalgae might also depend on the dominant N source taken up by the alga, i.e. NO_3^- or NH_4^+ (Foley and Koch 2010, Ochoa-Izaguirre and Soto-Jiménez 2015), in this study, NO_3^- was the only N_i source supplied. Therefore, changes observed in $\delta^{15}N$ values between N-deplete and N-replete blades must be due to changes in the external NO_3^- availability and/or to internal physiological processes that might affect the $\delta^{15}N$ signature. However, we do not discard that changes in $\delta^{15}N$ might also be influenced by the $\delta^{15}N$ signature of the NO_3^- source ($NaNO_3^-$) utilized during the incubations. In higher plants, when the nitrogen pool is in excess in the medium, $\delta^{15}N$ signature might be lower due to the discrimination against to the heavy isotope during enzymatic activity (Ostrom et al. 1997). However, further studies are required to determine how internal physiological processes of macroalgae (i.e. NO_3^- assimilation and enzymatic activity) might influence the fractionation of $\delta^{15}N$ within the algal cell.

5.4.2 The interactive effects of seaweed nitrogen status and pCO_2 on nitrogen physiology, growth and photosynthetic rates of *Macrocystis*.

The second hypothesis, that nitrogen status modulates the physiological response of *Macrocystis* to elevated pCO_2 was not supported. Photosynthetic and growth rates were similar for blades grown either under ambient (pCO_2 400 µatm; pH 8.00) or OA treatment (pCO_2 1200 µatm; pH 7.59), irrespective of the size of the internal NO_3^- pool and the total tissue N content. These results suggest that the tissue N status of *Macrocystis* does not influence on the growth and photosynthetic response of *Macrocystis* to elevated pCO_2 once NO_3^- is resupplied. N-deplete *Macrocystis* blades showed a rapid NO_3^- uptake and assimilation when NO_3^- availability increases, and NR was always active as long as there was NO_3^- available. Therefore, the resupply of NO_3^- (20 µM) to N-deplete blades, during pCO_2 incubations, seems to be sufficient to support high growth and photosynthesis either under ambient or elevated pCO_2 conditions, despite the low internal NO_3^- pool and low total tissue N content at the start of the incubation. Gerard (1982b) suggested that a concentration of 2 µM NO_3^- is sufficient to sustain a *Macrocystis* growth of 4% of per day. Therefore, concentrations of 20 µM are sufficient to sustain a growth rate of ≈13% per day recorded in this study.

Nitrate can be immediately reduced and assimilated into amino acids, which are incorporated into thallus growth (Young et al. 2007). Therefore, as the growth rate of *Macrocystis* was not enhanced by elevated pCO_2, their demand for NO_3^- did not increase. However, elevated pCO_2 did increase NO_3^- uptake and consequently the internal NO_3^- pool in N-deplete blades. This increased NO_3^- uptake was reflected in the internal NO_3^- pool, but NR activity was not affected. NO_3^- uptake and assimilation may be an uncoupled process in macroalgae, and NO_3^- can be temporally stored when NR is saturated (McGlathery et al. 1996). Indeed, as total tissue N content was neither higher

than the initial values nor the values recorded in N-deplete blades incubated in the ambient treatment (400 µatm/pH 8.00), this suggest that other nitrogenous compounds, i.e. amino acids, protein, chlorophyll, were not increased, and so increased NO_3^- uptake in N-deplete blades incubated under elevated pCO_2, was not associated with photosynthesis or growth. In this study other internal nitrogenous compounds such as proteins or pigments were not measured. However, it has been indicated that pigments and their associated proteins play an important role as storage of N in macroalgae, also increasing when nitrogen availability does (Kopczak 1994). Therefore, measurements of pigments, proteins or other nitrogenous compounds such as amino acids are important to consider for further studies.

In higher plants (i.e. C3 mechanism) when nutrient (i.e. NO_3^- and NH_4^+) supply is high and not limiting, elevated pCO_2 enhances photosynthesis and stimulates growth (Matt et al. 2001, and references therein). However, the relationship between those physiological processes in macroalgae may be more complex and not always coupled (Young et al. 2007). For *Macrocystis*, although the internal NO_3^- pool and total tissue N content were high in the N-replete blades, growth was not enhanced by elevated pCO_2. These results confirm the results of Chapters 3 and 4 (Fernández et al. 2014, 2015) that the growth of *Macrocystis* is saturated under the current Ci conditions. Contrary to *Macrocystis*, Gordillo et al. (2001) reported that the growth rate of *Ulva rigida* was significantly enhanced by elevated pCO_2 in N-replete compared to N-deplete thalli, but net photosynthesis was reduced. In N-deplete thalli of *U. rigida*, however, both growth and photosynthesis were severely reduced regardless of the pCO_2 present in the culture medium. *Macrocystis* growth was not reduced in N-deplete blades probably because total tissue N content was above the critical low value described for *Macrocystis* (1.1% dry weight, Gerard 1982a), while in *U. rigida* was < 1% dry weight (Gordillo et al.

2001). In addition, the reduced net photosynthesis, but enhanced growth rate observed in N-replete *U. rigida* thalli cultured under elevated pCO_2 (Gordillo et al. 2001) suggests that the reduction in proteins associated with photosynthesis (e.g. RuBisCO, chlorophyll-binding proteins), and the reduction in C losses in photosynthesis, might have provided more sources (i.e. C and N) to support higher growth rates. Therefore, even though elevated pCO_2 might enhance growth of some macroalgal species, a negative effect on other physiological processes could occur.

Generally, the effects of elevated pCO_2 on NR activity in macroalgae are mostly associated with an increase in NO_3^- uptake to support enhanced growth rate. For example, an increase in NR activity, NO_3^- uptake and growth rate was reported in *Hizikia fusiformis* cultured under elevated pCO_2 and NO_3^--enriched SW (Zou 2005). However, the NR activity of *Macrocystis* was unaffected by elevated pCO_2 irrespective of the N status of the alga. In contrast to *Macrocystis*, Gordillo et al. (2001) showed that the NR activity of *U. rigida* grown under a high [NO_3^-] was greatly enhanced by elevated pCO_2, but severely reduced under NO_3^- limitation regardless of the pCO_2 present in the medium. Since in the present study NO_3^- was supplied during pCO_2 incubations, NR remained active regardless of the N status of the alga. In this case, NR might be regulated more by external NO_3^- concentration than for internal NO_3^- pool. Since *Macrocystis*' growth is not stimulated by elevated pCO_2, there is no need to increase NR activity as the demand for nutrients is not enhanced.

The C:N ratio in *Macrocystis* was unaffected by the pCO_2 treatments, and it was mostly dependent on the N status of the alga. The similar C:N ratios observed in N-replete blades incubated either under ambient or elevated pCO_2 suggests that carbon and nitrogen were assimilated proportionally regardless of the pCO_2 in the medium. A similar pattern was observed in N-deplete blades. The amount of carbon fixed did not

significantly varied between N-deplete or N-replete blades either incubated under ambient or OA treatment, whereas N content varied significantly between N-replete and N-deplete being strongly influenced by the N status of the algae. Although, N-deplete blades were resupplied with NO_3^- during pCO_2 incubations, internal N content did not reach levels recorded before the pre-experimental incubations, but it was enough to support high growth rate during pCO_2 incubations.

Isotope signatures were mostly unaffected by the pCO_2 treatments. The $\delta^{13}C$ value is used to indicate the dominant Ci form (i.e. $CO_{2(aq)}$ or HCO_3^-) utilized by the alga to support photosynthesis (Raven et al. 2002). A change in the $\delta^{13}C$ value might indicates a shift between the Ci sources utilized (Fernández et al. 2015/Chapter 4). The $\delta^{13}C$ did not vary between N-replete blades incubated either under ambient (–15.18‰) or OA treatment (–15.25‰), indicating that the preference of *Macrocystis* by HCO_3^- as Ci source was not affected by pCO_2. However, in N-deplete blades a slight, but significant, change was observed between blades incubated under ambient (–16.54‰) and OA treatment (–17.64‰). Although $\delta^{13}C$ values varied between –15.18‰ and –17.64‰ in *Macrocystis* blades, the values were above –30‰, which indicates the operation of a CCM and direct or indirect use of HCO_3^- (Raven et al. 2002, Hepburn et al. 2011). Therefore, these results suggest that the direct and indirect mechanisms present in *Macrocystis*, i.e. external HCO_3^- dehydration mediated by CA_{ext} and uptake via an anion exchange (AE) protein, were not down-regulated under elevated pCO_2, which agrees with Chapters 3 and 4 (Fernández et al. 2014, 2015).

Foley and Koch (2010) suggest an inverse relationship between $\delta^{15}N$ value and external NO_3^- concentrations. This was supported by the results observed in this study. The $\delta^{15}N$ signatures of *Macrocystis* were unaffected by the pCO_2 treatments, but were strongly influenced by the N status of the algae. The values of $\delta^{15}N$ in N-deplete blades

were significantly higher than in N-replete blades, showing the same pattern observed after the pre-experimental incubations. Moreover, when the N-deplete blades were resupplied with NO_3^- (20 µM) in the pCO_2 incubations, incubated either under ambient or OA treatment, a lower $\delta^{15}N$ was observed compared to initial values, following the inverse relationship suggested by Foley and Koch (2010). However, for N-replete blades, the $\delta^{15}N$ signature was also lower compared to initial values, where one would expect a higher $\delta^{15}N$ according to the inverse relation between $\delta^{15}N$ and external NO_3^- concentrations. This result suggests that depending on the cultures condition of the algae, the $\delta^{15}N$ signatures may not only regulated by external NO_3^- concentrations, and as mentioned before the $\delta^{15}N$ signatures in macroalgae might also be regulated by internal physiological processes (i.e. NO_3^- assimilation and enzymatic activity).

In summary, *Macrocystis* exhibits an active NO_3^- uptake mechanism, which can rapidly be up-regulated after a period of low external NO_3^- availability. It can rapidly accumulate internal N pools when NO_3^- availability is increased (i.e. after 3 days under 80 µM). NR activity decreased after periods of low external NO_3^- availability, but it remained active, and so when external NO_3^- concentrations increase, this NO_3^- can be assimilated to rapidly restore its internal inorganic and organic pools. Since *Macrocystis* can use HCO_3^- as a Ci source to support photosynthesis, and it is Ci saturated under the current Ci ambient concentrations, elevated pCO_2 does not increase either its photosynthesis or growth, and consequently their demand for nutrients was not enhanced. The tissue N status did not affect the physiological response of *Macrocystis* to OA once the NO_3^- is resupplied. However, further long-term studies (several days to months) on elevated pCO_2 acclimation under different concentrations of nutrients will be important to further elucidate if nitrogen limitation might modify the *Macrocystis* response to OA.

Chapter 6: Effect of nitrogen source on nutrient uptake and pH changes within the diffusion boundary layer (DBL) of *Macrocystis* blades

6.1 Introduction

Physiological processes of seaweeds such as photosynthesis, respiration, and nutrient uptake depend on the transport of inorganic nutrients from the bulk seawater to the seaweed surface (Wheeler 1980, 1988, Hurd et al. 2000, 2014). To reach the seaweed surface, these nutrients have to cross the diffusion boundary layer (DBL), which is a concentration gradient formed by the uptake or efflux of molecules by the organism through which ions and molecules move by molecular diffusion from the seawater bulk to the thallus surface (Wheeler 1980, Denny 1993, Koch 1994, Hurd 2000). The thickness of the DBL is controlled by water motion (Wheeler 1980, Hurd et al. 1996). Fast flows around the seaweed produce a thin DBL, reducing the distance over which molecules travel, and thus metabolic processes can be enhanced (Wheeler 1980, Larned and Atkinson 1997). In slow flows, the flux of molecules to and from the thallus surface might be reduced by a thick DBL, which could limit metabolic processes (Hurd and Pilditch 2011, Hurd et al. 2014). Thus, the thickness of the DBL determines the flux of essential nutrients (i.e. CO_2, HCO_3^-, NO_3^-, NH_4^+), to and from the seaweed surface (Wheeler 1980, Lesser et al. 1994, Koch 1994).

For large, bladed seaweeds such as kelps, including *Macrocystis*, in a slow mainstream flow (<2-6 cm s^{-1}), the formation of a thick DBL can limit the flux of nutrients and metabolites to and from the blades (Wheeler 1980, Hurd et al. 1996, Enriquez and Rodriguez-Roman 2006, Mass et al. 2010). However, the flux of nutrients might also be influenced by the strength of the concentration gradient between the

seaweed and the surrounding seawater, and by the metabolic status of the algae (Hurd et al. 2014). For example, the intracellular nitrogen pools (NO_3^- and NH_4^+) may affect the rate at which the nutrient is taken up by the algae (Hwang et al. 1987, McGlathery et al. 1996, see Chapter 5). Furthermore, ions and molecules released by the algae by a metabolic process (e.g. O_2 released during photosynthesis), can be accumulated within the DBL, affecting the rate of other physiological processes and the seawater chemistry (e.g. pH and alkalinity) at the blade surface (Mass et al. 2010, Hurd et al. 2014). Therefore, physiological processes may not only be affected by the transfer of nutrients across of the DBL but also by the efflux of dissolved metabolic materials accumulated at the thallus surface (Hurd 2000).

It is well established that metabolic processes such as photosynthesis and respiration might alter the seawater chemistry at the seaweed surface due to the accumulation of various charged ions (De Beer and Larkum 2001, Hurd 2000, Larkum et al. 2003, Hurd et al. 2011, Beer et al. 2014). Photosynthetic products (OH^-) can increase the seawater pH (decreased $[H^+]$), which lead to a change in the DIC ratio present in the medium (HCO_3^-: CO_2). Respiration causes a decrease in the seawater pH (increased $[H^+]$) because of the production of CO_2 (Hurd et al. 2009, 2011). However, the change in seawater pH and consequently in $[H^+]$ due to other physiological processes like nutrient uptake and assimilation is not well established. It has been suggested that the seawater pH could be differently modified depending on which inorganic nitrogen (N_i) form is taken up by the algae (Raven and De Michelis 1979, Raven 1981, Geider and Osborne 1992, Hurd 2000).

Nitrate (NO_3^-) and ammonium (NH_4^+) are the main exogenous sources of inorganic nitrogen present in coastal seawater, and most seaweeds are able to utilize both N_i forms to support their growth (Ahn et al. 1998, Rees et al. 2007, Hurd et al.

2014, see Chapters 1 and 4). However, the assimilation of each N_i source might result in different metabolic fluxes, associated with the intracellular production of OH^- or H^+ (Raven and De Michelis 1979, Raven 1981, Raven 2013, Raven and Giordano 2015). Each NO_3^- ion assimilated produces about 0.7 OH^-, while each NH_4^+ assimilated produces about 1.3 H^+ (Raven and Jayasuriya 1977, Raven and De Michelis 1979, Raven and De Michelis 1980, Raven and Giordano 2015). These values also depend on which Ci source (CO_2 or HCO_3^-) is entering the cell, and (Raven and Giordano 2015). Since the cytoplasmic pH is not greatly affected by these metabolic fluxes (OH^-/H^+), it is assumed that extrusion of these excess charged ions out of the cytoplasm (either OH^- or H^+) must occur to maintain the intracellular acid-base balance, otherwise the cytoplasmatic pH would be greatly affected (Raven and Smith 1974, 1976, Smith and Raven 1976, Raven and De Michelis 1979, Raven 1980). In addition, an influx of H^+ might occur when NO_3^- is taken up by the algae (H^+/NO_3^- symport) (Raven and De Michelis 1979). It has been suggested that for algae, the ratio between each NO_3^- absorbed and H^+ absorbed ranged between 1-1.2; the influx of H^+ lead to an increase of the external SW pH (Fuggi et al. 1981). Thus, the uptake of H^+ and extrusion of OH^- associated with the NO_3^-uptake and assimilation, respectively, might increase the pH within of the DBL, while the efflux of excess H^+ produces during NH_4^+ assimilation might decrease the pH within of the DBL, similar to photosynthesis and respiration, respectively.

Such external changes in $[OH^-]$ and $[H^+]$ may also affect the alkalinity of seawater at the surface of the seaweed. Alkalinity is determined by the concentration of $HCO_3^- + 2CO_3^{2-} + B(OH^-)_4 + OH^- - H^+$ present in the SW, and therefore changes in OH^- and H^+ ion concentrations, associated with metabolic processes of seaweed may alter the SW alkalinity (Raven and Michelis 1979, Dickson 1981, Uusitalo 1996). It has

been reported that physiological processes such as NO_3^- assimilation increase alkalinity, while NH_4^+ assimilation and calcification decrease alkalinity, likely due to the extrusion of excess H^+ to the external medium (Hofslagare et al. 1983, Uusitalo 1996, Jokiel 2011, Beer et al. 2014). However, other metabolic processes such as respiration and photosynthesis do not alter the alkalinity because the proportion of protons in the medium remains unchanged as OH^- or H^+ to compensate for changes in the Ci forms (Uusitalo 1996, Beer et al. 2014). Therefore, changes in alkalinity observed during NO_3^- and NH_4^+ assimilation might reflect the net proton fluxes through the plasma membrane (Hofslagare et al. 1983, Uusitalo 1996).

Increased $CO_{2(aq)}$ concentration and consequently decreased SW pH (high $[H^+]$) due to ocean acidification (OA) might affect the physiological processes of macro- and microalgae (Zou 2005, Zou et al. 2011, Koch et al. 2013, Hofmann et al. 2013). The expected decrease of 0.3-0.4 units in pH by 2100 will lead to an increase of about 104-150% in $[H^+]$ (Caldeira and Wickett 2003). The increase in $[H^+]$ might affect the transport of metabolic H^+ out of the photosynthetic organism' cell into the DBL (Jokiel 2011). It has been suggested that if NO_3^- is transported together with an influx of H^+, NO_3^- uptake may be positively affected by higher $[H^+]$ under OA (Alexandre et al. 2012). Therefore, increases in pH within the DBL associated with the NO_3^- uptake and assimilation may be greater under OA conditions than under ambient conditions. Otherwise, NH_4^+ uptake may be negatively affected by higher $[H^+]$ under OA, because the efflux of H^+ associated with NH_4^+ assimilation may be reduced by higher external $[H^+]$ (because of the diffusion gradient strength), and higher $[H^+]$ might reduce the H^+-ATPase activity (Alexandre et al. 2012). Therefore, decreases in pH within the DBL associated with NH_4^+ assimilation may be smaller under OA conditions than ambient conditions.

Macrocystis forms dense beds which can greatly influence seawater velocity, inorganic nutrient concentrations and seawater chemistry within the kelp bed (Delille et al. 2000, Gaylord et al. 2007, Stewart et al. 2009, Hansen et al. 2011, Hofmann et al. 2011, Stephens and Hepburn 2014). Daily pH fluctuations within a *Macrocystis* forest have been associated with their physiological processes, i.e. increases in pH during day time are due to photosynthesis, while decreases in pH during night time are due to respiration (Cornwall et al. 2013). A similar pattern in pH fluctuations (high in the light and low in the dark) has been observed within the DBL in the coralline seaweed *Sporolithon durum* (Hurd et al. 2011). It is known that *Macrocystis* modifies the surrounding seawater due to physiological processes (i.e. photosynthesis and respiration), and the DBL thickness at the blade surface is influenced by the water velocity and blade morphology (Hurd and Pilditch 2011). However, little is known about how other physiological processes, i.e. N_i uptake and assimilation influence the pH within the DBL, and how low pH might affect those processes. To measure the changes in OH^-/H^+ fluxes related to the physiological processes of *Macrocystis* the formation of a thick DBL is required. Therefore, a slow flow of 0.8 cm s^{-1} was used in this study to allow the formation of a thick DBL.

The goals of this study were to test the hypotheses that (1) NO_3^- uptake will increase the pH within the DBL of *Macrocystis* under slow flow conditions, whereas NH_4^+ uptake will cause it to decrease; because photosynthesis might also cause an increase in pH within the DBL a nutrient-depleted treatment was included to test for this effect. Thus, increases in pH in the NO_3^- treatment (high pH due to photosynthesis + NO_3^- uptake) will be greater than under the nutrient-depleted seawater treatment (hereafter, NDSW) (photosynthesis alone), and increases in pH in the NH_4^+ treatment (increases in pH due to photosynthesis but decreases due to NH_4^+ uptake) will be

smaller than in the NSDW treatment. (2) Increases in pH within the DBL associated with NO_3^- uptake and assimilation will be greater under an OA treatment (pH = 7.65) than under an ambient treatment (pH = 8.00), whereas decreases in pH within the DBL associated with NH_4^+ assimilation will be smaller under an OA treatment than under an ambient treatment.

6.2 Materials and Methods

6.2.1 Seaweed collection

Young blades of *Macrocystis,* positioned directly behind the apical scimitar, were collected in July 2013 during low tide at the Aramoana (45°47'S, 170°43'E), Otago Harbour, New Zealand. Blades were always collected 3 days before the start of each set of experimental incubations. One blade was taken from each of 36 *Macrocystis* adult individuals, from the same position along each frond. Collected blades were transported to the laboratory 40 min away in an insulated container filled with ambient seawater (SW). In the laboratory, blades were cleaned of all the visible epibionts and standardized to a similar size of 15 × 3 cm with a fresh weight of 1.60 ± 0.03 (g ± SE). Blades were cut at 2 cm from the neumatocyst/blade junction using a razor blade. Thereafter, blade sections were incubated in eight 5 L glass jars (7 blade sections for each jar) containing filtered (0.5 µm pore size) nutrient-depleted SW (NDSW was changed every day; see below for SW treatment) and aerated constantly using an air pump. Cultures were maintained in a growth cabinet (Contherm Plant Growth Chamber, Contherm Scientific Co. Ltd., New Zealand) at 12 °C under a 12:12 h light:dark photoperiod and saturating light of 110 µmol photons m^{-2} s^{-1} of PAR. After three days of incubation in NDSW, *Macrocystis* blade sections were used in the experiments.

6.2.2 Preparation of nutrient-depleted seawater

Inorganic nutrients (i.e. NO_3^-, NH_4^+ and PO_4^{3-}) were depleted from the ambient SW using *Ulva* sp. 50 g of cleaned *Ulva* sp. were placed in a 40 L plastic tank filled with SW (0.5 µm filtered/UV sterilized) and aerated constantly using an air pump. After 8 h of incubation at 12 ˚C under a photon flux density of 110 µmol m^{-2} s^{-1}, SW was filtered using a Polycap TC filter capsule of 0.2 µm (Whatman), and seawater samples (10 mL)

were collected to measure nutrient concentrations (i.e. NO_3^-, NH_4^+ and PO_4^{3-}) as described below. Filtered SW was then stored overnight in a dark controlled temperature room (4 ˚C) to restore the seawater carbonate equilibrium. The next day water samples were collected to determine the seawater carbonate chemistry (i.e. pH, total alkalinity and DIC; see below for details). Inorganic nutrient concentrations, NO_3^-, NH_4^+ and PO_4^{3-} were about 0.0-0.2 µmoles L^{-1}, and the carbonate chemistry was not affected. Thereafter, NDSW was prepared every day for use in the N_i uptake experiments.

6.2.3 Experimental design

To obtain substantial N_i uptake rates and hence obtain a greater change in pH at the blade surface, within the DBL, *Macrocystis* blade sections were pre-incubated for three days in NDSW in order to reduce the internal soluble N_i pools (NO_3^- and NH_4^+; see Chapter 5). After that, pre-treated *Macrocystis* blade sections were used in experiments to examine the effect of nitrate (NDSW+NO_3^-) and ammonium (NDSW+NH_4^+) on the pH change at blade surface at two pH_T: ambient treatment (pH_T 8.00) and OA treatment (pH_T 7.65). Changes in pH at the blade surface were continuously monitored using a 50 µm pH micro-electrode (see below for details). To evaluate the effect of photosynthesis alone on pH within the DBL, NSDW was used. Experiments were conducted over 5 consecutive days; on each day one replicate of each treatment was performed (i.e. pH_T 8.00: NDSW+NO_3^-, NDSW+NH_4^+, NDSW; pH_T 7.65: NDSW+NO_3^-, NDSW+NH_4^+, NDSW; see below for details). To minimize the effect of the daytime on photosynthesis or N_i uptake, the order of the measurements was randomized every day.

6.2.4 Laboratory experimental set up

The pH fluctuation measurements and N_i uptake experiments were conducted in a 1 L glass beaker containing 0.9 L of SW-treatment (nutrient/pH). Pre-treated blade sections were placed on a small glass platform and attached to its edge, using a band to minimize blade movement. Then, the glass platform was placed inside of the 1 L beaker, and the beaker was sitting on top of a stirrer plate; the seawater was slowly mixed with a magnetic stirrer at 150 rpm (Fig. 6.1). This rpm represents a slow water speed of about 0.8 cm s^{-1}; measurements of water speed were made inside of the beaker with the platform and algae using a Vectrino Acoustic Doppler Velocimeter (Nortek AS, Vangkroken, Norway). All measurements were made under a saturating light intensity of 110 m^{-2} s^{-1} provided by Philips HPI- T 400 W quartz metal halide lamp (Philips) at 12 ˚C inside of the growth cabinet.

All treatments were prepared using NDSW. There were three nutrient treatments: nutrient-depleted seawater (NDSW), NO_3^- addition (NDSW+NO_3^-), and NH_4^+ addition (NDSW+NH_4^+). NO_3^- and NH_4^+ were added as $NaNO_3^-$ and NH_4^+Cl, respectively, to a final concentration of 20 µM. Each treatment was prepared at ambient treatment (pH_T 8.00) and OA treatment (pH_T 7.65) (n = 5 for each treatment). The OA treatment was achieved by bubbling with 100% CO_2 gas until the correct pH was reached. SW pH was then measured spectrophotometrically and on a total scale (pH_T). Each experimental treatment was prepared every day, and stored at the experimental temperature (12 ˚C). Initial SW samples were collected from each treatment to measure initial nutrient concentration (10 mL), dissolved inorganic carbon (DIC) (30 mL) and total alkalinity (A_T) (500 mL) as described below (see Chapter 4) (Table 6.1). Nutrient samples were stored at –20 ˚C until further analysis, and A_T and DIC samples were fixed with mercuric chloride.

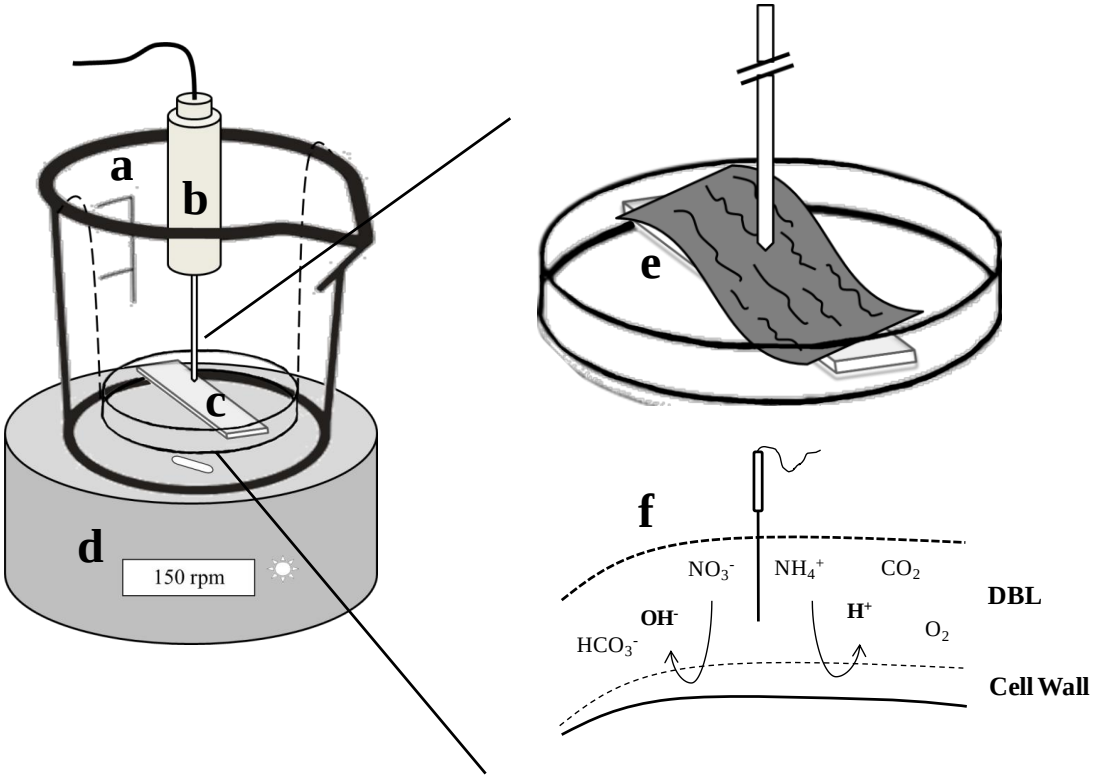

Figure 6.1: Experimental setup used for measuring pH changes within the diffusion boundary layer (DBL) in *Macrocystis* blade sections using a pH micro-electrode. (a) 1 L glass baker, (b) pH micro-electrode, (c) platform of glass where *Macrocystis* blade section was placed on, (d) stirrer plate at 150 rpm, and (e) *Macrocystis* blade section placed on the glass platform with the pH micro-electrode within the DBL (f) fluxes of molecules within the DBL.

Table 6.1: Initial inorganic nutrient (N_i) concentrations and seawater carbonate chemistry parameters recorded at the start of the experimental incubation. Values are the mean (n = 3-5) ± SE.

	Nutrient Treatments					
	NDSW		**NDSW+NO_3^-**		**NDSW+NH_4^+**	
pH treatments	**8.00**	**7.65**	**8.00**	**7.65**	**8.00**	**7.65**
N_i (µmoles L^{-1})						
NO_3^-	<0.001	0.62 ± 0.12	22.47 ± 0.71	21.84 ± 1.49	<0.001	<0.001
PO_4^+	<0.001	<0.001	<0.001	<0.001	<0.001	<0.001
NH_4^+	0.25 ± 0.04	<0.001	0.43 ± 0.08	0.36 ± 0.17	25.02 ± 2.19	26.30 ±0.53
SW carbonate chemistry						
A_T (µmol kg^{-1})	2230.70 ± 25.30	2226.85 ± 32.50	2218.87 ± 12.10	2199.97 ± 9.40	2231.50 ± 23.30	2200.60
DIC (µmol kg^{-1})	2051.05 ± 21.55	2154.07 ± 16.68	2061.72 ± 29.05	2159.73 ± 17.25	2053.82 ± 13.84	2140.47 ± 33.49
HCO_3^- (µmol kg^{-1})	1900.86 ± 32.79	2043.08 ± 19.72	1922.49 ± 42.65	2053.23 ± 17.49	1905.23 ± 20.85	2025.36 ± 40.33
Dissolved CO_2 (µmol kg^{-1})	17.74 ± 1.96	37.25 ± 4.94	21.59 ± 3.69	47.76 ± 6.91	17.57 ± 1.43	44.95 ± 10.49
pCO_2 (µatm)	409.58 ± 18.55	853.10 ± 41	425.85 ± 14.76	858.95 ± 43.66	410.66 ± 21.54	862.23 ± 31.51

6.2.5 Measurement of the diffusion boundary layer (DBL) thickness

The thickness of the DBL was estimated by measuring the O_2 concentration gradient at the blade surface determined using an O_2 micro-optode (needle type) (PreSens, Regensburg, Germany) (Hurd and Pilditch 2011). O_2 concentrations were measured above the *Macrocysti*s blade (n = 3) at 0.2 mm intervals over the first 1 mm and then at 1, 1.5, 3, 7, 11, 19, 31 mm. At each distance the O_2 concentration was recorded for 1 min. For all blade sections, the micro-optode was positioned on the top of the corrugation much closer to the edge of the blade, because the micro-optode tip was less disrupted by the up and down-blade movement. O_2 concentration gradients were measured under a slow water speed (0.8 cm s^{-1}) at the same temperature and light intensity described above. The DBL thickness was determined according to Hurd and Pilditch (2011).

6.2.6 pH changes at the blade surface of *Macrocystis* under different N_i sources measured at pH_T 8.00 and 7.65

The pH at the blade section surface of *Macrocystis* was measured under different N_i sources measured at pH_T 8.00 and 7.65. Experiments were conducted over five consecutive days, as described above. Each pre-treated blade section was randomly assigned to an experimental treatment, and experiments were started and finished at the same time every day (from 10:00 am to 18:00 pm). pH changes at the blade surface were determined using a calibrated pH micro-electrode of 50 µm tip diameter (Unisense, Aarhus, Denmark). Before the start of each measurement, the SW was vigorously mixed, and SW samples were collected to determine initial nutrients and DIC concentrations in order to determine uptake rates (see below). After that, the pH micro-electrode was positioned above the top of the blade section corrugation with a

manual micro-manipulator (Hurd et al. 2011). The pH was recorded for 75 min under a saturating light intensity of 110 m^{-2} s^{-1} at 12 ˚C in a slow water speed (0.8 cm s^{-1}). After recording the pH, *Macrocystis* blade section was removed and SW samples were collected for further nutrients, DIC and A_T analysis. In addition, controls without algae were run to determine the effect of each N_i treatment on the SW pH.

6.2.7 Inorganic nitrogen (NO_3^- and NH_4^+) and DIC uptake rates

Prior to the addition of the blade section into each experimental treatment, SW samples were collected to determine the initial N_i (10 mL) and DIC concentrations (30 mL). After 75 min incubation, the *Macrocystis* blade section was removed and SW samples were collected to determine the final concentrations present in the medium. SW samples were stored at –20˚ C until subsequent inorganic nitrogen analysis, and DIC samples were fixed with mercuric chloride. Both N_i uptake and DIC uptake rates (i.e. HCO_3^- and CO_2) were calculated by the disappearance of the nutrient from the medium, and standardized by the fresh weight of the algae.

6.2.8 Seawater sample analysis

Nutrient samples were analyzed using a QuickChem 8500 series 2 Automated Ion Analyzer (Lachat Instrument, Loveland, USA). Total alkalinity (A_T) was measured by the potentiometric method with a controlled titration cell, and DIC was measured directly by acidifying the sample (Dickson et al. 2007). A_T, DIC, pH, salinity, and temperature were used to calculate carbonate chemistry parameters using the program $SWCO_2$ (Hunter 2007).

6.2.9 Statistical analyses

Statistically significant differences in pH at the seaweed surface between nutrient treatments (i.e. NDSW+NO_3^-, NDSW+NH_4^+ and NDSW) under a same pH treatment were detected using analysis of variance (one-way ANOVA, $P < 0.05$). When significant differences were detected a Tukey's HSD test was performed. To test the differences between pH treatments (i.e. pH_T 8.00 and 7.65) Student's t-tests ($P < 0.05$) were conducted for each nutrient treatment after homogeneity (Levene's test) and normality (Shapiro-Wilk test) of data were satisfied. All analyses were performed using the statistical program SigmaPlot 11.0 (Systat Software, Inc.).

6.3 Results

6.3.1 The diffusion boundary layer (DBL) thickness

The DBL at the blade surface of *Macrocystis* was 0.7 ± 0.1 mm (± SE; n = 3) at the experimental flow of 0.8 cm s^{-1}.

6.3.2 pH changes at the blade surface of *Macrocystis* under different N_i sources measured at pH_T 8.00 and 7.65

The pH at the *Macrocystis* blade surface, measured over 75 min either under pH_T 8.00 (ambient) or pH_T 7.65 (OA), showed a similar trend of linear increase for all treatments (NDSW, NDSW+NO_3^-, NDSW+NH_4^+; Fig. 6.2). At pH_T 8.00, the increase in pH units across the treatments NDSW (0.113 ± 0.11 pH units ± SE), NDSW+NO_3^- (0.123 ± 0.019 pH units ± SE) and NDSW+NH_4^+ (0.107 ± 0.018 pH units ± SE) did not vary (ANOVA: $F_{3,98}$ = 0.140, P = 0.871, Fig. 6.3). Similarly, at pH_T 7.65, the increase in pH units did not vary across the treatments NDSW (0.182 ± 0.019 pH units), NDSW+NO_3^- (0.170 ± 0.005 pH units) and NDSW+NH_4^+ (0.168 ± 0.015 pH units) (ANOVA: $F_{3,98}$ = 0.279, P = 0.765, Fig. 6.3). Comparisons between pH treatments (pH_T 8.00 and 7.65) indicated that increases in pH units was greater at pH_T 7.65 than pH_T 8.00 for all treatments (NDSW, Student's t-test, t = -2.47, df = 8, P = 0.025; NDSW+NO_3^-, t = -2.408, df = 8, P = 0.047; NDSW+NH_4^+, t = -2.465, df = 8, P = 0.039; Fig. 6.3).

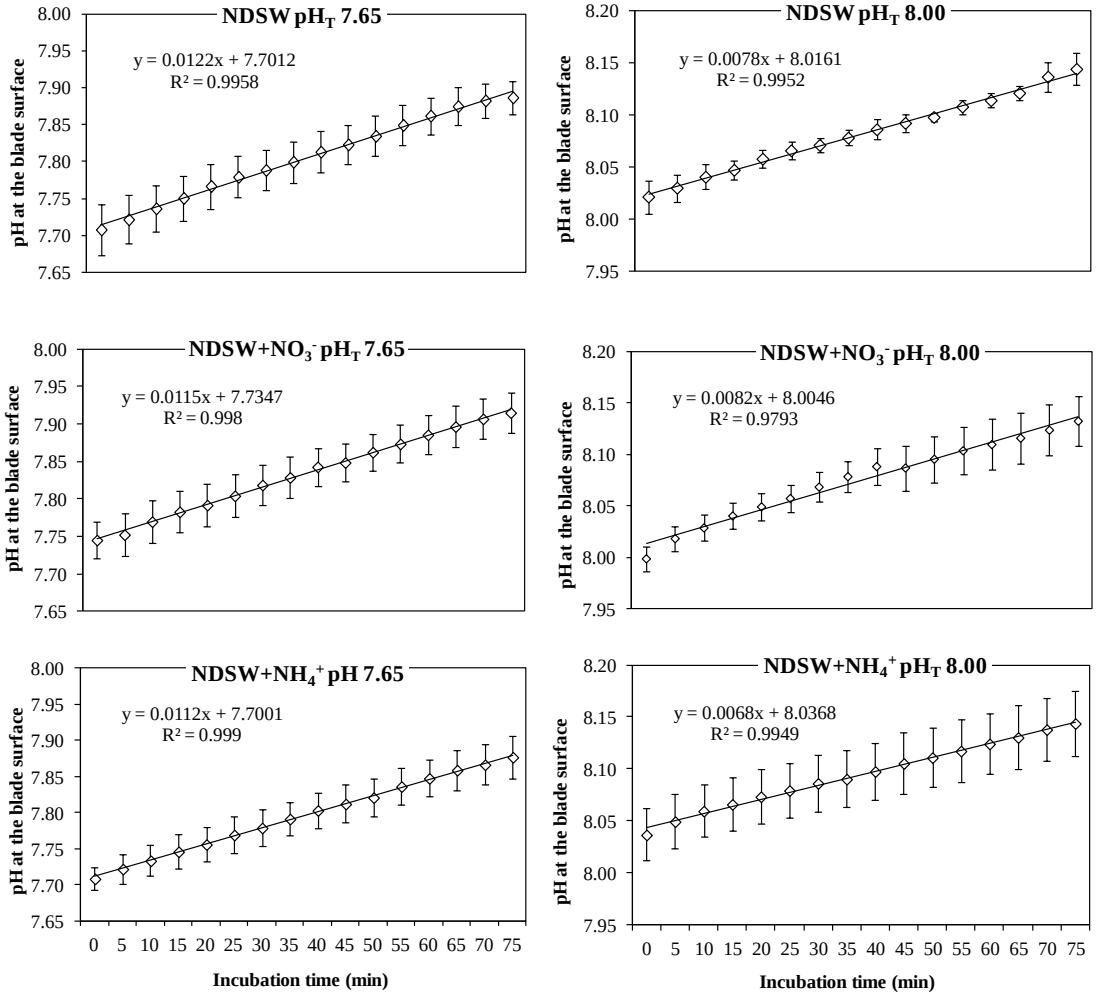

Figure 6.2: pH changes within the DBL of *Macrocystis* blade sections measured for 75 min with nutrient-depleted seawater (NDSW), NDSW+NO_3^- (20 µM) and NDSW+NH_4^+ (20 µM) at ambient (pH_T =8.00) and OA treatment (pH_T = 7.65) at a slow water speed (0.8 cm s^{-1}). Values are the mean (n = 5) ± SE.

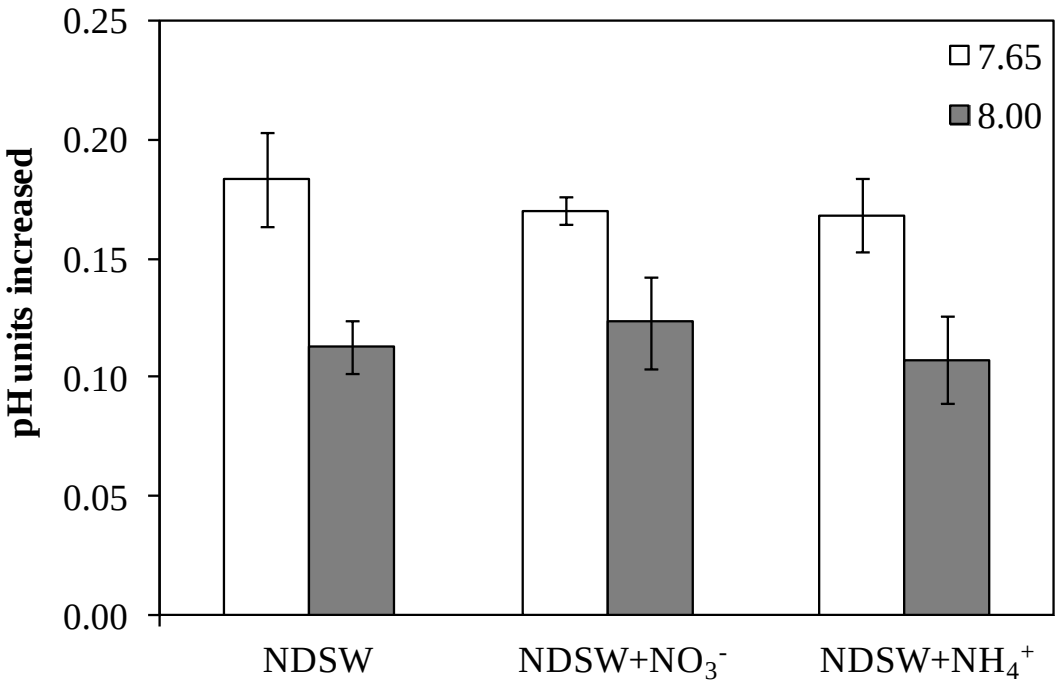

Figure 6.3: pH units increased within the DBL of *Macrocystis* blade sections after 75 min of incubation with nutrient-depleted seawater (NDSW), NDSW+NO_3^- (20 µM) and NDSW+NH_4^+ (20 µM) at ambient (pH_T =8.00) and OA treatment (pH_T = 7.65) at a slow water speed (0.8 cm s^{-1}). Values are the mean (n = 5) ± SE. Significantly different sub-groups: pH_T 8.00: NDSW = NDSW+NO_3^- = NDSW+NH_4^+; pH_T 7.65: NDSW = NDSW+NO_3^- = NDSW+NH_4^+ (ANOVA $p > 0.05$); pH_T 7.65 > 8.00 for all treatments (NDSW, NDSW+NO_3, NDSW+NH_4^+) (ANOVA $p < 0.05$).

6.3.3 Inorganic nitrogen (NO_3^- and NH_4^+) uptake rates

The NO_3^- uptake rates were similar at pH_T 8.00 (2.97 µmoles g^{-1} FW h^{-1}) and pH_T 7.65 (2.034 µmoles g^{-1} FW h^{-1}) (Student's t-test, t = -1.369, df = 7, P = 0.213, Fig. 6.4). Likewise, NH_4^+ uptake rates did not vary significantly between pH_T 8.00 (2.43 µmoles g^{-1} FW h^{-1}) and pH_T 7.65 (3.77 µmoles g^{-1} FW h^{-1}) (Student's t-test, t = 1.884, df = 7, P = 0.102, Fig. 6.4). However, at pH_T 7.65 NH_4^+ uptake rates were significantly higher compared to NO_3^- uptake rates (Student's t-test, t = 3.644, df = 8, P = 0.007, Fig. 6.4), while at pH_T 8.00, no significant differences were observed (Student's t-test, t = -0.590, df = 6, P = 0.577, Fig.6. 4).

6.3.4 DIC uptake rates and SW carbonate chemistry

The SW carbonate chemistry measured at the end of each incubation, showed that HCO_3^- uptake rates were similar across all treatments (NDSW, NDSW+NO_3^-, NDSW+NH_4^+; Fig. 6.5a) measured either under pH_T 8.00 (ANOVA: $F_{4,10}$ = 0.482, P = 0.630, Fig. 6.5a) or pH_T 7.65 (ANOVA: $F_{3,98}$ = 0.373, P = 0.698, Fig. 6.5a). When compared between pH treatments (pH_T 8.00 and 7.65), HCO_3^- uptake rate was unaffected by the pH in all treatments (NDSW, Student's t-test, t = 0.246, df = 8, P = 0.790; NDSW+NO_3^-, t = -0.160, df = 6, P = 0.878, NDSW+NH_4^+, t = 0.509, df = 8, P = 0.626; Fig. 6.5a).

Likewise, CO_2 uptake rates were similar across all treatments, measured either under pH_T 8.00 (ANOVA: $F_{4,10}$ = 0.483, P = 0.630, Fig. 6.5b) or pH_T 7.65 (ANOVA: $F_{4,10}$ = 0.233, P = 0.797, Fig. 6.5b). However, when compared between pHs (pH_T 8.00 and 7.65), CO_2 uptake was 67% higher at pH_T 7.65 than at pH_T 8.00 across all treatments (NDSW, Student's t-test, t = 5.306, df = 8, P < 0.001; NDSW+NO_3^-, t = 4.837, df = 6, P = 0.003; NDSW+NH_4^+, t = 4.299, df = 7, P < 0.001; Fig. 6.5b).

Total alkalinity measured at the end of each incubation was similar across the treatments (NDSW, NDSW+NO_3^-, NDSW+NH_4^+) either at ambient pH_T 8.00 (ANOVA: $F_{3,98}$ = 0.008, P = 0.991, Fig. 6.5c) or pH_T 7.65 (ANOVA: $F_{3,98}$ = 0.246, P = 0.786, Fig. 6.5c). When compared between pH treatments (pH_T 8.00 and 7.65) the final A_T measured after 75 min of incubation was not significantly affected either by NO_3^- uptake (Student's t-test, t = 0.233, df = 8, P = 0.823, Fig. 6.5c) or NH_4^+ uptake (Student's t-test, t = -0.227, df = 8, P = 0.826, Fig. 6.5c). Similar results were observed after incubations in NDSW (Student's t-test, t = 0.0787, df = 8, P = 0.939, Fig. 6.5c).

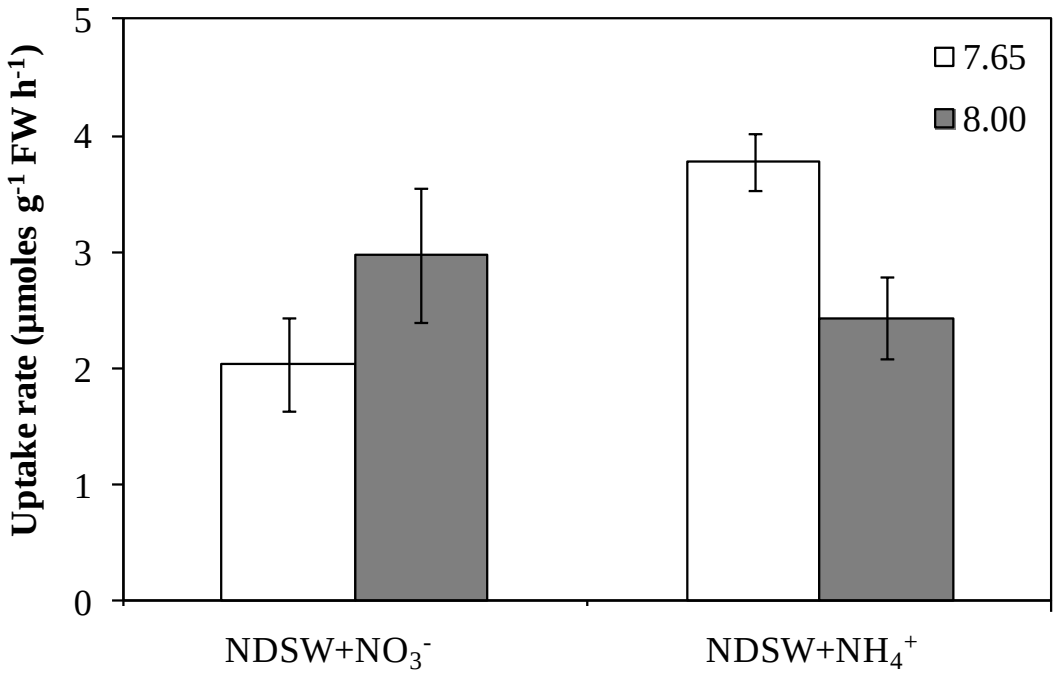

Figure 6.4: Inorganic nitrogen uptake rates (i.e. NO_3^- and NH_4^+) of *Macrocystis* blade sections after 75 min of incubation with NDSW+NO_3^- (20 µM) and NDSW+NH_4^+ (20 µM) at ambient (pH_T =8.00) and OA treatment (pH_T = 7.65) at a slow water speed (0.8 cm s^{-1}). Values are the mean (n = 5) ± SE. Significantly different sub-groups: NO_3^- uptake: 7.65 = 8.00; NH_4^+ uptake: 7.65 = 8.00; pH_T 7.65: NH_4^+ uptake > NO_3^- uptake; pH_T 8.00: NH_4^+ uptake > NO_3^- uptake (Student's t-test).

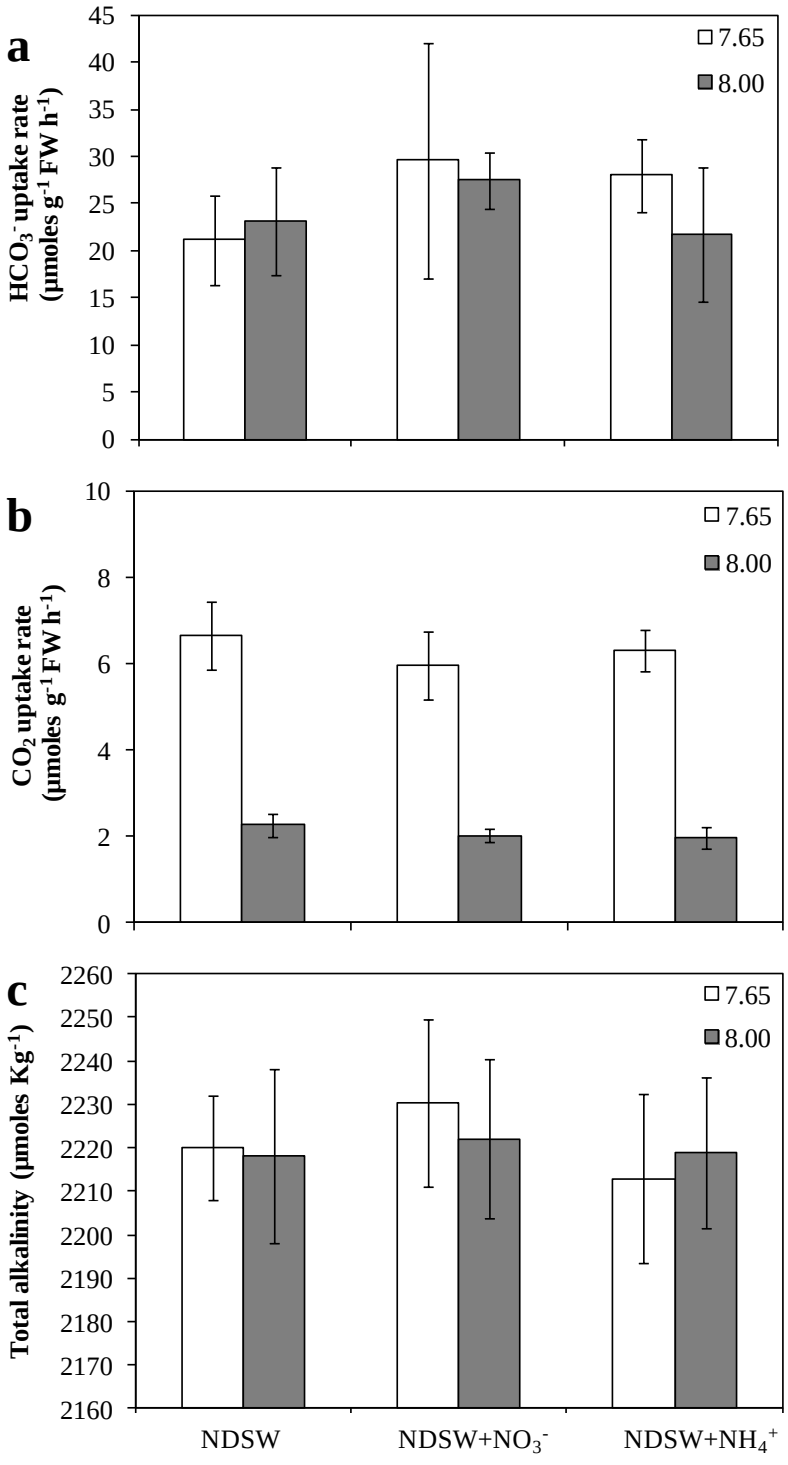

Figure 6.5: Bicarbonate (HCO_3^-) uptake rate of *Macrocystis* blade sections (a), CO_2 uptake rate of *Macrocystis* blade sections (b), and final total alkalinity (A_T) measured in the SW (c) after 75 min of incubation in nutrient-depleted seawater (NDSW), NDSW+NO_3^- (20 µM) and NDSW+NH_4^+ (20 µM) at ambient (pH_T =8.00) and OA treatment (pH_T = 7.65) at a slow water speed (0.8 cm s^{-1}). Values are the mean (n = 5) ± SE. Significantly different sub-groups: (a) no significant different between sub-groups (ANOVA $p > 0.05$), (b) pH_T 7.65: no significant differences between sub-groups; pH_T 8.00: no significant differences between sub-groups (ANOVA $p > 0.05$); across all

treatments (NDSW, NDSW+NO_3^-, NDSW+NH_4^+): pH_T 7.65 > 8.00 (ANOVA $p < 0.05$), (c) no significant different between sub-groups (ANOVA $p > 0.05$).

6.4 Discussion

The first goal of this study was to test the hypothesis that NO_3^- uptake will increase the pH within the DBL under a slow water flow condition, whereas NH_4^+ uptake will decrease it; however, the hypothesis was not supported. There was no difference in the pH changes measured at the blade section surface of *Macrocystis* incubated either with NO_3^- as N_i source or NH_4^+. In both cases, pH units increased linearly over time. These results suggest that the assimilation of NO_3^- and NH_4^+ by *Macrocystis* may not produce a shift in the intracellular pH associated with the production of OH^- or H^+, respectively. Extrusion of these charged ions outside the cell is required to prevent further changes in the intracellular pH. The increase in pH units observed under both N_i treatments suggests that changes in pH within the DBL are likely more associated with the photosynthesis process rather than with N_i assimilation.

To date, most studies on how macroalgal metabolism affect pH have evaluated the effect of photosynthesis and respiration on the bulk SW pH and/or on the proximity of the alga's surface (i.e. within the DBL) (Delille et al. 2000, De Beer and Larkum 2001, Middelboe and Hansen 2007ab, Hurd et al. 2011, Cornwall et al. 2013). However, studies performed under different Ni sources and with continuous pH measurements within the DBL in macroalgae are scarce. Raven and De Michelis (1979, 1980) reported that the acid-base regulation in the green freshwater microalga *Hydrodictyon africanum* depends on which N_i source (i.e. NO_3^- or NH_4^+) is being assimilated by the alga. Bulk SW pH was greatly reduced from pH 7.49 to 7.08 when NH_4^+ was supplied, after 1 h of incubation (Raven and De Michelis 1980). Reduction in pH was associated with NH_4^+ assimilation, because in a culture with no NH_4^+ addition, external SW pH was unchanged (Raven and De Michelis 1980). Similarly, this result is opposite to the result

observed in *Macrocystis*, where pH within of the DBL was not reduced when NH_4^+ was supplied. The non-acidification within the DBL (high $[H^+]$) during NH_4^+ uptake might be related to the pre-treatment of *Macrocystis* blade sections. *Macrocystis* blade sections were pre-incubated for 3 days in NDSW, hence internal N_i pools (i.e. NH_4^+) were reduced, and so resupply of NH_4^+ resulted in a high NH_4^+ uptake rate, but the new NH_4^+ entering into the cell was likely not immediately assimilated. Thus, it is possible that the incubation time (75 min) was not long enough to drive complete NH_4^+ assimilation and generate excess of H^+ that would be transported out of the cell decreasing the SW pH.

After a period of N_i starvation, NH_4^+ uptake by macroalgae is rapidly enhanced, occurring usually during the first 1 h of NH_4^+ resupply. However, once intracellular N pools are filled up, the assimilation rate of N into organic pools is controlled by internal N pools (e.g. amino acids), and can vary over longer scales of times (e.g. days to weeks) (Fujita 1985, McGlathery et al. 1996, Pedersen 1994). NH_4^+ assimilation involves the enzyme Glutamine synthetase GS, carbon skeletons, and energy (i.e. ATP), and internal pooling of NH_4^+ is required for GS to operate efficiently (Taylor and Rees 1999). Concentrating NH_4^+ prior to its assimilation might reduce considerably the resources (N and energy) required in making proteins and in running the transport and assimilation processes (Raven et al. 2008b). The initial rapid uptake, termed surge phase, last minutes to hours occurring as a function of time and /or the filling of internal N_i pools, and is followed by a constant N_i uptake rate that is internally controlled; a process known as the assimilation rate (Pedersen 1994). For example, in the green macroalga *Ulva lactuca* enhanced uptake occurred within the first 120-150 min of incubation, then the uptake rate remained constant for further 150 min (Pedersen 1994). This result suggests that in the first 2 h of incubation the main priority of the alga was to take up nutrients likely to refill the internal N_i pool, and assimilation may begin after 2 h of

incubation. These results agree with my suggestion that for N-deplete *Macrocystis* blade sections the 75 min of incubation under a high NH_4^+ concentration was likely not long enough to reach the second phase of assimilation, and the new NH_4^+ entering into the cell was stored (i.e. vacuole) before to be assimilated.

Nutrient uptake and assimilation processes in microalgae are highly coupled, and large storage vacuoles are scarce, and so most of the N_i entering into the cell must be immediately assimilated (Ullrich 1983, Eisele and Ullrich 1975, Inokuchi and Okada 2001). In contrast, macroalgae possess large intracellular vacuoles for NH_4^+ and NO_3^- storage, hence nutrient uptake and assimilation rates are not always highly coupled (Taylor and Rees 1999, Inokuchi and Okada 2001). This suggests that changes in $[H^+]$ in the medium may be faster and greater in microalgae than in macroalgae, and it could explain the differences observed between *Macrocystis* and the microalga *H. africanum* (Raven and De Michelis 1980). However, *H. africanum* is a big unicellular microalga with intracellular vacuoles for N_i storage (Ullrich 1983), and the metabolism of microalgae is also faster than the macroalgae's metabolism. Therefore, changes in H^+ fluxes in microalgal species may occur on a shorter scale of time min to hours than in macroalgal species.

Excess of OH^- generated after NO_3^- assimilation into NH_4^+ has been more extensively studied for freshwater algal species (Eisele and Ullrich 1975, Eisele and Ullrich 1977, Raven and De Michelis 1979, Deane-Drummond 1984, Ullrich et al. 1998). Eisele and Ullrich (1975, 1977) reported a stoichiometry closed to 1 (1 OH^-: 1 NO_3^-) between alkalinisation of the medium and nitrate uptake in the freshwater microalga *Ankistrodesmus braunii* in the presence of a Ci source (i.e. CO_2). A stoichiometry between OH^- and NO_3^- of 1: 1 occurs if there is no intracellular

biochemical OH^- removal (e.g. NH_4^+ assimilation into amino acids consumed the second OH^- produced after NO_3^- assimilation). In the absence of any Ci source the stoichiometry also increased to about 2 (2 OH^-: 1 NO_3^-) because NO_3^- may not be stored within the cell, and so most of the NO_3^- reduced is released as NH_4^+ outside of the cell, increasing the medium alkalinisation (high [OH^-]) (Eisele and Ullrich 1977). Similar results, a stoichiometry of about 1 (0.75 OH^-:1 NO_3^-) were observed by Raven and De Michelis (1979) in *H. africanum* grown with CO_2 as Ci source; pH in the medium increased from 6.92 to 7.33 after 4 weeks of incubation, and similar results were observed during a short term experiment (Raven and Jayasuriya 1977). In contrast, in our study NO_3^- uptake rate in *Macrocystis* did not increase the pH within the DBL. Similar results were observed when compared to *Macrocystis* blade sections incubated with NDSW, suggesting that the increases in pH within the DBL in both treatments were mainly due to photosynthesis rather than NO_3^- uptake. As explained above for NH_4^+ assimilation, it is possible that the incubation time utilized was not long enough to measure the production of OH^- after NO_3^- has been reduced and assimilated. Deane-Drummond (1984) did not observe a clear relationship between the efflux of OH^- and NO_3^- uptake in N-deplete *Chara corallina* cells after a short term experiment (< 1 h), and instead an acidification of the medium was observed. Like in *Macrocystis*, *C. corallina* cells were first pre-incubated with low NO_3^- concentrations (0.002 mmol L^{-1} KNO_3^-) and no internal NO_3^- pool was detected prior to the uptake experiment, but it was rapidly refilled after the 30 min uptake experiment (at 0.2 mmol L^{-1} KNO_3^-). Therefore, the rapid NO_3^- uptake observed during the first hour of incubation is likely associated with the refilling of the intracellular N_i pool (i.e. NO_3^-), suggesting that incubation time <1 h are probably not long enough to measure NO_3^- assimilation.

Furthermore, for the complete reduction of NO_3^- to NH_4^+, H^+ are required and OH^- must leave the cell to maintain the intracellular balance. Some authors have suggested that an H^+ co-transport or an OH^- counter-transport must occur across of the plasma membrane to maintain the intracellular pH (Eisele and Ullrich 1975, Raven and De Michelis 1979). Raven and De Michelis (1979) suggested that a co-transport (H^+/NO_3^-) occur in *H. africanum* with at least one H^+ entering into the cell per each NO_3^- taken up. In some microalgal species, nitrate uptake depends on a plasma membrane H^+-ATPase pump with a secondary active H^+ co-transport process (Ullrich et al. 1998). The presence of this mechanism may be detected by using a specific H^+-ATPase pump inhibitor (i.e. diethyl stillbestrol, DES) (Beilby 1984). Thus, if this mechanism is involved in NO_3^- uptake, the addition of DES must reduce NO_3^- uptake due to the inhibition of the ATPase pump (Deane-Drummond 1984). However, other authors have indicated that a counter-transport (OH^-/NO_3^-) is more likely to exist because the transport of H^+ into the cell during NO_3^- uptake might be pH dependent; the $[H^+]$ in the seawater is reduced at pH > 8.00 (Eisele and Ullrich 1975, Fuggi et al. 1981). In higher plants, a co-transport (H^+/NO_3^-) mechanism has been described; however, the influx of H^+ leads to a decrease in the intracellular pH when the reduction of NO_3^- was blocked by inhibiting nitrate reductase (NR) activity (Espen et al. 2004). The intracellular pH was regulated when NR was activated, suggesting that the reduction of NO_3^- is involved in pH homeostasis (Espen et al. 2004). Therefore, it can be assumed that when a co-transport H^+-NO_3^- exist the uptake of H^+ reduces the intracellular pH and therefore the OH^- produced after NO_3^- assimilation is not exuded outside of the cell to maintain the intracellular pH. Thus, changes in the extracellular pH may be associated with a co-transport H^+-NO_3^- or an efflux of OH^- after NO_3^- has been

assimilated; but not both. However, fluxes of H^+/OH^- through the plasma membrane might depend on the intracellular pH.

The transport, reduction and assimilation of NO_3^- in *Macrocystis* have not been extensively studied, and it is unknown whether or not there is a co-transport of H^+ during NO_3^- uptake. There are at least two ways, described for higher plants to prove the existence of this H^+/NO_3^- mechanism: (1) evaluate the effect alone of the NO_3^- uptake on the intracellular pH, blocking the NR activity with a specific inhibitor (i.e. Tungstate), and (2) NO_3^- uptake rates might be enhanced under low pH due to the high $[H^+]$ (Ullrich and Novacky 1990, Espen et al. 2004). In addition, this transport might be activated after a few days of NO_3^- starvation (Espen et al. 2004). *Macrocystis* blade sections were pre-incubated with low NO_3^- concentrations (< 0.25 µmoles L^{-1}), therefore if there is an H^+/NO_3^- co-transport present in *Macrocystis* initial pH would be more increased compared to the other two treatments (i.e. NDSW+NH_4^+ and NDSW) due to the influx of H^+ during the NO_3^- uptake experiment. In addition, NO_3^- uptake rates of *Macrocystis* were not enhanced under the low pH treatment (pH = 7.65) compared to the ambient treatment (pH = 8.00) (discussed below). This result suggests that this mechanism may not present in *Macrocystis*. However, further studies are required to describe the NO_3^- uptake mechanism and assimilation process in *Macrocystis* and to determine its effect on the intracellular pH and its regulation.

The second goal of this study was to test the hypothesis that increases in pH within the DBL associated with NO_3^- uptake and assimilation will be greater under an OA treatment (pH = 7.65) than under an ambient treatment (pH = 8.00), whereas decreases in pH within the DBL associated with NH_4^+ assimilation will be smaller under an OA treatment (pH = 7.65) than under an ambient treatment (pH = 8.00). The

pH within the DBL was more greatly modified under the OA treatment than under the ambient treatment irrespective of the N_i source supplied (NO_3^- or NH_4^+), and N_i uptake rates were not affected. NO_3^- uptake was not enhanced under the OA treatment, suggesting that H^+ may not be involved in the NO_3^- uptake by *Macrocystis*, and therefore greater increases in pH within the DBL observed in the OA treatment compared to the ambient treatment were not associated with NO_3^- uptake and assimilation. NH_4^+ uptake was not negatively affected by the OA treatment, which suggests that either the high external [H^+] did not negatively affect the H^+-ATPase pump or that excess of H^+ are not produced after NH_4^+ assimilation; this is supported by the observation of no differences in the pH changes within the DBL between nutrient treatments (i.e. NDSW+NO_3^-, NDSW+NH_4^+ and NDSW). Therefore, the greater changes in pH observed under the OA treatment across all the nutrient treatments compared to the ambient treatment suggest that photosynthesis may be the most important physiological process controlling the changes in pH within the DBL. Furthermore, the total seawater alkalinity was similar in the OA and ambient pH treatments across all nutrient treatments, suggesting that the proportion of base to protons in the medium was not changed, and from each Ci form (CO_2 or HCO_3^-) removed from the medium an OH^- or H^+ was generated (Uusitalo 1996). This result suggests that N_i transport, reduction and assimilation did not affect the balance between OH^- and H^+ in the external medium and therefore photosynthesis and Ci utilization were the main mechanisms regulating the acid/base medium.

The fluxes of H^+ and OH^- at the algal surface might also depend on which Ci source (i.e. CO_2 or HCO_3^-) is being utilized by the alga (Lucas 1983, Raven 1997, Larsson and Axelsson 1999, Moulin et al. 2011). Alhtough it is known that the utilization of CO_2 and HCO_3^- as Ci sources for photosynthesis results in an increase of

the external pH, for some macroalgal species and marine angiosperms the use of HCO_3^- results in an extrusion of H^+, generating localized acid zones within the DBL to enhance the conversion of HCO_3^- to CO_2 and consequently CO_2 diffusion into the cell, but OH^- may be relased in other sites along the cell membrane to counterbalance the local H^+ (Hellblom et al. 2001, Raven et al. 2008a, Moulin et al. 2011, Beer et al. 2014). However, Lin et al. (2013) observed an influx of H^+ instead of an efflux in the marine angiosperm *Zostera marina*, using a micro-electrode located at 5 µm from the leaf surface. This result suggests that the influx of H^+ under a saturating light intensity is associated with Ci utilization, e.g. direct use of CO_2 or a co-transport of H^+/HCO_3^- that leads to an increase in the external SW pH. In *Macrocystis*, the main mechanism of HCO_3^- uptake is via an anion exchange protein (AE), but CO_2 might also be used by simple diffusion (Fernández et al. 2014/ see Chapter 3). In the present study, HCO_3^- uptake in *Macrocystis* was similar between both pH treatments and across all the nutrient treatments, and so the greater changes in pH observed in the OA treatment might be associated with more diffusive entry of CO_2 into the cell that reduces the $[H^+]$ in the medium, leading to an increase in the external seawater pH (Beer et al. 2014). Moreover, as the pH within the DBL was not reduced either in the ambient or OA treatment across all the nutrient treatments, this suggests that the use of HCO_3^- in *Macrocystis* is not facilitated by the excretion of H^+ outside of the plasma membrane, which result in localized zones of low pH, as reported in other Laminariales species, i.e. *Saccharina latissima* (Axelsson et al. 2000).

The excess of H^+ under an OA scenario could affect important physiological processes in micro- and macroalgal species; however, to date the understanding of its effect on the intracellular pH regulation are poorly understood (Taylor et al. 2012). Phhysiological processes such as photosynthesis and growth require net uptake and

assimilation of inorganic nutrients such as CO_2, HCO_3^-, NH_4^+, and NO_3^-, across the plasma membrane, and usually the transport of these ions occur together with other anions (i.e. Na^+), H^+ or OH^-, and also energy is required (i.e. ATP) (Taylor et al. 2012 and references therein). With all these processes occurring at the same time within the algal cell, intracellular regulation is very important. Recent studies have observed that the passive outward flux of H^+ can occur in the microalga *Emiliana huxleyi* through H^+ channels and they might be negatively affected by the high $[H^+]$ outside the cell under an OA scenario because they are highly sensitive to changes in external pH as they depend on the trans-membrane H^+ electrochemical gradient (Suffrian et al. 2011, Taylor et al. 2011, 2012). In this study, N_i uptake by *Macrocystis* was not negatively affected by OA, indicating that a passive flux of H^+ might not occur in this species. Further studies are required for a better understanding of how internal physiological processes such as enzymatic activity and N_i reduction and assimilation are regulated, and how the intracellular pH homeostasis is maintained.

In summary, N_i uptake rates of *Macrocystis* did not modify the pH at the seaweed surface, within the DBL. Although the pH within the DBL increased under both treatments, similar results were observed under the NDSW treatment, suggesting that photosynthesis is likely the main physiological process modifying the pH within the DBL under a saturating light condition. If these experiments were repeated in the dark, where respiration would be the main physiological process modifying the pH at the thallus surface of a non-calcareous macroalga, then N_i uptake and assimilation may respond differently. Under the OA treatment (pH = 7.65) the pH within the DBL was more affected than under ambient conditions (pH = 8.00) irrespective of the N_i source supplied. These results suggest that under an OA scenario *Macrocystis* can modify its micro-environment within the DBL, and the physiological processes of photosynthesis

and N_i uptake will not be affected by low pH. However, both further long term studies (days to weeks) on elevated pCO_2/low pH conditions (OA) and descriptive studies on the transport and assimilation mechanisms of *Macrocystis* will be important to elucidate how increased in $[H^+]$ might affect their metabolic OH^-/H^+ fluxes and consequently their intracellular pH regulation.

Chapter 7: General Discussion

The overall goal of this thesis was to examine the effects of OA on photosynthesis, growth, and carbon and nitrogen metabolism of *Macrocystis*. In this final chapter, I will first review the key findings of each chapter, highlighting the more important physiological results and the possible implications for the species. Subsequently, I will combine the new information obtained on the C and N metabolism in this species in a mechanistic figure, summarizing NO_3^- uptake and assimilation processes, together with C interactions (Figure 7.1). This figure will also highlight which processes or transport mechanisms remain unknown in this species. This work presents the findings of short term (3-7 days) physiological responses of *Macrocystis* from New Zealand (summarized in Figure 7.2), and in the final section I will discuss how findings might be applied to the whole organism, highlighting the interactive effects of OA with other ongoing predicted environmental changes such as ocean warming and anthropogenic eutrophication. Finally, recommendations to take into account for future OA studies on macroalgal species are made.

7.1 Main findings

The research conducted in Chapter 2 described, for the first time, an optimized assay for determining external and internal CA activity in *Macrocystis*. The most important finding after the optimization of the CA assay was that CA_{int} activity was 2-fold higher than that CA_{ext} activity, suggesting that CA_{int} plays important roles such as intracellular pH regulation, internal Ci accumulation and CO_2 supply to RuBisCO. In addition, the low activity of CA_{ext} compared to the CA_{int}, suggested that externally catalyzed HCO_3^-

dehydration is not the only Ci acquisition mechanism present in the fast growing species *Macrocystis*.

The research presented in Chapter 3 demonstrated that the utilization of HCO_3^- by *Macrocystis* is mainly dependent on an anion exchange (AE) protein; the inhibition of the AE protein led to a decline of 55-65% of *Macrocystis* photosynthesis, with CA_{ext} making comparatively little (11-34%) contribution to the photosynthetic Ci acquisition. The present study is the first to describe the presence of the AE protein in this species. This is a more efficient mechanism than the external HCO_3^- catalyzed dehydration mediated by CA_{ext} (Beer et al. 2014). Therefore, direct HCO_3^- uptake via the AE protein and high internal CA_{int} activity may be an important adaptation of *Macrocystis* that allows it to inhabit environments with high daily pH fluctuations (7.9 to 9.1) and to supply sufficient amounts of CO_2 to RuBisCO to support high photosynthetic and growth rates. The high CA_{int} activity compared to CA_{ext} observed in this species is then explained by the continuous entry of HCO_3^- via the AE protein that must be dehydrated to supply CO_2 to RuBisCO. In addition, the functioning of both Ci acquisition mechanisms under low (7.65) and high pH (9.00) suggested that these mechanisms will not be down-regulated under a future elevated pCO_2 ocean, and therefore the preference and utilization of HCO_3^- by *Macrocystis* will mostly likely not be affected by OA.

The research presented in Chapter 4 demonstrated that elevated pCO_2 did not enhance either photosynthetic or growth rates of *Macrocystis*. This result strongly suggests that photosynthesis and growth of *Macrocystis* are carbon-saturated under the current Ci concentrations. Therefore, it is unlikely that the increase in pCO_2 ($\approx$ 40.35 µM) and HCO_3^- ($\approx$ 190 µM) predicted by 2100 will enhance *Macrocystis* photosynthesis or growth. In addition, CA_{ext} and CA_{int} were mostly not down-regulated

by elevated pCO_2, confirming the assertion from chapter 3. Although more diffusive entry of CO_2 into the algal cells may occur under OA, this does not mean that direct and/or indirect HCO_3^- uptake by *Macrocystis* will be down-regulated, because the CCMs increase the [CO_2] around RuBisCO above the CO_2 level achievable by passive diffusion (Raven et al. 2012).

The research presented in Chapter 5 showed that nitrogen metabolism (Figure 7.1) of *Macrocystis* is greatly modified by external NO_3^- availability. Important relationships between external NO_3^- availability, and NO_3^- uptake and assimilation, and internal NO_3^- pools were observed, e.g. higher NO_3^- uptake rates after a period of limited NO_3^- availability, and higher internal NO_3^- pool and NR activity after a period of sufficient NO_3^- supply. An understanding of these relationships are necessary to explain the growth responses of this species in the field, e.g. knowing the storage capacity of *Macrocystis* and NR assimilation rate, we can estimate how long this species may survive in environments with limited NO_3^- concentrations, and determine how fast it could assimilate a sporadic pulse of NO_3^- in the environment (e.g. coastal waters + eutrophication). In this study, internal NO_3^- pools of *Macrocystis* varied greatly with NO_3^- availability, and N metabolism was rapidly increased when NO_3^- was re-supplied after a few days of limited NO_3^- availability. NO_3^- uptake rates were regulated by internal NO_3^- pool size. These results strongly suggest that internal NO_3^- pools in macroalgae should be measured when conducting any nitrate uptake experiment, because it will probably influence uptake rates. The findings also support the assertion that *Macrocystis* is a 'seasonal responder' as suggested by Kain (1989). *Macrocystis* might exhibit different growth and NO_3^- storage capacity depending on the external NO_3^- availability, which can vary substantially between localities and seasons (Kopczak et al. 1991, Kopczak 1994).

In addition, all the physiological and biochemical parameters (i.e. $\delta^{15}N$) related to N metabolism measured in the present study, showed a fast response to the external NO_3^- availability in a short time-scale (hours-days). The rapid change in $\delta^{15}N$ values in *Macrocystis* blades, after 3 d of incubations under different NO_3^- concentrations suggests that $\delta^{15}N$ might be used as an indicator of external N_i availability, but only when one N_i source is supplied, as it may respond on a very short time-scale. The inverse relationship observed between $\delta^{15}N$ and external NO_3^- availability and total tissue N content suggests that nitrogen-limited conditions might cause a change in the nitrate assimilation, and therefore altered the isotope fractionation (Needoba et al. 2003). However, values of $\delta^{15}N$ of the enriched seawater with $NaNO_3^-$ could also influence the $\delta^{15}N$ values of *Macrocytsis* blades. The new biomass produced might have the same or similar $\delta^{15}N$ values as the nitrate source dissolved in the SW depending on the utilization and the assimilation rates. Teichberg et al. (2007) showed that in the green macroalgae, *U. lactuca*, $\delta^{15}N$ values decreased as total tissue N content increased. Those results suggest that NO_3^- assimilation might result in a change in the fractionation of $\delta^{15}N$ inside the algal cell. However, further studies on the fractionation of $\delta^{15}N$ during N uptake and assimilation are required for a better physiological understanding of this parameter in macroalgae.

Research reported in chapter 5 also revealed that the tissue N status did not modulate the response of *Macrocystis* to OA when NO_3^- is not limiting. As mentioned above, N metabolism of *Macrocystis* can be rapidly up-regulated, therefore low internal N reserves in N-deplete blades did not negatively affect *Macrocystis* photosynthesis or growth once NO_3^- was re-supplied. Irrespective of the N status of the alga, the OA treatment did not increase photosynthesis or growth, and consequently nutrient demand was not enhanced under the OA treatment. Interestingly, for N-replete blades

physiological parameters related to NO_3^- assimilation (i.e. NR, total tissue N content and internal NO_3^- pool) were equally down-regulated in both OA and ambient treatments compared to initial values at the start of the pCO_2 incubations. These results suggested that the N metabolism of *Macrocystis* is mainly regulated by external NO_3^- concentrations, and even if there are more internal N reserves to support higher growth or photosynthetic rates under OA, they are not enhanced, again supporting the findings from previous chapters 3 and 4.

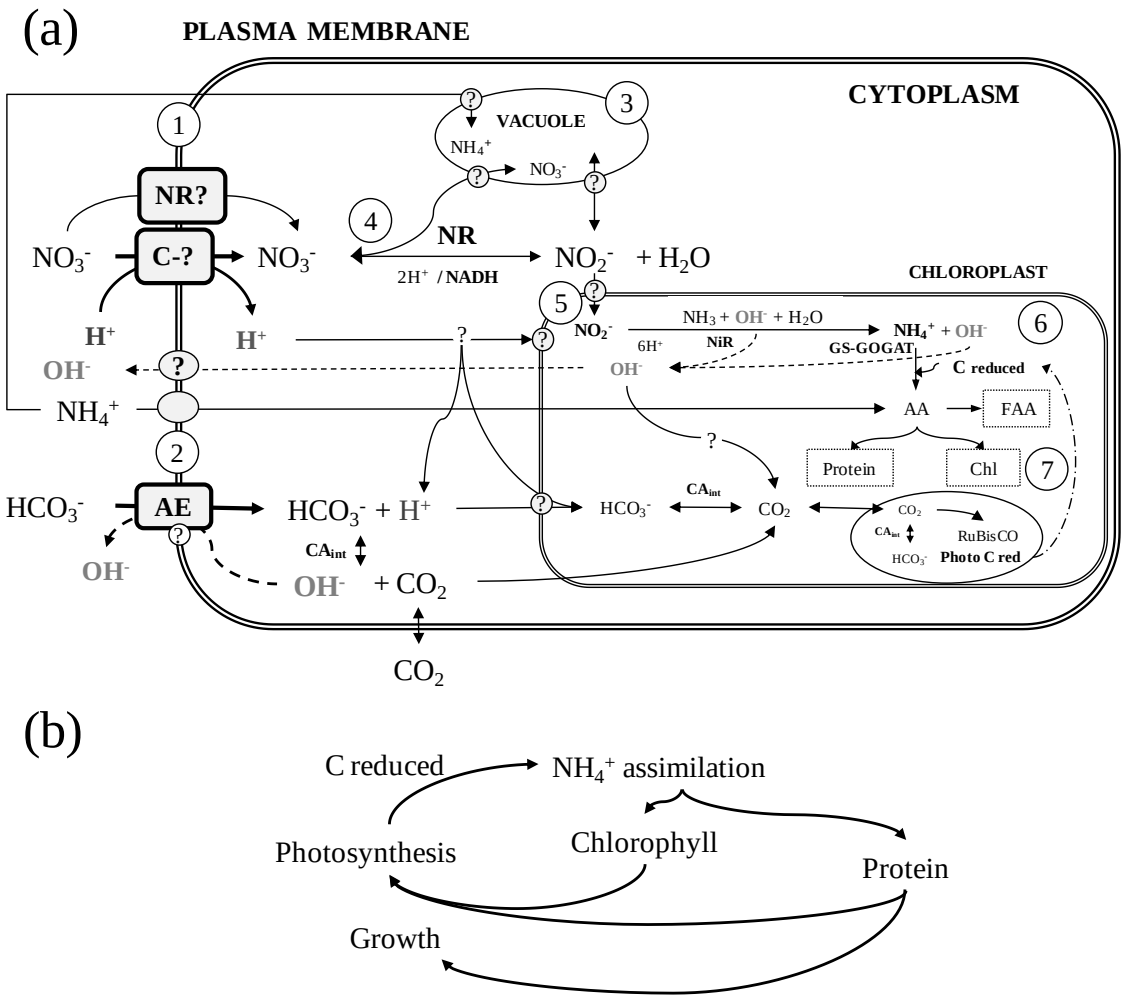

Figure 7.1: Scheme for carbon acquisition and accumulation, and inorganic nitrogen (N_i) uptake and assimilation, in *Macrocystis*. (a) Proposed scheme for N_i transport and reactions involved in nitrate (NO_3^-), nitrite (NO_2), ammonia (NH_3) and ammonium (NH_4^+) assimilation (see figure 3.5 for carbon scheme description). Transport and processes that are unknown are indicated in figure (?). (1) Possible transporters for NO_3^- through the plasma membrane: NR: nitrate reductase; C-: Co-transport of H^+-NO_3^- (1:1); Counter transport NO_3^-- OH^-, (2) transport of NH_4^+ through the plasma membrane via a passive or active uniport (Raven and Giordano 2015), (3) storage vacuole for NH_4^+, NO_3^- and NO_2?: internal N_i pools, (4) NO_3^- assimilation by NR, (5) NO_2 and NH_3 assimilation by NiR, (6) NH_4^+ assimilation by GS-GOGAT pathway, (7) incorporation of AA into protein and Chla, or storage as FAA, dash line boxes: represent organic N pools (Modified from Eisele and Ullrich 1975, Ullrich 1983). (b) Interactions between photosynthesis, N_i assimilation, and growth. Abbreviations: NiR: nitrite reductase; GS-GOGAT: glutamine synthethase-glutamine 2-oxoglutarate amino-transferase pathway; AA: amino acids; FAA: free amino acids; Chl: chlorophyll; Photo C red: photosynthetic carbon reduced; dashed line: OH^- efflux.

The research presented in Chapter 6 reveals the effects of transplasmalemma H^+/OH^- fluxes associated with N_i uptake and assimilation (i.e NO_3^- and NH_4^+) on external pH, within the DBL, might be insignificant compared to the effects of other physiological processes such as photosynthesis and respiration. The greatest change in pH within the DBL under an OA treatment at both N_i treatments, suggests that the internal regulation of the algae is different under low pH (high $[H^+]$), but whether or not this is only due to the photosynthetic Ci acquisition (fluxes of H^+/OH^-) is not clearly understood. Further descriptive studies on N_i uptake and assimilation processes in *Macrocystis* are required for a better understanding of how these fluxes works.

Overall, the present study reveals important new information about the Ci acquisition mechanisms, photosynthesis and growth of one of the most ecologically important macroalgal species of the Pacific temperate regions, *Macrocystis*. Knowledge of the photosynthetic carbon acquisition and whether or not photosynthesis and growth are carbon-saturated under the current ambient Ci concentrations are key issues to understand and predict how macroalgal species will respond to a future shift in the relative proportion of Ci: $CO_{2(aq)}$ and HCO_3^- (Koch et al. 2013, Raven and Hurd 2012). The results presented in this study, showed that increases in pCO_2 will not have significant effects on photosynthetic Ci acquisition and growth of *Macrocystis*. However, the interaction observed between external $[NO_3^-]$ and the NO_3^- uptake and assimilation processes in this species revealed that future changes in inorganic nutrient availability could have significant effects on its N metabolism, and consequently affect others physiological processes such as growth. This species inhabits environments with a wide depth-gradient of temperature, nutrients and light (Figure 7.2), and therefore different responses to OA may be expected under different incubation conditions of light, nutrients or temperature. Further works on the interactive effects of OA with other

environmental factors are required for a better understanding of the regulation of the physiological processes in this species.

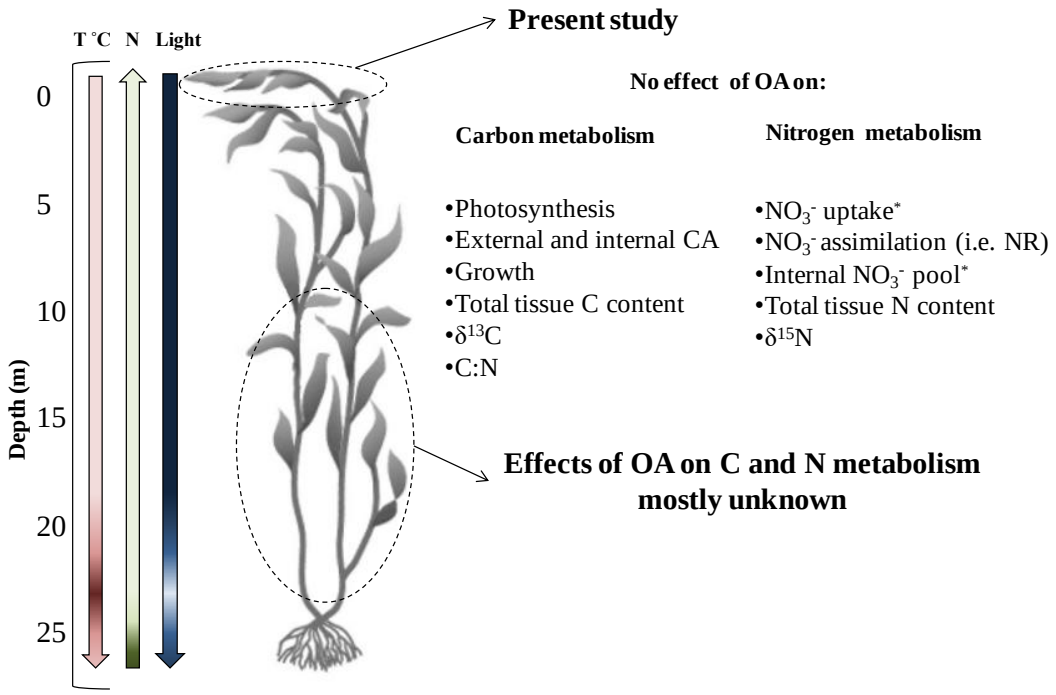

Figure 7.2: Summary of the present study that was focused on determining the effects of OA on C and N metabolisms of young blades (i.e. top of the canopy) of *Macrocystis*. On the left hand side, a representation of gradients of temperature (T °), nitrogen (N, i.e. NO_3^-) and light (PAR) to which an individual of *Macrocystis* can be exposed in its natural environment. * Positive effect only on N-deplete blades.

7.2 Future directions

7.2.1 Carbon metabolism

The present study showed the presence of two external mechanisms for HCO_3^- utilization in *Macrocystis*, and indicated that CA_{int} play an important role in the intracellular pH regulation, among others. However, the presence of other putative intracellular CCMs such as CA isoforms or chloroplast membrane Ci transporter that have been described for green macroalgae, *U. linza* and *U. rigida* (Zhang et al. 2012, Rautenberger et al. 2015), were not tested in *Macrocystis*. Further molecular studies looking for putative CCMs in *Macrocystis* will be of great importance to: (1) have a complete description of the functioning of CCMs in this species, (2) have a better understanding of its intracellular homeostasis (CO_2, HCO_3^-, H^+, OH^-), and (3) to know which and how Ci forms (i.e. CO_2 and HCO_3^-) are transported proximate to the fixation site of RuBisCO.

Other environmental factors such as temperature, nitrogen and light could also regulate the functioning of CCMs (Raven et al. 2012). Therefore, the Ci acquisition mechanisms described in this study for *Macrocystis* might be regulated by light or temperature rather than by external Ci concentrations. Hepburn et al. (2011) suggested that the responses of macroalgae to OA may likely vary between low- and high-light environments driving either the up- or down-regulation of the CCMs. *Macrocystis* is exposed to depth-dependent gradients of light, temperature and nitrate concentrations, and therefore metabolic processes might be depth-regulated in this species (Figure 7.2) (Konotichik et al. 2013). Light intensity decreases exponentially with depth, e.g. at 20 m values are about 1% of the surface PAR (Gerard 1984). It has already been shown that physiological processes of *Macrocystis* occurring in different parts of the kelp,

varying with the depth gradient, e.g. basal *Macrocystis* blades have a lower photosynthetic rate than blades from the surface, but a high NO_3^- assimilation (higher NR and NiR gene expression) (Colombo-Pallota et al 2006, Konotichik et al. 2013). The low photosynthetic rates in deeper waters (= low-light environment) suggest that the HCO_3^- acquisition mechanisms could be down-regulated by limited light conditions, and the diffusive entry of CO_2 could be already enough to support the lower photosynthetic rates in basal blades. Therefore, for *Macrocystis*, CCMs might vary within the individual depending on the depth gradient of light and temperature to which they are exposed, and increases in pCO_2 could have a more positive effect in deeper blades than blades from the surface. This also applies to macroalgal species inhabit a wide depth gradient, as suggested by Hepburn et al. (2011). Some deep water macroalgal species are strictly CO_2-users and as such solely rely on the diffusive CO_2 entry (Hepburn et al. 2011, Cornwall et al. 2015). However, given the low light intensity at depth to support lower photosynthetic rate, these species are most likely Ci saturated. Therefore, these species may be benefit from the increased diffusive entry of CO_2 under OA, but not under sub-saturating light (Rautenberger et al. 2015). In this regard, further studies on the regulation of the CCMs and the interaction with other physiological processes such as nitrogen uptake are required for a better understanding of the energetic metabolic costs. Under circumstances of climate change, such as OA and greater stratification of the mixed layer (less light availability; see section 7.2.2), mechanisms that involve less energetic cost, e.g. diffusive entry of CO_2 (Raven and Hurd 2012) and NH_4^+ assimilation (Pritchard et al. 2015) might be beneficial for the algae.

In addition, molecular studies on *Macrocystis* will be useful for a better understanding of the C and N metabolisms in this species. A recent study showed

differential gene expression across the depth gradient in *Macrocystis* (Konotchick et al. 2013). Genes associated with photosynthesis and carbon fixation had a higher expression in blades from the surface than basal blades, whereas genes associated with the N metabolism, i.e. NR, NiR, were higher in basal blades. This study strongly suggests that metabolic processes in *Macrocystis* are influenced by depth-dependent gradient of light, temperature and nutrients to which these individuals are exposed. However, *Macrocystis* also exhibits a wide geographic distribution around the world, with a latitudinal range from 54˚40'N to 54˚56'S (Alaska to Mexico; Peru to Argentina) (Graham et al. 2007), and will experience very different temperatures, light, and inorganic nitrogen regimes in each environment. Therefore, different physiological gene expression might be expected among populations. The study by Konotchick et al. (2013) provides a transcriptional profile of *Macrocystis* that might be used in further studies to determine the effects of further climate change (e.g. OA and temperature) on *Macrocystis*, and to examine differences between metabolic processes among populations and individuals exposed to different environmental gradients.

7.2.2 Ongoing climate change

OA will occur in synergy with other global environmental changes, such as increases in the ocean temperature (ocean warming); the surface ocean temperature is predicted to increase between 1.4˚C and 5.8˚C (IPCC 2013). A secondary effect of ocean warming will be an increase in the thermal stratification of seawater, reducing the nutrient supply from deeper waters to the surface (Guinotte and Fabry 2008). Increases in the stratification of the mixed layer could also increase the average irradiance above the thermocline, and affect negatively the light penetration below the thermocline due to by e.g. phytoplankton blooms (Boyd and Doney 2002, Steinacher et al. 2010, Raven 2011). Therefore, in a future ocean, photosynthesis and growth of macroalgae growing below

the thermocline may be negatively affected by reduced light. However, local changes such as increases in eutrophication are also expected in coastal waters (Wernberg et al. 2011). These predicted coastal changes might exacerbate or ameliorate the negative effects of others environmental factors on macroalgal species inhabit in coastal waters, as *Macrocystis* (see Figure 7.3 for a schematic illustration comparing today' ocean with a future predicted ocean).

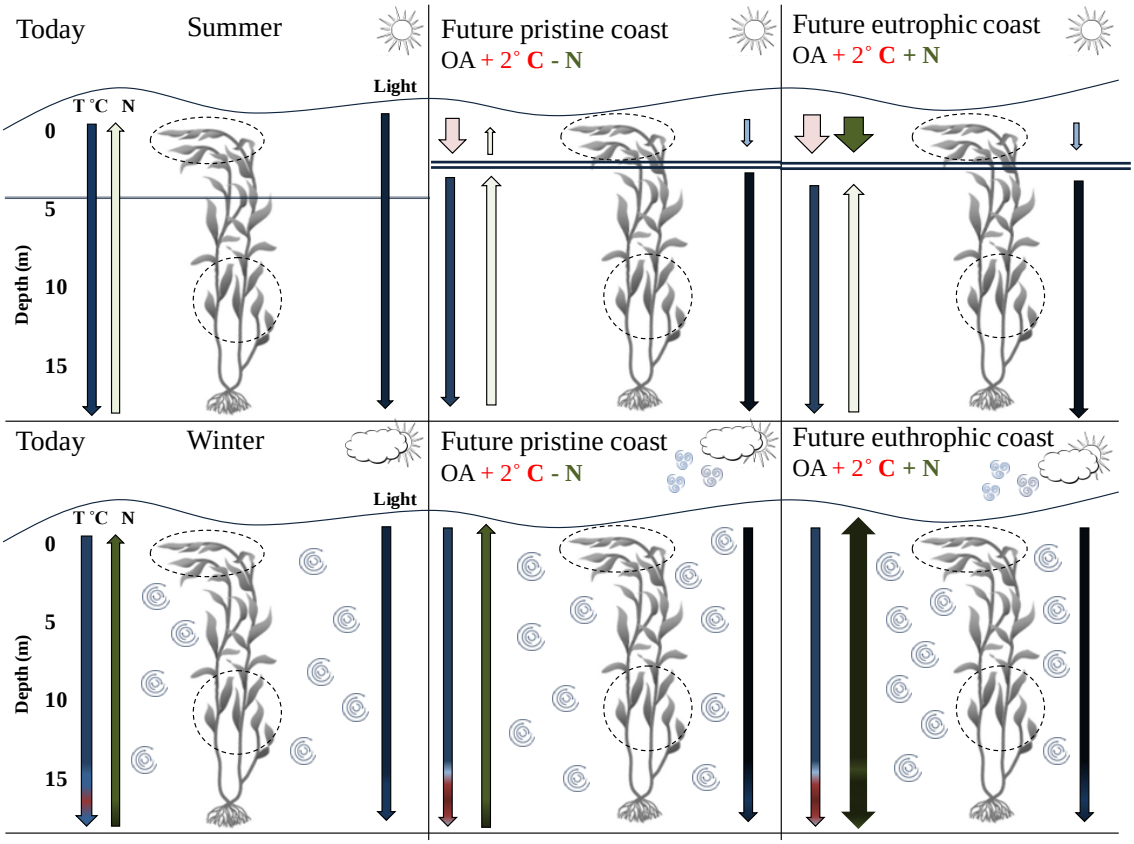

Figure 7.3: A schematic diagram comparing today's ocean with the predicted future changes in OA, anthropogenic eutrophication, ocean warming, and increases in the stratification of the mixer layer in two seasons: summer and winter. In summer, intensified stratification will lead to a decrease in the input of nutrients to the surface, and it will affect the light penetration to the bottom waters. However, in a future eutrophic coast, anthropogenic eutrophication could increase the nutrient concentrations in the surface, but surface waters will also get warmer and irradiances will be higher above the thermocline (Harley et al. 2006, Boyd and Law 2011). In winter, waters are well mixed, and the thermocline does not show a clear pattern with the depth as does in summer (Holt et al. 2010, 2014). For a future ocean, increases in storms will lead to a reduction in light in the surface waters (Boyd and Law 2011), but input of nutrients to the surface will not be limited. In a future eutrophic coast, concentrations of nutrients will be higher than in summer and in a pristine coast along the depth gradient. Individuals of *Macrocystis* were incorporated into the diagram to illustrate how the depth-gradient of nutrient, light and temperature to which this species is exposed will change in coastal waters of a future ocean.

Johnson et al. (2011) showed that populations of *Macrocystis* have been negatively affected by ocean currents with elevated temperatures and poor in nutrient concentrations in Tasmania, Australia. This observation suggests that populations of *Macrocystis* might be more affected by future predicted increases in temperature rather than by changes in pCO_2/pH. Temperature is an important factor controlling most of macroalgae performances, because influences on metabolic processes (e.g. growth and photosynthesis) and enzymatic mechanisms (Lobban and Harrison 1997, Harley et al. 2012). However, it is difficult to separate the effect of temperature from nitrogen (i.e. NO_3^-), because usually these two parameters co-vary inversely together in the oceans (Hernandez-Carmona et al. 2001). Another study on *Macrocystis* showed that growth was negatively affected by increased temperature alone, but was enhanced when both pCO_2 and temperature were increased; however, nutrient concentrations were not limited (Brown et al. 2014). Probably, under limited nutrient concentrations the response would be different due to the lack of nitrogen compounds (i.e. amino acids, protein) to support high growth (see below for discussion). The studies of Johnson et al. (2011) and Brown et al. (2014), give contrary predictions for the growth of *Macrocystis* in a future predicted ocean. Therefore, further studies that evaluate the effect of nitrogen, temperature and elevated pCO_2 alone on *Macrocystis* physiology and examine the interactive effects are required to predict the response of *Macrocystis* to a future predicted ocean conditions.

Irradiance, water temperature and nutrient availability are important environmental factors controlling *Macrocystis* growth, photosynthesis and N assimilation (North 1971, Wheeler and North 1980, Gerard 1984, Dean and Jacobsen 1984, Hernandez-Carmona et al. 2001, Johnson et al. 2011). It has been suggested that for *Macrocystis*, translocation of nitrogenous compounds occurs from the bottom

blades, which are usually exposed to cooler water with higher [NO_3^-], to the surface blades, which are usually exposed to warmer water with low [NO_3^-] (Jackson 1977, Hepburn et al. 2012, Konotchick et al. 2013). Simultaneously, the translocation of carbon compounds occurs from the surface to the bottom (Konotchick et al. 2013). The transport of C and N compounds along the thallus may be influenced by the future predicted changes in N availability, light and temperature. With more NO_3^- available in surface waters due to eutrophication (Figure 7.3), NO_3^- uptake and assimilation of apical blades could be enhanced, reducing the cost of N translocation from the bottom. However, increased temperature and low light availability (Figure 7.3) might affect negatively the enzymatic processes of apical blades reducing metabolic processes such as N assimilation and photosynthesis. As shown in Figure 7.1 these two mechanisms, carbon and nitrogen are tightly coupled: N assimilation provides the nitrogenous compounds required to support photosynthesis and growth, but photosynthesis provides the reduced carbon required for NH_4^+assimilation into amino acids. Therefore, further physiological studies on enzymatic regulation, e.g. thermal and light tolerance curves for NR and CA_{int} as well as for photosynthesis and growth, will be important to predict how increased temperature and low light availability could influence on the C and N metabolism in this species.

For coastal waters, the increase in temperature might be more variable than in the open ocean, and increases in eutrophication due to human activities may ameliorate the negative impact of ocean warming and OA reported on macroalgal species. However, a recent study showed that eutrophication in the coastal waters may lead to a further decline in pH of 0.05 units by 2100, and makes the coastal waters more susceptible to OA (Cai et al. 2011). As shown in this study, *Macrocystis* can modify its surroundings and its micro-environment, therefore a further decrease in pH of about

0.05 units should not influence on its physiology. Alternatively, increased temperature might affect marine communities causing a shift in the geographical range of the species, and increases in nutrient concentrations might benefit other opportunistic species, e.g. turf-forming and foliose algae (Connell and Russell 2010). Therefore, both OA and ocean warming could also affect indirectly *Macrocystis* abundance and distribution. Future work considering future predicted changes in coastal waters, e.g., increases in eutrophication, sedimentation, herbivory, and invasive species (Wernberg et al. 2011) should be conducted to determine the effects of climate change on populations and communities inhabiting in coastal waters.

7.3 Concluding Remarks

One of the main issues in order to predict a macroalgal respond to OA is understand the functioning of their C and N metabolisms. As shown in the present study the pathway of both mechanisms is complex, and both mechanisms are tightly coupled. Therefore, for a better understanding of how macroalgae will respond to OA it is strongly suggested that the following considerations should be taken into account: (1) determine the Ci source utilized by the alga and the main mechanisms for Ci acquisition with physiological experiments like the one used in the present study rather than using $\delta^{13}C$ signatures isotopes or pH drift experiment, which are useful to determine which Ci source is being utilized by the alga, but not to determine which mechanism are involved in the Ci utilization, (2) examine the regulation of the Ci mechanisms by external Ci concentrations, but also by other parameters such as light or temperature to not misinterpret the effect of OA on the down-regulation of those mechanisms, (3) understanding the metabolic fluxes of OH^-/H^+ are also of great importance to determine whether ot not the effect of OA on macroalgae physiology is only due to the changes in the relative proportion of relative proportion of Ci: $CO_{2(aq)}$ and $HCO_3^-$and low pH or

due to higher [H^+], which could affect the extrusion of metabolic H^+ affecting the internal cellular homeostasis, and (4) as nitrogen metabolism is tightly coupled to C metabolism, is of great importance to conduct the experiments under conditions of nutrients favourable for each species, as any negative effect on the N metabolism, e.g. nutrient limitation, will lead to a reduction in photosynthetic and growth rates of the species.

References

Ahn O, Petrell RJ, Harrison PJ (1998) Ammonium and nitrate uptake by *Laminaria saccharina* and *Nereocystis luetkeana* originating from a salmon sea cage farm. *J. Appl. Phycol.* 10:333–340.

Alexandre A, Silva J, Buapet P, Björk M, Santos R (2012) Effects of CO_2 enrichment on photosynthesis, growth, and nitrogen metabolism of the seagrass *Zostera noltii*. *Ecol. Evol.* 2:2625–2635.

Andría JR, Vergara JJ, Peréz-Lloréns JL (2000) Fractionation of carbonic anhydrase activity in *Gracilaria* sp. (Rhodophyta) and *Enteromorpha intestinalis* (Chlorophyta): changes in the extracellular activity in response to inorganic carbon levels. *Aust. J. Plant Physiol.* 27:1161–1167.

Andría JR, Brun FG, Peréz-Lloréns JL & Vergara JJ (2001) Acclimation responses of *Gracilaria* sp. (Rhodophyta) and *Enteromorpha intestinalis* (Chlorophyta) to changes in the external inorganic carbon concentration. *Bot. Mar*. 44:361–370.

Andría JR, Peréz-Lloréns JL, Vergara JJ (1999) Mechanisms of inorganic carbon acquisition in *Gracilaria gaditana* nom. prov. (Rhodophyta). *Planta*. 208:564–73.

Atkins, CA, Patterson BD, Graham D (1972) Plant carbonic anhydrases: I. Distribution of types among species. *Plant Physiol.* 50:214–217.

Axelsson L, Larsson C, Ryberg, H (1999) Affinity, capacity and oxygen sensitivity of two different mechanisms for bicarbonate utilization in *Ulva lactuca* L. (Chlorophyta). *Plant Cell Environ*. 22:969–978.

Axelsson L, Mercado JM, Figueroa FL (2000) Utilization of HCO_3^- at high pH by the brown macroalga *Laminaria saccharina*. *Eur. J. Phycol.* 35:53–59.

Axelsson L, Ryberg H, Beer S (1995) Two modes of bicarbonate utilization in the marine green macroalga *Ulva lactuca*. *Plant Cell Environ.* 18:439–445.

Badger MR, Andrews TJ, Whitney SM, Ludwig M, Yellowlees DC, Leggat W, Price GD (1998). The diversity and co–evolution of RUBISCO, plastids, pyrenoids and chloroplast–based CO_2 concentrating mechanisms in the algae. *Can J Bot* 76:1052–1071.

Badger MR, Bassett MB, Comins HN (1985) A model for HCO_3^- accumulation and photosynthesis in the Cyanobacterium *Synechococcus* sp. *Plant Physiol.* 77:465–471.

Badger MR, Price GD (1994) The role of carbonic anhydrase in photosynthesis. *Annu. Rev. Plant Physiol. Plant Mol. Biol*.45:369–392.

Beardall J, Beer S, Raven JA (1998) Biodiversity of marine plants in an era of climate change: some predictions based on physiological performance. *Bot. Mar.* 41:113–123.

Beardall J, Giordano M (2002) Ecological implications of microalgal and cyanobacterial CO_2 concentrating mechanisms and their regulation. *Funct. Plant. Biol.* 29:335–347.

Beardall J, Raven JA (2004) The potential effects of global climate change on microalgal photosynthesis, growth and ecology. *Phycologia* 43(1): 26–40.

Beardall J, Roberts S, Raven JA (2005) Regulation of inorganic carbon acquisition by phosphorus limitation in the green alga *Chlorella emersonii*. *Can. J. Bot.* 83:859–864.

Bédu S, Peltier G, Joset F (1989) Correlation between carbonic anhydrase activity and inorganic carbon internal pool in strain *Synechocystis* PCC 6174. *Plant Physiol.* 90:470–474.

Beer S (1994) Mechanisms of inorganic carbon acquisition in marine macroalgae (with special reference to the Chlorophyta). *Progr. Phycol. Res.* 10:179–207.

Beer S (1996) Photosynthetic utilization of inorganic carbon in *Ulva*. *Sci. Mar.* 60 (Supl. 1):125–28.

Beer S, Björk M, Beardall J (2014) Photosynthesis in the marine environment. Wiley-Blackwell, Iowa, USA, 208 pp.

Beer S, Israel A (1990) Photosynthesis of *Ulva fasciata*. IV. pH, carbonic anhydrase and inorganic carbon conversions in the unstirred layer. *Plant Cell Environ.* 13:555–60.

Beer T, Israel A, Helman Y, Kaplan A (2008) Acidification and CO_2 production in the boundary layer during photosynthesis in *Ulva rigida* (Chlorophyta) C. Agardh. *Israel J. Plant Sci.* 56:55–60.

Beilby MJ (1984) Current-voltage characteristics of the proton pump at *Chara* plasmalemma: I. pH dependence. *J. Membrane Biol.* 81:113–125.

Beman AM, Chow CE, King ALK, Fend Y, Fuhrmasn JA, Bates NR, Popp BN, Hutchins DA (2011) Global declines in oceanic nitrification rates as a consequence of ocean acidification. *Proc. Natnl. Acad. Scvi*. USA 108:208–213.

Bender D, Diaz-Pulido G, Dove S (2014) The impact of CO_2 emission scenarios and nutrient enrichment on a common coral reef macroalga is modified by temporal effects. *J. Phycol.* 50:203–215.

Bensoussan N, Gattuso JP (2007) Community primary production and calcification in a NW Mediterranean ecosystem dominated by calcareous macroalgae. *Mar. Ecol. Prog. Ser.* 334:37–45.

Berges JA (1997) Algal nitrate reductases. *Eur. J. Phycol.* 32:3–8.

Berman-Frank I, Zohary T (1994) CO_2 availability, carbonic anhydrase, and the annual dinoflagellate bloom in Lake Kinneret. *Limnol. Oceanogr*. 39(8):1822–1834.

Björk M, Haglund K, Ramazanov Z, García–Reina G, Pedersén M (1992) Inorganic–carbon assimilation in the green seaweed *Ulva rigida* C.Ag. (Chlorophyta). *Planta.* 187:152–156.

Björk M, Haglund K, Ramazanov Z, Pedersén M (1993) Inducible mechanisms for HCO_3^- utilization and repression of photorespiration in protoplasts and thalli of three species of *Ulva* (Chlorophyta). *J. Phycol.* 29:166–173.

Booth WA, Beardall J (1991) Effects of salinity on inorganic carbon utilization and carbonic anhydrase activity in the halotolerant alga *Dunaliella salina* (Chlorophyta). *Phycologia*. 30(2):220–225.

Bowes GW (1969) Carbonic anhydrase in marine algae. *Plant Physiol.* 44:726–732.

Boyd PW, Doney SC (2002) Modelling regional responses by marine pelagic ecosystems to global climate change. *Geophys. Res. Lett.* 29:1806–1810.

Boyd PW, Hutchins DA (2012). Understanding the responses of ocean biota to a complex matrix of cumulative anthropogenic change. *Mar. Ecol. Prog. Ser.* 470: 125–135.

Boyd PW, Law C (2011) An ocean climate change atlas for New Zealand waters. Niwa information series No 79 ISSN 1174–264X.

Brown MB, Edwards MS, Kim KY (2014) Effects of climate change on the physiology of giant kelp, *Macrocystis pyrifera*, and grazing by purple urchin, *Strongylocentrotus purpuratus*. *Algae* 29(3):203–215.

Brown MT, Nyman MA, Keogh JA, Chin NKM (1997) Seasonal growth of the giant kelp *Macrocystis pyrifera* in New Zealand. *Mar. Biol*. 129:417–424.

Butz RG, Jackson WA (1977) A mechanism for nitrate transport and reduction. *Phytochemistry* 16: 409–417.

Cai WJ, Hu X, Huang WJ, Murrell MC, Lehrter JC et al. (2011) Acidification of subsurface coastal waters enhanced by eutrophication. *Nat. Geosci*. 4:766–770.

Caldeira K, Wickett ME (2003) Anthropogenic carbon and ocean pH. *Nature* 425:365

Chapman ARO, Craigie JS (1977) Seasonal growth in *Laminaria longicruris*: relations with dissolved inorganic nutrients and internal reserves of nitrogen. *Mar. Biol.* 40:197–205.

Charpy–Roubaud C, Sournia A (1990) The comparative estimation of phytoplanktonic, microphytobenthic and macrophytobenthic primary production in the oceans. *Mar. Microb. Food Webs*. 4 (1):31–57.

Choo K, Snoeijs P, Pedersén M (2002) Uptake of inorhanic carbon by *Cladophora glomerata* (Chlorophyta) from the Baltic sea. *J. Phycol.* 38:493–502.

Chung IK, Beardall J, Mehta S, Sahoo D, Stojkovic S (2011) Using marine macroalgae for carbon sequestration: a critical appraisal. *J. Appl. Phycol.* 23:877–886.

Colombo–Pallotta MF, García–Mendoza E, Ladah L (2006) Photosynthetic performance, light absorption, and pigment composition of *Macrocystis pyrifera* (Laminariales, Phaeophyceae) blades from different depths. *J. Phycol*. 42:1225–1234.

Connell S, Russell B (2010) The direct effects of temperature and CO_2 on non–calcifying organisms: increasing the potential for phase shifts in kelp forests. *Proc. R. Soc. B.* 277:1409–1415.

Cook CM, Lanaras T, Colman B (1986) Evidence for bicarbonate transport in species of red and brown macrophytic marine algae. *J. Exp. Bot.* 37(180):977–984.

Cook CM, Lanaras T, Roubelakis-Angelakis KA (1988) Bicarbonate transport and alkalization of the medium by four species of Rhodophyta. *J. Exp. Bot.* 39(206):1185–1198.

Cornwall CE, Hepburn CD, McGraw CM, Currie KI, Pilditch CA, Hunter KA, Boyd PW, Hurd CL (2013) Diurnal fluctuations in seawater pH influence the response of a calcifying macroalga to ocean acidification. *Proc. R. Soc. B.* 280:20132201.

Cornwall CE, Revill AT, Hurd CL (2015) High prevalence of diffusive uptake of CO_2 by macroalgae in a temperate subtidal ecosystem. *Photosynth. Res.* DOI: 10.1007/s11120-015-0114-0.

Corzo A, Niell FX (1994) Nitrate–reductase activity and in vivo nitrate–reduction rate in *Ulva rigida* illuminated by blue light. *Mar. Biol.* 120:17–23.

Datta PK, Shepard TH (1959) Carbonic anhydrase: a spectrophotometric assay. *Arch. Biochem. Biophys.* 79:136–45.

Davison IR, Stewart WDP (1984) Studies on nitrate reductase activity in *Laminaria digitata* (Huds.) Lamour. II. The role of nitrate availability in the regulation of enzyme activity. *J. Exp. Mar. Biol. Ecol.* 79:65–78.

De Beer D, Larkum AWD (2001) Photosynthesis and calcification in the calcifying algae *Halimeda discoidea* studied with microsensors. *Plant Cell Environ*. 24:1209–1217.

Dean T, Jacobsen F (1984) Growth of juvenile *Macrocystis pyrifera* (Laminariales) in relation to environmental factors. *Mar. Biol.* 83:301–311.

Deane–Drummond CE (1984) Mechanism of nitrate uptake into *Chara corallina* cells: lack of evidence for obligatory coupling to proton pump and a new NO_3^-/NO_3^- exchange model. *Plant Cell Environ.* 7:317–323.

Delille B, Delille D, Fiala M, Prevost C, Frankignoulle M (2000) Seasonal changes of pCO_2 over a subantartic *Macrocystis* kelp bed. *Polar Biol.* 23:706–716.

Denny, MW (1993) Air and water. The biology and physics of life's media. By Princeton University Press, 341 pp.

Denny M, Wethey D (2001) Physical processes that generate patterns in marine communities. *In:* Marine Community Ecology. Bertness MD, Gaines SD, Hay ME [Eds.] Sinauer Associates, Sunderland, MA.

DeVoe H, Kistiakowsky GB (1961) The enzymic kinetics of carbonic anhydrase from bovine and human erythrocytes. *J. Am. Chem. Soc*. 83:274–280.

Dickson AG (1981) An exact definition of alkalinity, and a procedure for the estimation of alkalinity and total inorganic carbon from titration data. *Deep-Sea Res.* 28A:609–623.

Dickson AG, Sabine CL, Christian JR (2007) Guide to best practices for ocean CO_2 measurements. *PICES Special Publication*. 3:1–191.

Dodgson SJ, Tashian RE, Gros G, Carter ND (1991) The carbonic anhydrases: Cellular physiology and molecular genetics. Plenum, New York, 375 pp.

Drechsler Z, Beer S (1991) Utilization of inorganic carbon by *Ulva lactuca. Plant Physiol.* 97:1439–1444.

Drechsler Z, Sharkia R, Cabantchik ZI, Beer S (1993) Bicarbonate uptake in the marine macroalga *Ulva sp*. is inhibited by classical probes of anion exchange by red blood cells. *Planta*. 191:34–40.

Druehl LD (1984) Morphological and physiological responses of *Macrocystis pyrifera* to nitrate enrichment. *Hydrobiologia* 116/117:471–474.

Duarte, CM (1992) Nutrient concentration of aquatic plants: Patterns across species. *Limnol. Oceanogr*. 37(4): 882–889.

Edwards KF, Pfister CA, Van Alystyne KL (2006) Nitrogen content in the brown alga *Fucus gardneri* and its relation to light, herbivory and wave exposure. *J. Exp. Mar. Biol. Ecol.* 336:99–109

Eisele R, Ullrich WR (1975) Stoichiometry between photosynthetic nitrate reduction and alkalinisation by *Ankistrodesmus braunii*. *Planta* 123:117–124.

Eisele R, Ullrich WR (1977) Effect of glucose and CO_2 on nitrate uptake and coupled OH^- flux in *Ankistrodesmus braunii*. *Plant Physiol.* 59:18–21.

Enriquez S, Rodriguez–Roman A (2006) Effect of water flow on the photosynthesis of three marine macrophytes from a fringing reef lagoon. *Mar. Ecol. Prog. Ser*. 323:119–132.

Espen L, Nocito FF, Cocucci M (2004) Effect of NO_3^- transport and reduction on intracellular pH: an *in vivo* NMR study in maize root. *J. Exp. Bot*. 55(405):2053–2061.

Fabry VJ, Seibel BA, Feely RA, Orr JC (2008) Impacts of ocean acidification on marine fauna and ecosystem processes. *ICES J. Mar. Sci.* 65:414–432.

Fernández PA, Hurd CL, Roleda MY (2014) Bicarbonate uptake via an anion exchange is the main mechanism of inorganic carbon acquisition by the giant kelp *Macrocystis pyrifera* (Laminariales, Phaeophyceae) under variable pH. *J. Phycol.* 50(6):998–1008.

Fernández PA, Roleda MY, Hurd, CL (2015) Effects of ocean acidification on the photosynthetic performance, carbonic anhydrase activity and growth of the giant kelp *Macrocystis pyrifera*. *Photosynth. Res*. 124:293–304.

Figueroa FL, Viñegla B (2001) Effects of solar UV radiation on photosynthesis and enzyme activities (carbonic anhydrase and nitrate reductase) in marine macroalgae from southern Spain. *Rev. Chil. Hist. Nat*. 74:237–249.

Finelli CM, Helmuth BST, Dean Pencheff N, Wethey DS (2006) Water flow influences oxygen transport and photosynthetic efficiency in corals. *Coral Reefs* 25:47–57.

Flores-Moya A, Fernández JA (1998) Photosynthetic use of light and inorganic carbon in air and water by the intertidal alga *Petalonia fascia* (Scytosiphonales, Phaeophyta). *Phycol. Res.* 45:125–130.

Flores–Moya A, Gómez I, Viñegla B, Altamirano M, Pérez–Rodríguez E, Maestre C, Caballero RM, Figueroa F (1998) Effects of solar radiation on the endemic Mediterranean red alga *Rissoella verruculosa*: photosynthetic performance, pigment content and the activities of enzymes related to nutrient uptake. *New Phytol.* 139:673–683.

Foley MM, Koch PL (2010) Correlation between allochthonous subsidy input and isotopic variability in the giant kelp *Macrocystis pyrifera* in central California, USA. *Mar. Ecol. Prog. Ser*. 409:41−50.

Fram JP, Stewart HL, Brzezinski MA, Gaylord B, Reed DC, Williams SL, MacIntyre S (2008) Physical pathways and utilization of nitrate supply to the giant kelp, *Macrocystis pyrifera*. *Limnol. Oceanogr*. 53:1589–1603.

Fu LM, Zhao YH, Zhu YT (2012) Characterization of carbonic anhydrase II from *Chlorella vulgaris* in bio-CO_2 capture. *Environ. Sci. Pollut. Res.* 19(9):4227–3422.

Fuggi A, Di Martino Rigano V, Vona V, Rigano C (1981) Nitrate and ammonium assimilation in algal cell-suspensions and related pH variations in the external medium, monitored by electrodes. *Plant Sci. Lett.* 23:129–138.

Fujita RM (1985) The role of nitrogen status in regulation transient ammonium uptake and nitrogen storage by macroalgae. *J. Exp. Mar. Biol. Ecol*. 92:283–301.

Gaitán–Espitia JD, Hancock JR, Padilla–Gambiño JL, Rivest EB, Blanchette CA, Reed DC, Hofmann GE (2014) Interactive effects of elevated temperature and pCO_2 on early–life–history stages of the giant kelp *Macrocystis pyrifera*. *J. Exp. Mar. Biol. Ecol.* 457:51–58.

Gao K, Aruga Y, Asada K, Kiyohara M (1993) Influence of enhanced CO_2 on growth and photosynthesis of the red algae *Gracilaria* sp. and *G. chilensis*. *J. Appl. Phycol.* 5:563–571.

Garcia H, Gordon L (1992) Oxygen solubility in seawater: better fitting equations. *Limnol. Oceanogr.* 37:1307–1312.

García–Sanchez MJ, Fernández JA, Niell X (1994) Effect of inorganic carbon supply on the photosynthetic physiology of *Gracilaria tenuistipitata*. *Planta.* 194:55–61.

Gattuso JP, Gao K, Lee K, Rost B, Schulz KG (2010) Approaches and tools to manipulate the carbonate chemistry. *In* Riebesell U, Fabry VJ, Hansson L, Gattuso JP [Eds] *Guide to best practices for ocean acidification research and data reporting*. Luxembourg: Publications Office of the European Union, pp 41–51.

Gaylord B, Rossman JA, Reed DC (2007) Spatial patterns of flow and their modification within and around a giant kelp forest. *Limnol. Oceanogr*. 52:1838–1852

Geib K, Golldack D, Gimmler H (1996) Is there a requirement for an external carbonic anhydrase in the extremely acid–resistant green alga *Dunaliella acidophila? Eur. J. Phycol.* 31:273–284.

Geider RJ, Osborne BA (1992) Algal photosynthesis: the measurement of algal gas exchange. Chapman and Hall, New York, 256 pp.

Gerard V (1982a) Growth and utilization of internal nitrogen reserves by the giant kelp *Macrocystis pyrifera* in a low-nitrogen ambient. *Mar. Biol*. 66:27–35.

Gerard V (1982b) In situ rates of nitrate uptake by giant kelp, *Macrowstis pyrifera* (L.) C. Agardh: tissue differences, environmental effects, and predictions of nitrogen–limited growth. *J. Exp. Mar. Biol. Ecol.* 62:211–224.

Gerard V (1984) The light environment in a giant kelp forest: influence of *Macrocystis pyrifera* on spatial and temporal variability. *Mar. Biol.* 84:189–195.

Gerard VA (1986) Photosynthetic charactheristics of giant kelp (*Macrocystis pyrifera*) determined in situ. *Mar. Biol.* 90:473–482.

Giordano M, Beardall J, Raven JA (2005) CO_2 concentrating mechanisms in algae: mechanisms, environmental modulation, and evolution. *Annu. Rev. Plant Biol.* 56:99–131.

Giordano M, Maberly SC (1989) Distribution of carbonic anhydrase in British marine macroalgae. *Oecologia* 81:534–539.

Gómez I, Huovinen P (2010) Induction of phlorotannins during UV exposure mitigates inhibition of photosynthesis and DNA damage in the kelp *Lessonia nigrescens. Photochem. Photobiol*. 86:1056–1063.

Gómez I, Pérez–Rodríguez E, Viñegla B, Figueroa FL, Karsten U (1998) Effects of solar radiation on photosynthesis, UV-absorbing compounds and enzyme activities of the green alga *Dasycladus vermicularis* from southern Spain. *J. Photochem. Photobiol. B: Biol.* 47:46–57.

Gordillo FJ, Aguilera J, Jiménez C (2006) The response of nutrient assimilation and biochemical composition of Arctic seaweeds to a nutrient input in summer. *J. Exp. Bot.* 57:2661–2671.

Gordillo FJ, Niell FX, Figueroa FL (2001) Non–photosynthetic enhancement of growth by high CO_2 level in the nitrophilic seaweed *Ulva rigida* C. Agardh (Chlorophyta). *Planta* 213: 64–70.

Graham D, Atkins CA, Reed ML, Patterson BD, Smillie RM (1971) Carbonic anhydrase, photosynthesis and light-induced pH changes. *In* Hatch MD, Osmond CB, Slatyer RO [Eds.] *Photosynthesis and Photorespiration*. John Wiley and Sons, Inc., New York, 267–274 pp.

Graham D, Reed ML, Patterson BD, Hockley DG (1984) Chemical properties, distribution, and physiology of plant and algal carbonic anhydrases. *Ann. N.Y. Acad. Sci.* 429:222–237.

Graham D, Smillie RM (1976) Carbonate dehydratase in marine organisms of the Great Barrier Reef. *Aust. J. Plant Physiol*. 3:113–119.

Graham M, Vásquez J, Buschmann A (2007) Global ecology of the giant kelp *Macrocystis*: from ecotypes to ecosystems. *Oceanogr. Mar. Biol. Annu. Rev.* 45:39–88.

Granbom M, Pedersén M (1999) Carbon acquisition strategies of the red alga *Eucheuma denticulatum*. *Hydrobiologia*. 398/399:349–534.

Gravot A, Dittami SM, Rousvoal S, Lugan R, Eggert A, Colle J, Boyen C, Bouchereau A, Tonon T (2010) Diurnal oscillations of metabolite abundances and gene analysis provide new insights into central metabolic processes of the brown alga *Ectocarpus siliculosus*. *New Phytol.* 188:98–110.

Guinotte JM, Fabry VJ (2008) Ocean acidification and its potential effects on marine ecosystems. *Ann. NY Acad. Sci*. 1134: 320–342.

Gutow L, Rahman MM, Bartl K, Saborowski R, Bartsch I, Wiencke C (2014) Ocean acidification affects growth, but not nutritional quality of the seaweed *Fucus vesiculosus* (Phaeophyceae, Fucales). *J. Exp. Mar. Biol. Ecol*. 453:84–90.

Haglund K, Björk M, Ramazanov Z, Gárcia-Reina G, Pedersén M (1992a) Role of carbonic anhydrase in photosynthesis and inorganic–carbon assimilation in the red alga *Gracilaria tenuistipitata*. *Planta*. 187:275–281.

Haglund K, Pedersén M (1992) Growth of the red alga *Gracilaria tenuistipitata* at high pH. Influence of some environmental factors and correlation to an increased carbonic-anhydrase activity. *Bot. Mar*. 35:579–587.

Haglund K, Ramazanov Z, Mtolera M,. Pedersén M (1992b) Role of external carbonic anhydrase in light–dependent alkalization by *Fucus serratus* L. and *Laminaria saccharina* (L.) Lamour. (Phaeophyta). *Planta*. 188:1–6.

Haines KC, Wheeler PA (1978) Ammonium and nitrate uptake by the marine macrophytes *Hypnea musciformis* (Rhodophyta) and *Macrocystis pyrifera* (Phaeophyta). *J. Phycol.* 14:319–324.

Hansen AT, Hondzo M, Hurd CL (2011) Photosynthetic oxygen flux by *Macrocystis pyrifera*: a mass transfer model with experimental validation. *Mar. Ecol. Prog. Ser.* 434:45–55.

Harley CDG, Anderson KM, Demes KW, Jorve JP, Kordas RL, Coyle TA et al. (2012) Effects of climate change on global seaweed communities. *J. Phycol.* 48:1064–1078.

Harley CDG, Randall Hughes A, Hultgren KM,Miner BG, Sorte CJB et al. (2006) The impacts of climate change in coastal marine systems. *Ecol. Lett.* 9: 228–241.

Harrison PJ, Hurd CL (2001) Nutrient physiology of seaweeds: application of concepts to aquaculture. *Cah. Biol. Mar.* 42:71–82.

Hatch MD (1991) Carbonic anhydrase assay: Strong inhibition of the leaf enzyme by CO_2 in certain buffers. *Anal. Biochem.* 191:85–89.

Hay CH (1990) The distribution of *Macrocystis* (Phaeophyta, Laminariales) as a biological indicator of cool sea surface temperature, with special reference to New Zealand waters. *J. R. Soc. NZ*. 20:313–336.

Hellblom F, Beer S, Björk M, Axelsson L (2001) A buffer sensitive inorganic carbon utilization system in *Zostera marina*. *Aquat. Bot.* 69:55–62.

Hepburn CD, Frew RD, Hurd CL (2012) Uptake and transport of nitrogen derived from sessile epifauna in the giant kelp *Macrocystis pyrifera*. *Aquat. Biol.* 14:121–128.

Hepburn CD, Holborow JD, Wing SR, Frew RD, Hurd CL (2007) Exposure to waves enhances the growth rate and nitrogen status of the giant kelp *Macrocystis pyrifera*. *Mar. Ecol. Prog. Ser.* 339:99–108.

Hepburn CD, Hurd CL (2005) Conditional mutualism between the giant kelp *Macrocystis pyrifera* and colonial epifauna. *Mar. Ecol. Prog. Ser.* 302:37–48.

Hepburn CD, Hurd CL, Frew RD (2006) Colony structure and seasonal differences in light and nitrogen modify the impact of sessile epifauna on the giant kelp *Macrocystis pyrifera* (L.) C Agardh. *Hydrobiologia* 560:373–338.

Hepburn CD, Pritchard DW, Cornwall CE, McLeod RJ, Beardall J, Raven JA, Hurd CL (2011) Diversity of carbon use strategies in a kelp forest community: implica–tions for a high CO_2 ocean. *Glob. Change Biol.* 17:2488–2497.

Hernández-Carmona G, Robledo D, Serviere-Zaragoza E (2001) Effect of nutrient availability on *Macrocystis pyrifera* recruitment and survival near its southern limit off Baja California. *Bot. Mar.* 44 : 221–229.

Herfort L, Thake B, Roberts J (2002) Acquisition and use of bicarbonate by *Emiliania huxleyi*. *New Phytol.* 156:427–436.

van Hille RP (2001) Biological generation of reactive alkaline species and their application in a sustainable bioprocess for the remediation of acid metal contaminated wastewaters. Ph.D. Dissertation, Rhodes University, South Africa.

van Hille R, Fagan M, Bromfield L, Pott R (2014) A modified pH drift assay for inorganic carbon accumulation and external carbonic anhydrase activity in microalgae. *J. Appl. Phycol*. 26:377–385.

Hofmann GE, Smith JE, Johnson KS, Send U, Levin LA, et al. (2011) High-frequency dynamics of ocean pH: a multi-ecosystem comparison. *PLoS ONE* 6:e28983.

Hofmann LC, Straub S, Bischof K (2013) Elevated CO_2 levels affect the activity of nitrate reductase and carbonic anhydrase in the calcifying rhodophyte *Corallina officinalis. J. Exp. Bot.* 64(4):899–908.

Hofmann LC, Yildiz G, Hanelt D, Bischof K (2012) Physiological responses of the calcifying rhodophyte, *Corallina officinalis* (L.), to future CO_2 levels. *Mar. Biol.* 159:783–792.

Hofslagare O, Samuelson G, Sjöberg S, Ingri N (1983) A precise potentiometric method for determination of algal activity in an open CO_2 system. *Plant Cell Environ*. 6:195–201.

Hogetsu D, Miyachi S (1976) Role of carbonic anhydrase in photosynthetic CO_2 fixation in *Chlorella*. *Plant Cell Physiol*. 20(4):747–756.

Holt J, Schrum C, Cannaby H, Daewel H, Allen I et al. (2014) Physical processes mediating climate change impacts on regional sea ecosystems. *Biogeosciences Discuss.* 11:1909–1975.

Holt J, Wakelin S, Lowe J, Tinker J (2010) The potential impacts of climate change on the hydrography of the northwest European Continental shelf. *Prog. Oceanogr.* 86:361–379.

Hunter KA (2007) $SWCO_2$. Available at: http://neon.otago.ac.nz/research/mfc/people/keith_hunter/software/swco2 (accessed 5 October 2011).

Huovinen P, Gómez I, Orostegui M (2007) Patterns and UV sensitivity of carbon anhydrase and nitrate reductase activities in south Pacific macroalgae. *Mar. Biol.* 151:1813–1821.

Huovinen P, Leal P, Gómez I (2010) Interacting effects of copper, nitrogen and ultraviolet radiation on the physiology of three south Pacific kelps. *Mar. Freshwater Res*. 61:330–341.

Hurd, CH (2000) Water motion, marine macroalgal physiology, and production. *J. Phycol.* 36:453–472.

Hurd CL, Berges JA, Osborne J, Harrison PJ (1995) An in vitro nitrate reductase assay for marine macroalgae: optimization and characterization of the enzyme for *Fucus gardneri* (Phaeophyta). *J. Phycol*. 31:835–843.

Hurd CL, Cornwall CE, Currie K, Hepburn CD , McGraw CM, Hunter KA, Boyd PW (2011) Metabolically induced pH fluctuations by some coastal calcifiers exceed projected 22nd century ocean acidification: a mechanism for differential susceptibility? *Glob. Change Biol*. 17 (10):3254–3262.

Hurd CL, Durante KM, Harrison JP (2000) Influence of bryozoan colonization on the physiology of the kelp *Macrocystis integrifolia* (Laminariales, Phaeophyta) from nitrogen-rich and -poor sites in Barkley Sound, British Columbia, Canada. *Phycologia* 39(5):435–440.

Hurd CL, Harrison PJ, Dreuhl LD (1996) Effect of sea water velocity on inorganic nitrogen uptake by morphologically distinct forms of *Macrocystis integrifolia* from wave-sheltered and exposed sites. *Mar. Biol*. 126:205–214.

Hurd CL, Harrison PJ, Bischof K, Lobban CS (2014) Seaweed Ecology and Physiology. Cambridge University Press, Cambridge, United Kingdom, 551 pp.

Hurd CL, Hepburn CD, Currie KI, Raven JA, Hunter KA (2009) Testing the effects of ocean acidification on algal metabolism: considerations for experimental designs. *J. Phycol.* 45:1236–1251.

Hurd CL, Pilditch CA (2011) Flow induced morphological variations affect boundary–layer thickness of *Macrocystis pyrifera* (Heterokontophyta, Laminariales). *J. Phycol*. 47:341–351.

Hwang SPL, Williams SL, Brinkhuis BH (1987) Changes in internal dissolved nitrogen pools as related to nitrate uptake and assimilation in *Gracilaria tikvahiae* McLacklan (Rhodophyta). *Bot. Mar*. 30:11–19.

Ihnken S, Roberts S, Beardall J (2011) Differential responses of growth and photosynthesis in the marine diatom *Chaetoceros muelleri* to CO_2 and light availability. *Phycologia* 50:182–193.

Ikemori M, Nishida K, (1968) Carbonic anhydrase in the marine alga *Ulva pertusa*. *Physiol. Plant.* 21:292–297.

Inokuchi R, Okada M (2001) Physiological adaptations of glutamate dehydrogenase isozyme activities and other nitrogen-assimilating enzymes in the macroalga *Bryopsis maxima*. *Plant Sci*. 161:35–43.

IPCC (2013) Climate Change 2013: The Physical Science Basis. Contribution of Working Group I to the Fifth Assessment Report (AR5) of the Intergovernmental Panel on Climate Change. *In* Stocker TF, Qin D, Plattner GK, Tignor M, Allen SK, Boschung J, Nauels A, Xia Y, Bex V, Midgley PM [Eds.]. Cambridge University Press, Cambridge, UK/New York, NY, USA, 1535 pp.

Israel A, Beer S (1992) Photosynthetic carbon acquisition in the red alga *Gracilaria conferta* II. Rubisco carboxylase kinetics, carbonic anhydrase and HCO_3^- uptake. *Mar. Biol.* 112:697–700.

Israel AA, Friedlander M (1998) Inorganic carbon utilization and growth abilities in the marine red macroalga *Gelidiopsis* sp. *Israel J. Plant Sci.*46:117–124.

Israel A, Hophy M (2002) Growth, photosynthetic properties and Rubisco activities and amounts of marine macroalgae grown under current and elevated seawater CO_2 concentrations. *Glob. Change Biol.* 8:831–840.

Israel A, Katz S, Dubinsky Z, Merrill JE, Friedlander M (1999) Photosynthetic inorganic carbon utilization and growth of *Porphyra linearis* (Rhodophyta). *J. Appl. Phycol.* 11:447–453.

Jackson G (1977) Nutrients and production of giant kelp, *Macrocystis pyrifera*, off southern California. *Limnol. Oceanogr.* 22:979–995.

Johnson CR, Banks SC, Barrett NS, Cazassus F, Dunstan PK et al. (2011) Climate change cascades: shifts in oceanography, species' ranges and subtidal marine community dynamics in eastern Tasmania. *J. Exp. Mar. Biol. Ecol.* 400:17–32.

Johnston AM, Raven JA (1990) Effects of culture in high CO_2 on the photosynthetic physiology of *Fucus serratus*. *Br. Phycol. J.* 25:75–82.

Jokiel PL (2011) Ocean acidification and control of reef coral calcification by boundary layer limitation of proton flux. *Bull. Mar. Sc.* 87(3):639–657.

Jokiel PL, Rodgers KS, Kuffner IB, Andersson AJ, Cox EF, Mackenzie FT (2008) Ocean acidification and calcifying reef organisms: a mesocosm investigation. *Coral Reefs* 27:473–483.

Kain JM (1989) The seasons in the subtidal. *Br. Phycol. J.* 24:203–215.

Kawamitsu Y, Boyer JS (1999) Photosynthesis and carbon storage between tides in a brown alga, *Fucus vesiculosus*. *Mar. Biol.* 133:361–369.

Kernohan JC (1965) The pH-activity curve of bovine carbonic anhydrase and its relationship to the inhibition of the enzyme by anions. *Biochim. Biophys. Acta* 96:304–317.

Kevekordes K, Holland D, Häubner N, Jenkins S, Koss R, Roberts S, Raven JA, Scrimgeour K, Shelly K, Stojkovic S, Beardall J (2006) Inorganic carbon acquisition by eight species of *Caulerpa* (Caulerpaceae, Chlorophyta). *Phycologia* 45(4):442–449.

Klenell M, Snoeijs P, Pedersén M (2004) Active carbon uptake in *Laminaria digitata* and *L. saccharina* (Phaeophyta) is driven by a proton pump in the plasma membrane. *Hydrobiologia* 514:41–53.

Koch, EW (1994) Hydrodynamics, diffusion boundary layers and photosynthesis of the seagrasses *Thalassia testudinum* and *Cymodocea nodosa*. *Mar. Biol.* 118:767–776.

Koch M, Bowes G, Ross C, Zhang XH (2013) Climate change and ocean acidification effects on seagrasses and marine macroalgae. *Glob. Change Biol.* 19(1):103–132.

Koch EW, Ackerman JD, Verduin J, Keulen M (2006) Fluid dynamics in seagrass ecology—from molecules to ecosystems. *In:* Larkum AWD et al. [Eds.] *Seagrasses: Biology, Ecology and Conservation*, Springer, Netherlands, 193–225.

Konotchik T, Dupont CL, Valas RE, Badger JH, Allen AE (2013) Transcriptomic analysis of metabolic function in the giant kelp, *Macrocystis pyrifera*, across depth and season. *New Phytol.* 198:398–407.

Kopczak CD (1994) Variability of nitrate uptake capacity in *Macrocystis pyrifera* (Laminariales, Phaeophyta) with nitrate and light availability. *J. Phycol*. 30:573–580.

Kopczak CD, Zimmerman RC, Kremer JN (1991) Variation in nitrogen physiology and growth among geographically isolated populations of the giant kelp, *Macrocystis pyrifera* (Phaeophyta). *J. Phycol.* 27:149–158.

Kraemer GP, Chapman DJ (1991) Effects of tensile force and nutrient availability on carbon uptake and cell wall synthesis in blades of juvenile *Egregia menziesii* (Turn.) Aresch. (Phaeophyta). *J. Exp. Mar. Biol. Ecol.* 149:267–277.

Krebs HA, Roughton FJW (1948) Carbonic anhydrase as a tool in studying the mechanisms of reactions involving H_2CO_3, CO_2 or HCO_3^-. *Biochem. J.* 43:550–555.

Kroeker KJ, Kordas RL, Crim R, Hendriks IE, Ramajo L, Singh GS, Duarte CM, Gattuso JP (2013) Impacts of ocean acidification on marine organisms: quantifying sensitivities and interaction with warming. *Glob. Change Biol*. 19:1884–1896.

Kübler JE, Johnston AM, Raven JA (1999) The effects of reduced and elevated CO_2 and O2 on the seaweed *Lomentaria articulata*. *Plant Cell Environ.* 22:1303–1310.

Larkum AWD, Koch EMW, Kühl M (2003) Diffusive boundary layers and photosynthesis of the epiphytic algal community of coral reefs. *Mar. Biol*. 142:1073–1082.

Larned ST, Atkinson MJ (1997) Effects of water velocity on NH_4^+ and PO_4 uptake and nutrient–limited growth in the macroalga *Dictyosphaeria cavernosa*. *Mar. Ecol. Prog. Ser*. 157:297–302.

Larsson C, Axelsson L (1999) Bicarbonate uptake and utilization in marine macroalgae. *Eur. J. Phycol.* 34:79–86.

Larsson C, Axelsson L, Ryberg H, Beer S (1997) Photosynthetic carbon utilization by *Enteromorpha intestinalis* (Chlorophyta) from a Swedish rockpool. *Eur. J. Phycol.* 32:39–54.

Lartigue J, Sherman TD (2005) Response of *Enteromorpha sp*. (Chlorophyceae) to a nitrate pulse: nitrate uptake, inorganic nitrogen storage, and nitrate reductase activity. *Mar. Ecol. Prog. Ser.* 292:147–157.

Leal PP, Hurd CL, Roleda MY (2014) Meiospores produced in sori of nonsporophyllous laminae of *Macrocystis pyrifera* (Laminariales, Phaeophyceae) may enhance reproductive output. *J. Phycol*. 50:400–405.

Lesser MP, Weis VM, Patterson MR, Jokiel PL (1994) Effects of morphology and water motion on carbon delivery and productivity in the reef coral, *Pocillopora damicornis* (Linnaeus): Diffusion barriers, inorganic carbon limitation, and biochemical plasticity. *J. Exp. Mar. Biol. Ecol*. 178:153–179.

Lignell Å, Pedersén M (1989) Effects of pH and inorganic carbon concentration on growth of *Gracilaria secundata. Br. Phycol. J.* 24:83–89.

Lin A, Wang G, Zhou W (2013) Simultaneous measurements of H^+ and O_2 fluxes in *Zostera marina* and its physiological implications. *Physiol. Plant.* 148:582–589.

Lindskog S (1997) Structure and mechanism of carbonic anhydrase. *Pharmacol. Ther.* 74(1):1–20.

Lobban CS, Harrison PJ (1997) Seaweed ecology and physiology. Cambridge University Press, Cambridge, 384 pp.

Longphuirt SN, Eschmann C, Russell C, Stengel DB (2013) Seasonal and species–specific response of five brown macroalgae to high atmospheric CO_2. *Mar. Ecol. Prog. Ser*. 493:91–102.

Lucas WJ (1983) Photosynthetic assimilation of exogenous HCO_3^- by aquatic plants. *Ann. Rev. Plant Physiol.* 34:71–104.

Maberly SC (1990) Exogenous sources of inorganic carbon for photosynthesis by marine macroalgae. *J. Phycol.* 26(3):439–449.

Madsen TV, Enevoldsen HO, Jørgensen TB (1993) Effects of water velocity on photosynthesis and dark respiration in submerged stream macrophytes. *Plant Cell Environ.* 16: 317–322.

Madsen TV, Maberly SC (2003) High internal resistance to CO_2 uptake by submerged macrophytes that use HCO_3^-: measurements in air, nitrogen and helium. *Photosynth. Res.* 77:183–190.

Magnusson G, Larsson C, Axelsson L (1996) Effects of high CO_2 treatment on nitrate and ammonium uptake by *Ulva lactuca* grown in different nutrient regimes. *Sci. Mar*. 60:179–189.

Maren TH (1967) Carbonic anhydrase: Chemistry, physiology, and inhibition. *Physiol. Rev.* 47(4):595–791.

Mass T, Genin A, Shavit U, Grinstein M, Tchernov D (2010) Flow enhances photosynthesis in marine benthic autotrophs by increasing the efflux of oxygen from the organism to the water. *PNAS* 107 (6):2527–2531.

Matsuda Y, Kroth PG (2014) Carbon fixation in diatoms. *In* Hohmann-Marriott MF [Ed.] The structural basis of biological energy generation, *Advances in Photosynthesis and Respiration*, Springer Dordrecht Heidelberg London, New York, 335–362 pp.

Matt P, Geiger M, Walch-Liu P, Engels C, Krapp A, Sttit M (2001) Elevated carbon dioxide increases nitrate uptake and nitrate reductase activity when tobacco is growing on nitrate, but increases ammonium uptake and inhibits nitrate reductase activity when tobacco is growing on ammonium nitrate. *Plant Cell Environ*. 24:1119–1137.

McClintock M., Higinbotham N, Uribe EG and Cleland RE (1982) Active irreversible accumulation of extreme levels of H_2SO_4 in the brown alga, *Desmarestia*. *Plant Physiol.* 70:771–774.

McGlathery KJ (1992) Physiological controls of *Spyridea hypnoides* distribution: patterns along an eutrophication gradient in Bermuda. *Mar. Ecol. Prog. Ser*. 87:173–182.

McGlathery KJ, Pedersen MF (1999) The effect of growth irradiance on the coupling of carbon and nitrogen metabolism in *Chaetomorpha linum* (Chlorophyta). *J. Phycol*. 35:721–731.

McGlathery KJ, Pedersen MF, Borum J (1996) Changes in intracellular nitrogen pools and feedback controls on nitrogen uptake in *Chaetomorpha linum* (Chlorophyta). *J. Phycol.* 32:393–401.

McGraw CM, Cornwall CE, Reid MR, Currie KI, Hepburn CD, Hurd CL, Hunter KA (2010) An automated pH–controlled culture system for laboratory–based ocean acidification experiments. *Limnol. Oceanogr. Methods*. 8:686–694.

Mercado JM, Andria JR, Pérez–Llorens JL, Vergara JJ, Axelsson L (2006) Evidence for a plasmalemma–based CO_2 concentrating mechanism in *Laminaria saccharina*. *Photosynth. Res.* 88:259–268.

Mercado JM, Avilés A, Benítez E, Carrasco MPL, Clavero V, Niell FX (2003) Photosynthetic production of *Ulva rotundata* bliding estimated by oxygen and inorganic carbon exchange measurements in the field. *Bot. Mar.* 43:342–349.

Mercado JM, Carmona R, Niell FX (2000) Affinity for inorganic carbon of *Gracilaria tenuistipitata* cultured at low and high irradiance. *Planta* 210:758–764.

Mercado JM, Figueroa FL, Niell FX, Axelsson L (1997a) A new method for estimating external carbonic anhydrase activity in macroalgae. *J. Phycol.* 33:999–1006.

Mercado JM, Javier F, Gordillo L, Niell FX, Figueroa FL (1999) Effects of different levels of CO_2 on photosynthesis and cell components of the red alga *Porphyra leucosticta*. *J. Apply. Phycol*. 11:455–461.

Mercado JM, Gordillo FJL, Figueroa FL, Niell FX (1998) External carbonic anhydrase and affinity for inorganic carbon in intertidal macroalgae. *J. Exp. Mar. Biol. Ecol.* 221: 209–220.

Mercado JM, Niell FX (1999) Carbonic anhydrase activity and use of HCO_3^- in *Bostrychia scorpioides* (Ceramiales, Rhodophyceae). *Eur. J. Phycol.* 34:13–19.

Mercado JM, Niell FX, Figueroa FL (1997b) Regulation of the mechanism for HCO_3^- use by the inorganic carbon level in *Porphyra leucosticta* Thur. in Le Jolis (Rhodophyta). *Planta* 201:319–325.

Mercado JM, Niell FX, Gil-Rodríguez MC (2001) Photosynthesis might be limited by light, not inorganic carbon availability, in three intertidal Gelidiales species. *New Phytol*. 149:431–439.

Mercado JM, Sanchez P, Carmona R, Niell X (2002) Limited acclimation of photosynthesis to blue light in the seaweed *Gracilaria tenuistipitata*. *Physiol. Plantarum*. 114:491–498.

Mercado JM, de los Santos CB, Pérez–Lloréns JL, Vergara JJ (2009) Carbon isotopic fractionation in macroalgae from Cádiz Bay (Southern Spain): Comparison with other bio-geographic regions. *Estuar. Coast. Shelf S* 85:449–458.

Mercado JM, Viñegla B, Figueroa FL, Niell FX (1999) Isoenzymic forms of carbonic anhydrase in the red macroalga *Porphyra leucosticta*. *Physiol. Plant.* 106:69–74.

Middelboe A, Hansen P (2007a) Direct effects of pH and inorganic carbon on macroalgal photosynthesis and growth. *Mar. Biol. Res.* 3:134–144.

Middelboe AL, Hansen PJ (2007b) High pH in shallow-water macroalgal habitats. *Mar. Ecol. Prog. Ser.* 338: 107–117.

Miller AG, Colman B (1980) Evidence for HCO_3^- transport by the blue-green alga (Cyanobacterium) *Coccochloris peniocystis. Plant Physiol.* 65:397–402.

Millero F, Poisson A (1981) International one–atmosphere equation of state of seawater. *Deep–Sea Res*. 28A:625–629.

Miyachi S, Tsuzuki M, Avramova ST (1983) Utilization modes of inorganic carbon for photosynthesis in various species of *Chlorella*. *Plant Cell Physiol*. 24:441–451.

Moroney JV, Bartlett SG, Samuelsson G (2001) Carbonic anhydrases in plants and algae. *Plant Cell Environ*. 24:141–153.

Moroney JV, Husic HD, Tolbert NE (1985) Effect of carbonic anhydrase inhibitors on inorganic carbon accumulation by *Chlamydomonas reinhardtii*. *Plant Physiol.* 79:177–183.

Moulin P, Andria JR, Axelsson L, Mercado JM (2011) Different mechanisms of inorganic carbon acquisition in red macroalgae (Rhodophyta) revealed by the use of TRIS buffer. *Aquat. Bot*. 95:31–38.

Needoba JA, Waser NA, Harrison PJ, Calvert SE (2003) Nitrogen isotope fractionation in 12 species of marine phytoplankton during growth on nitrate. *Mar. Ecol. Prog. Ser.* 255:81–91.

Naldi M, Wheeler PA (1999) Changes in nitrogen pools in *Ulva fenestrata* (Chlorophyta) and *Gracilaria pacifica* (Rhodophyta) under nitrate and ammonium enrichment. *J. Phycol.* 35:70–77.

Nelson EB, Cenedella A, Tolbert NE (1969) Carbonic anhydrase levels in *Chlamydomonas*. *Phytochemistry.* 8:2305–2306.

North W (1971) The biology of giant kelp beds (*Macrocystis*) in California. *Nova Hedwigia* 32, 600 pp.

Ochoa–Izaguirre MJ, Soto–Jimenez MF (2015) Variability in nitrogen stable isotope ratios of macroalgae: consequences for the identification of nitrogen sources. *J. Phycol*. 51:46–65.

Okazaki M (1972) Carbonic Anhydrase in the calcareous red alga, *Serraticardia maxima. Bot. Mar.* XV:133–138.

Olischläger M, Wiencke C (2013) Ocean acidification alleviates low-temperature effects on growth and photosynthesis of the red alga *Neosiphonia harveyi* (Rhodophyta). *J. Exp. Bot.* 64(18):5587–5597.

Ostrom NE, Macko SA, Deibel D, Thompson RJ (1997) Seasonal variation in the stable carbon and nitrogen isotope biogeochemistry of a coastal cold ocean environment. *Geochim Cosmochim Acta* 61:2929–2942.

Pedersen MF (1994) Transient ammonium uptake in the macroalga *Ulva lactuca* (Chlorophyta): nature, regulation, and the consequences for choice of measuring technique. *J. Phycol*. 30:980–986.

Peréz-Lloréns JL, Brun FG, Andría J, Vergara JJ (2004) Seasonal and tidal variability of environmental carbon related physico–chemical variables and inorganic C acquisition in *Gracilariopsis longissima* and *Enteromorpha intestinalis* from Los Torunos salt marsh (Cádiz Bay, Spain). *J. Exp. Mar. Biol. Ecol*. 304:183–201.

Phillips JC, Hurd CL (2003) Nitrogen ecophysiology of intertidal seaweeds from New Zealand: N uptake, storage and utilisation in relation to shore position and season. *Mar. Ecol. Prog. Ser*. 264:31–48.

Price GD, Badger MR, Woodger FJ, Long BM (2008) Advances in understanding the cyanobacterial CO_2–concentrating–mechanism (CCM): functional components, Ci transporters, diversity, genetic regulation and prospects for engineering into plants. *J. Exp. Bot.* 59:1441–1461.

Pritchard D, Hurd C, Beardall J, Hepburn C (2015) Restricted use of nitrate and a strong preference for ammonium reflects the nitrogen ecophysiology of a light-limited red alga. *J. Phycol.* 51(2):277–87.

Ramazanov M, Semenenko VE (1988) Content of the CO_2–dependent form of carbonic anhydrase as a function of light intensity and photosynthesis. *Sov. Plant Physiol.* 35:340–344.

Rautenberger R, Fernández PA, Strittmatter M, Heesch S, Cornwall CE, Hurd CL, Roleda MY (2015) Saturating light and not increased carbon dioxide under ocean acidification drives photosynthesis and growth in *Ulva rigida* (Chlorophyta). *Ecol. Evol*. 5(4):874–888.

Raven JA (1980) Nutritional Strategies of submerged benthic plants: the acquisition of C, N and P by Rhizophytes and Haptophytes. *New Phytol*. 88:1–30.

Raven JA (1984) Energetics and Transport in Aquatic Plants. A R Liss, New York.

Raven JA (1986) Biochemical Disposal of Excess H^+ in Growing Plants? *New Phytol.* 104:175–206.

Raven JA (1991) Physiology of inorganic C acquisition and implications for resource use efficiency by marine phytoplankton: relation to increased CO_2 and temperature. *Plant Cell Environ*. 14:779–794.

Raven JA (1995) Photosynthetic and non–photosynthetic roles of carbonic anhydrase in algae and cyanobacteria. *Phycologia* 34(2):93–101.

Raven JA (1997) Inorganic carbon acquisition by marine autotrophs. *Adv. Bot. Res.* 27:85–209.

Raven JA (2011) Effects on marine algae of changed seawater chemistry with increasing atmospheric CO_2. *Biol. Environ.* 111B:1–17.

Raven JA (2013) Half a century of pursuing the pervasive proton. Lüttge U et al. [Eds.], *Progress in Botany*. Progress in Botany 74, Springer-Verlag Berlin Heidelberg, 3–34 pp.

Raven JA, Beardall J (2014) CO_2 concentrating mechanisms and environmental change. *Aquatic Bot.* 118:24–37.

Raven JA, Cockell CS, La Rocha CL (2008) The evolution of inorganic carbon concentrating mechanisms in photosynthesis. *Phil. Trans. R. Soc. B* 363:2641–2650.

Raven JA, De Michelis MI (1979) Acid-base regulation during nitrate assimilation in *Hydrodictyon africanum. Plant Cell Environ*. 2:245–257.

Raven JA, De Michelis MI (1980) Acid-base regulation during ammonium assimilation in *Hydrodictyon africanum*. *Plant Cell Environ*. 3:299–231.

Raven JA, Giordano M (2015) Combined nitrogen. *In* Borowitzka MA, Beardall J, Raven JA [Eds.], Heidelberg, Germany.

Raven JA, Giordano M and Beardall J (2008) Insights into the evolution of CCMs from comparisons with other resource acquisition and assimilation processes. *Physiol. Plant.* 133:4–14.

Raven JA, Giordano M, Beardall J, Maberly SC (2011) Algal and aquatic plant carbon concentrating mechanisms in relation to environmental change. *Photosynth. Res.* 109:281–296.

Raven JA, Giordano M, Beardall J, Maberly SC (2012) Algal evolution in relation to atmospheric CO_2: carboxylases, carbon–concentrating mechanisms and carbon oxidation cycles. *Phil. Trans. R. Soc. B* 367:493–507. DOI:10.1098/rstb.2011.0212.

Raven JA, Hurd CL (2012) Ecophysiology of photosynthesis in macroalgae. *Photosynth. Res*. 113:105–125.

Raven JA, Jayasuriya HD (1977) Active nitrate assimilation and hydroxyl ion efflux by *Hydrodictyon africanum*. In Thellier M, Monier A, Demarty M, Dainty J [Eds.] *Transmembrane Ionic Exchanges in Plants*. pCNRS Paris/University of Rouen Publications, 299–305 pp.

Raven JA, Johnston AM (1991) Mechanisms of inorganic-carbon acquisition in marine phytoplankton and their implications for the use of other resources. *Limnol. Oceanogr*. 36(8):1701–1714.

Raven JA, Johnston AM, Kübler JE, Korb R, McInroy SG et al. (2002) Mechanistic interpretation of carbon isotope discrimination by marine macroalgae and seagrasses. *Funct. Plant Biol.* 29:355–378.

Raven JA, Smith FA (1974) Significance of hydrogen ion transport in plant cells. *Can. J. Bot*. 52:1035–1048.

Raven JA, Smith FA (1976) Nitrogen assimilation and transport in vascular land plants in relation to intracellular pH regulation. *New Phytol*. 76:415–431.

Rees TAV, Dobson BC, Bijl M, Morelissen B (2007) Kinetics of nitrate uptake by New Zealand marine macroalgae and evidence for two nitrate transporters in *Ulva intestinalis* L. *Hydrobiologia* 586:135–141.

Rees TAV, Grant CM, Harmens HE, Taylor RB (1998) Measuring rates of ammonium assimilation in marine algae; use of the protonophore carbonyl cyanide *m*-chlorophenylhydrazone to distinguish between uptake and assimilation. *J. Phycol.* 34:264–72.

Reiskind JB, Seamon PT, Bowes G (1988) Alternative methods of photosynthetic carbon assimilation in marine macroalgae. *Plant Physiol.* 87:686–692.

Ren X, Lindskog S (1992) Buffer dependence of CO_2 hydration catalyzed by human carbonic anhydrase I. *Biochim. Biophys. Acta.* 1120:81–86.

Roleda MY, Boyd PW, Hurd CL (2012a) Before ocean acidification: calcifier chemistry lessons. *J. Phycol.* 48:840–843.

Roleda MY, Hurd CL (2012) Seaweeds responses to ocean acidification. *In* Wiencke C, Bischof K [Eds.] *Seaweed biology*. Ecological studies 219. Springer–Verlag, Berlin, 407–431 pp.

Roleda MY, Morris JN, McGraw CM, Hurd CL (2012b) Ocean acidification and seaweed reproduction: increased CO_2 ameliorates the negative effect of lowered pH on meiospore germination in the giant kelp *Macrocystis pyrifera* (Laminariales, Phaeophyceae). *Glob. Change Biol.* 18(3):854–864.

Rosman JH, Koseff JR, Monismith SG, Grover J (2007) A field investigation into the effects of a kelp forest (*Macrocystis pyrifera*) on coastal hydrodynamics and transport. *J. Geophys. Res.* 112:C02016, doi:10.1029/2005JC003430.

Rothäusler E, Gómez I, Hinojosa IA, Karsten U, Tala F, Thiel M. (2011) Physiological performance of floating giant kelp *Macrocystis pyrifera* (Phaeophyceae): Latitudinal variability in the effects of temperature and grazing. *J. Phycol.* 47:269–281.

Roughton FJW, Booth VH (1946) The effect of substrate concentration, pH and other factors upon the activity of carbonic anhydrase. *Biochem. J.* 40:319–330.

Rowlett RS, Silverman DN (1982) Kinetics of the protonation of buffer and hydration of CO_2 catalysed by human carbonic anhydrase II. *J. Am. Chem. Soc.* 104:6737–6741.

Rowlett RS, Chance MR, Wirt MD, Sidelinger DE, Royal JR, Woodroffe M, Wang YFA, Saha RP, Lam MG (1994) Kinetic and structural characterization of spinach carbonic- anhydrase. *Biochemistry* 33:13967–13976.

Sarker MY, Bartsch I, Olischläger M, Gutow L,Wiencke C (2013) Combined effects of CO_2, temperature, irradiance and time on the physiological performance of *Chondrus crispus* (Rhodophyta). *Bot. Mar*. 56:63–74.

Sharma A, Bhattacharya A, Singh S (2009) Purification and characterization of an extracellular carbonic anhydrase from *Pseudomonas fragi*. *Process Biochem*. 44:1293–1297.

Smith RG, Bidwell RGS (1987) Carbonic anhydrase-dependent inorganic carbon uptake by the red macroalga, *Chondrus crispus*. *Plant Physiol*. 83:735–738.

Smith RG, Bidwell RGS (1989) Mechanism of photosynthetic carbon dioxide uptake by the red macroalga, *Chondrus crispus. Plant Physiol.* 89:93–99.

Smith FA, Raven JA (1976) Nitrogen assimilation and transport in vascular land plants in relation to intracellular pH regulation. *New Phytol.* 76:415–431

Smith FA, Raven JA (1979) Intracellular pH and its regulation. *Annu. Rev. Plant Physiol*. 30:289–311.

Solomonson LP, Barber MJ (1990) Assimilatory nitrate reductase: functional properties and regulation. *Annu. Rev. Plant. Physiol. Plant Mol. Biol.* 41:225–253.

Spalding MH (2008) Microalgal carbon–dioxide–concentrating mechanisms: *Chlamydomonas* inorganic carbon transporters. *J. Exp. Bot.* 59:1463–1473.

Steemann NE (1960) Uptake of CO_2 by the plant. *In* Ruhland W [Ed.] *Encyclopaedia of plant physiology*. Vol 1. Springer-Verlag, Berlin, 70–84 pp.

Steinacher M, Joos F, Frolicher TL, Bopp L, Cadule P, Cocco V, Doney SC, Gehlen M, Lindsay K, Moore JK, Schneider B, Segschneider J (2010) Projected 21st century decrease in marine primary productivity: a multi–model analysis. Biogeosciences 7:979–1005.

Steinberg PD (1985) Feeding preferences of *Tegula funebralis* and chemical defences of marine brown algae. *Ecol. Monogr*. 55:333–349.

Steneck RS, Graham MH, Bourque BJ, Corbett D, Erlandson JM, Estes JA, Tegner MJ (2002) Kelp forest ecosystems: biodiversity, stability, resilience and future. *Environ. Conserv.* 29(4):436–459.

Stephens TA, Hepburn CD (2014) Mass-transfer gradients across kelp beds influence *Macrocystis pyrifera* growth over small spatial scales. *Mar. Ecol. Prog. Ser.* 515:97–109.

Stewart HL, Fram JP, Reed DC, Williams SL, Brzezinski MA, MacIntyre S, Gaylord B (2009) Differences in growth, morphology and tissue carbon and nitrogen of

Macrocystis pyrifera within and at the outer edge of a giant kelp forest in California USA. *Mar. Ecol. Prog. Ser*. 375:101–112.

Stitt M, Krapp A (1999) The interaction between elevated carbon dioxide and nitrogen nutrition: the physiological and molecular background. *Plant Cell. Environ*. 22:583–621.

Stojkovic S, Beardall J, Matear R (2013) CO_2–concentrating mechanisms in three southern hemisphere strains of *Emiliania huxleyi. J. Phycol.* 49:670–679.

Stöhr C, Tischner R, Ward MR (1993) Characterization of the plasma-membrane-bound nitrate reductase in *Chlorella saccharophila* (Kriiger) Nadson. *Planta* 191:79–85.

Strickland JDH, Parsons TR (1968) A practical handbook of seawater analysis. Fisheries Research Board of Canada, Ontario, Canada, 310 pp.

Stum W, Morgan JJ (1981) Aquatic Chemistry. Wiley.

Suárez–Álvarez S, Gómez–Pinchetti JL, García–Reina G (2012) Effects of increased CO_2 levels on growth, photosynthesis, ammonium uptake and cell composition in the macroalga *Hypnea spinella* (Gigartinales, Rhodophyta). *J. Appl. Phycol.* 24(4):815–823.

Suffrian K, Schulz KG, Gutowska MA, Riebesell U, Bleich M (2011) Cellular pH measurements in *Emiliania huxleyi* reveal pronounced membrane proton permeability. *New Phytol*. 190:595–608.

Sültemeyer D (1998) Carbonic anhydrase in eukaryotic algae: characterization, regulation, and possible function during photosynthesis. *Can. J. Bot.* 76: 962–972.

Sültemeyer D, Heinrich P, Fock P, Canvin DT (1990) Mass spectrometric measurement of intracellular carbonic anhydrase activity in high and low Ci cells of *Chlamydomonas*. *Plant Physiol.* 94:1250–1257.

Surif MB, Raven JA (1989) Exogenous inorganic carbon sources for photosynthesis in seawater by members of the Fucales and the Laminariales (Phaeophyta): ecological and taxonomic implications. *Oecologia* 78:97–105.

Swanson AK, Fox CH (2007) Altered kelp (Laminariales) phlorotannins and growth under elevated carbon dioxide and ultraviolet–B treatments can influence associated intertidal food webs. *Glob. Change Biol.* 13:1696–1709.

Taylor AR, Brownlee C, Wheeler GL (2012) Proton channels in algae: Reasons to be excited. *Trends Plant Sci.* 17(11):675–684.

Taylor AR, Chrachri A, Wheeler G, Godbard H, Brownlee C (2011) A voltage-gated H^+ channel underlying pH homeostasis in calcifying coccolithophores. *PLoS Biol.* 9, e1001085.

Taylor MW, Rees TAV (1999) Kinetics of ammonium assimilation in two seaweeds, *Enteromorpha* sp. (Chlorophyceae) and *Osmundaria colensoi* (Rhodophyceae). *J. Phycol*. 35:740–746.

Teichberg M, Heffner LR, Fox S, Valiela I (2007) Nitrate reductase and glutamine synthetase activity, internal N pools, and growth of *Ulva lactuca*: response to long and short–term N supply. *Mar. Biol.* 151: 1249–1259.

The Royal Society (2005) Ocean acidification due to increasing atmospheric carbon dioxide. Policy document 12/05 Royal Society, London. The Clyvedon Press Ltd, Cardiff.

Thom, RM (1996) CO_2–enrichment effects on eelgrass (*Zostera marina* L.) and bull kelp (*Nereocystis luetkeana* (Mert.) P.&R.). *Water Air Soil Poll.* 88:383–391.

Thomas TE (1983) Ecological aspects of nitrogen uptake in intertidal macrophytes, PhD Thesis, University of British Columbia, Vancouver, 203 pp.

Thomas TE, Harrison PJ (1985) Effect of nitrogen supply on nitrogen uptake, accumulation and assimilation in *Porphyra perforata* (Rhodophyta). *Mar. Biol.* 85:269–278.

Thomas TE, Harrison PJ (1987) Rapid ammonium uptake and nitrogen interactions in five intertidal seaweeds grown under field conditions. *J. Exp. Mar. Biol. Ecol.* 107:1–8.

Thomas TE, Harrison PJ (1988) A comparison of in vitro and in vivo nitrate reductase assays in three intertidal seaweeds. *Bot. Mar*. 31:101–107.

Tischner R, Ward MR, Huffaker RC (1989) Evidence for a plasma-membrane-bound nitrate reductase involved in nitrate uptake of *Chlorella sorokiniana*. *Planta* 178:19–24.

Toth GB, Pavia H (2001) Removal of dissolved brown algal phlorotannins using insoluble Polyvinylpolypyrrolidone (PVPP). *J. Chem. Ecol*. 27:1899–1910.

Tsuzuki M (1983) Mode of HCO_3^- utilization by the cells of *Chlamydomonas reinhardtii* grown under ordinary air. *Z. Pflanzenphysiol*. 110:29–37.

Tsuzuki M, Miyachi S (1989) The function of carbonic anhydrase in aquatic photosynthesis. *Aquat. Bot*. 34:85–104.

Tsuzuki M, Shimamoto T, Yang SY, Miyachi S (1984) Diversity in intracellular locality, nature, and function of carbonic anhydrase in various plants. *Ann. N.Y. Acad. Sci*. 429:238–240.

Turpin DH (1991) Effects of inorganic N availability on algal photosynthesis and carbon metabolism. *J. Phycol.* 27:14–20.

van Tussenbroek BI (1989) Seasonal growth and composition of fronds of *Macrocystis pyrifera* in the Falkland Islands. *Mar. Biol*. 100:419–430.

Ullrich CI, Novacky AJ (1990) Extra– and intracellular pH and membrane potential changes induced by K^+,Cl^-,$H_2PO_4^-$ and NO_3^- uptake and fusicoccin in root hairs of *Limnobium stoloniferum*. *Plant Physiol.* 94:1561–1567.

Ullrich WR (1983) Uptake and reduction of nitrate: Algae and fungi. In Läuchli A, Bielesk RL [Eds], *Encyclopaedia of plant physiology*. N.S. vol. 15A: Inorganic plant nutrition, Springer, Berlin Heidelberg New York London Paris Tokyo, 376–397 pp.

Ullrich WR, Lazarova J, Ullrich CI, Witt FG, Aparicio PJ (1998) Nitrate uptake and extracellular alkalinisation by the green alga *Hydrodictyon reticulatum* in blue and red light. *J. Exp. Bot.* 49(324):1157–1162.

Uusitalo J (1996) Algal carbon uptake and the difference between alkalinity and high pH ("alkalization"), exemplified with a pH drift experiment. *Sci. Mar*. 60 (Supl. 1):129–134.

Vergara JJ, Bird KT, Niell FX (1995) Nitrogen assimilation following NH_4^+ pulses in the red alga *Gracilariopsis lemaneiformis*: effect of C metabolism. *Mar. Ecol. Prog. Ser*. 122:253–263.

Viñegla B, Segovia M, Figueroa FL (2006) Effect of artificial UV radiation on carbon and nitrogen metabolism in the macroalgae *Fucus spiralis* L. and *Ulva olivascens* Dangeard. *Hydrobiologia* 560:31–42.

Warrier RR, Lalitha S, Chellappan S (2014) A modified assay of carbonic anhydrase activity in tree species. *BBR-Biochemistry and Biotechnology report* 3(1):48–55.

Waygood ER (1955) Carbonic anhydrase (plant and animal). *In* Colowick SP, Kaplan NO [Eds.] *Methods in Enzymology*. Vol. 2. Academic Press, New York, 836–46 pp.

Weaver CI, Wetzel RG (1980) Carbonic anhydrase levels and internal lacunar CO_2 concentrations in aquatic macrophytes. *Aquat. Bot*. 8:173–186.

Wernberg T, Russell BD, Moore PJ, Ling SD et al. (2011) Impacts of climate change in a global hotspot for temperate marine biodiversity and ocean warming. *J. Exp. Mar. Biol. Ecol.* 400:7–16.

Wheeler WN (1980) Effect of boundary layer transport on the fixation of carbon by the giant kelp *Macrocystis pyrifera*. *Mar. Biol.* 56:103–110

Wheeler WN (1988) Algal productivity and hydrodynamics– a synthesis. *Prog. Phycol. Res.* 6:23–58.

Wheeler PA, North WJ (1980) Effect of nitrogen supply on nitrogen content and growth rates of juvenile *Macrocystis pyrifera* (Phaeophyta) sporophytes. *J. Phycol*. 16:577–582.

Wheeler PA, North WJ (1981) Nitrogen supply, tissue composition and frond growth rates for *Macrocystis pyrifera* off the coast of southern California. *Mar. Biol*. 64:59–69.

Wheeler WN, Srivastava LM (1984) Seasonal nitrate physiology of *Macrocystis integrifolia*. *J. Exp. Mar. Biol. Ecol*. 76:35–50.

Wilbur K M, Anderson NG (1948) Electrometric and colorimetric determination of carbonic anhydrase. *J. Biol. Chem*. 176:147–54.

Xu Y; Feng L, Jeffrey PD, Shi Y, Morel FM (2008) Structure and metal exchange in the cadmium carbonic anhydrase of marine diatoms. *Nature* 452:56–61.

Xu Z, Gao K (2009) Impacts of UV radiation on growth and photosynthetic carbon acquisition in *Gracilaria lemaneiformis* (Rhodophyta) under phosphorus-limited and replete conditions. *Funct. Plant. Biol.* 36:1057–1064.

Xu ZG, Zou DH, Gao KS (2010) Effects of elevated CO_2 and phosphorus supply on growth, photosynthesis and nutrient uptake in the marine macroalga *Gracilaria lemaneiformis* (Rodophyta). *Bot. Mar.* 53:123–129.

Young E, Berges J, Dring M (2009) Physiological responses of intertidal marine brown algae to nitrogen deprivation and resupply of nitrate and ammonium. *Physiol. Plant.* 135:400–441.

Young EB, Dring MJ, Savidge G, Birkett DA, Berges JA (2007) Seasonal variation in nitrate reductase activity and internal N pools in intertidal brown algae correlate with ambient nitrate availability. *Plant Cell Environ.* 30:764–774.

Young EB, Giordano M, Beardall J (2001) Inorganic carbon acquisition by *Dunaliella tertiolecta* (Chlorophyta) involves external carbonic anhydrase and direct HCO_3^- utilization insensitive to the anion exchange inhibitor DIDS. *Eur. J. Phycol.* 36:81–88.

Young EB, Lavery PS, van Elven B, Dring MJ, Berges JA (2005) Nitrate reductase activity in macroalgae and its vertical distribution in macroalgal epiphytes of seagrasses. *Mar. Ecol. Prog. Ser.* 288:103–114.

Zhang X, Hu H, Tan T (2006) Photosynthetic inorganic carbon utilization of gametophytes and sporophytes of *Undaria pinnatifida* (Phaeophyceae). *Phycologia* 45(6):642–647.

Zhang X, Ye N, Liang C, Mou S, Fan X, Xu J, et al. (2012) De novo sequencing and analysis of the *Ulva linza* transcriptome to discover putative mechanisms

associated with its successful colonization of coastal ecosystems. *BMC Genom.* 13:565.

Zimmerman RC, Kremer JN (1986) In situ growth and chemical composition of the giant kelp, *Macrocystis pyrifera*: response to temporal changes in ambient nutrient availability. *Mar. Ecol. Prog. Ser*. 27: 277–285.

Zou D (2005) Effects of elevated atmospheric CO_2 on growth, photosynthesis and nitrogen metabolism in the economic brown seaweed, *Hizikia fusiforme* (Sargassaceae, Phaeophyta). *Aquaculture* 250: 726–735.

Zou DH, Gao KS (2004) Comparative mechanisms of photosynthetic carbon acquisition in *Hizikia fusiforme* under submersed and emersed conditions. *Acta Bot. Sin*. 46:1178–1185.

Zou DH, Gao KS (2009). Effects of elevated CO_2 on the red seaweed *Gracilaria lemaneiformis* (Gigartinales, Rhodophyta) grown at different irradiance levels. *Phycologia* 48:510–517.

Zou DH, Gao KS (2010a) Photosynthetic acclimation to different light levels in the brown marine macroalga, *Hizikia fusiform*is (Sargassaceae, Phaeophyta). *J. Appl. Phycol.* 22:395–404.

Zou DH, Gao KS (2010b) Acquisition of inorganic carbon by *Endarachne binghamiae* (Scytosiphonales, Phaeophyceae). *Eur. J. Phycol.* 45(1):117–126.

Zou DH, Gao KS, Chen W (2011a) Photosynthetic carbon acquisition in *Sargassum henslowianum* (Fucales, Phaeophyta), with special reference to the comparison between the vegetative and reproductive tissues. *Photosynth. Res.* 107:159–168.

Zou DH, Gao KS, Luo H (2011b) Short- and long-term effects of elevated CO_2 on photosynthesis and respiration in the marine macroalga *Hizikia fusiformis*

(Sargassaceae, Phaeophyta) grown at low and high N supplies. *J. Phycol.* 47:87–97.

Zou DH, Gao KS, Xia JR (2003) Photosynthetic utilization of inorganic carbon in the economic brown alga, *Hizikia fusiforme* (Sargassaceae) from the South China Sea. *J. Phycol*. 36:1095–1100.

Zou DH, Xia JR, Yang YF (2004) Photosynthetic use of exogenous inorganic carbon in the agarophyte *Gracilaria lemaneiformis* (Rhodophyta). *Aquaculture* 237:421–431.

Appendix

9.1 Appendix 1

J. Phycol. 50, 998–1008 (2014)

DOI: 10.1111/jpy.12247

BICARBONATE UPTAKE VIA AN ANION EXCHANGE PROTEIN IS THE MAIN MECHANISM OF INORGANIC CARBON ACQUISITION BY THE GIANT KELP *MACROCYSTIS PYRIFERA* (LAMINARIALES, PHAEOPHYCEAE) UNDER VARIABLE pH[1]

Pamela A. Fernández[2]

Department of Botany, University of Otago, PO Box 56, Dunedin 9054, New Zealand

Catriona L. Hurd

Department of Botany, University of Otago, PO Box 56, Dunedin 9054, New Zealand

Institute for Marine and Antarctic Studies (IMAS), University of Tasmania, Private Bag 129, Sandy Bay, Hobart, Tasmania 7001, Australia

and Michael Y. Roleda

Department of Botany, University of Otago, PO Box 56, Dunedin 9054, New Zealand

Bioforsk Norwegian Institute for Agricultural and Environmental Research, Kudalsveien 6, Bodø 8049, Norway

Macrocystis pyrifera **is a widely distributed, highly productive, seaweed. It is known to use bicarbonate (HCO_3^-) from seawater in photosynthesis and the main mechanism of utilization is attributed to the external catalyzed dehydration of HCO_3^- by the surface-bound enzyme carbonic anhydrase (CA_{ext}). Here, we examined other putative HCO_3^- uptake mechanisms in *M. pyrifera* under pH_T 9.00 (HCO_3^-: CO_2 = 940:1) and pH_T 7.65 (HCO_3^-: CO_2 = 51:1). Rates of photosynthesis, and internal CA (CA_{int}) and CA_{ext} activity were measured following the application of AZ which inhibits CA_{ext}, and DIDS which inhibits a different HCO_3^- uptake system, via an anion exchange (AE) protein. We found that the main mechanism of HCO_3^- uptake by *M. pyrifera* is via an AE protein, regardless of the HCO_3^-: CO_2 ratio, with CA_{ext} making little contribution. Inhibiting the AE protein led to a 55%–65% decrease in photosynthetic rates. Inhibiting both the AE protein and CA_{ext} at pH_T 9.00 led to 80%–100% inhibition of photosynthesis, whereas at pH_T 7.65, passive CO_2 diffusion supported 33% of photosynthesis. CA_{int} was active at pH_T 7.65 and 9.00, and activity was always higher than CA_{ext}, because of its role in dehydrating HCO_3^- to supply CO_2 to RuBisCO. Interestingly, the main mechanism of HCO_3^- uptake in *M. pyrifera* was different than that in other Laminariales studied (CA_{ext}-catalyzed reaction) and we suggest that species-specific knowledge of carbon uptake mechanisms is required in order to elucidate how seaweeds might respond to future changes in HCO_3^-:CO_2 due to ocean acidification.**

Key index words: **bicarbonate; carbon acquisition; carbon dioxide; carbonic anhydrase; inorganic carbon; macroalgae; *Macrocystis pyrifera*; ocean acidification; photosynthesis**

Abbreviations: **AE, anion exchange; A_T, total alkalinity; AZ, acetazolamide; CA, carbonic anhydrase; CA_{ext}, external carbonic anhydrase; CA_{int}, internal carbonic anhydrase; Ci, inorganic carbon; DIC, dissolved inorganic carbon; DIDS, 4,4′-diisothiocyanatostilbene-2,2′-disulfonate; NPS, net photosynthesis; NSW, natural sea water; OA, ocean acidification; VAN, vanadate**

Seaweeds are the base of the food web and major contributors to benthic primary production in coastal ecosystems, providing both food and habitat for fish and invertebrates. Their high productivity enables them to fix large amounts of carbon, contributing around 10% of total marine production (Charpy-Roubaud and Sournia 1990, Bensoussan and Gattuso 2007, Graham et al. 2007, Koch et al. 2012). To support photosynthesis and growth, seaweeds require an exogenous inorganic carbon (Ci) source. Today's oceans contain ~2.1 mol · m^{-3} of dissolved inorganic carbon (DIC) at pH ~8.07 and 15°C, which exist as bicarbonate (HCO_3^-; 91%), carbonate (CO_3^{2-}; 8%), and dissolved carbon dioxide ($CO_{2\ (aq)}$; 1%) (Roleda and Hurd 2012); only CO_2 and HCO_3^- can be used as CO_2 source for photosynthesis. Although only a small proportion of Ci exists as CO_2, this uncharged molecule readily diffuses into the seaweed cell, whereas the most abundant form of Ci, HCO_3^-, cannot diffuse through the lipid bilayer of the plasma membrane (Raven 1997). Due to the low CO_2 concentration in seawater, it is not surprising that most seaweed have developed mechanisms for using the abundant

[1]Received 27 March 2014. Accepted 28 August 2014.
[2]Author for correspondence: e-mail pamela.fernandez@botany.otago.ac.nz
Editorial Responsibility: T. Wernberg (Associate Editor)

9.2 Appendix 2

Photosynth Res
DOI 10.1007/s11120-015-0138-5

REGULAR PAPER

Effects of ocean acidification on the photosynthetic performance, carbonic anhydrase activity and growth of the giant kelp *Macrocystis pyrifera*

Pamela A. Fernández[1] · Michael Y. Roleda[1,2] · Catriona L. Hurd[1,3]

Received: 3 December 2014 / Accepted: 31 March 2015

Abstract Under ocean acidification (OA), the 200 % increase in $CO_{2(aq)}$ and the reduction of pH by 0.3–0.4 units are predicted to affect the carbon physiology and growth of macroalgae. Here we examined how the physiology of the giant kelp *Macrocystis pyrifera* is affected by elevated pCO_2/low pH. Growth and photosynthetic rates, external and internal carbonic anhydrase (CA) activity, HCO_3^- versus CO_2 use were determined over a 7-day incubation at ambient pCO_2 400 µatm/pH 8.00 and a future OA treatment of pCO_2 1200 µatm/pH 7.59. Neither the photosynthetic nor growth rates were changed by elevated CO_2 supply in the OA treatment. These results were explained by the greater use of HCO_3^- compared to CO_2 as an inorganic carbon (Ci) source to support photosynthesis. *Macrocystis* is a mixed HCO_3^- and CO_2 user that exhibits two effective mechanisms for HCO_3^- utilization; as predicted for species that possess carbon-concentrating mechanisms (CCMs), photosynthesis was not substantially affected by elevated pCO_2. The internal CA activity was also unaffected by OA, and it remained high and active throughout the experiment; this suggests that HCO_3^- uptake via an anion exchange protein was not affected by OA. Our results suggest that photosynthetic Ci uptake and growth of *Macrocystis* will not be affected by elevated pCO_2/low pH predicted for the future, but the combined effects with other environmental factors like temperature and nutrient availability could change the physiological response of *Macrocystis* to OA. Therefore, further studies will be important to elucidate how this species might respond to the global environmental change predicted for the ocean.

Keywords Carbonic anhydrase · Inorganic carbon uptake · Macroalgae · *Macrocystis pyrifera* · Ocean acidification · Photosynthesis

Introduction

Since the Industrial Revolution, the emissions of CO_2 into the atmosphere have increased considerably, from ~280 to 395 µatm, due to human activities such as burning fossil fuels, deforestation, cement manufacture and others land-use changes (Caldeira and Wickett 2003; The Royal Society 2005). This trend is projected to continue by a minimum rate of 0.5 % per year throughout the next century, reaching levels of ~1000 µatm of CO_2 by 2100 (IPCC 2013). Approximately one-third of these CO_2 emissions will be absorbed by the world's oceans, increasing $CO_{2(aq)}$ and decreasing the pH of the surface waters, making them more acidic and altering the seawater carbonate chemistry, a process known as ocean acidification (OA) (The Royal Society 2005; Guinotte and Fabry 2008). By 2100, the $CO_{2(aq)}$ concentration will be double the existing level, leading to an estimated drop in pH of 0.3–0.4 units from the current global ocean surface average of ~8.15–7.75 (IPCC 2013). These predicted changes in seawater carbonate chemistry can influence important biological and physiological processes of calcifying and non-calcifying marine organisms (both autotrophs and heterotrophs) (The Royal Society 2005).

✉ Pamela A. Fernández
pamela.fernandez@botany.otago.ac.nz

[1] Department of Botany, University of Otago, PO box 56, Dunedin 9054, New Zealand

[2] Biofrank Norwegian Institute for Agricultural and Environmental Research, Kudalsveien 6, 8049 Bodø, Norway

[3] Institute for Marine and Antarctic Studies (IMAS), University of Tasmania, Hobart, TAS 7001, Australia

Published online: 14 April 2015